UK Society for Biomaterials Annual Conference 2025 (UKSB2025)

UK Society for Biomaterials UKSB at Lancaster University

With generous support from:

https://doi.org/10.5281/zenodo.16416539

UK Society for Biomaterials Annual Conference 2025 (UKSB2025)

The UK Society for Biomaterials (UKSB) is an interdisciplinary society, with a broad membership including folks in academic, clinical and industry settings, representing the UK-based community engaged in biomaterials development and their collaborators worldwide. The UKSB Annual Conference 2025 (UKSB2025) will be held at Lancaster University. The UKSB award winners will deliver exciting lectures:

- President's Prize: Professor Sarah Cartmell, University of Manchester.
- Alan Wilson Memorial Lecture Award: Professor Maisoon Al-Jawad, University of Leeds.
- Larry Hench Award: Dr Jessica Senior, University of Huddersfield.

Venue: Lancaster University, Lancaster, UK.

Dates: 30/06/2025-02/7/2025.

Sponsors: We thank the conference sponsors for support in a variety of forms.

- **Industry:** ArmaTrex, Bruker, Design for AM Network, Invibio (Victrex), Medilink, Metrohm, Nikon, Schrödinger, Wonderful Scientific.
- **Elsevier:** Biomaterials Advances, Biomaterials and Biosystems.
- **Royal Society of Chemistry:** Biomaterials Science, Journal of Materials Chemistry B, Materials Advances, Materials Horizons, RSC Pharmaceutics.
- **Wiley:** Advanced Engineering Materials, Advanced Healthcare Materials, Advanced NanoBiomed Research, Advanced Sensor Research, Advanced Therapeutics.

https://doi.org/10.5281/zenodo.16416539

Foreword

Welcome to the 2025 Annual Conference of the UK Society for Biomaterials (UKSB). This is a milestone year for our Society as we celebrate our 25th anniversary, which is a moment of pride for all those who have been part of this journey. Over the past quarter of a century, the UKSB has grown into a dynamic and diverse community, committed to advancing biomaterials science and providing a platform to help build meaningful collaborations and friendships across disciplines.

As we reflect on our achievements and look to the future, this year's conference is an opportunity to celebrate our continued growth and to reaffirm our mission: to bring people together, and to support the development of the next generation of biomaterials scientists. We are especially focused on creating an inclusive and welcoming environment, where all members – regardless of career stage or background – feel empowered to contribute and connect.

Our annual meeting remains a cornerstone of the Society's activity. It provides a vital space for networking, knowledge exchange, and professional development. The 2025 scientific programme reflects the evolving nature of our field, spanning a wide range of topics and encouraging meaningful discussion, collaboration, and fresh ideas. We strongly encourage you to make the most of the sessions, engage with new colleagues, and take time to reflect on how your work fits into the broader biomaterials landscape.

We are particularly proud of our efforts to support early-career researchers. Many of our junior members, whose formative years were impacted by the pandemic, are now attending in-person scientific meetings for the first time. We invite you all to make them feel welcome, and to foster the sense of community and mentorship that is the hallmark of UKSB.

This year has also seen an exceptional number of high-quality applications for our awards and travel grants. We are pleased to be supporting members attending this conference and other events through our different funding initiatives. In addition, our prize winners this year exemplify excellence and dedication—not only in research, but in their commitment to the advancement of biomaterials as a whole.

I would like to extend a heartfelt thank you to the UKSB Council members, whose tireless work behind the scenes ensures the smooth running and continual development of the Society. Your

https://doi.org/10.5281/zenodo.16416539

feedback as members is essential in helping us shape the future of the UKSB, so I encourage you to attend the Annual General Meeting during this conference and share your thoughts. Looking beyond this event, we're excited to support and participate in major upcoming conferences, including the European Society for Biomaterials (ESB) 2025, and many other important gatherings across our international community. If you plan to attend, please represent the UKSB proudly – as a vibrant and collaborative hub for biomaterials research in the UK and beyond.

Here's to 25 years of progress – and to a bold, inclusive, and innovative future.

Dr Adrian Boyd

President, UK Society for Biomaterials

https://doi.org/10.5281/zenodo.16416539

Welcome from the Local Organising Committee for #UKSB2025

The local organising committee would like to extend a very warm welcome to you all for the 25th UKSB Annual Conference being held this year at Lancaster University campus in Bailrigg. This meeting offers an opportunity for those working in the field of biomaterials (academia, public/private sectors [e.g., UKRI, NHS, industry, etc.] and the third sector [e.g., charities, NGOs, etc.]) to engage with each other and develop existing/new collaborations. The UKSB network welcome newcomers from any career stage and strongly supports opportunities for the development of students and early career researchers (this year with a variety of oral/poster presentation and networking opportunities). We hope you enjoy the conference, (both the scientific sessions and the social programme) and to explore Lancaster and the surrounding area. With sustainability in mind, we are largely paperless; we have also kept the conference to a single-track session to ensure maximum exposure to all contributors.

Local Organising Committee

- Chair: Dr John Hardy (Department of Chemistry at Lancaster University).
- Dr Timothy Douglas (School of Engineering at Lancaster University).
- Dr Jemma Kerns (Lancaster Medical School at Lancaster University).
- Dr Richard Mort (Division of Biomedical and Life Sciences at Lancaster University).
- Prof. Ihtesham Rehman (School of Medicine and Dentistry at the University of Lancashire).
- Prof Ben Robinson (Department of Physics at Lancaster University).
- Dr Naval Singh (School of Engineering at Lancaster University).

https://doi.org/10.5281/zenodo.16416539

Conference Information

Conference abstract submissions

We are delighted to have received submissions for oral/poster presentations from academia, public/private sectors (e.g., UKRI, NHS, industry, etc.) and the third sector (e.g., charities, NGOs, etc.). Abstract templates are available from the UKSB2025 website. Abstracts should be submitted via email to: UKSB2025@gmail.com

Submissions should be aligned with topical coverage that includes but is not limited to:

- Additive Manufacturing
- Advanced Antimicrobial Materials
- Advanced Engineering Materials
- Advanced Therapeutics
- Bioelectronics and Biosensors
- Dental and Orthopaedic Materials
- Drug Delivery
- Neuroscience & Neurotechnology
- Prosthetics and Orthotics
- Tissue Engineering and Regenerative Medicine

With the move towards "Open Science" it is possible to upload your presentations (e.g., posters or slide decks) to open access repositories such as F1000 (an open research publisher and services provider that enables researchers, funders, research institutions, societies, and associations to accelerate the reach of knowledge; https://www.f1000.com/resources-for-researchers/how-to-publish-your-research/article-types/) or Zenodo (a general-purpose open repository developed under the European OpenAIRE program that enables researchers to deposit research papers, data sets, research software, reports, and any other research related digital artefacts; https://zenodo.org/). For submissions a persistent digital object identifier (DOI) is created to facilitate the stored items to be citeable. **Only upload documents to these repositories with the agreement of all co-authors/sponsors.**

https://doi.org/10.5281/zenodo.16416539

Conference abstract submissions, registration and accommodation

Accommodation is available on campus (including accessible accommodation) that can be reserved on the registration website and in the city (e.g., via Booking.com). We encourage you to use public transport to/from/within Lancaster and to walk between venues (where possible) and recognising the challenges of visiting the campus we include parking permits in the registration fee.

- Conference registration via the conference website.
- Early bird student (i.e., on/before 30/04/2025): £180.
- Early bird non-student (i.e., on/before 30/04/2025): £210.
- Normal student (i.e., after 30/04/2025): £200.
- Normal non-student (i.e., after 30/04/2025): £230.

Public/private sector and third sector involvement

We are particularly keen to engage with folks in the public/private sectors (e.g., UKRI, NHS, industry, etc.) and the third sector (e.g., charities, NGOs, etc.) to deliver the maximum impact from the conference, and therefore have oral/poster presentations from non-academic speakers, exhibition spots, and networking opportunities (multiple coffee/tea breaks; 3 lunches; 2 poster/networking sessions; 2 conference meals, and others). We welcome sponsorship in any form (e.g., headline sponsors, supporting sponsors, poster session sponsors, abstract book sponsors/advertising, exhibitors, donations). Contact us via email to: UKSB2025@gmail.com to chat in detail about potential opportunities (e.g., oral/poster presentations, technology showcasing, etc.), e.g., via MS teams.

https://doi.org/10.5281/zenodo.16416539

Prizes

- Oral presentation (Early Career Researchers): 1st, 2nd, 3rd.
- Flash presentation (Early Career Researchers): 1st, 2nd, 3rd.
- Best posters (Student): 1st, 2nd, 3rd.
- ArmaTrex poster prize: 1st.
- RSC poster prizes: Biomaterials Science; Materials Advances; Materials Horizons; RSC Pharmaceutics; Journal of Materials Chemistry B.
- Wiley poster prizes: 1st, 2nd.

Acknowledgements

First and foremost, we would like to thank Dale Walker (Events Manager at Lancaster University) for her patience and support throughout the planning and execution of the conference, particularly helping folks find accommodation at the last minute.

For insightful discussions regarding the knowledge exchange and design of impactful conferences, we thank Dr Martin Gilmore (Head of Partnerships & Business Engagement: Engineering & Physical Sciences at Lancaster University); and for thoughts on conference promotion we thank Ellen Greyling, both at Lancaster University.

For insightful discussions regarding the conference planning we thank Professor Julian Jones at Imperial College London; and specifically for insightful discussions regarding the Early Career Takeover sessions, we thank Dr Tanveer Tabish at the University of Oxford and Dr Nicola Contessi Negrini at Imperial College London.

For support with conference administration (name badges, poster boards, welcome desk, etc.) we thank Daniel Baines, Carmen Barker Benavides, Gaurav Dubey, Leena Duong, Nikita Lad, Dr Sam Robertshaw and Dr Sam Rust.

For support with peer review of abstracts and oral/poster presentations we thank the conference organising committee, the UKSB council members, Katie Morton at the Royal Society of Chemistry, and the audience.

https://doi.org/10.5281/zenodo.16416539

For musical entertainment we thank:

- Monday 30th of June 2025: Another Mister (contactable via: https://www.facebook.com/Anothermister/).
- Tuesday 1st of July 2025: Daniel Smith (contactable via: d.e.smyth1@gmail.com), and the 7/6 Jazz Combo (contactable via: http://www.ulms.org.uk/)

Once again, we thank the conference sponsors for support in a variety of forms that helped subsidise the costs associated with the conference, without these contributions the conference would not have been possible; their engagement before, during and after the conference will help ensure the maximum impact of the conference.

- **Industry:** ArmaTrex, Bruker, Design for AM Network, Invibio (Victrex), Medilink, Metrohm, Nikon, Schrödinger, Wonderful Scientific.
- **Elsevier:** Biomaterials Advances, Biomaterials and Biosystems.
- **Royal Society of Chemistry:** Biomaterials Science, Journal of Materials Chemistry B, Materials Advances, Materials Horizons, RSC Pharmaceutics.
- **Wiley:** Advanced Engineering Materials, Advanced Healthcare Materials, Advanced NanoBiomed Research, Advanced Sensor Research, Advanced Therapeutics.

Save the date: the UK Society for Biomaterials Annual Conference in 2026 will be held on the 9th and 10th of July 2026 at Keele University and will be organised by Dr Pooya Davoodi, Prof. Ying Yang, and others.

https://doi.org/10.5281/zenodo.16416539

Sponsor information

ArmaTrex Ltd.

The ArmaTrex products designed and developed by a former commercial diver, soldier, maritime security operator and explorer, also the Director of Operations; conducted deep sea salvage operations on the wreck of the RMS Titanic. The two products; the ArmaTrex META (Medical Emergency Trauma Appliance) limb splint system and the SLETCHER an innovative rescue and extrication stretcher; both designed for the medical responder, rescue industry and military, remote location and wilderness for use in austere and hostile environments.

- Organisation website: https://armatrex.co.uk/
- Contact: Dik Barton (Founder & Chief Operating Officer) and Adele Davydaitis (Business Development Director).
- Email: info@armatrex.co.uk or admin@armatrex.co.uk
- LinkedIn: https://www.linkedin.com/in/dik-barton-30132118/

Bruker

Bruker Corporation makes scientific instruments for molecular/materials research, and industrial/applied analysis. Bruker's differentiated high-value life science research and diagnostics solutions enable scientists to make breakthrough discoveries and develop new applications that improve the quality of human life.

- Organisation website: https://www.bruker.com/en.html
- Contact: Joerg Barner, Application Scientist.
- Email: Joerg.Barner@bruker.com

https://doi.org/10.5281/zenodo.16416539

Design for AM Network

The purpose of the EPSRC Design for AM Network is to connect the wider UK Design for AM academic research community alongside those in the industry.

- Organisation website: https://www.designforam.ac.uk/
- Email: design.for.am@lboro.ac.uk

Elsevier

Elsevier is a publishing company.

- Organisation website: https://www.elsevier.com/en-gb
- Contact: Jacqueline Zhu or Emma Xu.
- Email: jieyi.zhu@elsevier.com or Emma.XU@elsevier.com

Biomaterials Advances

Formerly known as Materials Science and Engineering: C, with a 2022 IF of 7.9.

Editor-in-Chief: Manuel Salmeron-Sanchez.

Biomaterials Advances includes topics at the interface of the biomedical sciences and materials engineering. These topics include:

https://doi.org/10.5281/zenodo.16416539

- Bioinspired and biomimetic materials for medical applications
- Materials of biological origin for medical applications
- Materials for "active" medical applications
- Self-assembling and self-healing materials for medical applications
- "Smart" (i.e., stimulus-response) materials for medical applications
- Ceramic, metallic, polymeric, and composite materials for medical applications
- Materials for in vivo sensing
- Materials for in vivo imaging
- Materials for delivery of pharmacologic agents and vaccines
- Novel approaches for characterizing and modeling materials for medical applications

Manuscripts on biological topics without a materials science component, or manuscripts on materials science without biological applications, will not be considered for publication in Biomaterials Advances. New submissions are first assessed for language, scope and originality (plagiarism check) and can be desk rejected before review if they need English language improvements, are out of scope or present excessive duplication with published sources.

Biomaterials Advances sits within Elsevier's biomaterials science portfolio alongside Biomaterials, Materials Today Bio and Biomaterials and Biosystems. As part of the broader Materials Today family, Biomaterials Advances offers authors rigorous peer review, rapid decisions, and high visibility. We look forward to receiving your submissions!

Metrics:

- CiteScore: 17.7
- Impact Factor: 6.0
- Time to first decision: 5 days
- Review time: 97 days
- Submission to acceptance: 117 days
- Acceptance to publication: 8 days
- Acceptance rate: 18%

Abstracting and indexing:

- Scopus
- Medline
- SNIP
- Science Citation Index Expanded (SCIE)

https://doi.org/10.5281/zenodo.16416539

Medilink North of England

Medilink North of England brings together the NHS, industry and academia to increase innovation and improve patient care in the North. Its primary focus is on helping organisations to grow by providing cost-effective specialist consultancy support to become more competitive and profitable in the UK and Internationally.

- Organisation website: https://www.medilinkuk.com/medilink-north-of-england/
- Contact: Patrick Trotter, Strategy, Innovation, Product Development and Commercialisation Expert.
- Email: p.trotter@medilink.co.uk
- LinkedIn: https://www.linkedin.com/in/ptrotter/

Metrohm

Metrohm offers a wide range of analytical instrumentation, laboratory equipment, and accessories.

- Organisation website: https://www.metrohm.com/en_gb.html
- Contact: Jayan Tailor, Technical sales specialist at Metrohm.
- Email: jayan.tailor@metrohm.co.uk
- LinkedIn: https://www.linkedin.com/in/jayan-tailor-364611167/

https://doi.org/10.5281/zenodo.16416539

Nikon

Nikon Corporation is a Japanese optics and photographic equipment manufacturer.

- Organisation website: https://www.nikon.co.uk/en_GB
- Contact: Dr Niall Mahon, Key Account Manager (North) @ Nikon Healthcare UK.
- Email: Niall.Mahon@nikon.com
- LinkedIn: https://www.linkedin.com/in/niall-mahon-phd-b75044153/

Royal Society of Chemistry (RSC)

The RSC is a learned society in the United Kingdom with the goal of advancing the chemical sciences. Organisation website: https://www.rsc.org/

Biomaterials Science

- Editor-in-Chief: Jianjun Cheng
- Scope: New concepts in biomaterials design, studies into the interaction of biomaterials with the body, and the use of materials to answer fundamental biological questions. Papers do not necessarily need to report a new biomaterial but should provide novel insight into the biological applications of the biomaterial.
- Time to first decision: 37* days
- Impact Factor: 5.7
- Journal website: https://pubs.rsc.org/en/journals/journalissues/bm#!recentarticles&adv

https://doi.org/10.5281/zenodo.16416539

Journal of Materials Chemistry B

- Editor-in-Chief: Jessica Winter
- Scope: High quality studies of novel materials chemistry, bringing a molecular picture to bear on a given material's suitability as a biomaterial with applications in biology and medicine.
- Time to first decision: 45* days
- Impact Factor: 5.7
- Journal website: https://pubs.rsc.org/en/journals/journalissues/tb#!recentarticles&adv

Materials Horizons

- Editor-in-Chief: Martina Stenzel
- Scope: Materials Horizons is a leading journal for the publication of exceptionally high quality, innovative materials science. The journal places an emphasis on original research that demonstrates a new concept or a new way of thinking (a conceptual advance), rather than primarily reporting technological improvements. However, outstanding articles featuring truly breakthrough developments such as record performance of materials alone may also be published in the journal.
- Time to first decision: 33* days
- Impact Factor: 0.7
- Journal website: https://pubs.rsc.org/en/journals/journalissues/mh#!recentarticles&adv

Materials Advances

- Editor-in-Chief: Anders Hagfeldt and Jessica Winter
- Scope: Experimental or theoretical studies that report new understanding, applications, properties and synthesis of materials, building on and complementing the materials content already published across the Royal Society of Chemistry journal portfolio.
- Time to first decision: 42* days

https://doi.org/10.5281/zenodo.16416539

- Impact Factor: 4.7
- Journal website: https://pubs.rsc.org/en/journals/journalissues/ma#!recentarticles&adv

RSC Pharmaceutics

- Editor-in-Chief: Yvonne Perrie
- Scope: RSC Pharmaceutics is a new gold open access journal leading the way in the field of Pharmaceutics. This journal publishes research focused on formulating a drug into a medicine, with the intention of achieving controllable drug delivery with high efficacy. Research sharing new scientific findings from across the areas of chemistry, materials science, biomedical sciences, pharmaceutics and drug delivery are all welcomed.
- Time to first decision: 54* days
- Impact Factor: N/A
- *Time to first decision in 2024 (peer reviewed)
- Journal website: https://pubs.rsc.org/en/journals/journalissues/pm#!recentarticles&adv

https://doi.org/10.5281/zenodo.16416539

Schrödinger

Schrödinger

Schrödinger's computational platform, powered by physics, is transforming the way therapeutics and materials are discovered to make innovations of the future achievable, today. Use the QR codes to in the figure below to access a competition for a place on one of Schrödinger's online certificate courses.

https://doi.org/10.5281/zenodo.16416539

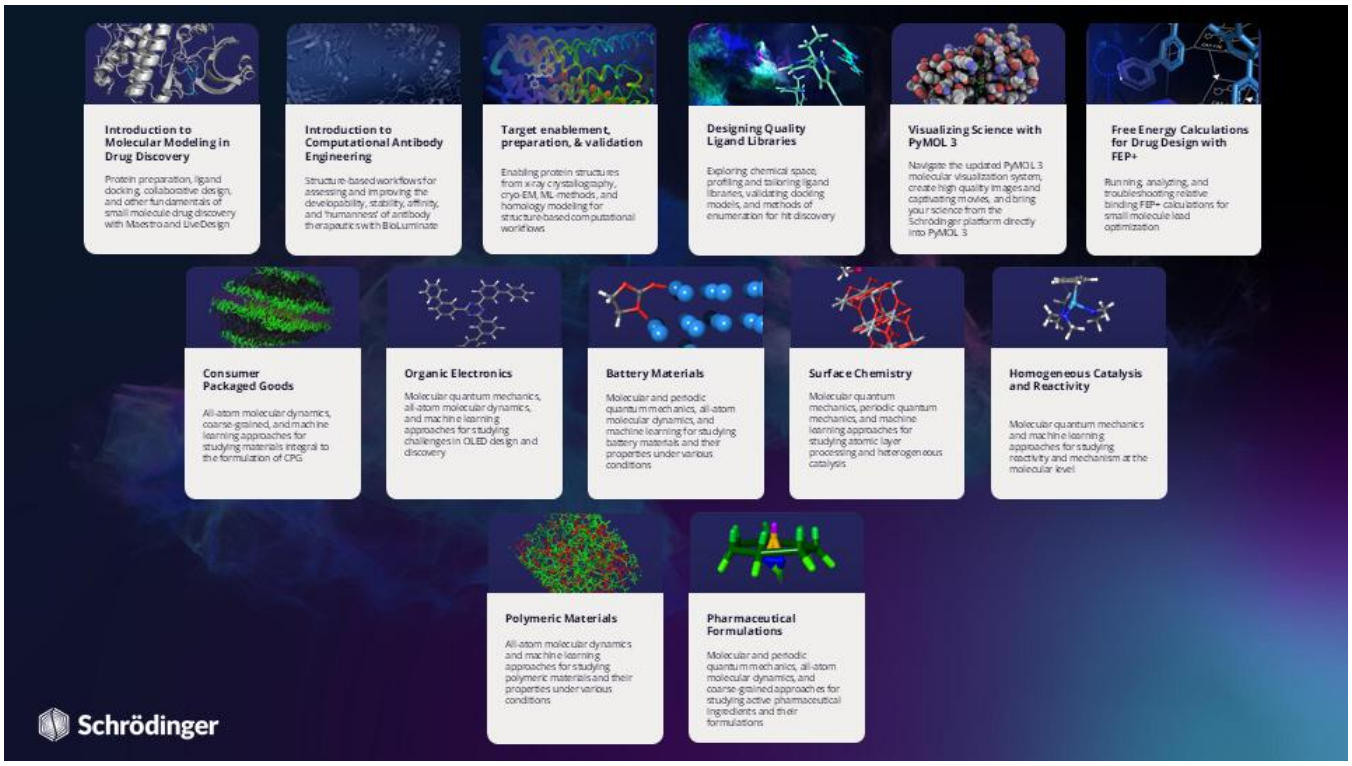

- Organisation website: https://www.schrodinger.com/
- Contact: Dr Patrick Heasman, Materials Science Academic Account Manager.
- Email: patrick.heasman@schrodinger.com
- LinkedIn: https://www.linkedin.com/in/patrick-heasman/

https://doi.org/10.5281/zenodo.16416539

Victrex and Invibio

Invibio, part of the Victrex plc group of companies, is a global leader in providing high-performance biomaterial solutions to medical device manufacturers. The company provides PEEK-OPTIMA™ polymers, advanced technical research and support and manufacturing of components for spine, trauma and orthopaedic and medical segments for the development of long-term implantable medical devices.

- Organisation website: https://invibio.com/en/about-invibio
- Contact: Andy Anderson, Head of R&D.
- Email: aanderson@victrex.com
- LinkedIn: https://www.linkedin.com/in/andy-anderson-victrex-peek/

Wiley

Wiley is a publishing company.

- Organisation website: https://www.wiley.com/en-gb
- Related journals: Advanced Engineering Materials, Advanced Healthcare Materials, Advanced NanoBiomed Research, Advanced Sensor Research, Advanced Therapeutics.

https://doi.org/10.5281/zenodo.16416539

Wonderful Scientific

Wonderful Scientific is the proud distributor of NeoScan.com benchtop Micro-CT and Nano-CT products in the UK and Ireland. We are committed to providing the highest quality instruments to our customers. NeoScan scanners are the most advanced and innovative in the market. The recently launched N90 is the world's first bench-top Nano-CT and has 300nm spatial and 40nm voxel size at maximum resolution. The N80 scanner is the best-in-class scanner and is ideal for high resolution bone analysis and visualisation. The N80 has a sealed transmission X-ray source with a 2um spot size and movable target repositioning, radiation hardened camera protection, 2:1 fibre optics, active artefact suppression, new precision stepper motors and all new software. The resulting benefits make it the most robust, long lasting, scientific grade bench-top Micro-CT on the market today. We offer 5 MicroCT scanners and our latest NXL can accommodate very large samples up to 540mm in length.

- Organisation website: https://wonderfulscientific.com/
- Contact: Dr Andrew Lonergan, Director and Founder.
- Email: andrew@wonderfulscientific.com
- LinkedIn: https://www.linkedin.com/in/andrew-lonergan-80005016/

https://doi.org/10.5281/zenodo.16416539

Academic Journal Special Issues

Elsevier

Biomaterials and Biosystems is an open access, interdisciplinary journal published by Elsevier, positioned within its biomaterial's science portfolio alongside Biomaterials, Materials Today Bio, and Biomaterials Advances. With a CiteScore of 7.9 (covering 2021–2025) and sits in the 46th percentile in the Biomaterials category and 83rd in Biomedical Engineering category, the journal aims to publish high-quality research at the intersection of engineering, chemistry, biology, and medicine. It focuses on research, technology development, and clinical translation related to innovative biomedical devices, biological systems, and their applications for human health, as well as exploring the ethical and social implications of advancements in biomedical engineering. The journal is committed to maintaining the highest standards of integrity, confidentiality, and ethical conduct while disseminating knowledge, tools, and discoveries that can improve healthcare and quality of life.

UK Society for Biomaterials Special Issue 2025

Submission deadline: 31 December 2025

https://www.sciencedirect.com/special-issue/321189/uk-society-for-biomaterials-special-issue-2025

Authors should click 'Submit your article' and then, under 'Select Article Type' to select either VSI: UKSB2025_Full length article for research papers or VSI: UKSB2025_Review article for review papers.

https://doi.org/10.5281/zenodo.16416539

Emerald Insight

Now in its 30th year, the Rapid Prototyping Journal (RPJ) was the first journal dedicated to the publication of research for the range of technologies that we now refer to as additive manufacturing. Over the past three decades, RPJ has maintained its role as a leading international journal for the dissemination of research in additive manufacturing, 3D printing, advanced materials, digital fabrication processes, and the associated technologies that support them. RPJ publishes original research that explores not only technical innovation but also practical applications, from new material development and process optimisation to system integration and computational design strategies. Connecting academic research with real-world industrial applications, the journal serves a diverse audience of academic researchers, scientists, engineers and practitioners shaping the field of digital manufacturing. RPJ welcomes article submissions of high-quality pieces of research presented at the UKSB2025 Conference that fits the scope of RPJ.

MDPI: Materials "Biomaterials Science—Select Papers from the UKSB 2025 Conference."

Biomaterials aid in the delivery of solutions to diseases/injuries for the global population. Biomaterials research and development requires insights from researchers based in academic and industrial settings, underpinning millions of jobs worldwide. The UK Society for Biomaterials (UKSB) is an interdisciplinary society, with a broad membership including people in academic, clinical, and industrial settings, representing the UK-based community engaged in biomaterials development and their collaborators worldwide. We invite researchers to contribute original findings to this Special Issue of Materials.

Website: https://www.mdpi.com/journal/materials/special_issues/0VGI0295BN

https://doi.org/10.5281/zenodo.16416539

Wiley

Call for papers – Invitation to authors to submit articles to Wiley for peer review.

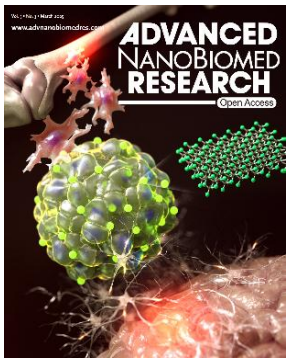

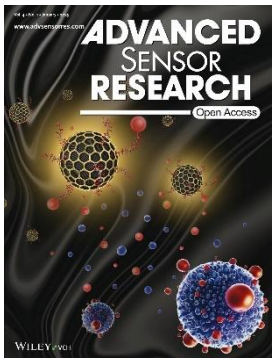

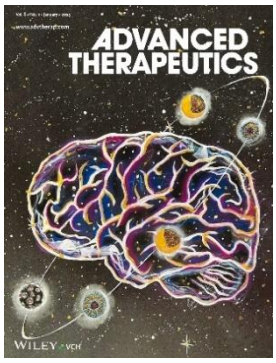

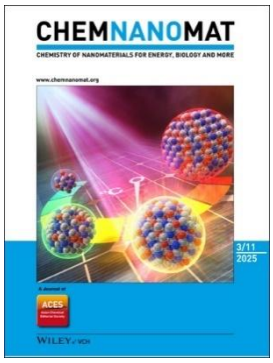

Special Collection in Advanced NanoBiomed Research, Advanced Sensor Research, Advanced Therapeutics and ChemNanoMat

Biosensors & Biomaterials @ UKSB2025; Guest-Editor: John G. Hardy

Submission Deadline: **October 31st, 2025**; submissions at

https://www.editorialmanager.com/advnanobiomedres/ for Advanced NanoBiomed Research

https://www.editorialmanager.com/advsensorres/ for Advanced Sensor Research

https://www.editorialmanager.com/advtherap for Advanced Therapeutics

http://www.editorialmanager.com/cnma for ChemNanoMat

Dear **UKSB2025** presenters,

We are planning to publish a special collection highlighting the most exciting new results presented at this year's **UKSB2025** across our Journals **Advanced NanoBiomed Research, Advanced Sensor Research, Advanced Therapeutics** and **ChemNanoMat.** In collaboration with the Guest Editor, and the Editorial Offices, we cordially invite you to contribute a **Research Article** or **Review Article** based on your oral or poster presentation.

Advanced NanoBiomed Research provides an Open Access home for cutting-edge nanomedicine, bioengineering and biomaterials research aimed at improving human health. The journal captures a broad spectrum of research from multi- and interdisciplinary fields of biomedicine, bioengineering and health-related materials science as well as precision and personalized medicine, drug delivery, and artificial intelligence-driven health science (https://advanced.onlinelibrary.wiley.com/journal/26999307). **Advanced Sensor Research**, part of the prestigious Advanced Portfolio, is the open access home for ground-breaking

https://doi.org/10.5281/zenodo.16416539

research on sensing materials, devices, and their applications (https://advanced.onlinelibrary.wiley.com/journal/27511219). **Advanced Therapeutics** is a unique multidisciplinary therapeutics journal publishing the best research in targeted drug delivery, cellular and genetic therapies, personalized medicines and theranostics, as well as pharmacology, toxicology and drug discovery. Innovative therapeutic approaches as well as clinical studies are especially welcome (https://advanced.onlinelibrary.wiley.com/journal/23663987) and **ChemNanoMat** is an international nanoscience journal connecting nano chemistry with materials science. With a broad scope, the journal covers all aspects of the chemistry of nanomaterials, nanotechnology, nanomedicines, and their interdisciplinary applications (https://aces.onlinelibrary.wiley.com/journal/2199692x).

Please note, that manuscripts considered for this special collection will be evaluated using the same high standards and peer-review process as regular submissions to our journals. Accepted papers will be published online as soon as possible. The online publication date will be the official publication date of your paper. Manuscripts should be submitted directly to the **journals** by following the links given above. You should **mention the conference** in your cover letter and select the appropriate topical section/category **Biosensors & Biomaterials @ UKSB2025** during online submission to expedite handling. If you believe that your work fits well to one of our other Wiley Journals **Advanced Healthcare Materials** or **Advanced Engineering Materials** email us at advhealthmat@wiley-vch.de or aem@wiley-vch.de, respectively, or submit your article directly to one of the journals and mention the conference in your cover letter.

We look forward to receiving your contribution!

John G. Hardy (Guest Editor), Irem Bayindir-Buchhalter (Editor-in-Chief, Advanced NanoBiomed Research), Marc Zastrow (Editor-in-Chief, Advanced Sensor Research), Christine Mayer (Editor-in-Chief, Advanced Therapeutics) and Ulrike Kauscher Pinto (Editor-in-Chief, ChemNanoMat)

https://doi.org/10.5281/zenodo.16416539

PS. All articles published by **Advanced NanoBiomed Research** and **Advanced Sensor Research** are fully open access (OA) and **Advanced Therapeutics** and **ChemNanoMat** are hybrid OA/subscription journals: OA means that all articles are immediately freely available to read, download, and share. To cover the cost of publishing your funder or institution may have an agreement with Wiley for payment of article publication charges; please visit the following page for details: https://authorservices.wiley.com/author-resources/Journal-Authors/open-access/affiliation-policies-payments/index.html

https://doi.org/10.5281/zenodo.16416539

Schedule

The conference will be held at Lancaster University, from 30/06/2025-02/7/2025, with Lancaster University Management School as the base venue.

Venues

- Oral Presentations in Lecture Theatre 15, Lancaster University Management School.
- Poster Presentations in the Foyer of Lancaster University Management School.
- Sponsors showcases in the Foyer of Lancaster University Management School.
- Catering (coffee, lunch, etc.) in the Foyer of Lancaster University Management School.
- Accommodation is available on campus (including accessible accommodation), and in addition to this, we encourage you to use public transport to/from/within Lancaster and to walk between venues (where possible).
- Other rooms in Lancaster University Management School have been reserved for any meetings you need to attend online or in person.

Conference meals

- Monday 30th of June 2025, Barbecue and drinks 7–10 pm at Health Innovation One.
- Tuesday 1st of July 2025, Dinner and drinks 7–10 pm at Lancaster House Hotel.

How to find us: https://www.lancaster.ac.uk/about-us/maps-and-travel/

Table 1. Schedule for day 1 Monday 30th of June 2025.

Time	Activity
Midday to 1pm	Lunch, registration & poster setup.
1.00-1.05 pm	Welcome from conference chair Dr John Hardy (Lancaster University, UK) and UKSB President Dr Adrian Boyd Ulster University, UK)
1.05-3.00 pm	**Session: Dental and Orthopaedic Biomaterials.** Session Chairs: Peter Dyer, OBE (University of Lancashire, UK) and Dr Timothy Douglas (Lancaster University, UK).

https://doi.org/10.5281/zenodo.16416539

1.05-1.35 pm	Prof. Maisoon Al-Jawad (University of Leeds, UK) **Alan Wilson Memorial Lecture:** Shining a light on Biomaterials in Dentistry.
1.35-1.45 pm	Dr Victor Villapun (University of Birmingham, UK) Rapid design of bioinspired alloys through conventional and additively manufacturing techniques.
1.45-1.55 pm	Dr Ian Smith (University of Manchester, UK) Incorporation Of Engineered Collagen Peptides Into 3D-Printable Hydrogels For Osteogenic And Adipogenic Mesenchymal Stem Cell Differentiation.
1.55-1.59 pm	Dr Nael Berri (University of Bath, UK) Repurposing Laboratory Plastic into Functional Fibrous Scaffolds via Green Electrospinning for Cell Culture and Tissue Engineering Applications.
1.59-2.03 pm	Bhuvaneshwari Anbazhagan (University of Manchester, UK) Engineering ECM-Enriched 3D Hydrogels for Enhanced Osteogenic Differentiation of Bone Marrow Mesenchymal Stem Cells.
2.03-2.07 pm	Daniel Kerr Baines (Lancaster University, UK) Effect of poly-γ-glutamic acid molecular weight on the properties of whey protein isolate hydrogels.
2.07-2.11 pm	Frances Hasson (Ulster University, UK) Advanced 3D Printing of PEKK/hydroxyapatite Composites via Fused Filament Fabrication (FFF) for Medical Implants.
2.11-2.15 pm	Arian McAllion (Ulster University, UK) Impact of Corrosion Study Parameters on the Degradation Rate of Magnesium Alloy.
2.15-2.19 pm	Ellamay McIlhatton (Ulster University, UK) Enhancing Corrosion Resistance of WE22 Magnesium Alloy with Calcium Phosphate Coatings for Resorbable Bone Fixation Applications.
2.19-2.23 pm	Amy Morgan (University of Sheffield, UK) A polyHIPE dermal scaffold featuring rete ridges for full-thickness wound healing.

https://doi.org/10.5281/zenodo.16416539

2.23-2.27 pm	Reshma McMullan (Ulster University, UK) 3D Printing of Polyaryletherketone (PAEK)/Apatite composites for lattice structures for orthopaedic implants.
2.27-2.42 pm	Prof. Rizwan Gul (University of Engineering and Technology, Peshawar, Pakistan) Effects of Different Crosslinking Techniques on UHMWPE/Antioxidants Blends Performance: A Path to Superior Service Life of Total Joint Replacements.
2.42-2.54 pm	Dr Yanghee Kim (University of Southampton, UK) Immunomodulatory phenotype transition following nanoclay phagocytosis in macrophages.
2.54-3.30 pm	Coffee & check-in collection & poster setup
3.30-5.00 pm	**Session: Early Career Researcher Takeover - Session 1** Session Chairs: Session Chair: Dr Tanveer Tabish (University of Oxford, UK) and Dr Timothy Douglas (Lancaster University).
3.30-3.42 pm	Dr Silviya Halacheva (University of Buckingham, UK) Trimethoxy silyl end-capped hyperbranched polyglycidol/polycaprolactone particle gels for cell delivery and tissue repair. Mechanical properties, biocompatibility and biodegradability studies.
3.42-3.46 pm	Nicola Kelly (University of Liverpool, UK) Novel Electrospun Materials for the Advancement of Lateral Flow Diagnostics.
3.46-3.50 pm	Arjan Sall (University of Birmingham, UK) Shape Memory Polymer-Enabled Minimally Invasive Blood Pressure Sensor: PCL-PDMS Polyurethane Integration via Photolithographic Microfabrication.
3.50-3.54 pm	Josh Fletcher (Lancaster University, UK) Resonant cavity enhanced photodetectors for non-invasive glucose detection.
3.54-3.58 pm	Moira Lorenzo-Lopez (University of Liverpool, UK). A Passive Nanorheological Tool to Characterise Hydrogels.

https://doi.org/10.5281/zenodo.16416539

3.58-4.02 pm	Joseph (Joe) Weightman (University of Birmingham, UK) Structural polymer as suspending media for lightsheet fluorescent microscopy.
4.02-4.06 pm	Georgios Mikalef (University of Birmingham, UK) Material Characterisation of Electroactive (AMPS-co-PEGDA) hydrogels.
4.06-4.10 pm	Skylar Rees (University of Aberystwyth, UK) Optimisation of Bioresorbable Implant Degradation with Machine Learning.
4.10-4.14 pm	Mariam Olabisi Ashimi (Queen Mary University of London, UK) Physio-mechanical Characterisation of Olive Stone Powder-Tapioca Starch Biocomposites for Sustainable Food Packaging.
4.14-4.18 pm	Genevieve Schleyer (University of Liverpool, UK) Development of an experimental model for quantifying the effect of cell monolayers on nanoparticle dynamics.
4.18-4.22 pm	Aziz A Alrwaili (University of Sheffield, UK) The molecular landscape of transformed and non-transformed cells in an engineered fibrous microenvironment.
4.22-4.26 pm	Mary Heim (University of Edinburgh, UK) Dual-Action Adenosine-Functionalized Scaffolds for Macrophage Reprogramming and Thyrocyte Support.
4.26-4.30 pm	Jess Hollett (University of Liverpool, UK) Development of an in vitro wound healing model for large conjunctival defects.
4.30-4.34 pm	Sertan Kiziloz (University of Brighton, UK) Optimising host response biology to advance wound dressing efficacy.
4.34-4.38 pm	Mingda Lu (University of Sheffield, UK) Replicating the tendon-to-bone interface through the creation of electrospun scaffolds with chemical and mechanical gradients.
4.38-4.42 pm	Nevena Slavova (University of Sheffield, UK) Tissue Engineered Vascular Grafts.
4.42-5.07pm	Dr Jessica Senior (University of Huddersfield, UK)

https://doi.org/10.5281/zenodo.16416539

	Larry Hench Young Investigators Prize Lecture: Biomaterials in Translation – Impact on Bioengineering Wound Models for Training and Education.
5.00-6.00 pm	Posters/refreshments.
5.10-5.40 pm	UKSB AGM.
6.00-7.00 pm	Break, check in and go to Health Innovation One (Lancaster Medical School)
7.00-10.00 pm	Dinner at Health Innovation One.

Table 2. Schedule for day 2 Tuesday 1st of July 2025.

Time	**Activity**
9-9.30 am	Coffee, tea and biscuits
9.30-11.03 am	**Session: Early Career Researcher Takeover - Session 1** Session Chairs: Dr Jessica Senior (University of Huddersfield, UK) and Dr Naval Singh (Lancaster University, UK).
9.30-9.42 am	Dr Tanveer Tabish (University of Oxford, UK) Nitric oxide releasing materials (NORMs) for cardiovascular therapeutics.
9.42-9.46 am	Hilal Mete Gunaydin (University of Birmingham, UK) Development and Characterization of Multi-Material Hydrogels for Mimicking Skin Layers.
9.46-9.50 am	Federico Delle Fave (University of Rome Tor Vergata, Italy) Effects of LDH-treated surfaces on biofilm formation.
9.50-9.54 am	Mehmet Gunen (University of Sheffield, UK) Development of an Antifungal Smart Biomaterial with Engineered Microenvironments for Corneal Regeneration.
9.54-9.58 am	Rosie Hood (University of Sheffield, UK) Decalcifying and antibacterial bilayer grafts for vascular tissue engineering.
9.58-10.02 am	Cadhan O'Garra (University of Liverpool, UK) Fabrication of Antibacterial NO Releasing Cellulose Acetate Nanofibers.

https://doi.org/10.5281/zenodo.16416539

10.02-10.06 am	Grace Ritchie (University of Liverpool, UK) Real-time label-free exploration of the dynamics and interactions of bacteriophages.
10.06-10.10 am	Imogen Walker (University of Liverpool, UK). Development of Inhaled Therapeutic Polymeric Nanoparticles for the Treatment of Respiratory Infections.
10.10-10.14 am	Louis Johnson (University of Sheffield, UK) Testing a GDNF-eluting conduit in a mouse model of nerve injury.
10.14-10.18 am	Nimeet Desai (University of Liverpool, UK) Mucoadhesive Hydrogel-Nanofiber Composites for Sustained Ocular Chemotherapy in Conjunctival Melanoma.
10.18-10.22 am	Ziyue Su (University of Liverpool, UK) Development of Delivery Platforms for RNA-Based Immunotherapy in Breast Cancer.
10.22-10.26 am	Ece Tezsezen (University of Liverpool, UK) Engineering Magnetic nanobots for Boron Neutron Capture Therapy Applications.
10.26-10.30 am	Connor Proctor (University College London, UK) 2D and 3D Printed Cobalt Phosphate Bioactive Glass-Polycaprolactone (CoPBG-PCL) Scaffolds for HIF-1α directed Diabetic Bone Regeneration.
10.30-10.34 am	Patricia Santos (University of Manchester, UK) Formulating L-alanine-based poly(ester amide) inks for 3D printing and scaffold-guided tissue regeneration.
10.34-10.38 am	Lukas Weber (University of Manchester, UK) Melt electrowriting of a bacterial polyester for shoulder tendon repair.
10.38-11.04 am	Coffee, tea and biscuits.
11.05 am - 1.10 pm	**Session: Advanced Therapeutics - Part 1** Session Chairs: Dr Sandra Borbor-Sawyer (Buffalo State University, USA) and Dr Naval Singh (Lancaster University, UK).

https://doi.org/10.5281/zenodo.16416539

11.05-11.22 am	Prof. Vitaliy Khutoryanskiy (University of Reading, UK) Galleria mellonella larvae as an in vivo model for evaluating antimicrobial biomaterials.
11.22-11.34 am	Dr Francesco Giorgi (University of Liverpool, UK) Multi-Layer Infection-on-a-Chip Platform for Real-Time Evaluation of Antimicrobial Therapies.
11.34-11.44 am	Dr Vahid Heravi Shargh (University of Liverpool, UK) NO-releasing liposomal formulations for treatment of respiratory infections.
11.44-11.56 am	Dr Svetlana Zolotovskaya (University of Dundee, UK) Advanced antibacterial surfaces by integrating laser surface structuring with biopolymer composite coating.
11.56-12.08 pm	Dr Jenny Shepherd (University of Leicester, UK) Perivascular biodegradable mesh for the controlled delivery of the corticosteroid dexamethasone for treatment of vein graft disease.
12.08-12.18 pm	Dr Dan Baiocco (University of Birmingham, UK) Biodegradable and Biocompatible Plant-based Chitosan-Pyrophosphate Micropowders for Potential Haemostatic applications.
12.18-12.28 pm	Dr Caroline Taylor (University of Sheffield & University of Leeds, UK) Versatile Twin Layer Macromolecular Fibres for Advanced Tissue Engineering Applications.
12.28-12.40 pm	Dr Elisa Mele (Loughborough University, UK) Electrospinning of Poly(lactic acid) for the generation of bioactive materials.
12.40-1.10 pm	Prof. Manuel Salmeron-Sanchez & Dr Graham Day (University of Glasgow, UK) **Biomaterials Advances Keynote Lecture:** Engineered biomaterials for regeneration and mechanobiology.
1.10-1.40 pm	Lunch
1.10-1.40 pm	UKSB Council meeting (Lecture Theatre 19, Lancaster University Management School).
1.40-3.05 pm	**Session: Advanced Therapeutics - Part 2**

https://doi.org/10.5281/zenodo.16416539

	Session Chair: Dr Richard Mort (Lancaster University, UK).
1.40-1.57 pm	Prof. Ruman Rahman (University of Nottingham, UK) Intraoperative drug delivery via an injectable hydrogel confers survival benefit against childhood hindbrain tumour xenografts.
1.57-2.09 pm	Dr Sandra Borbor-Sawyer (Buffalo State University, USA) In Vitro and In Vivo Evaluation of LHRH-Conjugated Drugs for Targeted Treatment of Triple-Negative Breast Cancer.
2.09-2.21 pm	Dr Arathyram Ramachandra Kurup Sasikala (University of Bradford, UK) PiezoMagnetic Nanoparticles (PMNPs): A Multimodal, Non-Invasive Theranostic Platform for Post-Surgical Osteosarcoma Therapy and Bone Regeneration.
2.21-2.31 pm	Dr Abhinav Thareja (University of Birmingham, UK) Mechanotransduction of T-Cell receptor and mechanosensitive ion-channels via remote magnetic field application to modulate human T-cell activation in-vitro.
2.31-2.48 pm	Prof. Steve Rimmer (University of Bradford, UK) Smart Polymers in the fight against anti-microbial resistance.
2.48-3.05 pm	Prof. Martin Desimone (Universidad de Buenos Aires, Argentina) Exploring Novel Biomaterial Strategies for Tissue Engineering and Drug Delivery.
3.05-3.25 pm	Coffee, tea and biscuits
3.25-5.18 pm	**Session: Advanced Therapeutics - Part 2** Session Chair: Dr Jenny Shepherd (University of Leicester, UK)
3.25-3.42 pm	Prof. Sub Reddy (University of Central Lancashire, UK) High-Affinity nanoMIPs: Synthetic Antibody Alternatives for Diagnostics.
3.42-3.54 pm	Dr Helen Willcock (Loughborough University, UK) Polymer particles for sensing and imaging.
3.54-4.06 pm	Dr Samit Chakrabarty (University of Leeds, UK) Sharper Signals, Smarter Wearables: Engineering the Future of Biosensing.

https://doi.org/10.5281/zenodo.16416539

4.06-4.18 pm	Dr Tim Douglas (Lancaster University, UK) **Provocation:** Two figures "behind the scenes" Languages Other Than English (LOTEs) and the hidden, unpublished stories of scientists.
4.18-4.48 pm	Phil Smith, MBA (4D Biomaterials, UK) **Industry Keynote Lecture:** Commercialising a novel biomaterial.
4.48-5.18 pm	Prof. Sarah Cartmell (University of Manchester, UK) **UKSB President's Prize Lecture:** Biomaterials, 3D Co-Cultures and Medical Devices: Translation and Tips.
5.18-6.00 pm	Posters/refreshments.
6.00-7.00 pm	Break
7.00 pm onwards	Dinner at Lancaster House Hotel.

Table 3. Schedule for day 3 Wednesday 2nd of July 2025.

Time	**Activity**
9-9.30 am	Coffee, tea and biscuits.
9.30-11.26 am	**Session: Advanced Engineering Materials - Part 1** Session Chairs: Dr Pooya Davoodi (Keele University, UK) and Dr John Hardy (Lancaster University, UK).
9.30-9.42 am	Dr Nazia Mehrban (University of Bath, UK) Designing 'smart' biomaterials: from regenerative medicine to integrative envelopes for robotic implants.
9.42-9.52 am	Dr. Gildacio Chaves Filho (University of Manchester, UK) Carrageenan-Gel-MA Hydrogels for Bone Tissue Engineering Scaffolds.
9.52-10.02 am	Dr Vera Citro (University of Liverpool, UK) Layered Biofabrication of Trabecular Meshwork Analogues Using MEW and Hydrogel-Based Cell Printing.

https://doi.org/10.5281/zenodo.16416539

10.02-10.14 am	Dr James Armstrong (University of Bristol, UK) Design of Biomaterials for Bioprinting and Engineering Neurovascular Tissues.
10.14-10.26 am	Prof. Rebecca Killick (Lancaster University, UK) Using Machine Learning for reducing training in mice experiments.
10.26-10.56 am	Amy Beale (Replacing Animal Research, UK) **Industry Keynote Lecture:** Furthering Replacement.
10.56-11.26 am	Dr Ulrike Kauscher Pinto (Wiley) **Industry Keynote Lecture:** How to Publish with Impact.
11.26-11.50 am	Coffee, tea and biscuits.
11.50 am - 1.35 pm	**Session: Advanced Engineering Materials – Part 2** Session Chairs: Prof. Ying Yang (Keele University, UK) and Dr Jemma Kerns (Lancaster University, UK).
11.50-12.02 pm	Dr Steve Hall (Lancaster University, UK) The Development of Drug Delivery Biomaterials for the Treatment of Cytotoxic Snakebite Envenoming.
12.02-12.14 pm	Dr Tom Robinson (University of Birmingham, UK) Bioactive Polysaccharide-Protein Interactions Inhibit Fibrosis.
12.14-12.24 pm	Dr Thomas Fruleux (University of Galway, Galway, Ireland) Development of cellulose-based membrane for artificial lung applications.
12.24-12.34 pm	Dr Zoe Schofield (University of Birmingham, UK) Alcohol Induced Dancing Particles.
12.34-12.46 pm	Dr Tim Douglas (Lancaster University, UK) Whey Protein Isolate (WPI): a versatile, low cost biomaterial as a coating, scaffold and as a drug delivery vehicle.
12.46-12.58 pm	Dr Ketan Pancholi (Robert Gordon University, Aberdeen, UK) Harnessing Ultrasound for Biomaterial Design: Sono-crystallisation of Hydrophobic APIs and Antibodies.
12.58-1.10 pm	Dr Pooya Davoodi (Keele University, UK)

https://doi.org/10.5281/zenodo.16416539

	A Photocrosslinkable Granular Hydrogel–Chondrocyte Spheroid Composite for Enhanced Cartilage Repair.
1.10-1.15 pm	Patrick Heasman (Schrödinger) **Industry Flash Presentation:** Designing the next generation of materials starts at the molecular level.
1.15-1.35 pm	Prizes (Adrian Boyd (Ulster University, UK) and Katie Morton (RSC)) and closing comments (Adrian Boyd and John Hardy).
1.30-2.15 pm	Lunch.

https://doi.org/10.5281/zenodo.16416539

Abstracts

https://doi.org/10.5281/zenodo.16416539

UKSB prize winners' abstracts

https://doi.org/10.5281/zenodo.16416539

Alan Wilson Memorial Lecture:
Shining a light on Biomaterials in Dentistry.

Al-Jawad, M. [a,*]

[a] School of Dentistry, Faculty of Medicine and Health, University of Leeds, Leeds, UK.

* Corresponding author(s) e-mail(s): M.Al-Jawad@leeds.ac.uk

Abstract

Synchrotron x-rays are a powerful tool to study the physico-chemical properties of hard tissues and biomaterials. In this talk I will present my work spanning two decades using synchrotron techniques to study the hierarchical structure of dental enamel in health and disease, and to develop innovative biomaterials for repair and replacement of dental enamel lost through caries (tooth decay), erosion, or dental disease.

Biosketch

Maisoon Al-Jawad is Professor of Biological Physics and Biomineralisation within the School of Dentistry at the University of Leeds. She is a physicist by training, and her area of expertise is in the highly interdisciplinary research fields of biomineralisation and biomimetic materials, at the interface of physics, materials, biology, biomedicine and dentistry. She combines in-house biophysical techniques with use of international advanced science facilities (synchrotron and neutron scattering techniques) to drive forward our understanding of hard tissue structures at multiple length-scales and interactions at protein-mineral interfaces to enable translation of oral and musculoskeletal sciences to innovative clinical applications.

Photo. Professor Maisoon Al-Jawad

References

1) LeBlanc, A.R.H., et al. *Nature Ecology & Evolution*. **2024**, 8, 1711-1722.
2) Deng X, et al. *Materials Today Bio*. **2021**, 11, 100119.
3) Elsharkawy S, et al. *Nature Communications*. **2018**, 9, 2145.

https://doi.org/10.5281/zenodo.16416539

Larry Hench Young Investigators Prize Lecture: Biomaterials in Translation – Impact on Bioengineering Wound Models for Training and Education.

Senior, J. [a,*]

[a] Department of Pharmacy, University of Huddersfield, Huddersfield, UK.

* Corresponding author(s) e-mail(s): J.J.Senior2@hud.ac.uk

Abstract

Wound care specialists are faced with limited resources that enable them to safely and effectively develop their debriding and wound management skills. Current training resources include citrus peels and cadavers, either exhibiting poor mechanical resemblance to wounds in live humans or lacking in supply, which subsequently causes a significant risk when translation to patients is inevitably mismatched. This talk will guide you through our recent advancements in bioengineering a range of true-to-life wound simulations with various aetiologies. Our models encompass a range of skin tones, removable slough, and debridable skin necrosis using 100% natural and sustainable biomaterials. We have further established wound tear simulations, diabetic foot ulcer models, and incorporated other anatomical features including hair, fat and bone to enhance realism and further educate the end-user. We have successfully supplied model units to many educational institutions, academies, NHS trusts, and wound care businesses worldwide, improving awareness, training and education opportunities and allowing the demonstration of wound care products. We envisage that our wound models will help contribute to the knowledge and confidence of our wound care workforce in a cost-effective manner, ultimately leading to improved patient outcomes.

Biosketch

Jessica Senior was awarded a bachelor's in medical biology, a master's in pharmaceutical and analytical, and PhD in tissue engineering, before postdoctoral research. She returned to Huddersfield as a Research and Teaching Fellow in 2021, became a lecturer in Pharmaceutics in 2023, and was promoted to Senior Lecturer in 2024.

Photo. Dr Jessica Senior.

References

1) Senior, J., *et al. In Vitro Models*. **2024**, 3, 81-89.
2) Senior, J., *et al. Advanced Functional Materials*. **2019**, 29, 1904845.

https://doi.org/10.5281/zenodo.16416539

UKSB President's Prize Lecture:
Biomaterials, 3D Co-Cultures and Medical Devices: Translation and Tips.

Cartmell, S. [a,*]

[a] School of Engineering, The University of Manchester, Manchester, UK.

* Corresponding author e-mail: sarah.cartmell@manchester.ac.uk

Photo. Prof. Sarah Cartmell

Abstract: I am very honoured to be recipient of the UKSB President's Award. UKSB is such an important society for our community and has helped me greatly through my career to network, share and gather ideas and facilitate mentoring that has helped place me in the position I am today. The presentation I will give will take you through key moments in my career and offer top tips for those considering a similar path. My career started with my PhD in phosphate-based glass research at Liverpool University and my PDRA in bioreactor design and coculture in orthopaedic tissue engineering at GeorgiaTech, Atlanta USA. I will describe starting a new PDRA and then new career journey as independent lecturer and senior lecturer at Keele University with more research on bioreactors, 3D tissues, and mechanotransduction. I will also describe my move to move to Manchester University in 2010 as a Reader and then Professor, where I continued more bioreactor design, electrical stimulation work, translation of medical devices and patent filing. In particular, the ongoing journey of tendon repair and electrical stimulation products will be described along with running an active Centre for Doctoral Training in Biomedical Materials. Recent collaboration with oncologists and biologists to translate the 3D tissue engineering concepts for early cancer detection and toxicology models will also be described.

Biosketch: Sarah is Vice Dean and Head of School of Engineering at the University of Manchester. Sarah was appointed Professor of Bioengineering at the University of Manchester in 2014 in the School of Materials after joining Manchester in 2010. She received a B.Eng. in Materials Science with Clinical Engineering and a Ph.D. degree in Clinical Engineering from the University of Liverpool in 1996 and 2000, respectively and then furthered her studies at GeorgiaTech, Atlanta for two years as a postdoctoral research fellow. She joined Keele University in 2002 where she continued her postdoctoral studies until obtaining a Lecturership

https://doi.org/10.5281/zenodo.16416539

and then a Senior Lecturer position in orthopaedic tissue engineering in 2008. Sarah was head of the Department of Materials 2019-2023 at the University of Manchester and is now a Senate member due to her Head of School role. Sarah was the UK Biomedical Materials champion for The Royce Institute of a £235 million UK government investment for advanced materials 2017-21. In this activity, she has created an interaction of a 200 strong stakeholder working group of UK academics and industry. She has prepared and led community day and strategic working group meetings. In this role she has led the creation of UK landscape activity in the biomedical materials area and has liaised with many UK and international academics and industry. Sarah has been awarded over 60 grants, >£14 million of grants as lead PI and >£26 million as both PI and CI from over 20 different competitive sources ranging from government, charity and industry. She is President of the UK Tissue and Cell Engineering Society. She has over 100 publications with over 6500 citations, 200 published abstracts and has given over 100 invited keynotes in the field of tissue engineering and regenerative medicine. All these publications have a common theme of orthopaedic engineering with a particular focus on X-Ray evaluation of tissue engineering constructs and biomaterials and the response of orthopaedic cells to a variety of stimuli such as mechanical forces, electrical stimulus, statins and a variety of different novel materials to support their growth into the correct tissue type/shape. She has recently created a spin off company named Retendon Ltd to translate her tendon repair product portfolio. She has been a review panel member for the government funding such as the BBSRC, MRC and Innovate UK and has been an external evaluating panel member and UK expert advisor to the European Union as a member of The European Cooperation in the field of Scientific and Technical Research (COST) in the ‘Biomedicine and Molecular Biosciences’ Domain. She is also a reviewer for ERC, EU H2020 Marie Skłodowska Curie Award Individual Fellowships and Integrated Training Networks, Natural Sciences and Engineering Research Council of Canada, Irish Research Council, Czech Science Foundation and Israel Science Foundation. She is the Speciality Chief Editor for Regenerative Technologies, a section of Frontiers in Medical Technology Journal and is an associate editor for ‘Science and Technology of Advanced Materials (STAM)’.

References

1) Ker, D.F.E., *et al*. *Frontiers in Bioengineering and Biotechnology*, **2024**, 12, 1489256.
2) Xue, R., *et al*. *Frontiers in Medical Technology*, **2024**, 6, 1269861.

https://doi.org/10.5281/zenodo.16416539

Industry abstracts

https://doi.org/10.5281/zenodo.16416539

Industry Keynote Lecture: Commercialising a novel biomaterial.

Smith, P. [a,*]

[a] 4D Medicine Ltd, MediCity, D6 Thane Road, Nottingham, NG90 6BH, UK.

* Corresponding author(s) e-mail(s): p.smith@4dbiomaterials.co.uk

Abstract

The generation of impact from university research has become a political priority in the UK over recent years. With world-leading academic institutions and highly supportive tax relief schemes for early-stage investors, there are growing expectations for what the UK should be achieving in this space. However, the survival rate for university spinouts is notoriously low as there are many challenges to be faced on the journey to a successful business exit or share listing. In this lecture, a veteran technology-transfer entrepreneur highlights some of the key considerations for people setting out on such a journey, drawing on his recent experience of commercialising a novel biomaterial.

Biosketch

Phil Smith has been involved in managing University spinouts for over 15 years, having previously worked in materials-related product development, research and management roles in the aerospace and utility industries. Since April 2020, Phil has been the CEO of 4D Medicine Ltd, a spin-out from the Universities of Birmingham and Warwick, commercialising a range of novel degradable biomaterials in the form of implantable medical devices.

Phil became a Chartered Engineer in 1998 after previously being awarded a BSc in Materials Science and Technology from Brunel University of London and an MBA from the University of Warwick.

Photo. Phil Smith, MBA.

https://doi.org/10.5281/zenodo.16416539

Industry Keynote Lecture: Furthering Replacement.

Beale, A [a,*]

[a] Replacing Animal Research, UK.

* Corresponding author(s) e-mail(s): amy@replacinganimalresearch.org.uk

Abstract: The exploration and consideration of alternatives to animal use in scientific research and testing is not just an important element of responsible and ethical research practice, but also a legal requirement under the Animals (Scientific Procedures) Act 1986 (ASPA). The 3Rs Principles of Replacement, Reduction and Refinement in UK and EU legislation, requires alternative approaches replacing or avoiding the use of animals in experiments to be used wherever scientifically possible. However, implementation of the 3Rs is not fulfilled as it should be. Replacement is often not thoroughly considered, and scepticism about its achievability is widespread. A 2023 report on the role of review and regulatory approvals processes for animal research in supporting the implementation of the 3Rs concluded that 'Replacement does not seem to be covered well by any of the review processes' and that alternatives are rarely suggested by project licence reviewers.[1] Elsewhere reviews of Project Licences approved and issued by the Home Office regulator, provide evidence that researchers are not adequately exploring opportunities for animal-free options.[2] Replacement can be more challenging to address in basic and applied research due to the diverse range of methods and approaches available across disciplines to answer research questions. This is compounded by familiarity with established in vivo approaches. Replacing Animal Research have been working with the scientific community for over 50 years to help further the replacement of animals in medical research. Today the charity supports scientists and research reviewers with tools and training to help address gaps and opportunities to implement replacement more robustly, for example by using the Replacement Checklist[3]. Replacing Animal Research provide research grants, publish a peer-reviewed journal in partnership with SAGE Publishing[4], offer training on finding and reviewing replacements[5], and collaborate with others to explore issues such as Animal Bias in publishing[6]. Alongside work to support scientific research other strategic workstreams of the charity, we influence education and shape policy to help create a world where human-relevant research methods are the norm in biomedical research.

https://doi.org/10.5281/zenodo.16416539

Biosketch

Amy Beale was awarded a bachelor's in equine science and a PGCE in secondary science education. After over 15 years teaching science in various schools across the UK and a stint working at RSPCA Education she started work for Replacing Animal Research (then Fund for the Replacement of Animals in Medical Experiments) in 2018.

Photo. Amy Beale.

References

1) The Role of review and regulatory approvals processes for animal research in supporting implementation of the 3Rs (2023), https://nc3rs.org.uk/role-review-and-regulatory-approvals-processes-animal-research-supporting-implementation-3rs-2023 (accessed June 2025).

2) Animals in Science Committee. Antibody report by the Project Licence Strategic Review subgroup (2022) (accessible), https://www.gov.uk/government/publications/review-of-antibody-licences-report-by-the-animals-in-science-committee/antibody-report-by-the-project-licence-strategic-review-subgroup-accessible (accessed June 2025).

3) J. Jukes, Beale A and Camp C, Alternatives to Laboratory Animals, 2025, volume 53, issue 2, page. 72

4) ATLA https://journals.sagepub.com/home/atl (accessed June 2025).

5) Searching for Replacements, https://replacinganimalresearch.org.uk/resources/searching-for-alternatives/ (accessed June 2025)

6) Coalition to illuminate and Address Animal Methods Bias, https://www.animalmethodsbias.org/about (accessed June 2025)

https://doi.org/10.5281/zenodo.16416539

Industry Keynote Lecture: How to Publish with Impact

Kauscher Pinto, U. [a,*]

[a] Wiley-VCH GmbH, Weinheim, Germany.

* Corresponding author(s) e-mail(s): ukauscherp@wiley.com

Abstract

The publishing process is an integral part of building a career as a researcher. Recently, scientific publishing has undergone many changes and is continuing to develop rapidly. While high publishing standards, scientific integrity and speedy publication remain top priorities, important new developments like the use of GenAI are now also garnering greater attention.

This session offers an insider's perspective on scientific publishing, with a focus on editorial workflows, peer review, and strategies for successful manuscript publication. Dr. Kauscher Pinto will explore the value of publishing research, the editor's role in shaping scientific communication, and the key stages of the peer review process. Attendees will gain practical guidance on crafting impactful titles, abstracts, and cover letters to boost the visibility and influence of their work. Designed for both early-career and established researchers, this talk offers actionable insights into navigating the publishing landscape and effectively communicating research to a global audience.

Biosketch

Ulrike Kauscher Pinto studied chemistry and earned her PhD in organic and supramolecular chemistry at the Universität Münster (Germany). She was then a postdoctoral DFG fellow at Imperial College London (UK), where she focused on bioengineering of extracellular vesicles and ran a cryoTEM service for her colleagues. After having worked for 5 years as an editor for Wiley's *Advanced* Portfolio (Advanced Materials, Advanced Functional Materials, Advanced Healthcare Materials etc.), she is now the Editor-in-Chief for two journal titles: ChemNanoMat and ChemPlusChem.

Photo: Dr Ulrike Kauscher Pinto.

Faculty abstracts

In Vitro and In Vivo Evaluation of LHRH-Conjugated Drugs for Targeted Treatment of Triple-Negative Breast Cancer

Sandra M. Borbor-Sawyer*[a,b,c], John D. Obayemi [b,d], Ali A. Salifu [b,d], Chukwudalu C. Nwazojie [c], Vanessa O. Uzonwanne [b], Olushola S. Odusanya [e], and Winston O. Soboyejo [b,c,d].

a. Department of Biology, State University of New York, Buffalo State University, Buffalo, New York, 14222, USA

b. Department of Mechanical and Materials Engineering, Worcester Polytechnic Institute, Worcester, MA 01609, USA

c. Department of Materials Science and Engineering, African University of Science and Technology, Km 10 Airport Road, Abuja, 900107, Nigeria

d. Department of Biomedical Engineering, Gateway Park Life Sciences Center, 60 Prescott Street, Worcester Polytechnic Institute (WPI), Worcester, MA 01605, USA

e. Biotechnology and Genetic Engineering Advanced Laboratory, Sheda Science and Technology Complex (SHESTCO), Abuja, 900107, Nigeria

* Corresponding author(s) e-mail(s): borborsm@buffalostate.edu

Prodigiosin and paclitaxel were conjugated with Luteinizing Hormone-Releasing Hormone (LHRH) to enable targeted treatment of triple-negative breast cancer (TNBC). These model drugs were encapsulated within Poly(Lactic Acid-Glycolic Acid) (PLGA) based drug delivery vehicles (DDVs). Physicochemical characterization was conducted to evaluate their properties. The controlled release of the drugs was evaluated in vitro under normal and hyperthermic conditions (37°C, 41°C, and 44°C). Biocompatibility and therapeutic efficacy were assessed through in vitro cytotoxicity assays and in vivo

Introduction

Triple-negative breast cancer (TNBC) remains a clinical challenge due to its aggressiveness and poor response to conventional chemotherapy. We present a biomaterials-based strategy for localized and targeted drug delivery using biodegradable drug delivery vehicles (DDVs). These DDVs were engineered to minimize toxicity while enhancing site-specific therapeutic effects following tumor resection.

Materials and methods

models, highlighting the potential of this targeted approach in cancer therapy.

Results

The drug delivery vehicles (DDVs) exhibited release kinetics that aligned with the Korsmeyer-Peppas model. In vitro studies showed that drug-loaded formulations caused significant cytotoxicity in triple-negative breast cancer (TNBC) cells. In vivo treatment with these LHRH-based drug formulations significantly prolonged survival and reduced local tumor recurrence following surgical resection.

Discussion

This study highlights the potential of targeted delivery systems, specifically PGS-LHRH and PTX-LHRH, for treating triple-negative breast cancer (TNBC) cells. In vitro analysis indicates that these formulations are effective at reducing TNBC cell viability, suggesting enhanced specificity due to LHRH. Additionally, in vivo results show that these DDVs can effectively prevent locoregional recurrence of TNBC after surgical resection. These findings build upon prior research and lay a strong foundation for innovation in translational biomaterials in oncology.

Figure.

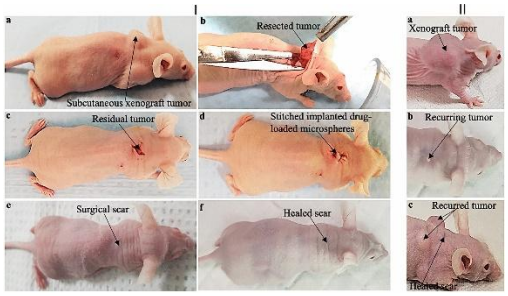

Acknowledgements

For financial support we thank:

- World Bank
- Pan-African Materials Institute (PAMI)
- African Union Commission
- Worcester Polytechnic Institute

Reference

S. M. Jusu, J. D. Obayemi, A. A. Salifu et al., *Sci. Rep.,* 2020, 10, 14188. https://doi.org/10.1038/s41598-020-71129-0

Sharper Signals, Smarter Wearables: Engineering the Future of Biosensing.

Chakrabarty, S. [a,*]

[a] School of Biomedical Sciences, University of Leeds, Leeds LS2 9JT, UK.

* Corresponding author(s) e-mail(s): S.Chakrabarty@leeds.ac.uk

Introduction

Wearable biosensors are increasingly central to healthcare, rehabilitation, and human-machine interfacing. However, challenges remain in capturing high-quality, interpretable signals in real-world conditions. This presentation will explore a research programme led by Dr. Samit Chakrabarty that addresses these challenges through the integration of signal processing, neurophysiology, and materials science. The seminar draws on three key studies that collectively advance the fidelity, resolution, and physiological insight of surface electromyography (sEMG) in wearable systems.

Materials and Methods

The first strand of this work introduces the Filter and Aggregate Synchrosqueezed Transform (FAST), a novel signal processing method that enhances time-frequency resolution by aggregating multiple synchrosqueezed transforms. FAST enables the detection of subtle, transient features in biosignals that are often lost using conventional techniques [1].

The second strand focuses on the non-invasive detection of muscle fatigue and neural compensation, using sEMG to quantify physiological adaptations during fatigue. This work provides a framework for interpreting changes in muscle activity over time and under load [2].

The third strand involves the development of flexible, biocompatible electrodes using conductive nanocomposites. These materials are designed to improve skin conformity and signal stability. While not used in the FAST or fatigue studies, they represent a parallel effort to enhance the physical interface of wearable systems.

Conceptually, this work is informed by the high-density, stretchable sEMG electrode system developed by Yang et al. [3], which demonstrates the potential of conformable, long-term wearable arrays for monitoring muscle stress and fatigue. Their findings provide a valuable reference point for designing future

wearable systems that combine material innovation with physiological insight.

Results

Across these studies, the integration of advanced signal processing and physiological insight has led to improved detection of muscle activation patterns, fatigue-related changes, and transient frequency shifts in sEMG signals. The development of novel electrode materials complements these findings by addressing the mechanical and electrical challenges of long-term wearable use.

Discussion

This seminar-style presentation highlights a cohesive research trajectory aimed at engineering smarter, more adaptive wearable biosensing systems. By combining innovations in signal analysis, physiological modelling, and materials engineering, Dr. Chakrabarty's work contributes to the development of wearable technologies that are not only more robust and accurate, but also more informative about the underlying neural mechanisms they aim to monitor.

Acknowledgements

For financial support we thank the Wings for Life foundation, BBSRC and the University of Leeds.

References

1) Desai, A., Richards, T., Chakrabarty, S., TechRxiv, 2021. https://doi.org/10.36227/techrxiv.15177819.v1
2) Zhao, B., Charoonsrisawad, K., Ichiyama, R., & Chakrabarty, S. (2025). Cambridge Open Engage. doi:10.33774/coe-2025-j3v1z
3) Yang, Y., et al., Nature Communications, 2023, 14, 6942. https://www.nature.com/articles/s41467-023-42149-x

A Photocrosslinkable Granular Hydrogel–Chondrocyte Spheroid Composite for Enhanced Cartilage Repair

Atwal, A.[1], Mahnavi, A.[1], Forsyth, N.R.[1,2], Snow, M.[3], Davoodi, P.[1,2]

[1] Guy Hilton Research Centre, Keele University, Staffordshire ST4 7QB, UK

[2] Vice Principals' Office, University of Aberdeen, Kings College, Aberdeen AB24 3FX, UK

[3] The Robert Jones and Agnes Hunt Hospital, Oswestry, Shropshire SY10 7AG, UK

* Corresponding author(s) e-mail(s): p.davoodi@keele.ac.uk

Introduction

Cartilage defects present a significant clinical problem due to their limited capacity for self-repair, often leading to osteoarthritis. Autologous chondrocyte spheroid therapy (Spherox) shows potential but faces challenges such as slow production, weak integration, and poor mechanical properties. Hydrogels offer ECM-mimetic properties and minimally invasive delivery [1], however, traditional bulk hydrogels often exhibit nanoporous architectures that impede cellular infiltration [2]. To overcome these limitations, we have developed a photopolymerizable granular hydrogel system designed to incorporate chondrocyte spheroids, aiming to facilitate enhanced cell migration and support endogenous tissue repair mechanisms.

Materials and methods

Gelatin, hyaluronic acid (HA), and platelet (PL) lysate were functionalized with methacryloyl groups using methacrylic anhydride. The resulting polymers were dissolved in a photoinitiator solution (Irgacure 2959), loaded into a syringe, and exposed to UV light (λ = 365 nm) for 10 seconds to achieve partial crosslinking, which was then extruded through a series of syringes (18G to 30G) to fragment the bulk hydrogel into variously sized microparticles. Chondrocyte spheroids were produced using microwell arrays and mixed with the granular hydrogel before photo-annealing. The system was thereafter characterised for mechanical and biochemical properties.

Results

The granular hydrogel system was successfully generated through partial crosslinking, mechanical fragmentation, centrifugation-mediated jamming, and photo annealing (Fig. 1a). Varying the microparticle size modulated the porosity of the hydrogel, leading to downstream effects on cell behaviour. Relative to the bulk hydrogel, granular hydrogels demonstrated enhanced cell proliferation and increased tissue deposition, including aggrecan,

collagen type II, and glycosaminoglycans (GAGs) (Figure 2b–c).

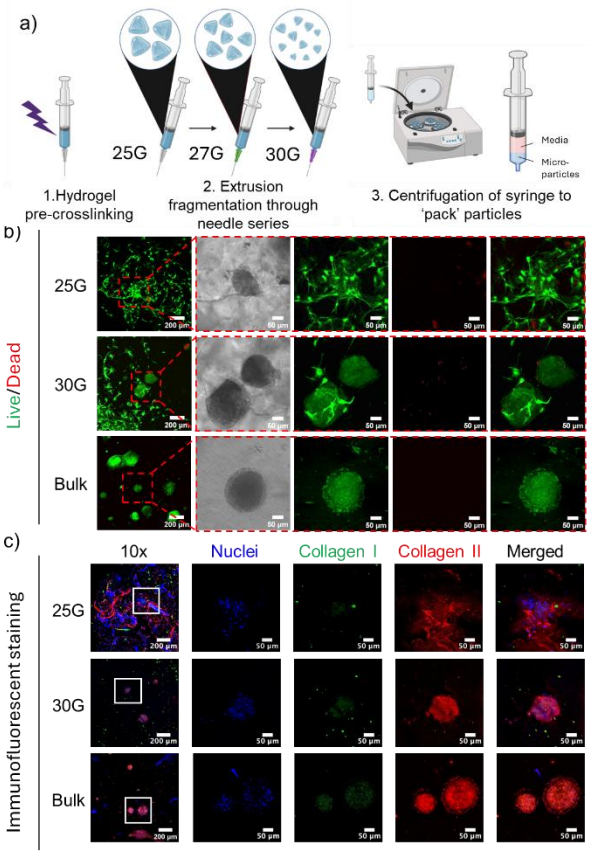

Figure 1. A) Schematic overview of system fabrication. B) Live/Dead staining after 31 days of culture. C) Immunofluorescent staining for cartilage-specific protein markers.

Discussion

In contrast to conventional bulk hydrogels, whose porosity is constrained by crosslinking density and polymer concentration, the designed granular system forms an interconnected microporous network via interstitial spaces between packed microgels. This structure is modulated by microparticle size and the degree of jamming induced through centrifugation. Rheological analysis showed that the granular hydrogel exhibits shear-thinning and self-recovery behaviour, supporting its suitability for minimally invasive arthroscopic delivery. *In vitro* and *ex vivo* studies demonstrated that the system facilitates cell infiltration, spheroid outgrowth, and neotissue formation characteristic of hyaline cartilage. Notably, the granular hydrogel enables decoupling of matrix stiffness from microporosity, offering greater control over the cellular microenvironment.

Acknowledgements

We thank North Staffordshire Medical Institute for funding the project and Keele University for funding PhD studentships.

References

[1] A. Atwal, T. P. Dale, M. Snow, N. R. Forsyth, P. Davoodi. Adv Colloid Interface Sci, 103030, 2023.

[2] H. Lee, D. Mooney, M. Levenston, O. Chaudhuri, *Nature Mater* 1243–1251 2017.

Exploring Novel Biomaterial Strategies for Tissue Engineering and Drug Delivery.

Desimone, M.F. [a, b]*

[a] Universidad de Buenos Aires, Consejo Nacional de Investigaciones Científicas y Técnicas (CONICET), Instituto de Química y Metabolismo del Fármaco (IQUIMEFA), Facultad de Farmacia y Bioquímica, Buenos Aires, Argentina.

[b] Instituto de Ciências Biológicas (ICB), Universidade Federal do Rio Grande - FURG, Rio Grande, RS, Brazil.

* Corresponding author(s) e-mail(s): desimone@ffyb.uba.ar

Introduction

The pursuit of advanced biomaterial strategies is central to revolutionizing tissue engineering and drug delivery, tackling persistent limitations in regenerative medicine and targeted therapeutics. There is an increasing medical need for the development of new materials that could replace damaged organs, improve healing of critical wounds or provide the environment required for the formation of a new healthy tissue. This presentation will explore novel approaches from our laboratory in tissue engineering, focusing on bio-inspired scaffolds with inherent therapeutic properties and innovative delivery systems for bioactive natural compounds, achieved through the integrated use of biomaterials design, 3D printing technology, and *Cannabis sativa* extracts (CSE).

Materials and methods

This presentation will showcase several distinct projects that explore innovative biomaterial strategies. These include:

1. The pioneering use of a standardized CSE to investigate its effects on neuroinflammation and locomotor outcome after spinal cord injury (SCI) in rats. [1]

2. The unconventional approach of developing collagen hydrogels loaded with silver nanoparticles and CSE to create a nanocomposite biomaterial with enhanced antimicrobial and antioxidant properties. [2]

3. The investigation of alginate microencapsulation as a new platform for the efficient delivery of Cannabidiolic Acid (CBDA), evaluating its antioxidant and antimicrobial properties, as well as its cytotoxicity. [3]

4. The novel design and fabrication of a bioink made with gelatin and alginate that was able to be printed using an extrusion

3D bioprinter to create scaffolds for soft-tissue applications. These scaffolds were then loaded with CSE. [4]

For each project, unique material combinations, fabrication methodologies (extrusion 3D bioprinting, microflow-dripping), advanced characterization methods (swelling assessment, SEM, mechanical testing, antioxidant and antimicrobial assays), and innovative *in vitro/in vivo* evaluation models (cell culture, rat model) were employed, as detailed in our respective studies.

Results

Our research unfolded in a logical progression to harness the therapeutic potential of Cannabis sativa. Initially, we established the promising anti-inflammatory and functional recovery-promoting effects of its extracts in the context of spinal cord injury. This foundational work then led us to develop hydrogel systems incorporating these natural compounds, aiming to leverage their inherent antioxidant and antibacterial properties for improved biomaterial functionality. In parallel, we also explored alginate microencapsulation as a distinct route for the controlled release of CBDA and its associated bioactivities. Ultimately, to achieve sophisticated control over scaffold architecture and drug delivery, we integrated 3D printing technology to fabricate scaffolds loaded with CSE for soft-tissue engineering.

Discussion

These exploratory strategies demonstrate the potential of combining advanced biomaterials with natural compounds like CSE and their components to pave the way for transformative clinical applications in areas such as wound healing and infection control.

Acknowledgements

For financial support we thank Universidad de Buenos Aires, UBACYT 20020150100056BA and PIDAE2022 and CONICET PIP 11220200102598CO.

References

1) J. Del Care *et al*., Neuroscience, 2025, **573**, 468.

2) P.E. Antezana, S. Municoy, C.J. Perez and M.F. Desimone, *Antibiotics*, 2021, **10**, 1420.

3) P.E. Antezana, S. Municoy, F.M. Silva Sofras, M.G. Bellino, P. Evelson and M.F. Desimone, *International Journal of Pharmaceutics*, 2025, **669**, 125076

4) P.E. Antezana, S. Municoy, G. Orive and M.F. Desimone, *Polymers*, 2022, **14**, 4506.

Two drivers of science "behind the scenes": Languages Other Than English (LOTEs) and the hidden, unpublished stories of scientists

Douglas, T.E.L.*

School of Engineering, Lancaster University, UK.

t.douglas@lancaster.ac.uk

Provocation

If you speak ENGLISH, and you're a scientist, WHY learn another language ?! Because, ENGLISH is THE language of science, isn't it?

(I'll stop writing like Donald Trump now…)

No, it's not the language of science.

But… everything's in English, all the articles and conference presentations! (I'm aware this abstract is in English!)

However, the situation is more complex, but we're scientists, we love complexity…

A lot of science (not all) may be published and presented in English, But... we must look behind the scenes… it's not all done or discussed in English.

Science is based on collaboration, which is based on interpersonal relationships, which are based on conversations, which are based on language.

Your research is unique, but your story as a researcher is also unique. However, we don't talk about the role of language or the role of RELATIONSHIPS. Many of these stories are not in English (or not completely in English).

What's your story? Let's not just be interested in science, but in scientists

In this short provocation I hope to show (1) Why it's worth learning Languages Other Than English (LOTEs)

(2) How to learn LOTEs as a scientist

(3) The value of "behind-the-scenes" stories. Not only the results of research, but the story of the interpersonal relationships behind the results.

To practice what I preach, I explain this in several LOTEs under this link: https://www.youtube.com/watch?v=b8HRRMDBHWM&lc=Ugz4A4yRB7YhqToOfg94AaABAg

Whey Protein Isolate (WPI): a versatile, low cost biomaterial as a scaffold and as a drug delivery vehicle

Douglas, T.E.L.*

[a] School of Engineering, Lancaster University, UK.

t.douglas@lancaster.ac.uk

Introduction

Whey Protein Isolate (WPI) is an inexpensive by-product of the dairy industry; 3/4 is beta-lactoglobulin (β-LG). WPI solutions form hydrogels upon heating; crucially, they can be sterilized by autoclaving. This talk will describe the use of WPI hydrogels as scaffolds for cells and carriers of hydrophobic substances.

Materials and methods

WPI hydrogels 15% to 40% (w/v) have been synthesized[1]; inorganic particles, including aragonite, have easily been added during hydrogel formation [2]. Hydrophobic molecules such as phloroglucinol (PG), the fundamental subunit of marine polyphenols, cannibinoids and poly-gamma-glutamic acid (PGGA), were incorporated during hydrogel formation [3-5].

Results and Discussion

WPI hydrogels are suitable substrates for bone-forming cells[2] and human umbilical vascular endothelial cells (HUVEC) [1]. Aragonite[2] and PGGA[5] enhanced osteoblastic differentiation. PG[3] was incorporated leading to antimicrobial activity without a loss of cytocompatibility. Cannabinoids[4] promote cell proliferation.

Conclusion

WPI hydrogels are suitable scaffolds for cells and carriers for hydrophobic molecules

References

1) H. Genç et al, *Molecules*, 2023, **28**, 20A.

2) D. Gupta et al, *Materials and Design*, 2020, **188**, 11.

3) V. Platania et al. *Materials Science and Engineering: C*, 2021. **129**, 112412.

4) D.K. Baines et al. *Gels*, accepted 21/05/2025

5) D.K. Baines et al. *Gels*, 2023, **10**, 18

MULTI-LAYER INFECTION-ON-A-CHIP PLATFORM FOR REAL-TIME EVALUATION OF ANTIMICROBIAL THERAPIES

Xie, R.[1] *, Giorgi, F.[1] *, Chen, R.[2], Percival, S.[2], Han, M.[1], Lopez, M.L.[1]

[1] School of Engineering, University of Liverpool - The Quadrangle, Liverpool, L69 3BX, UK

[2] Biofilm Centre, 5D Health Protection Group, Liverpool, Merseyside, UK

*e-mail: Ruoxiao.Xie@liverpool.ac.uk, francesco.giorgi@liverpool.ac.uk

Introduction

The skin serves as the body's primary barrier against microbial colonisation, yet it remains highly vulnerable to infection—particularly in the context of chronic wounds, burns, and biomaterial-associated interventions [1]. Despite advances in antimicrobial therapies and biomaterial design, a persistent gap exists in physiologically relevant in vitro models capable of replicating the complexity of cutaneous tissue and its interaction with pathogens. Traditional monolayer cultures and static infection assays often fail to capture the dynamic, multilayered nature of skin and the spatial-temporal progression of infection [2]. Staphylococcus aureus, a leading cause of these infections, can penetrate multiple skin layers, making effective intervention particularly challenging [3]. Current skin-on-a-chip models lack integrated vasculature and immunocompetence, restricting their utility in simulating infection dynamics or evaluating advanced antimicrobial products [4]. In response, we developed M-LICES (Multi-Layer Infection-on-a-Chip Evaluation System), a vascularized, immunocompetent, multilayer skin-on-a-chip platform designed to emulate the structural and functional complexity of human skin. This innovative model enables high-resolution monitoring of infection progression and therapeutic efficacy in real time, bridging a critical gap in the evaluation of biomaterials and anti-infective agents.

Materials and methods

The engineered model comprises two distinct cellular layers: a basal matrix of human dermal fibroblasts embedded within a fibrin-based matrix, and an upper layer of human epidermal keratinocytes cultured at the air-liquid interface to mimic the epidermis. Microchannels, mimicking vasculature, were integrated within the collagen matrix and seeded with microvascular

endothelial cells to generate perfusable structures (Fig. 1A-1B).

The model was infected with Staphylococcus aureus to simulate cutaneous infection. To monitor infection progression and biofilm development, we employed a multi-technique approach including microscopy analysis with two photon confocal microscopy and SEM for real-time monitoring of infection progression, biofilm formation and structural changes post-infection. Comparative analysis was performed using a patented porcine skin models as biological benchmark.

Antimicrobial efficacy was assessed by treating infected models with a selection of pharmaceutical agents and a novel formulation of AgZn nanoparticles. Outcomes included quantification of bacterial load (CFU), biofilm mass (confocal microscopy), and structural evaluation (SEM).

Results

The model successfully emulates the layered architecture of human skin, with well-differentiated keratinocytes forming an epidermal-like layer atop a stable matrix of fibroblasts embedded within fibrin gel. The embedded microchannel network remained perfusable, ensuring nutrient delivery and supporting the inclusion of immune cells for potential immunocompetence.

Following inoculation, Staphylococcus aureus was observed to colonize the uppermost region of the model, particularly at the interface between the epidermal layer and the external environment. Two-photon confocal microscopy enabled real-time, high-resolution imaging of bacterial presence and distribution, while SEM imaging confirmed the development of biofilm-like structures on the surface of the tissue model. Assessment of antimicrobial interventions revealed variable biofilm disruption, with AgZn nanoparticles demonstrating the significant reduction in biomass and structural integrity of the biofilm. Compared to porcine skin explants, the model reproduced key infection and treatment trends but also offered distinct advantages: it enabled precise spatial control of infection, non-destructive, high-resolution imaging, and systematic modulation of host–pathogen interactions in a way not feasible with ex vivo tissues.

Discussion and Conclusion

This multi-layer vascularized skin-on-a-chip model replicates key structural and functional features of human skin, enabling controlled simulation of infection and real-time, high-resolution monitoring of biofilm formation. By combining biological relevance with advanced imaging and reproducibility, the model overcomes limitations of traditional ex vivo systems.

These capabilities position the platform not just as a biological mimic, but as an advanced, mechanistically insightful alternative for preclinical screening — with the potential to accelerate antimicrobial development and reduce reliance on animal models.

This work establishes a robust foundation for next-generation infection models in translational microbiology and antimicrobial research).

References

[1] Sandoz, H. (2022. Nursing Standard, 37(10), 75–82.

[2] Mathes, S. H., Ruffner, H., Graf-Hausner, U. (2014). Advanced Drug Delivery Reviews, 69–70, 81–102.

[3] Tong, S. Y. C., Davis, J. S., Eichenberger, E., Holland, T. L., Fowler, V. G. (2015). Clinical Microbiology Reviews, 28(3), 603–661.

[4] Wufuer, M., Lee, G., Hur, W., Jeon, J., Kim, B. J., Choi, T. H. (2016). Scientific Reports, 6, 37471.

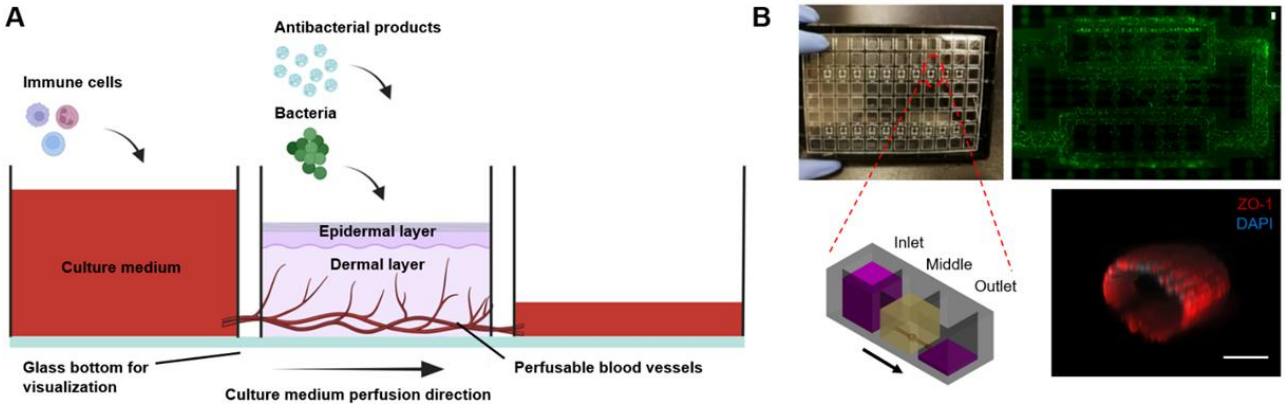
A
Antibacterial products
Immune cells
Bacteria
Culture medium
Epidermal layer
Dermal layer
Glass bottom for visualization
Perfusable blood vessels
Culture medium perfusion direction
B
Inlet
Middle
Outlet
ZO-1
DAPI

Figure 1.

A Path to Superior Service Life of Total Joint Replacements

Gul, R.M. [a,*], Khan, F.N. [b,*], Khalil, M.K. [a]

[a] Department of Mechanical Engineering, University of Engineering and Technology, Peshawar, Pakistan [b] Faculty of Materials and Chemical Engineering, GIK Institute of Engineering Sciences and Technology, Topi, Pakistan

* rgul@uetpeshawar.edu.pk and fahd@giki.edu.pk

Introduction

Ultra-high molecular weight polyethylene (UHMWPE) is the material of choice for use in total Joint replacement (TJRs) as a bearing surface[1]. The main reasons of UHMWPE failure as a liner in artificial joints are due to wear debris generation (osteolysis) and oxidation embrittlement [2, 3]. The wear associated problem of medical implant is managed through crosslinking while antioxidants are blended with UHMWPE to cope with the problem of oxidation embrittlement induced due to crosslinking[4,5]. In this research two difference antioxidants (vitamin E and Irganox) are blended with UHMWPE and crosslinked using three different techniques (radiation, bulk chemical and surface chemical) to compare the performance of the blends as liner for TJRs.

Materials and methods

Vitamin E (VE) and Irganox are blended with UHMWPE in concentration of 0.5% by weight and are crosslinked through radiation crosslinking (dose=150 kGy), bulk chemical crosslinking (Dicumyl Peroxide (DCP)=1% wt.) and surface chemical crosslinking which include doping of the blends in DCP (temperature:80°C, time:4h) and decomposition (temperature:150°C, time:4h). The performance of the processed materials was evaluated and compared by measuring the crosslink density, oxidation induction time (OIT), crystallinity and mechanical properties of Control-UHMWPE, VE-UHMWPE and Irganox-UHMWPE samples

Results

Among the antioxidants blends Irganox-UHMWPE blend showed both higher crosslink density and OIT when compared with the VE-UHMWPE blend processed by all the three different techniques. While Control-UHMWPE show the lowest OIT but crosslink density higher than VE-UHWMPE. For example, when radiation crosslinked, Irganox-UHMWPE has higher crosslink density of 274.5 mol/m^3 and OIT of 48.8 min., compared to VE-UH having crosslink density of 196.9 mol/m^3 and OIT of 26.2

min. While radiation crosslinked Control-UHMWPE had a crosslink density of 226.2 mol/m^3 and OIT of 0.8 min.

Discussion

Similar trends were observed when comparing the crosslink density and OIT of the three different types of samples (Control-, VE- and Irganox-UHMWPE) for the three different crosslinking techniques (radiation, bulk chemical and surface chemical). However, radiation crosslinking results in higher crosslink density, followed by surface chemical, and it was least in case of bulk chemical crosslinking. We expect that the wear resistance of the radiation crosslinked blends (for this radiation dose) will be higher than the others as it results in higher crosslink density.

Acknowledgements

Funding provided by National Research Program for Universities (NRPU), Higher Education Commission, Islamabad, Pakistan (Grant: 20-16020).

References

1) O. Hussain, B. Ahmad, and S. Saleem, *International Journal of Materials Engineering Innovation,* 2023, **14.2**, page. 95.
2) S. Liza *et al.*, *Tribology and Sustainability,* CRC Press, 2021, page. 353.
3) M. Tan *et al.*, *Eng. Failure Anal.*, 2020, **109**, page. 12.
4) S. Paladugu and R. Sreekanth, *Materials Today: Proceedings*, 2022, **56**, page. 1097.
5) Y. Ren *et al.*, *ACS Appl. Bio Mater.,* 2020, **3**, page. 547.

Trimethoxy silyl end-capped hyperbranched polyglycidol/polycaprolactone particle gels for cell delivery and tissue repair. Mechanical properties, biocompatibility and biodegradability studies.

González-Chomón, C [1], Garamus, V. M [2], Hoyland, J. [3] and Halacheva, S. S [4],*

[1] University of Bolton, Deane Road, Bolton, Greater Manchester BL35AB, UK;

[2] Helmholtz-Zentrum Hereon, Max-Planck-Str., 21502 Geesthacht, Germany;

[3] The University of Manchester, Oxford Rd, Manchester M13 9PL, UK;

[4] School of Postgraduate Medicine and Allied Health, Apollo Buckingham Health Science Campus, University of Buckingham, Crewe Green Road, Crewe, Cheshire CW1 5DU, UK

* Correspondence: silviya.halacheva@buckingham.ac.uk

Introduction

Recently polymer scaffolds based on hydrophilic hyperbranched polyglycidol (HBPG) have attracted considerable attention in tissue engineering because of their high functionality, their desirable mechanical properties, solubility in aqueous media and biocompatibility.1 In this study we investigate the relationship between the structure, mechanical properties, and performance of the novel PCL-HBPG/1SiHBPG gel scaffolds that have been developed for soft tissue regeneration. The copolymers were composed of a middle block of hydrophobic PCL and outer moieties of hydrophilic HBPG and trimethoxysilyl HBPG (SiHBPG).2,3 In aqueous solution, at concentrations above their corresponding critical aggregation concentration, the PCL-HBPG/1SiHBPG copolymers readily self-assemble into large multicore structures composed of PCL domains and HBPG/1SiHBPG corona. The particles were stabilized by numerous hydrogen-bonds from the HBPG moieties as well as via formation of siloxane crosslinks. The particles formed from the more hydrophilic copolymers were only slightly affected by an increase in temperature, whereas the most hydrophobic copolymers formed more compact and tight particles/domains at elevated temperatures.

Materials and methods

The copolymers used in the present study were synthesized as described elsewhere.2 and characterized by gel permeation chromatography, 1HNMR, thermogravimetric analysis and dynamic scanning calorimetry. They feature constant molar mass of the PCL middle block and HBPG/1SiHBPG contents varying from 45 – 90 mol% for the HBPG and from 0.6 – 1.4

mol% for the SiHBPG, respectively. Their aqueous solutions in the concentration range from 1mg/ml were investigated by dye solubilization, turbidimetry, light scattering, SAXS and rheology. Cell viability was determined using immortalised human chondrocyte cell line by MTT assay. The biodegradation studies were carried out by addition of 100 µL of 5% lipase solution in 10 mL phosphate buffered saline to the gel at 37 °C

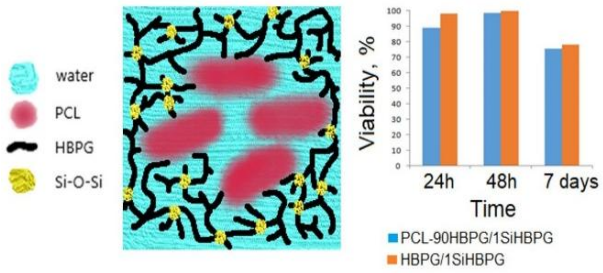

Figure 1. PCL-HBPG/SiHBPG particles' gel

Results

We applied a completely new approach for the development of the gel scaffolds. In the first step, the physical gels were formed by crosslinking the interpenetrating shells of the PCL-HBPG/1SiHBPG particles via numerous inter- and intramolecular hydrogen bonds formed within the HBPG/1SiHBPG moieties as well as the ability of the PCL to diffuse into the different domain. In the second step, the physical network was locked in place due to the gradual hydrolysis (and subsequent Si–O–Si crosslink formation) of trimethoxysilyl groups. The cytotoxicity results with immortalized chondrocyte cells revealed that the new PCL-HBPG/1SiHBPG gels show very good biocompatibility, with at least 75% cell viability after 7 days of incubation, (**Figure 1**). The PCL-45HBPG/1SiHBPG gels were biodegradable upon the addition of lipase.

Discussion

Our investigation clearly shows that variations in the hydrophobic/hydrophilic portions of the copolymers determined the macroscopic properties of the PCL-HBPG/1SiHBPG systems. The sol–gel phase transition was only observed for the most hydrophobic system, PCL-45HBPG/1SiHBPG, at low temperatures. The elastic properties of PCL-45HBPG/1SiHBPG were attributed to the hydrophobic interaction between the PCL segments and the numerous hydrogen bonds formed between HBPG/1SiHBPG moieties. Increases in the temperature and the hydrophilic content resulted in the disintegration of the PCL domains and the occurrence of a flow zone. The PCL-HBPG/1SiHBPG particle gels showed a steady increase in the gels' elasticity over time at low temperatures, which was

attributed to the gradual crosslinking of the trimethoxysilyl groups. They feature high elasticity and undergo enzyme-triggered disassembly. The gels are biocompatible and have the potential to invoke cell attachment and differentiation without the need for exogenous biological stimuli. A successful outcome of this study will be the prospect of a new minimally invasive approach for tissue regeneration that is currently not available.

Acknowledgements

We are grateful to the EPSRC for financial support (EP/M02881X/1). The SAXS study was supported by the European Commission under the sixth Framework Program through the Key Action: Strengthening the European Research Area, Research Infrastructures (Contract RII3-CT-2003-505925, Grant Agreement No. 226507-NMI3).

References

1) Calderón, M.; Quadir, M.A.; Sharma, S.K.; Haag, R. Dendritic Polyglycerols for Biomedical Applications. Advanced Materials 2010, 22, 190–218
2) González-Chomón, C.; Garamus, V.M.; Rangelov, S.; Ebdon, J.R.; Novakov, C.; Halacheva, S.S. Eur. Polym. J. 2019, 112, 648–659
3) González-Chomón, C.; Garamus, V.M.; Hoyland, J.; Halacheva, S. S. J. Compos. Sci. 2023, 7, 451.

THE DEVELOPMENT OF DRUG DELIVERY BIOMATERIALS FOR THE TREATMENT OF CYTOTOXIC SNAKEBITE ENVENOMING

Hall, S.R.[a,*], Cobb, T.[a], Gray, M.[a], De Castro, G.[a], Baines, D. [a], Donnelly, R[b], Douglas, T.[a]

[a] Lancaster University, UK. [b] Queen's University Belfast, UK.

* Corresponding author(s) e-mail(s): s.r.hall@lancaster.ac.uk

Introduction

Kofi Annan called snakebite "The biggest public health crisis you've never heard of"1. Almost 3 million people are envenomed by snakes annually, killing at least 138,000 and causing catastrophic injury to 400,0002. The injuries caused by snakebite can be devastating and are often caused by cytotoxic (cell killing) snake venoms which cause what is termed "tissue necrosis" of the skin and muscle around the snakebite site3. Unfortunately, the only currently available specific treatment for snakebite, antivenom, is expensive, must be administered in hospital intravenously (IV), and is largely ineffective at treating this necrosis4. My previous research has shown how small molecule drug inhibitors of specific snake venom toxin families, when injected directly into the envenoming-site in vivo, can drastically reduce the resulting skin necrosis (dermonecrosis)5–7. However, to translate such prehospital snakebite therapies into the real world, inexpensive biomaterials containing such drugs and capable of delivering them rapidly into a snakebite wound and that are easy enough to use that they could be self-administered by the snakebite victim themselves in an emergency, thereby buying them time to reach hospital for further treatment, must be developed.

Materials and methods

Whey protein isolate (WPI) in the form of hydrogels containing Drug X (currently unnamed to protect potential future IP) were cut into consistently sized discs. These discs, or those from no-drug containing control hydrogels, were soaked in cell culture medium for up to 24 hours, after which the supernatant was collected and used to treat epidermal keratinocytes (HaCaT cells) exposed to venom from the spitting cobra, *Naja nigricollis*, for a further 24 hours. Then, cell viability was quantified using resazurin assays and %-cell viability calculated, from which concentration-response curves were created and the venom-inhibiting ability of the Drug X-containing hydrogels determined.

Results

Drug X-containing hydrogels inhibited the cytotoxic potency of *N. nigricollis* venom in the HaCaT cell viability assays to a similar extent to what was observed with our Drug X (not within hydrogels) positive controls. Close to complete cytoprotection (i.e. close to 100% cell viability in cells treated with venom + Drug A-containing hydrogel supernatant) was observed.

Discussion

These results show that drugs which inhibit snake venom toxins and contained within WPI hydrogels can be successfully stored and later released into standard cell medium, after which they can then inhibit the cytotoxic action of spitting cobra venom in cell culture experiments. This suggests that such hydrogels could potentially be used in the future to create drug-containing wound dressings or as components of transdermal microneedle patches that could be used to deliver venom toxin-inhibiting drugs directly into the affected tissues of snakebite victims. Such therapies could be carried on one's person or within first aid kits kept in nearby villages, thereby significantly reducing the time it takes a snakebite victim to receive treatment and ultimately helping to save the lives and limbs of many thousands of people every year.

Acknowledgements

For financial support we thank the Friends of Lancaster University in America (FLUA; Global Impact Small Grant to SRH), the Department of Biomedical & Life Sciences at Lancaster University (Start-Up Package to SRH), and Faculty of Science and Technology at Lancaster University for the DB's doctoral studentship.

References

1)K. Annan, Snakebite: https://www.kofiannanfoundation.org/combatting-hunger/public-health-snakebite/, (accessed 5.1.22).

WHO, Snakebite Envenoming, https://www.who.int/news-room/fact-sheets/detail/snakebite-envenoming, (25.4.25).

2) D. Chakrabarty and A. Sarkar, in Snake Venoms, Springer, 2016, p1.

3) R. H. Clare t al. Trends Pharmacol Sci, 2021, 42, 340–353.

4) T. Y. Du et al. Sci Transl Med, 2024, 16, 1-12.

5) K. E. Bartlett at al. Proc Natl Acad Sci U S A, 2024 121, 1-12.

7) S. R. Hall et al. Nat Commun, 2023, 14, 1-15.

Galleria mellonella larvae as an *in vivo model* for evaluating antimicrobial biomaterials

Khutoryanskiy, V. [a]*, Satmbekova, D., [a,b], Walton, G.-[c], Dala-Ali, Z.[a]

[a] Reading School of Pharmacy, University of Reading, UK.

[b] Department of Medicine and Healthcare, Al-Farabi Kazakh National University, Kazakhstan

[c]Department of Food and Nutritional Sciences, University of Reading, UK

* Corresponding author e-mail: v.khutoryanskiy@reading.ac.uk

Introduction

Galleria mellonella, the greater wax moth larva, is a practical and ethically acceptable alternative to mammalian models for early-stage testing of antimicrobial biomaterials[1]. This model is particularly useful due to its well-developed innate immune system, which is similar to that of vertebrates. Additionally, *Galleria mellonella* can be studied at 37°C, closely mimicking the physiological conditions of mammalian hosts, making it a suitable model for evaluating the *in vivo* effectiveness of antimicrobial agents. We developed both systemic (bacterial injection) and topical (burn with bacterial application) infection models to assess the *in vivo* efficacy of antimicrobial polymers, peptides, nanoparticles, and formulations.

Materials and methods

Galleria mellonella larvae were infected systemically (injection) or topically (thermal injury plus bacteria) using *Staphylococcus aureus* and *Escherichia coli*. Larval survival, melanisation, and activity were monitored following treatment with antimicrobial polymers, peptides, nanoparticles, and various formulations.

Results

Injection of a bacterial suspension into *Galleria mellonella* larvae leads to the development of systemic infection, typically accompanied by visible darkening due to melanisation, and ultimately resulting in larval death (**Figure 1**).

Figure 1. Experiments in live larvae: before infection (A); injection of bacteria in larvae (B); development of infection and death of larvae (C and D)

Discussion

Administering antimicrobial agents 1-hour post-infection has a significant impact on

larval survival, with the outcomes varying based on the efficacy and toxicity of the compounds being tested. The survival rate is influenced by several factors, including the antimicrobial dose relative to the bacterial concentration at the site of infection, as well as the inherent toxicological properties of the agent. In some instances, the antimicrobial agents effectively combat the infection, resulting in enhanced survival rates in the infected larvae. However, in other cases, the same agents may exhibit toxic effects that outweigh their antimicrobial efficacy, leading to a reduction in larval survival. This is particularly evident when certain antimicrobial compounds, although non-toxic to healthy larvae, induce harmful effects when administered to infected ones, possibly due to the altered immune response or the increased susceptibility of the larvae during infection. These findings emphasise the complexity of balancing antimicrobial effectiveness and toxicity, highlighting the need for careful optimisation of dosage and formulation to achieve the desired therapeutic outcome without causing harm to the host organism.

Acknowledgements

VK acknowledges the Royal Society for supporting his industry fellowship (IF\R2\222031). DS acknowledges the JSC “Center for International Programs” (Kazakhstan) for supporting her postdoctoral fellowship at the University of Reading.

References

1) G. Menard, A. Rouillon, V. Cattoir and P.-Y. Donnio, *Frontiers in Cellular and Infection Microbiology*, 2021, 11:782733.

Using Machine Learning for reducing training in mice experiments

Killick, R [a*]

[a] School of Mathematical Sciences, Lancaster University, UK

* Corresponding author(s) e-mail(s): r.killick@lancaster.ac.uk

Introduction

This talk will discuss the potential of modern data science / machine learning / AI (pick your favourite buzz word) techniques for aiding the 3R's (Replacement, Reduction, Refinement) agenda in animal research. Through discussion of a collaboration between Lancaster University and Manchester University on Riccardo Storchi's 3R's postdoctoral fellowship, I will motivate the need for true interdisciplinary collaboration to achieve step change. The collaboration designed a new set of experiments for monitoring mice in minimally modified habitats to assess sightedness without requiring learning. Crucially, rodent learning was avoided using a combination of machine learning for object (mouse) identification within the habitat and changepoint detection for segmenting behaviour to associate with sightedness. This combination of state-of-the-art statistical and computational techniques coupled with a refinement of the experimental conditions demonstrated that a reduction in both the number and stress of animals is possible.

The talk is designed to be a motivator for future collaborations with statistical and computational scientists and thus accessible to a wide audience.

References

1) Storchi, R., Rodgers, J., Gracey, M. *et al. Scientific Reports*, **2019**, 9, 10396. https://doi.org/10.1038/s41598-019-46836-y

Immunomodulatory phenotype transition following nanoclay phagocytosis in macrophages

Kim, Y-H[a], Oreffo, ROC[a], Tabata, Y.[b], Dawson J-[a,*]

[a] Bone and Joint Research Group, Centre for Human Development, Stem Cells & Regeneration, Institute of Developmental Sciences, University of Southampton, Southampton, UK

[b] Department of Plastic and Reconstructive Surgery, Graduate School of Medicine, Kyoto University, Kyoto, Japan

* Corresponding author(s) e-mail(s): Yanghee.Kim@soton.ac.uk & jid@soton.ac.uk

Introduction

Macrophages are key regulators of immune responses to damaged tissue and foreign bodies such as biomaterials. A critical early process in their function is phagocytosis—the uptake of heterogeneous target particles. While it is well established that particle size and shape influence macrophage phenotype and function in tissue regeneration[1], the relationship between phagocytosis and macrophage behaviour, including underlying pathways, remains unclear. Nanoclay particles (Laponite) have recently garnered attention in regenerative medicine as self-assembling matrices and drug delivery modifiers[2]. This study investigates how nanoclay particle phagocytosis affects macrophage phenotype and function.

Materials and methods

Mouse bone marrow-derived macrophages were isolated from Balb/c male mice (4–8 weeks old) and cultured with varying concentrations of nanoclay (50, 100, 500, and 1000 µg/mL) for 1 and 3 days. Intracellular and extracellular particle localisation was assessed via transmission electron microscopy and confirmed using energy-dispersive X-ray spectroscopy. Macrophage phenotype was analysed by flow cytometry, cytokine levels in the culture medium by ELISA, gene expression by quantitative PCR, and signalling pathway involvement by western blotting.

Results

Nanoclay particles were observed both intracellularly and extracellularly across all nanoclay concentrations examined. A significant increase in M1-like macrophages was detected at 100 µg/ml nanoclay after 24 hours ($p < 0.034$). By day 3, M1-like populations declined while M2-like populations increased. Correspondingly, levels of anti-inflammatory genes Il10 and Tgfb1 were significantly elevated ($p < 0.017$, $p < 0.032$), and pro-inflammatory Tnfα expression was significantly reduced at all nanoclay concentrations ($p < 0.04$).

Furthermore, inhibition of phagocytosis with cytochalasin D led to increased M1 marker expression and decreased PI3K/AKT pathway activity.

Discussion

The current findings demonstrate that nanoclay-induced M2 polarisation is dependent on macrophage phagocytosis and is regulated via the PI3K/AKT pathway. Phagocytosis of biomaterials plays a crucial role in modulating macrophage phenotype and function, thereby influencing inflammatory responses in tissue regeneration with significant implications for patient health.

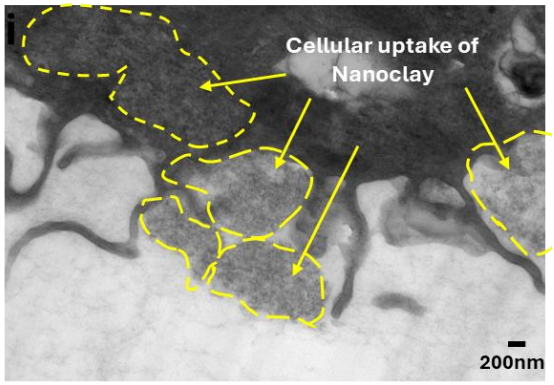

Figure 1. TEM observation of nanoclay particles taken up by macrophages.

Acknowledgements

Supported by an MRC-AMED Regenerative Medicine and Stem Cell Research Initiative (ref.MR/V00543X/1).

References

1) Y-H. Kim, ROC. Oreffo, JI. Dawson, *Bone*, 2022, **159**, 11639
2) Y-H. Kim, et al. *Nature Communications*, 2020, **11**, 1-9

Designing 'smart' biomaterials: from regenerative medicine to integrative envelopes for robotic implants.

Mehrban, N. [a,*]

[a]Department of Life Sciences, University of Bath, UK, BA2 7AY.

*Corresponding author(s) e-mail(s): nm2051@bath.ac.uk

Introduction

Surgical attempts to repair diseased and damaged tissues are limited primarily by reduced functional restoration, patient discomfort and high healthcare costs associated with inflammation and failed implants. Biomaterials used to overcome some of these issues are often limited by the chemistry and architecture which don't accurately reflect the internal environment of the body.

We design and manufacture novel 'smart' biomaterials, often inspired by nature, which control cell behaviour and offer better integration with healthy tissue.[1-4]

Materials and methods

Standard solid-phase synthesis techniques were used to manufacture novel alpha-helical peptides to form the backbone of our hydrogel-based biomaterials including the cell-interacting motifs. All peptides are purified by reversed-phase HPLC, and their masses confirmed by MALDI-TOF mass spectrometry. Gels were formed by mixing 2mM stock solutions of peptide1/peptideN_3 (p1/p1N_3) and peptide2 (p2) in a buffered solution at pH 7.4 and decorated using copper-catalysed azide-alkyne cycloaddition ('click chemistry').

We are currently expanding the profile of these novel peptides using nanocages to build a new class of biomaterials with gradient stiffnesses for smart, integrative device envelopes.

Results & Discussion

We have shown that by mimicking some of the chemistry and architecture of native extracellular matrix proteins, our self-assembling hydrogels are capable of reorganising and reconstructing damaged tissue matrix, promoting repair and reducing chronic inflammation when implanted. In this presentation I will be covering our design criteria and explaining how we have adapted our *de novo* peptide-based system to promote migration, proliferation, and functional differentiation in several different cell types to address key medical challenges, such as integration with healthy tissue.

I will also be introducing a second novel material my group have been working on more recently[5], towards developing soft robotic envelopes with a gradient stiffness and modifiable chemistry. This work is part of a UK-based consortium bringing together academics, clinicians, medical technology specialists and ethics advisors with the aim of creating implantable soft robotic muscles.

Acknowledgements

We thank the BBSRC, EPSRC and AMS for their support over the years. We also thank researchers from the Mehrban group and collaborators at University of Bristol, University College London, University of Pittsburgh, Cardiff University, The Open University and University of Exeter for their contributions.

References

1) D.A. Scott, A. Wasmuth, E. Abelardo *et al.*, *Advanced Functional Materials*, 2025, **35**, 2410333.

2) N. Mehrban, D. Cardinale, S.C. Gallo *et al.*, *Materials Science and Engineering C*, 2021, **122**, 111935.

3) N. Mehrban, C.P. Molina, L.M. Quijano *et al.*, *Acta Biomaterialia*, 2020, **111**, 141-152.

4) N. Mehrban, B. Zhu, F. Tamagnini *et al.*, *ACS Biomaterial Science & Engineering*, 2015, **1**, 431-439.

5) L. Anderson, A.P. Hunter, M.J. Kershaw *et al.*, *Nanoscale*, 2024, **16**, 14802-14812.

Electrospinning of Poly(lactic acid) for the generation of bioactive materials

Mele, E. [a,*]

[a] Materials Department, Loughborough University, Loughborough LE11 3TU, UK

[b] Affiliation 2, Country.

* Corresponding author: e.mele2@lboro.ac.uk

Introduction

Electrospinning is a method to manufacture polymeric fibres with micro-to nanometre diameters, high surface area, controlled porosity and distinct morphological features.[1] The rising demand for these high-performance materials, in sectors such as healthcare, filtration, textile, and energy, is driving the global electrospinning market. The biomedical and healthcare sector is the largest consumer of electrospun fibres, with products such as scaffolds for tissue engineering, wound dressings, and drug delivery systems. However, most of the commercial biomedical components are made of bioinert electrospun fibres. Here, naturally derived systems were used to impart bioactivity to poly(lactic acid) electrospun fibres and their role on the properties of the resulting fibres was investigated.[2-5]

Materials and methods

Poly(lactic acid) (PLA 4060D, MW = 120,000 g/mol, amorphous polymer with an L-lactide content of around 88 wt%) was purchased from NatureWorks LLC; acetone and essential oils, such as limonene, black pepper and clary sage, were purchased from Sigma-Aldrich. All chemicals were used without further purification. PLA solutions for electrospinning were prepared by dissolving the polymer in acetone at a concentration of 14% w/v, and the bioactive ingredients were added in the solution before electrospinning. For the electrospinning process, a high voltage power supply was used. All experiments were conducted in normal environmental conditions. Characterisation techniques, like Scanning Electron Microscopy, Differential scanning calorimetry, Thermogravimetric Analysis, tensile tests, were used to determine the properties of the electrospun fibres. The bioactivity of the electrospun mats was tested by conducting experiments with bacteria and cells.

Results and Discussion

In this research, the encapsulation of natural materials, like plant extracts, was effective in generating bioactive PLA electrospun nanofibers (for example, antibacterial properties) and impacted on

the morphological and physical properties of the resulting mats. The addition of essential oils generated thermodynamic instabilities during the electrospinning process, leading to the formation of fibres with a nano-textured surface and nanoporosity.

The effect of plants extracts on the properties of the PLA electrospun fibres over time periods longer than 14 days was investigated under different storage conditions. It was shown that the properties of composite fibres evolved over time due to the evaporation of the natural compounds, with a consequent impact on the thermal and mechanical stability of medical devices consisting of these systems. However, the degree of change seen is not expected to impact the material functionality in service, especially when considering an application like a wound dressing.

Acknowledgements

For financial support we thank the Royal Society.

References

1) E. Mele, *Polymers*, 2020, **12**, 908.
2) W. Zhang, C. Huang, O. Kusmartseva, N. L. Thomas, E. Mele, *Reactive and Functional Polymers*, 2017, **117**, 106.
3) P. Wang, E. Mele, *Materials* 2018, **11**, 923.
4) L. Williams, F. L. Hatton, M. C. Righetti, E. Mele, *Polymers*, 2024, **16**, 1005.
5) G. Milanesi, B. Vigani, S. Rossi, G. Sandri, E. Mele, Polymers 2021, **13**, 2582.

Harnessing Ultrasound for Biomaterial Design: Sono-crystallisation of Hydrophobic APIs and Antibodies

Horacek, F.[a], Pancholi, Ketan*.[a], Njuguna, J [a], Welgamage Don, A.[b], Faraz Amini Boroujeni[c], Prentice, P.[c]

a School of Computing, Engineering & Technology, Robert Gordon University, United Kingdom

b School of Pharmacy and Life Sciences, Robert Gordon University, United Kingdom

c School of Physics and Astronomy, University of Glasgow, United Kingdom

* Corresponding author: k.pancholi@rgu.ac.uk

Introduction

Protein crystallization is pivotal for drug design and crystallography studies[1,2,3]. This work develops a novel continuous crystallization platform combining ultrasound[4], electromagnetic fields, microbubbles, and temperature control for forming uniform therapeutic protein crystals. Sono-crystallisation—the use of constant high-frequency focussed ultrasound field to trigger and control crystal formation—offers a single, scalable route for engineering both low-molecular-weight, water-insoluble active pharmaceutical ingredients (APIs) and high-molecular-weight protein therapeutics such as antibodies. When an acoustic field (20 kHz–2 MHz) of constant pressure is applied on small area of a supersaturated solution, acoustic cavitation produces micron-scale vapour bubbles that grow and implode in microseconds, generating localised hot spots (ΔT ≈ 1000 K), high pressures (ΔP ≈ 100 MPa) and radial shock waves. Primary nucleation is promoted by (i) transient pressure drops at bubble interfaces where molecules adsorbs[5], which lower the free-energy barrier for cluster formation, and (ii) radical-induced surface activation that supplies heterogeneous nucleation sites. Secondary nucleation and growth are accelerated by intense micro-mixing: shear fields and acoustic micro-streaming disrupt concentration boundary layers around nascent crystals, sustaining high supersaturation while limiting agglomeration.

For hydrophobic APIs, ultrasound enables (1) rapid generation of sub-5 μm crystals with narrow size distribution, enhancing dissolution rate, and (2) polymorph selection via pulse-width tuning that biases nucleation kinetics overgrowth. For antibodies—traditionally resistant to orderly crystallisation—moderate-intensity sonication (< 2 W cm^{-2}) induces metastable

mesoscopic clusters that template well-ordered crystal lattices without denaturing the protein, achieving yields > 70 % and diffraction-quality crystals within hours rather than days. The same cavitation-driven phenomena thus bridge the molecular-weight gap, delivering a versatile processing tool that unifies formulation of poorly soluble small-molecule drugs and structurally complex biologics. Furthermore, a new possibility of progress in this area will also be discussed.

Materials and Methods

Initial sonocrystallization proof-of-concept involved lysozyme in a capillary exposed to high-intensity focused ultrasound (Figure 1). Crystal imaging and sizing were performed using ImageJ. Future work includes acoustic pressure measurement, protein expression, and fabrication of a flow-cell-based hybrid crystallizer.

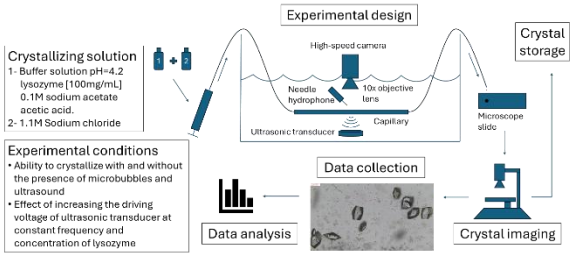

Figure 1: Diagram showing the evolution from proof-of-concept to a hybrid sonocrystallization setup, with microfluidic integration and acoustic monitoring.

Results

Lysozyme crystal size decreased with increased ultrasound amplitude, though nonlinearly (**Figure 2 and 3**). The standard deviation of the protein crystal size also seems to increase with the ultrasound amplitude. The frequency of the ultrasound was kept constat at 692 kHZ as it will cavitate the microbubble nuclei. Observed microbubble induced cavitation

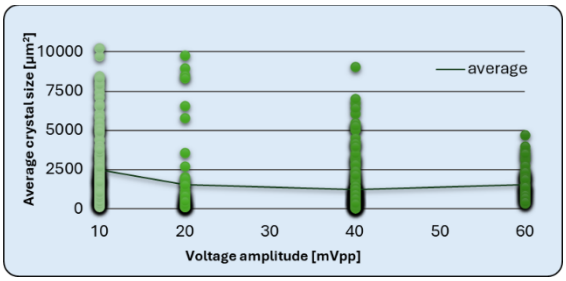

Figure 1 – Effects of rising voltage amplitude on average crystal size 50mg/mL lysozyme - 692kHz - 1000cycles = 1450µs

suggests a possible secondary nucleation pathway. ELISA testing of post-crystallization protein activity will validate structural preservation. With controlled parameters, the diffraction quality protein crystals can be produced reliably.

Discussion

The platform's integration of hybrid stimuli supports precise control over crystallization variables, with potential for tailoring crystal morphology and stability for drug delivery. Target proteins include membrane and

antimicrobial resistance proteins—difficult to crystallize with existing methods.

Acknowledgements

We thank Robert Gordon University for funding a multidisciplinary studentship.

References

1. D. A. Dmitrieva, E. A. Pustovalova, I. A. Serebryakova, O. V. Bocharova and S. A. Shilova, *Biochemistry (Moscow)*, 2023, **88**, 1201–1215.

2. S. B. Ebrahimi and D. Samanta, *Nat. Commun.*, 2023, **14**, 1234.

3. L. Fang, X. Zhang, Y. Wang, Y. Liu and Y. Zhang, *Ultrason. Sonochem.*, 2021, **76**, 105650.

4. N. Fatemi, K. Wang, A. J. Norouzi, M. Parviz and A. R. Minerick, *Langmuir*, 2019, **35**, 60–69.

5. E. Stride, K. Pancholi, M. J. Edirisinghe and S. Samarasinghe, *J. R. Soc. Interface*, **2008**, *5*, 807–811.

Intraoperative drug delivery via an injectable hydrogel confers survival benefit against childhood hindbrain tumour xenografts.

Moloney, C. [a,b], McCrorie, P. [a], ElSherbeny, A. [b], Porter, H. [a], Bastiancich, C. [c], Silka, H. [d], Handley, P. [e], Dredge, K. [e], Wicher, G. [f], Grundy, G. [a], Brem, H. [d], Forsberg-Nilsson, K. [f], Smith, S.J. [a], Tyler, B [d], Alexander, C. [b], Rahman, R. [a,*]

[a] School of Medicine, Biodiscovery Institute, University of Nottingham, UK.

[b] School of Pharmacy, University of Nottingham, UK.

[c] Aix-Marseille Université, Marseille, France.

[d] Department of Neurosurgery, Johns Hopkins University, Baltimore, Maryland, USA.

[e] Zucero Therapeutics Ltd., Suite 1.11, Westlink Court, Darra, Queensland, Australia.

[f] Department of Immunology, Uppsala University, Uppsala, Sweden.

Email: Ruman.Rahman@nottingham.ac.uk

Introduction

Intraoperatively applied local drug delivery systems offer a means of overcoming poor blood brain barrier (BBB) drug permeability. We previously reported on the intraoperative application of a mouldable and temperature-sensitive poly(lactic-co-glycolic acid)-poly(ethylene glycol) (PLGA/PEG) paste loaded with combination chemotherapeutics, to the resection cavity of an orthotopic syngeneic malignant brain tumour model, whereby a significant increase in overall survival benefit was observed as compared to standard treatment [1,2]. However, there is a paucity of localised delivery systems for childhood tumours arising in the hindbrain. Here we demonstrate applicability of an injectable (sol-to-gel) hydrogel against Myc-amplified medulloblastoma (MB) and atypical teratoid/rhabdoid tumours (AT/RT), neoplasms associated with poor prognoses and debilitating quality of life.

Materials and methods

poly(ethyleneglycol)-poly(caprolactone)-poly(ethyleneglycol) (PECE) hydrogel loaded with chemotherapeutics identified as effective against primary MB and AT/RT *in vitro*, was prepared as an injectable and biodegradable formulation. CHIR99021 (glycogen synthase kinase-3 inhibitor), ribavirin (guanosine analogue) and PG545 (heparanase inhibitor) were chosen as ideal candidates for intraoperative delivery, based upon an inability to effectively traverse the BBB.

Results

The hydrogel alone was well-tolerated, and drug-loaded hydrogel achieved > 1-month therapeutic release, commensurate with any oncological treatment gap post-surgery. Orthotopic xenograft tolerability and efficacy studies against G3 MB indicated a comparable median survival in treatment arms receiving radiotherapy (XRT), or CHIR99021- and PG545-loaded LDDS. However, combined XRT and LDDS potentiated survival, including establishing long-term survivors. Median survival of AT/RT arms receiving XRT alone was comparable to that of CHIR99021- and ribavirin-loaded LDDS, with long-term survivors observed only in the latter arm.

Discussion

Intraoperative localised drug delivery against cerebellar brain tumours using PECE offers a promising novel therapeutic alternative and encourages the possibility of circumventing radiation-induced adverse effects for young children impacted by these diseases (**Figure 1**).

Acknowledgements

For financial support we thank The Little Princess Trust and The Children's Cancer and Leukaemia Group (Grant Ref: CCLGA 2019 32).

References

1) S.J. Smith, B.M. Tyler, T. Gould *et al*, *Clinical Cancer Research*, 2019, **25(16)**, 5094-5106.
2) R. Serra, S.J. Smith, J. Rowlinson *et al*, *British Journal of Cancer*, 2024, **131(11)**, 1858-1868.

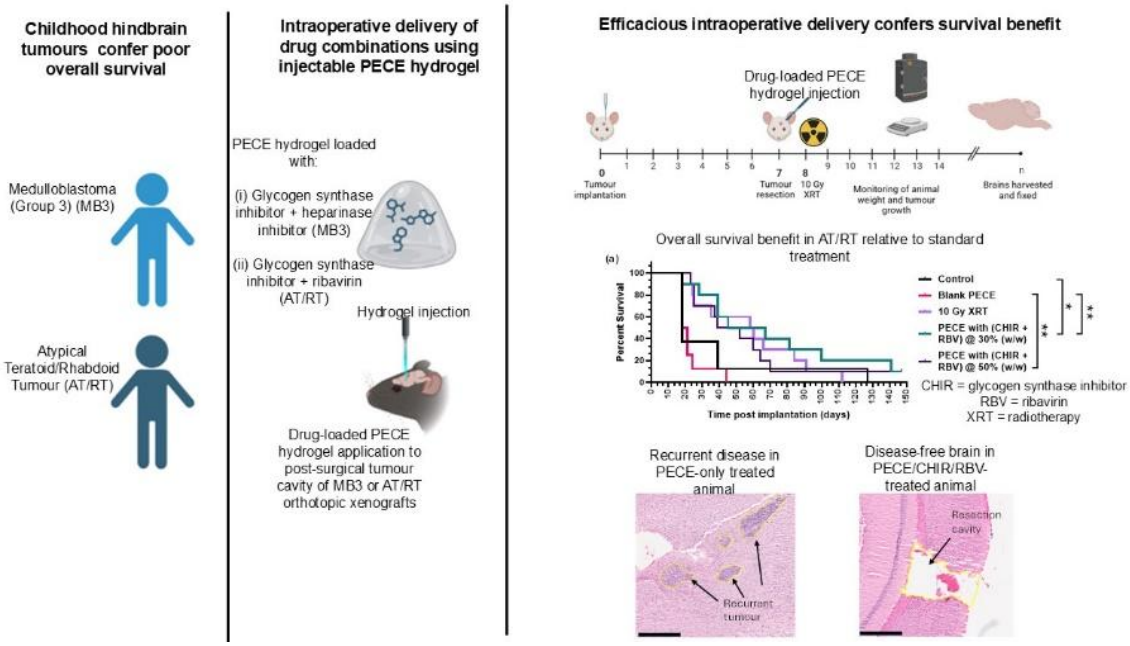

Figure 1. Intraoperative combination drug delivery using PECE hydrogel confers survival benefit to childhood brain tumour orthotopic xenografts.

Platform for Post-Surgical Osteosarcoma Therapy and Bone Regeneration

Arathyram Ramachandra Kurup Sasikala [a]*, Vignesh Krishnamoorthi Kaliannagounder [b], , Afeesh Rajan Unnithan [a]

[a] Centre for Pharmaceutical Engineering Science, School of Pharmacy and Medical Sciences, University of Bradford, UK

[b] School of Engineering, Newcastle University, Claremont Road, Newcastle upon Tyne, UK

* Corresponding author(s) e-mail(s): a.ramachandrakurupsasikala@bradford.ac.uk

Introduction

Osteosarcoma is a highly aggressive bone cancer with limited treatment options, often resulting in tumour recurrence, drug resistance, and large post-surgical bone defects[1,2]. To address these challenges, we developed PiezoMagnetic Nanoparticles (PMNPs)—a multifunctional nanoplatform combining piezoelectric barium titanate and superparamagnetic iron oxide. PMNPs enable magnetic hyperthermia, photothermal and photodynamic therapies, along with multimodal imaging and bone-targeted delivery via risedronate3. Importantly, they promote bone regeneration through non-invasive electrical stimulation using low-intensity pulsed ultrasound (LIPUS). This "theranogeneration" strategy integrates cancer therapy, diagnosis, and regeneration into a single system, offering a novel, non-invasive approach for post-surgical osteosarcoma management.

Materials and methods

PiezoMagnetic nanoparticles (PMNPs) were synthesised by coating solvothermally prepared tetragonal barium titanate nanoparticles with iron oxide via coprecipitation. Risedronate was loaded for bone targeting. PMNPs were characterised using TEM, XRD, Raman, XPS, UV–vis, FT-IR, and magnetic measurements. Electrochemical and piezoelectric properties were assessed using impedance spectroscopy and a nanogenerator device. Heat generation was tested under AMF; LIPUS was applied to study drug release. Cellular uptake, cytotoxicity, and anticancer effects were analysed in MC3T3 and Saos-2 cells. Regenerative potential was evaluated via LIPUS-stimulated osteoblast cultures using viability assays, cytoskeletal staining, Alizarin Red S, and calcium quantification.

Results and Discussion

The multifunctional PiezoMagnetic nanoparticles (PMNPs) exhibited excellent

structural integrity, with HR-TEM and XRD confirming the formation of tetragonal BTNPs and surface-coated Fe_3O_4. Raman and XPS analyses validated crystallinity and risedronate (RIS) functionalisation. Electrochemical impedance spectroscopy revealed improved conductivity, while ferroelectric testing confirmed intrinsic piezoelectricity. PMNPs generated significant voltage output under mechanical stress, successfully powering capacitors and LEDs. In vitro, PMNPs demonstrated excellent biocompatibility and were efficiently internalised by osteoblasts and osteosarcoma cells. Under AMF and NIR exposure, PMNPs induced robust magnetic hyperthermia, photothermal, and photodynamic effects, leading to significant apoptosis in Saos-2 cells. SHG and confocal imaging enabled label-free nanoparticle tracking. LIPUS stimulation enhanced RIS release, promoting osteogenic differentiation and calcium deposition in MC3T3 cells. Overall, the results confirm that PMNPs function as a promising theranostic nanoplatform for non-invasive cancer therapy and bone regeneration, combining multimodal treatment efficacy, imaging, and electroactive tissue regeneration in a single, targeted nanosystem.

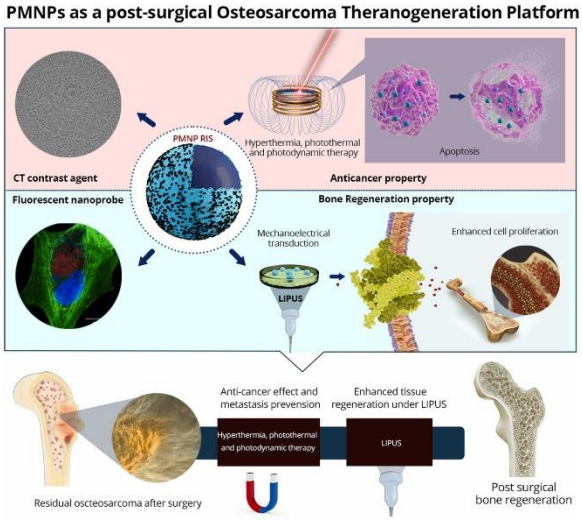

Figure 1. Schematic illustration depicting the stepwise theranostic strategy of PiezoMagnetic Nanoparticles (PMNPs): multimodal treatment of osteosarcoma via magnetic hyperthermia, photothermal and photodynamic therapies, followed by LIPUS-stimulated osteogenesis for bone regeneration.

References

1) I.E. Palama, V. Arcadio, S. D'Amone, M. Biasiucci, G. Gigli, B., Sci. Rep. (2017), p. 7

2) R.K. Heck, T.D. Peabody, M.A. Simon, Ca-Cancer J. Clin., 56 (6) (2006), pp. 366-375.

3) W. Liu, A. Hajibeigi, M. Lin, C.L. Rostollan, Z. Kovacs, O.K. Oz, et al., Bioorg. Med. Chem. Lett., 18 (17) (2008), pp. 4789-4793

High-Affinity nanoMIPs: Synthetic Antibody Alternatives for Diagnostics

Reddy, S.M. *

[a] Chemistry Division, School of Pharmacy & Biomedical Sciences, Centre for Smart Materials, Institute of Materials and Investigative Sciences
University of Central Lancashire, Preston, PR1 2HE, United Kingdom

* *Corresponding author(s) e-mail(s): smreddy@uclan.ac.uk*

Introduction

Antibodies are produced by the body playing a crucial role in the natural immune response to harmful substances such as viruses, bacteria and chemicals. Antibodies are also being used widely in protein diagnostics and sensors to detect infection and disease. Antibody application in diagnostics presents issues related to their ethical sourcing, cost of production, temperature and pH instability. Synthetic receptors such as nanoscale molecularly imprinted polymers (nanoMIPs) are being intensively researched as stable and low-cost alternatives to biological antibodies in diagnostic and medical imaging applications. They can be rapidly produced (in a matter of hours) and these smart materials offer the promise of replacing antibodies in protein immunodiagnostics, biosensors, protein extraction and therapeutics. There is still a gap in economically scaling up the mass production of nanoMIPs.

We address this using our proprietary bioreactor-type approach where the protein template is re-usable because it is tethered to bespoke (size-tuned) microwave synthesised magnetic nanoparticles (MNP).[1]

Materials and methods

All monomers, proteins and reagents were used as received from Merck. Recombinant nucleocapsid protein for SARS-CoV-2 was purchased from BioservUK Ltd (Rotherham, UK). DropSens disposable screen-printed electrodes (Au-BT) were purchased from Metrohm (Runcorn, Cheshire, UK). A range of characterisation techniques were using to characterise MNPs (DLS, TEM) and nanoMIPs (DLS, AFM, electrochemistry and SPR).

Results

The MNPs are size-tunable[1], have high stability, small size, rapid reaction kinetics, and ease of surface functionalisation allowing the tethering of proteins (**Figure 1**). We subsequently demonstrate a facile

one-day method to produce five batches of up to 10 mg/mL each of high affinity nanoMIPs using our protein functionalised MNP solid-phase process.[1,2] Crucially, the protein functionalised MNP can be regenerated for subsequent cycles of nanoMIP synthesis with no deterioration in nanoMIP affinity between cycles thereby reducing the cost burden on template requirement and offering a sustainable approach to scale the synthesis of these antibody replacement materials to gramme scale quantities within a day.

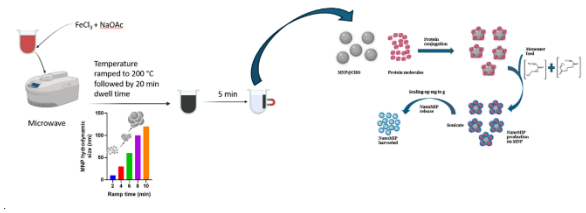

Figure 1: Microwave synthesis of MNPs and subsequent nanoMIP synthesis

The nanoMIPs demonstrated high (antibody-like) sub-nanomolar affinity for its protein target.

Discussion

Our nanoMIP production method delivers a high yield, short time to production and reduced number of steps involved while still offering acceptable protein binding affinities. Additionally, our ability to simply separate the MNP@protein particles using an external magnet and re-use it for multiple nanoMIP synthesis cycles with an overall <20% reduction in nanoMIP yield is a key step change compared to existing methods, offering scaling in yield and minimising target template required. We therefore present a facile route to produce nanoMIPs in large industrially relevant quantities (100s of mg) and at short timescales (within a day). Our method offers realistic opportunities for industry to adopt such materials as an antibody replacement technology in diagnostics, biological extraction and therapeutics.

Acknowledgements

For financial support we thank the University of Central Lancashire, The Royal Society of Chemistry COVID-19 Action fund (H20-188) and RSC Research Enablement Grant (E22-5899202825), and the Daiwa Anglo-Japanese Foundation (13094/13916).

References

1) S. Reddy, A. Stephen, M. Holden, W. Stockburn, S. Dennison, *Biomaterials Science*, 2024, **12**(22), 5845.

2) A. Stephen, T. Mercer, W. Stockburn, S. Dennison, J. Readman, S. Reddy, *Materials Advances*, 2025, **6**, 2016.

Smart Polymers in the fight against anti-microbial resistance

Rimmer, S. [a,b]*

[a] Molecular Titans Ltd, UK

[b] University of Bradford, UK

* Corresponding author(s) e-mail(s): S.Rimmer@bradford.ac.uk

Abstract

Stimulus responsive polymers (or smart polymers) have been widely studied mand whist the response of these materials to changing environment (ie to stimuli) can take a number of forms the most studied area involves a reversible change in solvation. This can occur at upper or lower critical temperatures and is generally regarded as a switch from an equilibrium fully solvated “coil” state to a partially solvate “globular” state. In part this transition mirrors protein refolding of peptide segments in response to stimuli but in these natural systems the changes are from quasi-stable non-equilibrium states.

Several stimuli have been well reported including pH, salt, temperature, stress fields but in our work, we have shown that it is possible to induce the transition by binding to biological entities. The key to this type of response is the branched nature of the amphiphilic polymers and location of the ligands at chain ends. In early work we assumed that on binding the whole of polymer coil became desolvated but as our work progressed, we gathered evidence that showed that the desolvation is occurring at a segment level; the length of these smart segments remains an unanswered question, but a working hypothesis is that the critical segment is average sequence before the first branch point.

In this presentation we will show how we synthesise the polymers, how we journey to develop a better theory of the response behaviour and the applications of these systems as diagnostics. Our systems provide data on infection with bacteria or fungi; provide new lab. tools and can be used to manipulate human and microbial cells.

Over 20 years we have reported the performance and behaviour of these systems, and we produced prototype wound dressings, ophthalmic swabs and now focus on urinary tract infections and other infectious disease states. Our aim is now mainly to translation and commercialisation in real clinical and community scenarios via our new spin out:

“Molecular Titans”. We will describe vital data on this journey including routes to scale up and waste minimisation, biocompatibility and efficacy.

Bioactive Polysaccharide-Protein Interactions Inhibit Fibrosis

Brunet, M.Y.[a], Chapple I.[b], Heagerty, A.H.M.[c], Miljus, T.[d], Calebiro, D.[d], Metcalfe, A.D.[a], Grover, L.M.[a], Gillis, R.B.[e], Kitchen, P.[f], Robinson T.E. [a,*]

[a] Healthcare Technologies Institute, University of Birmingham, UK

[b] School of Dentistry, University of Birmingham, UK

[c] Institute of Inflammation and Aging, University of Birmingham, UK

[d] Department of Metabolism and Systems Science, University of Birmingham, UK

[e] National Centre for Molecular Hydrodynamics, University of Nottingham, UK

[f] Health and Life Sciences, Aston University, UK

* Corresponding author(s) e-mail(s): T.E.Robinson@bham.ac.uk

Introduction

Polysaccharides are used extensively as structural biomaterials, to augment drug release profiles and act as tissue engineering scaffolds. In these applications the polysaccharides are considered biologically inert, however there is growing evidence that some polysaccharides can exhibit considerable therapeutic efficacy.

Scarring and fibrosis can affect almost every organ in the body, causing disfigurement, disability and even death. On a cellular level, scarring occurs when transforming growth factor beta 1 (TGFβ1) causes fibroblasts to transdifferentiate into ‘activated’ myofibroblasts, which are far more contractile and able to rapidly produce ECM: this is essential for fast healing, but continued activity leads to fibrosis.

The aim of this study was to investigate whether polysaccharides can dampen this effect, by interacting with TGFβ1 and preventing it from binding its receptor and thus curbing excessive fibrosis.

Materials and methods

Fibrosis was modelled *in vitro* by exposing human dermal fibroblasts to transforming growth factor beta 1 (TGFβ1), triggering myofibroblast transdifferentiation. The extent of this was measured through immunofluorescence imaging and RT-qPCR, with alpha smooth muscle actin as the primary marker of myofibroblast transdifferentiation.

Biophysical methods were utilised to directly probe the interaction between the polysaccharides and TGFβ1.

Results

Several polysaccharides were investigated in the *in vitro* model, and while some showed no effect, others displayed considerable efficacy. Carrageenans, particularly the iota subtype, significantly prevented myofibroblast transdifferentiation, in a concentration dependent manner (Figure 1).

Dynamic light scattering showed the formation of large particles when carrageenan and TGFβ1 were combined, suggesting aggregation. Flow induced dispersion analysis corroborated this finding, showing an increase in hydrodynamic radius of TGFβ1 in the presence of the polysaccharide, as well as an increase in spike count, suggesting aggregation, and tryptophan emission, which is direct evidence of a molecular interaction.

Discussion

This data suggests that carrageenan strongly binds TGFβ1, preventing it from interacting with the receptors on fibroblasts that cause myofibroblast transdifferentiation, and thus inhibiting the fibrotic response.

As a structural biomaterial, this presents the opportunity to formulate carrageenan into a structured fluid, to combine its bioactivity with material properties to improve retention, and additional beneficial properties such as lubrication. The long use of carrageenans in food and pharmaceuticals will minimise translational hurdles, allowing such therapies to reach the market, and human benefit, sooner.

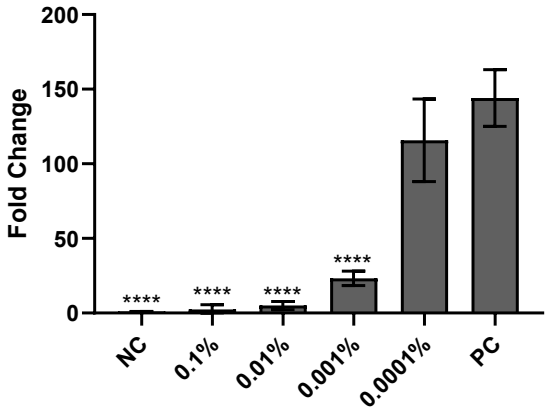

Figure 1. Fold change in αSMA gene expression at different iota carrageenan concentrations

Acknowledgements

I would like to thank DEBRA UK and the Rosetrees Trust for their financial support of this work.

Biomaterials Advances Keynote Lecture: Engineered biomaterials for regeneration and mechanobiology

Day, G.; [a,b] Salmeron-Sanchez, M. [a,b]*

[a] Professor of Biomedical Engineering at the University of Glasgow, UK.

[b] ICREA Research Professor at Institut de Bioenginyeria de Catalunya (IBEC).

* Manuel.Salmeron-Sanchez@glasgow.ac.uk

Abstract

The physical properties of the extracellular matrix (ECM) and the use of growth factors are powerful tools to control cell behaviour, including fundamental processes such as cell migration and (stem) cell differentiation. Integrins are mechanotransductors that feel and respond towards the mechanical properties of the ECM. We have developed material systems that allow simultaneous stimulation of integrins and growth factors receptors. We have engineered polymers and 3D hydrogels that unfold and assemble proteins to allow exposure of the integrin and growth factor binding regions. For example, we show the use of BMP-2 in synergy with α5β1 integrins to promote osteogenesis and regeneration of critical-sized defects. Further, we have developed interfaces that bind latent proteins that induce integrin-mediated mechanical activation of growth factors. We will demonstrate the use of TGF-β1 that is released and activated by using engineered surfaces that organise fibronectin to promote binding of LTBP1 and enable integrin B1 to pull on active TGFB1. In the second part of the talk, we will use surfaces of controlled viscosity in our pathway to engineer and understand the viscoelastic properties of the ECM. We use supported lipid bilayers that are functionalised with either RGD (integrin binding) or HAVDI (cadherin binding) to demonstrate the molecular clutch is engaged on surfaces of high enough viscosity and, importantly, that it is weaken upon N-cadherin binding, controlled by the competition between vinculin and α-catenin for actin filaments. We then introduced substrates of controlled elasticity and viscosity, first in 2D using polyacrylamide hydrogels that were further patterned using fibronectin and then in 3D using PEG-hydrogels functionalised with fibronectin. We will discuss the unexpected interplay between viscoelasticity, cell adhesion and molecular clutch engagement. We introduce Brillouin microscopy as a way to follow the evolution of the viscoelastic properties of cells and the engineered hydrogels in 3D in a non-invasive way and in real time.

Perivascular biodegradable mesh for the controlled delivery of the corticosteroid dexamethasone for treatment of vein graft disease

S.Kasi , J.Shepherd *

University of Leicester, United Kingdom.

* Corresponding author e-mail: js1005@leicester.ac.uk

Introduction

The long saphenous vein (LSV) sees regular use as a vein graft for coronary artery bypass within the NHS, primarily due to its length and ease of access. The LSV successfully restores blood flow to the coronary artery [1] but hemodynamics and the high pressure within the thin walls of LSV triggers a cascade of events. These events eventually lead to blockage of veins and vein graft failure [2]. Pre-treating LSVs with dexamethasone (dex) has been shown to arterialise the vein thus eliminating vein graft failure [3]. Targeted dexamethasone delivery to LSVs can promote patency rates while avoiding toxic doses of dex administered centrally to patients. This work considers the development of external unidirectional drug delivering conduits for targeted drug delivery. Collagen was the primary choice of biomaterial to contain and deliver dex; due to its excellent biocompatibility and hypothesised lack of influence upon drug on release.

Materials and methods

Collagen slurry of multiple solid loadings (0.5%(w/v), 1%(w/v), and 2%(w/v)) were prepared by swelling type 1 collagen in 0.05M of acetic acid and homogenising at 10000rpm for 25 minutes. The homogenised slurry was degassed and desired drug concentration (20uM-200uM) added. Post drug incorporation, the slurry was vortex at 4500rpm for 3-5 minutes and poured into a silicone mould (dimensions calculated from circumference of LSV). Samples were lyophilised to produce porous collagen sheets containing dex prior to be being rolled and adhered using 2%(w/v) collagen slurry. A short lyophilisation cycle produced adhered collagen sheets. Nonporous collagen films (1%(w/v)) were produced by air drying collagen slurry over well plate lids. Further, the non-porous collagen film was adhered to drug containing porous collagen sheets using 2%(w/v) collagen slurry and lyophilised. Hence, the unidirectional conduit was successfully produced as shown in fig. (1).

Results

Scanning electron microscopy (SEM) images of the porous drug loaded collagen sheets exhibited good connectivity and porosity across all drug doses and concentrations of collagen. SEM images of the conduits after a month of degradation exhibited good integration between the porous collagen sheet and non-porous collagen films as shown in fig. (2). Drug release studies performed using UV spectroscopy at 240nm for various drug concentration and density of collagen helped elucidate drug loading and release mechanism. Physiologically relevant drug release was observed without burst response during the whole intended period of application of conduits as per the clinician's specification.

Discussion

The multiple layers within the conduit remained integrated after 31 days of degradation. Particularly significant was that the collagen film adhered on the conduit, remained nonporous after degradation; this is hypothesised to support continued unidirectional drug release. Ongoing studies with in-vitro and ex vivo models will confirm the efficiency of the designed conduit. Further these conduits can also help understanding drug uptake mechanisms extra-venously, allowing a comparison of efficiency with intravenous drug delivery.

Fig.1.SEM image of cross section of conduits showing integration of non-porous film and porous collagen sheet after degradation study.

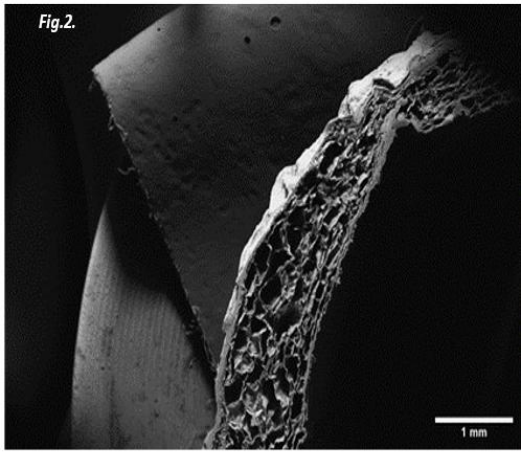

Fig.2. Unidirectional drug delivering conduit produced by multi-step lyophilisation process.

Acknowledgements

For financial support we thank University of Leicester's future 100 scholarship, the technical help and support of the staff and microanalysis equipment at the Hercules facility at University of Leicester supported by EPSRC grant EP/X0114614/1.

References

1) Diodato and Chedrawy, **2014**, 10.1155/2014/726158.

2) Ladak et al., **2022**, http://dx.doi.org/10.1093/eurheartj/ehac544.3084.

3) Zakkar et al., **2011**, https://doi.org/10.1161/circulationaha.110.979542.

Nitric oxide releasing materials (NORMs) for cardiovascular therapeutics

Tabish, Tanveer A.

Radcliffe Department of Medicine, University of Oxford, UK

* Corresponding author e-mail: tanveer.tabish@cardiov.ox.ac.uk

Introduction: For more than a century, nitric oxide (NO) donating formulations such as organic nitrates and nitrites have been a cornerstone for the treatment of cardiovascular diseases. These donors primarily produce NO systemically, however it would be desirable to deliver the right amount of NO to a precise location at the right time. To address this need, we hypothesised that graphene-based nanomaterials can be developed to store and release therapeutic amounts of NO in a controlled fashion.

Methodology & results: We describe the design and characterisation of a novel NO delivery system via the incorporation of sodium nitrite as a NO source into porous graphene oxide nanosheets (termed NO@Th-PGO) **(Figure)**. The exchange between functional groups and the corresponding morphologies were confirmed by X-ray diffraction (XRD), Fourier transform infrared spectroscopy (FTIR), Raman spectroscopy and scanning electron microscopy (SEM). The real-time release of NO from NO@Th-PGO was measured using a free radical analyser equipped with NO electrode and the total capacity for NO production by ozone-chemiluminescence. The NO release was sustained at >5 × $x10^{-10}$ mol cm^{-2} min^{-1} for at least 3 hours, which is comparable to production by healthy endothelium (cf, 0.5 – 4 $x10^{-10}$ mol cm^{-2} min^{-1}). The underlying mechanism of NO release likely involves a role for thiols as a reducing agent, thereby converting graphene-conjugated nitrite into NO. To test whether NO released from NO@Th-PGO is localised intracellularly, we used a fluorescent NO-specific probe, 4-amino-5- methylamino-2′,7′-difluorofluorescein (DAF-FM DA) for real-time imaging. This detected the release of NO from NO@Th-PGO in both vascular endothelial and smooth muscle cells. Furthermore, exposure of vascular cells to NO@Th-PGO *in vitro* increased endothelial cell proliferation and inhibited smooth muscle cell growth.

Conclusions: Here we demonstrate the utility of porous graphene as a NO delivery vehicle to release physiologically relevant amounts of NO in culture. This work highlights the potential of these formulations as a promising strategy for the treatment of cardiovascular diseases.

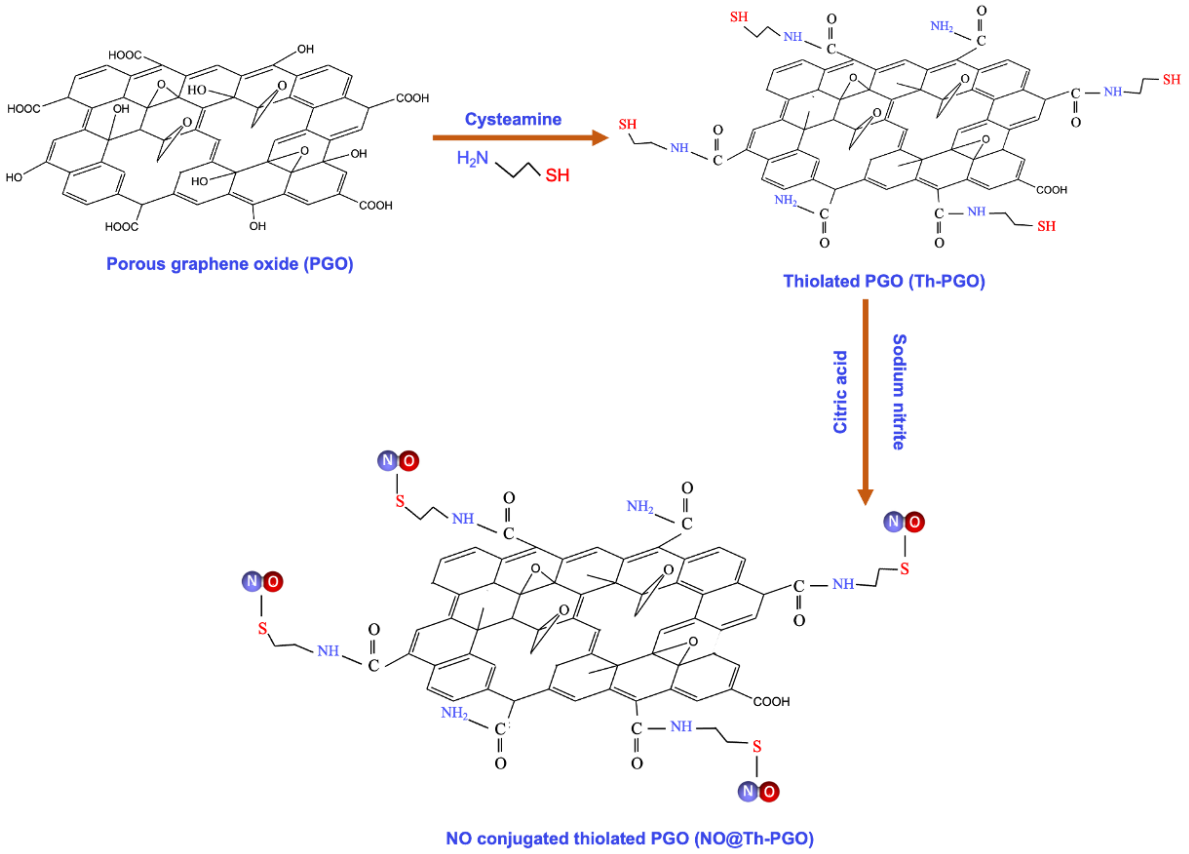

Figure: Schematic showing crosslinking of thiol groups to porous graphene oxide (PGO) followed by conjugation of acidified nitrite.

Acknowledgements

This work was supported by a British Heart Foundation (BHF) Fellowship (FS/ATA/21/20015) to Dr Tabish.

Polymer particles for sensing and imaging.

Willcock, H.
Loughborough University, UK.
Email: h.willcock@lboro.ac.uk

Introduction

Polymers are versatile and robust platforms for functional groups, and their composition and morphology can be easily tuned using techniques such as reversible addition fragmentation chain transfer (RAFT) polymerisation. Stimuli responsive or "smart" polymers switch their properties rapidly on response to changes in temperature or pH, and this can be used to modify the behaviour of materials.

Discussion

Some of our recent examples of polymers in imaging materials and nanocomposites will be described. A new strategy for the preparation of Magnetic Resonance Imaging (MRI) agents from polymerizable Gd containing metal complexes will be shown[1].

Following this, tuning of the particle size by controlling the block length ratios of larger PPEGMA/MEM-b-PMMA assemblies will be described, demonstrating limits to their size and stability[2]. Current work based on the incorporation of MRI active and luminescent monomers into responsive polymer particles to allow switchable systems will be highlighted.

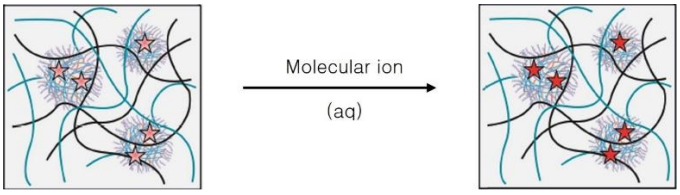

Figure 1. Representation of our anion sensing technology[3].

Finally, our patented dual encapsulation technique to allow anion sensing luminescent probes to be trapped within hydrogels for continuous sensing of a variety of analytes will be described (Figure 1).[3]

References

1) Chemical Science, 2021, 12, 3999-4013.
2) Polymer Chemistry, 2022,13, 4124-4135.
3) Europe (EP3844241A1), United States (US2021230479A1) and Australia (AU2019328725A1). Chemical Communications, 2024,60, 284-287.

Advanced antibacterial surfaces by integrating laser surface structuring with biopolymer composite coating

Wang, Y., Dong, Y., Wackerow, S., Abdolvand, A., Zolotovskaya, S.A. *, Zhao, Q.
School of Science & Engineering, University of Dundee, Dundee DD1 4HN, UK
* Corresponding author e-mail: s.a.zolotovskaya@dundee.ac.uk

Introduction

Health-associated infections (HAIs) remain a major clinical concern, often arising from biofilm-contaminated medical devices such as catheters, prosthetics, and orthopaedic implants. These biofilm-related infections pose significant treatment challenges due to the protective nature of biofilms. In the EU alone, ~4.1M patients are affected by ~4.5M episodes of HAIs annually, incurring financial losses of ~€7B. In the US, similar infections account for over US$6.5B, including direct costs associated with 16M extra days of hospital stay. The efficacy of conventional antibiotic therapies is increasingly compromised by the emergence of antimicrobial resistance (AMR). Projections indicate that drug-resistant infections could result in ~10M deaths per year by 2050, highlighting the urgent need for alternative, antibiotic-free antimicrobial strategies.1 Surface morphology and chemistry play critical roles in bacterial attachment and colonisation. Existing surface modification approaches typically target a single antimicrobial pathway - either physical or chemical. Physical methods typically include topographical alterations, while chemical approaches often involve antimicrobial coatings.

This study presents an innovative hybrid antibacterial approach that combine both physical and chemical cues by coupling laser surface structuring with a composite biopolymer coating. Specifically, laser-induced periodic surface structures were integrated with a polydopamine-chitosan-silver nanoparticle composite coating to produce hybrid surfaces with significantly enhanced antibacterial and antibiofilm performance. These surfaces achieved bactericidal efficiencies of 96.9% against E. coli and 91.9% against S. aureus after a 16-h incubation period. Furthermore, the surfaces effectively inhibited E. coli attachment and biofilm formation over a 24-h incubation period, demonstrating strong potential for clinical applications.

Materials and methods

Laser surface structuring was performed on as-received titanium (Ti) foils using a frequency-doubled Nd:YAG laser system (Talisker Ultra, Coherent), operating at a 10-ps pulse duration and 50-kHz repetition rate. This resulted in formation of low spatial frequency laser-induced periodic surface structures (LIPSS) with an average period of ~350 nm. The LIPSS-textured Ti surfaces (Ti-LIPSS) were subsequently coated with a polydopamine–chitosan (PDA-CS) composite via electroless deposition in a weakly acidic aqueous solution. This followed by the silver nanoparticles (AgNP) deposition on the PDA-CS-coated Ti-LIPSS substrates (Ti-PCA@LIPSS).

Results

The antibacterial efficacy of untreated Ti, Ti-LIPSS, Ti-PCA, and hybrid Ti-PCA@LIPSS surfaces was evaluated using two representative bacterial strains: E. coli and S. aureus. Bacterial adhesion was assessed at incubation periods of 2, 6, 12, and 16h. All surface modifications significantly reduced bacterial attachment compared to the untreated Ti surface. Ti-LIPSS and Ti-PCA exhibited only marginal differences in the total number of adhered E. coli and S. aureus. In contrast, the hybrid Ti-PCA@LIPSS surface consistently demonstrated the lowest bacterial adhesion across all incubation periods.

At the 2-h incubation mark, the Ti-PCA@LIPSS surface achieved bacterial inhibition rates of 88.6% for E. coli and 80.0% for S. aureus. This enhanced early-stage antibacterial performance is attributed to the synergistic effect of the LIPSS topography - which disrupts initial bacterial adhesion - and the bactericidal activity of the PCA coating, including the increased loading of CS and AgNPs facilitated by the structured surface. At longer incubation time, the hybrid surface maintained its antibacterial efficacy, showing a sustained reduction in both total and viable bacteria relative to the Ti-LIPSS and Ti-PCA surfaces alone. This superior performance demonstrates the importance of integrating both mechanical and chemical cues, which influence different stages of bacterial adhesion and survival. The maximum bactericidal efficiencies reached 96.6% for E. coli and 91.9% for S. aureus after 16h, highlighting the effectiveness of the multifunctional design in activating complementary antibacterial pathways.

To further assess biofilm formation, E. coli incubation was extended to 24h (Figure 1).

Substantial bacterial attachment and biofilm development were observed on untreated Ti and Ti-LIPSS surfaces. In comparison, the Ti-PCA surface exhibited reduced bacterial aggregation and improved resistance to biofilm formation (Figure 1a). The Ti-PCA@LIPSS surface (Figure 1 b-d) showed the most effective suppression of bacterial attachment and complete inhibition of biofilm formation after 24h, confirming the long-term antibacterial potential of the hybrid surface.

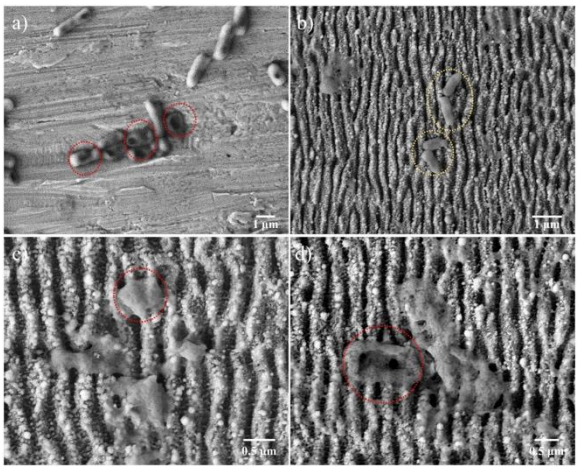

Figure 1. Representative SEM images of *E. coli* on the Ti-PCA (a) and Ti-PCA@LIPSS surfaces (b-d) after 24h incubation time.

Discussion

Conventional antibacterial technologies typically target bacterial attachment through either surface topography modification or chemical coatings, each leveraging a single mode of action. Hybrid strategy that combines both physical and chemical antibacterial mechanisms is emerging as a compelling solution, overcoming the individual limitations of each approach. This integrated strategy offers the potential for enhanced antibacterial performance, improved durability, and increased biocompatibility.

References

1. E. Utt, C. Wells, Pharmaceuticals Policy and Law, 2016, 18, 179.

2. Y. Wang, Y. Dong, Y. Quan, S. Wackerow, A. Abdolvand, S.A. Zolotovskaya, Q. Zhao, Advanced Materials Interfaces, 2025, 12, 2400660.

ECRs: Postdoctoral researchers' abstracts

Biodegradable and Biocompatible Plant-based Chitosan-Pyrophosphate Micropowders for Potential Haemostatic applications

Baiocco, D. [a,b*], Zhang Z. [b], Grover, L.M [a,b,*]

[a] Healthcare Technologies Institute, Institute of Translational Medicine, Birmingham, UK

[b] School of Chemical Engineering, University of Birmingham, Birmingham, UK.

* l.m.grover@bham.ac.uk ; d.baiocco@bham.ac.uk

Introduction

Haemostasis remains a critical challenge, particularly in managing torrential bleeding, where rapid and effective clotting is essential.[1] Conventional haemostatic agents often exhibit limitations, including heat generation and degradability issues, thereby necessitating the development of novel engineered materials. Composite materials, such as pyrophosphate (pyr)-based particles, have demonstrated significant pro-thrombogenic potential, especially when combined with peptide drugs.[2] Yet, peptide-based formulations are undesirably costly. Recently, biopolymer-assisted (e.g. animal-sourced chitosan) haemostatic agents have drawn interest due to their inherent haemostatic efficacy. However, haemostatic formulations featuring the synergistic action from both organic and inorganic materials have not been largely investigated. Moreover, no related reports centring on biodegradable, biocompatible, plant-based chitosan (pCh) have appeared in the public domain.[3]

Materials and methods

We investigated the feasibility of developing finely dispersed pCh-pyr hybrids through ionic interaction at a controlled pH of ~5.1 to maximise the electrostatic interaction between the two species. Structural and physicochemical properties, including morphology, surface topography, and mechanical strength, were systematically analysed via scanning electron microscopy (SEM), Raman spectroscopy, and micro-manipulation based on diametrical compression between two parallel surfaces.[4]

Results

Free-flowing micropowders of pCh-pyr hybrid crystals (HyCs), with a particle size of 46.4 ± 2.1 μm, were successfully obtained. Morphological analysis (**Figure 1**) revealed relatively large and irregularly shaped HyCs, indicative of the unique structural arrangement induced by the rapid ionic crosslinking. The mechanical compression strength of the HyCs was 2.4 ± 0.3 MPa, with a Young's modulus of 0.18

± 0.04 GPa, suggesting a degree of ductility that may enhance their adaptability to wound beds. Furthermore, the presence of pyr and pCh in HyCs suggest a high water absorption capacity and antimicrobial activity, reinforcing their potential for haemostatic applications.

Discussion

The integration of pCh with pyr yielded a novel hybrid material with promising mechanical properties, enhanced water uptake, and a distinctive structural morphology. These findings suggest strong potential for next generation of biodegradable haemostatic agents. Future work will entail the quantification of the haemostatic performance of pCh-pyr HyCs (e.g. blood clotting time, antimicrobial activity). Details of this work will be presented.

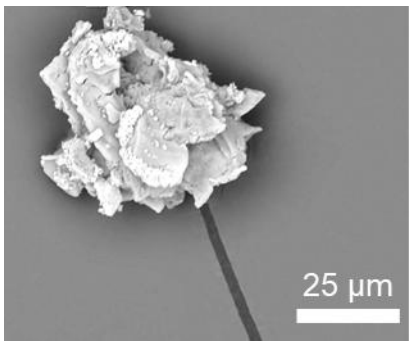

Figure 1. SEM micrograph of a single pCh-pyr HyC.

Acknowledgements

For financial support we thank National Institute for Health and Care Research (NIHR203395) and the European Health and Digital Executive Agency (grant number 101092242).

References

1) B. Guo, R. Dong, Y. Liang and M. Li, *Nature Reviews Chemistry*, 2021, **5**, page. 773-791
2) D.C. Bassett, T.E Robinson, R.J. Hill, L.M. Grover and J.E. Barrelet, *Biomaterials Advances*, 2022, **140**, 213086
3) D. Baiocco, M. Al-Sharabi, B.T. Lobel, O.J. Cayre, A.F. Routh and Z. Zhang, *ACS Omega*, 2024, **9(26)**, 28385-28396
4) G. Sun, Z. Zhang, *International Journal of Pharmaceutics*, **242(1-2)**, 307-311

Repurposing Laboratory Plastic into Functional Fibrous Scaffolds via Green Electrospinning for Cell Culture and Tissue Engineering Applications

Berri, N. [a,c], Moise, S. [a,c], Keirouz, A. [a], Jennings, A.[b], Castro Dominguez, B [a,d], Leese, H.S.[a,c] *

[a] Department of Chemical Engineering, University of Bath, Bath, BA2 7AY, UK.

[b] Department of Mechanical Engineering, University of Bath, Bath, BA2 7AY,

[c] Centre for Bioengineering & Biomedical Technologies (CBio), UK.

[d] Centre for Digital Manufacturing and Design (dMaDe), UK.

* Corresponding author(s) e-mail(s): H.S.Leese@bath.ac.uk

Introduction

Plastic waste is a significant environmental challenge, contributing to global warming throughout its life cycle[1]. While efforts to address this issue are underway at international, national, and industry levels, developing sustainable practices within laboratory settings is also essential. This study explores repurposing plastic lab waste through green solvents processing for electrospinning eco-friendly fibrous membranes. Integrating these solvents enhances environmental sustainability without compromising fibre quality. This approach not only repurposes discarded lab plastics but also provides a sustainable alternative to traditional tissue culture plastics.

Materials and methods

Electrospun scaffolds were fabricated using green solvents (Cyrene and Dimethyl carbonate) and polystyrene Petri dishes. Scaffolds were characterized using scanning electron microscopy (SEM), attenuated total reflectance Fourier-transform infrared spectroscopy (ATR-FTIR), and porometry to assess morphology, chemical composition, and porosity. Biological characterization included confocal microscopy, metabolic assays, and Alizarin red staining. MG-63 osteoblast-like cells were employed for in vitro studies. Osteogenic differentiation was induced using media supplemented with dexamethasone, ascorbic acid, and β-glycerophosphate. Prior to cell seeding, scaffolds underwent oxygen plasma surface treatment to enhance cell attachment. MG-63 cells were then seeded onto the plasma-treated, green solvent-based scaffolds to evaluate cellular responses and osteogenic potential.

Results

Electrospun scaffolds constructed with green solvent-based spinning dopes

yielded both aligned and non-aligned fibre configurations with mechanical properties comparable to cancellous bone. Biocompatibility and osteogenic potential were confirmed using MG63 osteoblast-like cells, which exhibited increased DNA content and metabolic activity over time. Confocal microscopy revealed that the green scaffold alignment influenced cell morphology, while osteogenic differentiation was supported by mineral deposition on both scaffold types[2].

Discussion

This study demonstrates that green electrospinning can repurpose laboratory plastic waste into functional, sustainable biomaterial scaffolds. Utilising green solvents, the process offers environmental and cost benefits without compromising scaffold quality. The mechanical properties are comparable to cancellous bone, and MG63 cell assays confirmed biocompatibility, adhesion, proliferation, and osteogenic differentiation. Confocal microscopy revealed that fibre alignment influences cell morphology and mineral deposition. These findings highlight the potential of integrating green electrospinning with lab plastic recycling as a sustainable approach for tissue engineering.

Acknowledgements

This work was founded by BioMed 4.0, EPSRC grant code EP/V051083/1.

References

1) Chawla, S., Varghese, B. S., Hussain, C. G., Keçili, R., & Hussain, C. M. (2022). Environmental impacts of post-consumer plastic wastes: Treatment technologies towards eco-sustainability and circular economy. Chemosphere, 308, 135867.

2) Berri, N., Moise, S., Keirouz, A., Jennings, A., Castro-Dominguez, B., & Leese, H. S. (2025). Repurposing Laboratory Plastic into Functional Fibrous Scaffolds via Green Electrospinning for Cell Culture and Tissue Engineering Applications. *ACS Biomaterials Science & Engineering*.

Carrageenan-Gel-MA Hydrogels for Bone Tissue Engineering Scaffolds

Chaves Filho, G.P. [a, b*], Santos, P. [a]., Ramos, A.P. [b], Domingos, M. [a]

[a] Department of Mechanical and Aerospace Engineering, School of Engineering, Faculty of Science and Engineering & Henry Royce Institute, The University of Manchester, Manchester, UK

[b] Department of Chemistry, Faculty of Philosophy, Science and Letters at Ribeirão Preto, University of São Paulo, Ribeirão Preto, Brazil;

* Corresponding author(s) e-mail(s): gildacio.chavesfilho@manchester.ac.uk

Introduction

Engineering bioinks that combine mechanical robustness, bioactivity, and printability remains a core challenge in bone tissue engineering. Gelatin methacryloyl (Gel-MA) hydrogels are promising due to their tunable properties and biocompatibility, yet they often lack sufficient mechanical strength for hard tissue applications. In this study, we explore the incorporation of 0.5% (w/v) carrageenan into GelMA hydrogels to enhance their rheological behavior and mechanical performance without compromising biocompatibility. We further evaluate their potential to support human mesenchymal stem cell (hMSC) viability and osteogenic differentiation *in vitro*.

Materials and methods

Gel-MA was synthesized from porcine gelatin and characterized by ^{1}H-NMR to determine its degree of functionalization[1]. Composite hydrogels were prepared by adding 0.5% carrageenan to 10% Gel-MA (w/v). Rheological properties were assessed via flow sweep, amplitude sweep, photorheology, and frequency sweep. Mechanical strength was tested using a TA ElectroForce 5500. Swelling ratio was measured, and morphology analyzed by SEM. hMSCs were encapsulated, and viability and proliferation were evaluated using LIVE/DEAD™ and PrestoBlue™ assays over 21 days. Osteogenic potential was assessed by ALP activity and RT-qPCR of RUNX2, ALP, BGLAP, COL1A, SP7, and SPP1. Matrix mineralization was confirmed by Alizarin Red S and Von Kossa staining.

Results

Carrageenan functionalization imparted shear-thinning behavior to the hydrogels and significantly enhanced their mechanical integrity, as evidenced by increased elastic modulus and failure strain compared to

GelMA-only controls. Rheological analysis revealed elevated storage modulus values and an expanded linear viscoelastic range, indicating improved structural stability and printability.

The carrageenan-GelMA hydrogels also showed a slightly higher swelling ratio, greater apparent porosity, and reduced pore size by SEM. Notably, the photocrosslinking kinetics remained unaffected by carrageenan incorporation.

Encapsulated hMSCs exhibited viability above 90% throughout the 21-day culture period, with a progressive increase in metabolic activity, suggesting sustained proliferation. Gene expression analysis demonstrated upregulation of key osteogenic markers in the carrageenan-functionalized hydrogels, corroborated by elevated ALP activity and enhanced extracellular matrix mineralization.

Discussion

The addition of carrageenan to GelMA hydrogels enhanced mechanical strength, shear-thinning behavior, and rheological performance, addressing key limitations for 3D printing in bone tissue engineering. These improvements, including the shear-thinning profile, higher storage modulus, and broader viscoelastic range, supported better printability and structural integrity.

Biocompatibility was maintained, with hMSCs remaining highly viable and metabolically active over 21 days. The modified hydrogels also exhibited greater porosity, smaller pore size, and a slightly increased swelling ratio, potentially improving cell-matrix interactions. Moreover, carrageenan-Gel-MA gels promoted osteogenic differentiation, as indicated by upregulated gene expression and elevated ALP activity.

Together, these results highlight carrageenan-GelMA hydrogels as promising osteoinductive bioinks with well-balanced mechanical and biological performance for bone scaffold bioprinting.

Acknowledgements

For financial support we thank FAPESP for the scholarship 2024/16384-7.

References

1. Sun, M., Sun, X., Wang, Z., Guo, S., Yu, G., & Yang, H. (2018). Synthesis and Properties of Gelatin Methacryloyl (GelMA) Hydrogels and Their Recent Applications in Load-

Bearing Tissue. Polymers, **10(11)**,
1290.

Layered Biofabrication of Trabecular Meshwork Analogues Using MEW and Hydrogel-Based Cell Printing

Citro, V.[a], Sheridan, C.M[a], Paxton N.C.[b] Bosworth, L.A.[a,*]

[a] Department of Eye and Vision Science, Institute of Life Course and Medical Sciences, Faculty of Health and Life Sciences, University of Liverpool, Liverpool, UK

[b] Centre for Biomedical Technologies, Queensland University of Technology (QUT), Brisbane, Australia

* lucy.bosworth@liverpool.ac.uk

Introduction

Glaucoma is a leading cause of irreversible blindness, driven by elevated intraocular pressure resulting from impaired aqueous humor outflow through the trabecular meshwork (TM)[1]. The TM's unique structure and biomechanical properties are key to regulating this outflow. Engineered TM models provide a valuable platform to investigate these structure–function relationships and inform regenerative strategies.

Materials and methods

Hierarchical poly(ε-caprolactone) (PCL) scaffolds (80 µm thick) were fabricated via melt electrowriting (MEW), using both curly and straight fiber morphologies to generate distinct porosity profiles. Human NTM$_5$ trabecular meshwork cells were incorporated into the scaffolds using a BIONOVA X digital light processing 3D bioprinter (Fig.1). GelMA (95% degree of methacrylation) and alginate were employed as bioinks (Cellink), varying the mechanical stiffness from stiff to soft matrices, respectively.

Cell proliferation and viability were assessed over 7 days using PicoGreen and Live/Dead assays, respectively. Cell response to mechanical environment was assessed by immunofluorescence: α-smooth muscle actin (α-SMA), actin filaments (phalloidin), fibronectin, and vinculin. Phagocytic activity was analysed by encapsulating fluorescent tracer particles within the hydrogel constructs and assessing cellular uptake.

Results

Live/Dead revealed a progressive increase in cell viability over time, with notably enhanced proliferation observed in GelMA-based hydrogels (Fig.1C). In these stiffer environments, cells exhibited localized clustering and segregation at the gel boundaries, whereas a more homogeneous distribution was maintained in alginate-

based constructs. Immunofluorescence demonstrated culture duration and hydrogel stiffness influenced expression of α-SMA, actin filaments, vinculin, and fibronectin, indicating matrix- and time-dependent modulation of cytoskeletal organization and ECM remodelling. Cells cultured directly on MEW fibers displayed elevated phagocytic activity (tracer particle internalization increased). In contrast, hydrogel encapsulation attenuated this phagocytic response, suggesting a protective or modulating role of the hydrogel environment.

Discussion

This study demonstrates the potential of combining MEW scaffolds with cell-laden hydrogels to mimic the complex architecture and mechanical microenvironment of human TM. The use of GelMA and alginate allowed constructs engineered with distinct stiffness profiles, which in turn directly influenced cell behavior. Stiffer GelMA hydrogels promoted rapid cell proliferation and viability over time, likely due to the increased mechanical cues supporting cytoskeletal tension and matrix adhesion. However, cellular segregation at the gel boundaries was observed, suggesting limited migratory capacity in denser matrices. In contrast, alginate-based constructs facilitated a more uniform cell distribution, potentially due to their softer and more permissive network. Protein expression patterns further reflected the influence of substrate stiffness and culture duration. Increased levels of α-SMA, vinculin, and fibronectin in stiffer environments suggest a transition toward a contractile, ECM-remodeling phenotype, aligning with known mechanosensitive responses of TM cells. Interestingly, cells cultured directly on MEW fibers exhibited increased phagocytic activity, a response often seen in stress-related or inflammatory contexts, such as in tumor-associated stromal environments. The incorporation of hydrogel layers attenuated this effect, pointing to a protective role of the ECM-like matrix in buffering excessive cellular activation. These results underscore the importance of tuning both mechanical and structural parameters to replicate physiologically relevant TM environments and opens new avenues for modeling pathological states such as glaucoma.

Figure 1. Biofabrication of trabecular meshwork-like scaffolds. *A) Schematics of MEW PCL scaffolds combined with cell-laden hydrogels. B) SEM images of MEW scaffolds with straight and curly fiber architectures, and confocal microscopy image demonstrating integration of printed hydrogel (GelMA or alginate) with underlying fiber network. C) Live/Dead assay of NTM$_5$ cells cultured on curly MEW fibers, curly fibers with GelMA, and curly fibers with alginate after 7 days.*

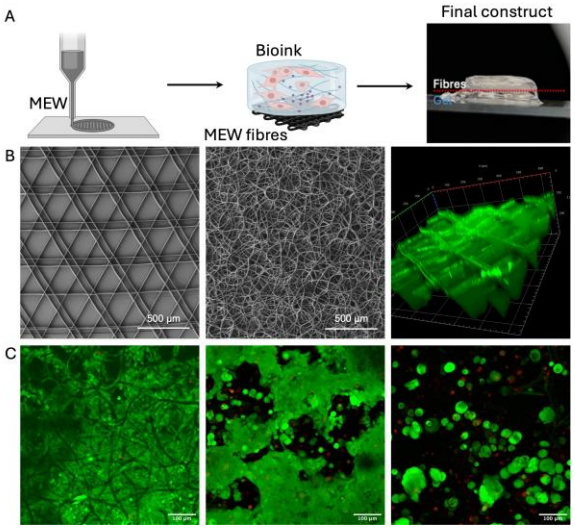

Acknowledgements

Thanks to University of Liverpool for funding this research.

References

Fan, X. et al. Replacement of the Trabecular Meshwork Cells-A Way Ahead in IOP Control? Biomolecules 11, (2021)

Development of cellulose-based membrane for artificial lung applications

Thomas Fruleux [a], Jiemin Wang [a], Catalina Vallejo-Giraldo [a], Mizi Fan [b], Mark Brassil [c], Manus Biggs [a *]

[a] CURAM, Research Ireland Centre for Medical Devices, University of Galway, Ireland

[b] Brunel University, Kingston Ln, London, Uxbridge UB8 3PH, United Kingdom

[c] Smart Reactors, Galway Technology Park, Parkmore Road, Galway H91 AY0Y, Ireland

* Corresponding author(s) e-mail(s): manus.biggs@universityofgalway.ie

Introduction

End-stage lung disease represents the third leading cause of death worldwide,[1] accelerated by increasing rates of tobacco smoking and exposure to air pollutants which further raise the number of patients with lung disease thus creating an urgent need for new therapeutic strategies. Extracorporeal membrane oxygenation (ECMO) and mechanical ventilation can be temporarily used as a bridge to lung transplantation for patients too sick to wait until a donor lung becomes available. These devices utilise a porous membrane which allows for gas transfer at the blood-device interface, facilitating blood oxygenation. Although ECMO can prevent patient death, challenges include device-related infection, bleeding, thrombosis, cost, and low patient quality of life

Due to the high surface area, high mechanical strength and low toxicity, nanocellulose (NC) can be used for the fabrication of cytocompatible, renewable and highly porous membranes for ECMO.

Materials and methods

Drop-cast nanocellulosic films and electrospun nanocellulose membrane (Figure 1) were investigated as potential novel ECMO materials through in vitro analysis of cytocompatibility.

Results & Discussion

Analysis of primary human umbilical endothelial cell (HUVECs) proliferation on NC materials was assessed for up to 3 weeks in vitro (Figure 2). It was observed that material formulation impacted cell proliferation and cell morphology at early timepoints (Figure 3). Critically, NC formulation was also observed to modulate endothelial barrier integrity, through changes in VE-cadherin expression after 3 days. These results indicate the cytocompatibility of NC-based materials

and their potential as functional ECMO devices.

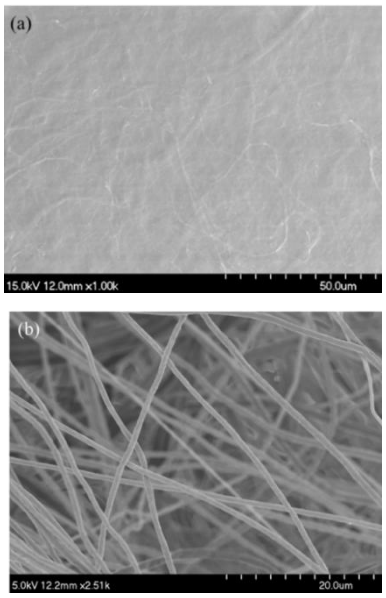

Figure 1. Microscopic analysis of (a) NC Film and (b) NC Membrane

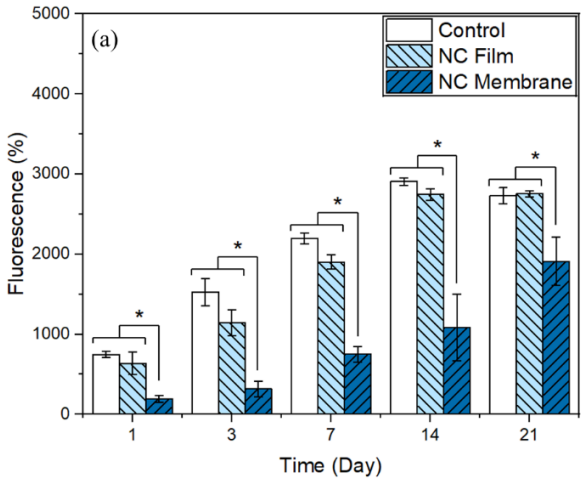

Figure 2. Evolution of HUVECs proliferation on tissue culture plate (control), NC Film and NC Membrane over a 3-week period.

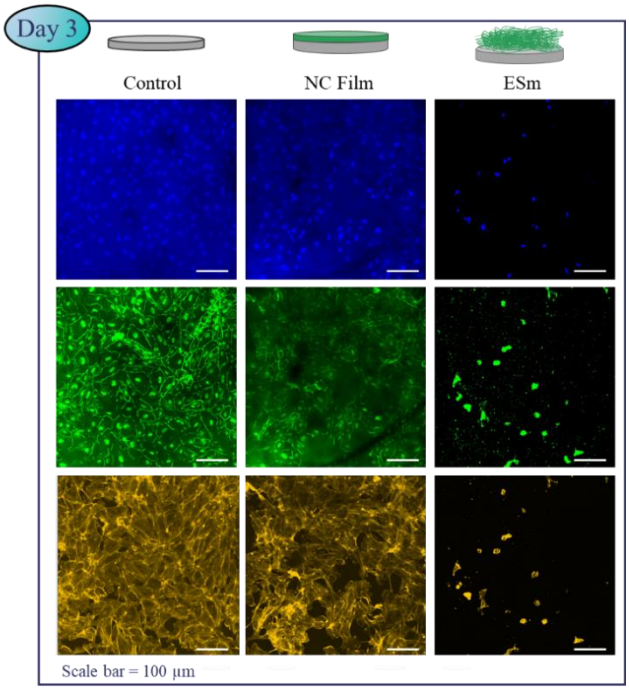

Figure 3. Influence of material selection on the morphometric indicators and barrier integrity of HUVEC cells. (blue = nucleus, yellow = cytoplasm, green = VE-cadherin)

Acknowledgements

For financial support we thank…

References

1) Jutta Arens, Oliver Grottke, Axel Haverich, Lars S Maier, Thomas Schmitz-Rode, Ulrich Steinseifer, HP Wendel and Rolf Rossaint, *ASAIO Journal*, August 2020, p847-854. 10.1097/MAT.0000000000001139

Alcohol Induced Dancing Particles

Schofield, Z.[a*], Goffrey, T. [a,b], Grover, L.M [a]

[a] Healthcare Technologies Institute, University of Birmingham, UK.

[b] Centre for Fusion Space and Astrophysics, University of Warwick, UK.

* Corresponding author(s) e-mail(s): s.zoe@bham.ac.uk

Introduction

Self-propelling particles move by converting energy from the environment (chemical, electrical, thermal, etc.) into mechanical motion[1]. Recent interest in them has increased, since they have found use as models of surface swarming by microbes and as toxicity sensors1. They have significant potential for directed drug delivery if their movement could be predicted and controlled. To enable this, it is essential to better understand what drives movement of the particles. Here, we aim to control the speed, time of propulsion and directionality of particles by altering the constraints of the environment in which they are allowed to move, and by altering the surface tension around particle using ethanol as a propellent to push the particle around the environment.

Materials and methods

3% (w/v) chitosan (medium molecular weight, Sigma Aldrich, UK) solutions, CS, were prepared with 0.2 M Acetic Acid (Sigma Aldrich, UK) and varying ethanol (HPLC grade, Fisher Scientific, UK) concentrations (40-100 % v/v). Sodium Hydroxide (NaOH, Fisher Scientific) pellets were dissolved in deionised water (Purite, 300) at 2-4 M for the sol-gel transition. CS solutions were mixed with varied ethanol concentrations to form chitosan with ethanol solutions, CEW solutions, similarly to Kumar, P. et al.[2]. To capture the particles self-propelling through a NaOH bath (50 mL added to 100x100 mm petri dish). The NaOH bath temperature was also altered from 25-50 C. CEW solutions were injected via a syringe pump at 50 µL/min and a Photron SA3 fast camera was positioned directly above the NaOH bath. The imaging speed was set to 50 frames per second. The videos were then processed into a binary image to ease tracking using the Fiji plug in TrackMate[3]. The data was then extracted from TrackMate and an inhouse Matlab script was used for tracking analysis.

Results

CEW solution, bottom 88% CEW solution both in 100 mm petri dish compared to polar plots which are both 86% CEW

solution in 10 mm (left) and 100 mm (right) petri dish. The bottom plot indicates how temperature influences time of propulsion.

Sol-gel particles were created using the syringe pump injection metho. With CEW solutions with 86% (v/v) ethanol particle area variation was minimal (29 ± 1.4 mm^2). The temporal evolution of speed (**Figure 1**) shows intermittent behaviour, characterised by short phases of rapid acceleration followed by rapid deceleration. However, in some cases there is a clear exponential decay. Furthermore, it was possible to control directionality of the particles by altering the channel width. The particle moves predominantly vertically in the 10 mm width channel compared to the 100 mm width (**Figure 1**). Finally, the temperature will influence the diffusion of EtOH from the particle as well as the sol-gel transition rate reducing the time at which the particles move up until 40 C before increasing again at 50 C.

Discussion

The Marangoni effect is an attractive concept to propel particles as it does not require external stimuli to control the movement of particles. By controlling the release of ethanol from the chitosan particles it will be possible to programme the speed, sporadic and directionality of propulsion[4,5].

The release of ethanol will be determined by the rate at which the sol-gel transition takes place within the NaOH bath. This can be controlled using temperature. The sporadic speed profile indicates intermittent driving force followed by a viscous drag deceleration. Whereas the speed profile exhibiting an exponential decay over time still could be due to the sol-gel transition which takes place from the surface towards the centre of the particle reducing the presence of ethanol at the surface of the particle. There does seem to be some correlation with ethanol concentration, yet better control of ethanol release is required. It should also be noted that ethanol concentration will influence the viscosity of the CEW solution which will affect the speed profile.

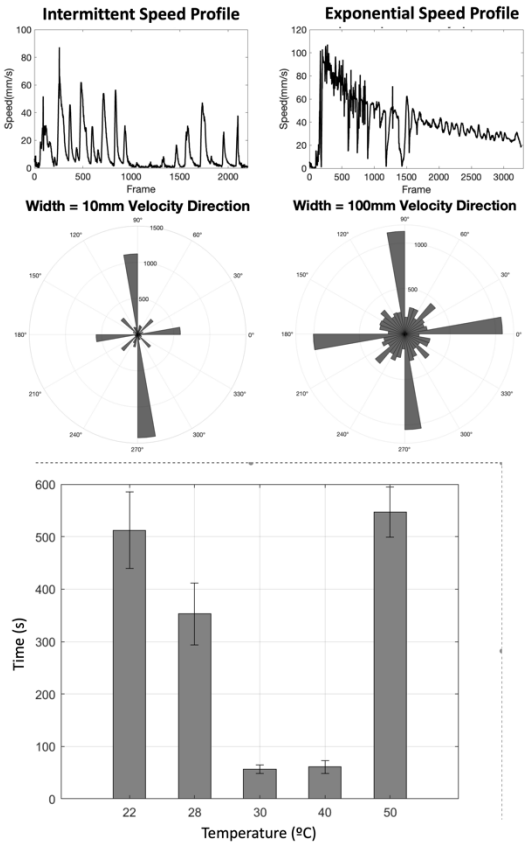

Figure 1: Examples of both speed profiles exhibited by particles. Top 86%

Acknowledgements

This work was funded by UK Research and Innovation (UKRI) under the UK government's Horizon Europe funding guarantee [grant number 101092242]. Views and opinions expressed are however those of the author(s) only and do not necessarily reflect those of the European Union

References

1) Sharma, R., et al, *Langmuir*, **28**, 10128–10135, 2012.

2) Kumar, P., et al., Chaos, **32**, 2022

3) Ershov, D., et alNature Methods, **19**, 829–832, 2022

4) Kwak, B., et al., Scientific Reports, **11**, 2021

5) Piras, C. C., et al, Low-Molecular-Weight Gelator', Chemistry - A European Journal, 27, 14527–14534, 2021.

Incorporation Of Engineered Collagen Peptides Into 3D-Printable Hydrogels For Osteogenic And Adipogenic Mesenchymal Stem Cell Differentiation

Ian P. Smith [1,2], Stephen M. Richardson [1], Marco Domingos [2] and Jordi Bella [1*]

[1] Division of Cell Matrix Biology and Regenerative Medicine, School of Biological Sciences, Faculty of Biology, Medicine and Health, Manchester Academic Health Science Centre, University of Manchester, Manchester M13 9PT, UK [2] Department of Mechanical and Aerospace Engineering, School of Engineering, Faculty of Science and Engineering and Henry Royce Institute, University of Manchester, Manchester, M13 9PY, UK

* Corresponding author e-mail: jordi.bella@manchester.ac.uk

Introduction

Type I collagen is commonly used as a biocompatible substrate in regenerative medicine therapies and in vitro research models. This natural biopolymer, however, is not the sole extracellular matrix (ECM) component found in human tissues and alone cannot fully recapitulate the extracellular landscape that cells interact with in vivo. This highlights an important consideration for cellular therapies – do the adhesion interactions between cells and the ECM components selected for biomaterials matter for tissue regeneration? To help answer this question we have modelled the cell adhesion binding motifs present on mammalian fibrillar collagens by synthesising collagen peptides which provide cellular adhesion in a specific manner to α1β1 integrin, α2β1 integrin and discoidin domain receptors 1/2 (DDR1/2). Using in vitro modelling, we evaluate the phenotypic changes of human mesenchymal stem cells (MSCs) when cultured on substrates which dictate a single mechanism of adhesion. We also demonstrate the functionalisation of these collagen peptides into viscoelastic hydrogels suitable for 3D bioprinting.

Materials and methods

Synthetic collagen peptides with 36-42 amino acids containing binding sequences specific to α1β1 integrin (GLOGEN, GFOGEN; O: hydroxyproline), α2β1 integrin (GROGER) and DDR1/2 (GVMGFOGPRGQO) were obtained commercially (AAPPTec, USA). Circular dichroism (CD) spectroscopy was used to confirm the correct collagen triple helical conformation of these peptides and to measure their melting temperatures. Human MSC, fibroblast and fibrosarcoma cell lines were cultured in 2D on peptide coatings. Integrin-peptide binding specificity was confirmed using integrin subunit blocking antibodies. Commercial acrylamide hydrogels (SoftWell, USA) were functionalised covalently with the collagen peptides before morphological and

phenotypic analysis of MSC adhesion. Collagen peptides were also functionalised to gellan gum hydrogels using carbodiimide chemistry, before rheological characterisation and optimisation to create a cell-compatible biomaterial suitable for 3D extrusion bioprinting.

Results

Molar ellipticity spectra confirmed the triple helical conformation for all collagen peptides. CD spectroscopy was also used to measure the melting temperature of each peptide, which were all sufficiently high (38°C - 58°C) to prevent helical unfolding at physiological temperatures. Fibrosarcoma cell adhesion was only observed to the GROGER peptide, confirming that this motif binds specifically to α2β1 integrin. Inhibition of fibroblast and MSC binding to GFOGEN and G[F/L]OGEN peptides when incubated with α1 and β1 blocking antibodies confirmed the binding specificity of these sequences to α1β1 integrin. The differential expression of focal adhesions and MSC lineage markers were also observed for MSCs cultured on peptide-coated substrates. Rheological characterization of peptide-functionalised gellan gum hydrogels confirmed that this biomaterial maintained its viscoelastic properties post carbodiimide functionalisation and ionic cross-linking. Cell viability was also shown to be unaffected after encapsulation and extrusion of the cell-laden hydrogels, and cell-laden hydrogels were successfully bioprinted into a suspension bath without compromising viability. MSCs encapsulated in peptide-functioanlised hydrogels were differentiated towards adipo-, osteo-, chondrogenic lineages. The GROGER peptide-functionalised hydrogels promoted the expression of adipogenic and osteogenic genes in comparison to non-functionalised gels.

Discussion

Triple helical collagen peptides capable of binding to specific integrins and discoidin domain receptors 1/2 and with sufficient thermal stability for in vitro studies were successfully produced. Peptide functionalised hydrogels were also successfully created, enabling the presentation of specific adhesion motifs to cells in 3D. The pro-osteogenic phenotype observed in MSCs differentiated in GROGER-functionalised hydrogels suggests that α2β1 integrin binding plays a role in mediating osteogenic differentiation. This finding could inform future biomaterial design for regenerative medicine research.

Versatile Twin Layer Macromolecular Fibres for Advanced Tissue Engineering Applications

Taylor, C.S.[a,b,*], Madj, H.[c], Gregory, D.A[a], Farr, N.T[a], Alenezi, H[c], Welsh, G.I[d], Edirisinghe, M[c], Roy, I[a].

[a]School of Chemical, Materials and Biological Engineering, The University of Sheffield, Sheffield, S3 7HQ, UK

[b]Institute of Medical and Biological Engineering, School of Biomedical Sciences, Faculty of Biological Sciences, University of Leeds, Leeds, UK

[c]Department of Mechanical Engineering, University College London, London WC1E 7JE, UK

[d]Bristol Renal, Translational Health Sciences, Bristol Medical School, University of Bristol, Bristol, BS1 3NY, UK

Email: C.Taylor1@leeds.ac.uk

Introduction

Many biomaterials are inert, and those that are bioactive, aiding tissue regeneration, are costly to use. Pressurised gyration has been shown to produce hybrid core sheath polymer fibres, which can utilise strength from the core material, and bioactivity/functionality from the fibre sheath material, for a wide range of tissue engineering applications.

Materials and methods

PHAs were produced by bacterial fermentation and characterised as per the methods by Basnett et al.[1] Core sheath fibres were produced by pressurized gyration. Fibres were characterised and a variety of different cell types, were cultured on fibres for 7 days. Cells were stained with cell specific antigens and imaged using confocal microscopy to ascertain *in vitro* responses.

Results

Four different polymer fibres were produced from pressurized gyration; PHA sheath:PLA core fibres, PLA sheath:PHA core fibres, virgin PLA fibres and virgin PHA fibres. The addition of the PHA sheath to PLA fibres significantly supported adhesion of NG108-15 neuronal cells, C2C12 myoblast cell, Human Primary Osteoblasts, BRIN-BD11 rat pancreatic beta cells, and HaCaT immortalised human keratinocytes. Fibres with a higher young's modulus better supported human osteoblast mineralisation, whereas softer fibres, such as the PHA virgin fibres, better promoted collagen

expression from Human Glomerular Podocytes and Endothelial cells.

Discussion

Pressurised gyration is a scalable, cost-effective technique to manufacture core sheath fibres, compared to conventional techniques that have the potential for various tissue engineering applications.

References

1) Basnett et al. ACS Appl. Mater. Interfaces, 2021, 13, 28, 32624–32639.

Mechanotransduction of T-Cell receptor and mechanosensitive ion-channels via remote magnetic field application to modulate human T-cell activation in-vitro

Thareja, A. [a,b,c,*], Clarke, J. [a,d], Oo, Y [b,c,] El Haj, A. [a,c]

[a] Healthcare Technologies Institute, Institute of Translational Medicine, University of Birmingham, UK

[b] Centre for Liver and Gastrointestinal Research, Institute of Biomedical Research, Institute of Immunology and Immunotherapy, University of Birmingham, UK

[c] National Institute for Health and Care Research Birmingham Biomedical Research Centre (NIHR Birmingham BRC), Institute of Translational Medicine, University of Birmingham, UK

d Medical Research Council Translational Immune Discovery Unit, John Radcliffe Hospital, University of Oxford, United Kingdom

* Corresponding author's e-mail: a.thareja@bham.ac.uk

Introduction

Anti-cancer adoptive cell immunotherapies have recently achieved a major boost as promising treatment modality. Recruitment of patient's own T-cells to target and produce an immune response in tumour microenvironment requires activation and differentiation of naïve T-cells mediated by T-cell receptor (TCR) complex. Recent research in T-cell mechanobiology has established that TCR acts as an anisotropic mechanosensor, which can convert mechanical forces into biochemical cues required for activation, differentiation, and proliferation, upon signalling by mechanosensitive ion-channels, in a process called mechanotransduction. We demonstrate a novel immunoengineering strategy of TCR mechanotransduction called Magnetic Ion Channel Activation (MICA) by application of an external magnetic field onto magnetic artificial antigen presenting cell (aAPC) tagged T-cells.

Materials and methods

Commercially available magnetic core-shell particles with a superparamagnetic magnetite core were surface functionalized with monoclonal antibodies against TCR-CD3 activation complex and mechanosensitive ion-channels like PIEZO1 to function as aAPCs. This was achieved via orientational Fc binding on protein-G coating for increased availability of Fab receptor binding sites in a 2-step

carbodiimide coupling to the carboxyl groups. Naïve T-cells were isolated by negative selection magnetic enrichment from human peripheral blood mononuclear cells (PBMCs) taken from haemochromatosis (HFE) patient blood and labelled with magnetic aAPCs. Labelled cells were then activated in-vitro upon application of an external repeating pulsed magnetic field onto the aAPC-tagged cells for 1 to 4 hours which in-turn produced mechanical stresses on the TCR-CD3 complex resulting in an effector response via downstream signalling pathways. The effector response by surface activation markers was then measured as an endpoint 16 hour post magnetic field application by immunophenotyping of surface activation markers including CD69, CD25, CD154, CD134, CD137, and HLA-DR (MHC-II), by multi-parameter flow-cytometry. Further, differentiation and expansion of activated T-cells over multiple days was measured by proliferation and cell-cycle markers.

Results

Synergistic mechanotransduction of TCR-CD3 complex and PIEZO1 in naïve T-cells induced significantly increased activation and reduced expansion times compared to only CD3 and only PIEZO1 groups, and with labelled cells without magnetic field application.

Discussion

This work confirms that mechanical activation of PIEZO1 ion-channel supplements the activation of TCR-CD3 complex. The easily scalable MICA platform can modulate T-cell activation by using magnetic aAPCs and provides an improved activation and expansion over currently available commercial technologies for adoptive T-cell immunotherapies.

Acknowledgements

We would like to thank our funders - the European Research Council for the ERC advanced grant DYNACEUTICS, and the National Institute for Health and Care Research Birmingham Biomedical Research Centre (NIHR Birmingham BRC) for generously funding this research.

Rapid design of bioinspired alloys through conventional and additively manufacturing techniques

Villapun, V.M.[a],*, Rabbitt, D.[a], Carter, L.N.[a], Page, O.[a], Hanley, S.[b], Nicum, A.[a], Cox, S. [a,*]

[a] School of Chemical Engineering, University of Birmingham, Birmingham, B15 2TT UK.

[b] Institute of Inflammation and Ageing, University of Birmingham, Birmingham B15 2TT, UK

* Corresponding author(s) e-mail(s): v.m.villapun@bham.ac.uk, s.c.cox@bham.ac.uk

Introduction

Metallic devices are broadly employed as biomaterials, equating to 70-80% of implants globally[1,2]. However, the need for metal implantable devices in a 11.4 billion industry is superseded by 2-23% failing rates of dental implants and 10% revision rates of hip arthroplasties[3,4], critically calling for novel alloy systems.

The biomedical industry focuses on the use of stainless steels, cobalt-chromium and titanium (e.g. Ti-6Al-4V) based alloys[2,5]. Nevertheless, the long-term impact of alloying elements in normal bodily function has become a concern with elevated metal levels detected in patients and reports suggesting inhibition of cell behaviour[6-9]. Historically, these materials were developed in alternative industries, e.g. aerospace, and later repurposed to the medical field[10]. Their development was centered on mechanical/corrosion resistance and cytotoxicity, thus, disregarding critical design area as stress shielding, inflammation, and infection[11]. From an alloy development perspective, careful selection of metallic elements can be harnessed to guide the immune response, improve angiogenesis, enhance biomineralization, provide antimicrobial activity and limit mechanical properties. This leads to an upper bound of ~$7.6*10^5$ multicomponent systems that directly assess biological benefits[12]. Nevertheless, each of these alloys should be compositionally and microstructurally optimised[12]. With hundreds of combinations per system, exploring such design space is a daunting process.

Herein, we will show the work developed over the last years in the Centre for Custom Medical Devices to rapidly explore tailor-made alloys from a biological perspective.

Materials and methods

This alloy discovery vision was developed through several example systems. First, conventional alloy casting and heat treatment techniques (homogenization and ageing) were employed to fundamentally link the influence of composition and microstructure with mechanical,

antimicrobial and biological properties of the Ti-Cu and Ti-Cu-Mo systems. Then, blended powder and Laser powder bed fusion (L-PBF) were explored as high throughput approaches for early alloy analysis. In situ powder blends of different elements (e.g. Ti, Cu, Ag, Mo, Sn) were prepared and either mechanically compressed or processed by L-PBF through a reduced build volume (RVB) system to manufacture pure/graded samples.

Produced parts were microstructurally (SEM, EDX, XRF), mechanically (tensile/compressive, micro-harness) analyzed and tested in vitro for antimicrobial, cytotoxicity, mineralization, vascularization and immune responses.

Results and discussion

Conventionally treated $Ti_{33}Cu$/$Ti_{11.5}Cu$ samples resulted in a prevalence of Ti_2Cu precipitates driving both antimicrobial and cytotoxic properties. Nevertheless, its effectiveness was linked with intermetallic morphology as highlighted by a decrease in alloy efficacy as the quantity of Cu-rich phases increased. On the other hand, PBF-LB alloys with reduced Cu content (3 wt.%) outperformed conventional alloys against pathogenic *S. aureus* and *E. coli* without enhanced toxicity. This improvement was attributed to the finer grain structure which accelerated ionic release.

Further analysis of PBF-LB parts revealed process driven variations with Ti-Sn characterized by a homogeneous solid solution while Ti-Mo required homogenization of un-melted particulates to enhance expression of anti-inflammatory markers. Finally, PBF-LB resulted in an effective technique to produce graded samples (**Figure 1**) with biological evaluation rapidly suggesting 10%Cu as the main threshold to enact an antimicrobial and non-toxic effect.

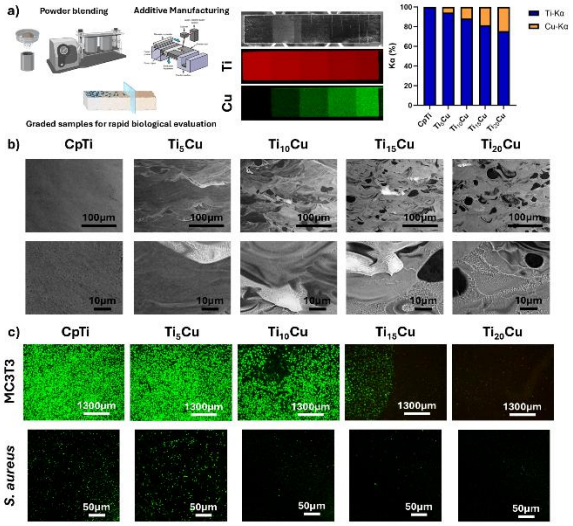

Figure 1 Example of Ti-Cu graded sample manufactured with PBF-LB, including a) XRF, b) SEM-BSC and biological images of seeded c) MC3T3 and *S. aureus* cells

Conclusions

These results indicate that powder blending, and PBF-LB are powerful techniques for the rapid evaluation of biologically driven alloy systems, however, further work is required to understand process driven variations.

Acknowledgements

This study was financially supported by UKRI Future Leaders Fellowship MR/T017783/1.

References

1) Li, Y., et al., Materials (Basel), 2014. 7(3): p. 1709-1800.
2) Rack, H.J. and J.I. Qazi, Materials Science and Engineering: C, 2006. 26(8): p. 1269-1277.
3) Medical alloys and market-Global forecast, EMR (2023)
4) Kenney, Connor, et al. Journal of orthopaedics 16.5, 2019: p. 393-395.
5) Bocchetta, P., et al., Coatings, 2021. 11(5).
6) Catalani, S., et al., Clinical Toxicology, 2013. 51(7): p. 550-556.
7) Bistolfi, A., et al. HIP International, 2018. 28(5): p. 522-530.
8) Hanawa, T., Materials Science and Engineering: C, 2004. 24(6): p. 745-752.
9) Thompson, G.J. and D.A. PuleoBiomaterials, 1996. 17(20): p. 1949-1954.
10) Rabbitt, Daisy, et al. Rethinking Biomedical Titanium Alloy Design: A Review of Challenges from Biological and Manufacturing Perspectives. Advanced Healthcare Materials 14.4, 2025: p 2403129.
11) Villapun Puzas, Victor Manuel, et al.. ACS Biomaterials Science & Engineering 8.10, 2022: p. 4311-4326.
12) Kuroda, D., Niinomi, M., Morinaga, M., Kato, Y., & Yashiro, T., Materials Science and Engineering: A, 243(1-2), 1998: p. 244-249.

ECRs: Postgraduate researchers' abstracts

The molecular landscape of transformed and non- transformed cells in an engineered fibrous microenvironment

Alrwaili, A. [a], Ortega Asencio, I. [a], Lambert, D [a,*]

[a] University of Sheffield, United kingdom

* Corresponding author(s) e-mail(s): aaalrwaili1@sheffiled.ac.uk

Introduction

Mechanobiology studies how mechanical forces impact cells and tissues, particularly in cancer, where altered mechanical properties drive malignant progression. Identifying molecular processes that regulate cancer through cell mechanics could help develop anti-metastasis drugs (Rezk et al., 2021). The aim is to explore how changes in the morphology and chemistry of electrospun fibrillar matrices can reverse the mechanoresponse of transformed cells to normal.

Materials and methods

Scaffold Manufacture.

To produce the scaffolds, we used a PHD2000 syringe pump connected to an Alpha IV Brandenburg power source. The polymer that was expelled from the syringe pump was collected on a grounded collection plate placed above it. To ensure proper separation of the fibrous membrane from the collector, the collection plate was wrapped in parchment paper. We prepared polymer solutions using polycaprolactone (PCL) which is a hydrophobic, slow-degrading, biocompatible, synthetic thermoplastic polymer that is often used in biomedical applications at 15%.

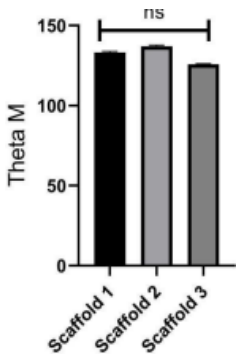

Figure 1. Contact angle of the scaffolds was measured by using a contact angle measurement instrument, n=3

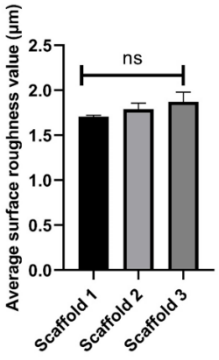

Figure 2. The Y axis demonstrates the average surface roughness. The x-axis

demonstrates the number of scaffolds that were tested. n=3.

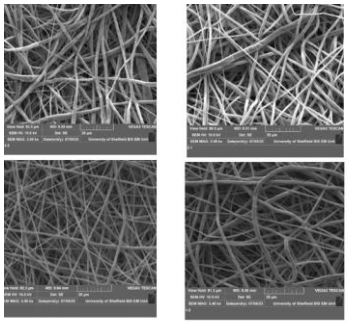

Figure 3. Scanning electron microscopy (SEM) images of electrospun polycaprolactone (PCL) scaffolds with distinct architectures. The top row shows 3D PCL scaffolds characterized by a highly porous, multi-layered fiber arrangement, enabling increased surface area and spatial complexity.

Cell Culture

BjhTERT cells, which are immortalised neonatal fibroblasts, were used as a model for normal, non-transformed, and non-invasive cells. In contrast, the isogenic BjhTERT-SV40T-H-RasV12 cell line, modified to overexpress SV40T and H-RasV12 oncogenes, displays transformed and invasive tumor-like characteristics (Hahn et al., 1999).

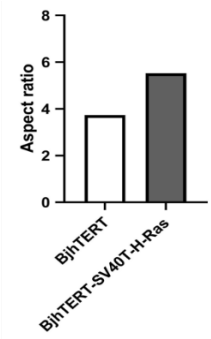

Figure 4. The aspect ratio of immortalised Bjhtert cells (dark grey) and metastasising BjhtertSV40TRasV12 cells without (white), n=3

Quantitative PCR (qPCR)

was performed on BJhtert and BJ-Ras cells to assess gene expression profiles. The analysis aimed to compare molecular differences between the immortalized BJhtert fibroblasts and their Ras-transformed counterparts.

Results

Mechanical testing showed no significant difference in scaffold hardness at room temperature. Contact angle measurements confirmed the hydrophobic nature of the scaffolds (all >90°). Aspect ratio analysis revealed morphological distinctions between normal and cancerous fibroblasts. BJ-RAS cells, transformed by oncogenic RAS, displayed enhanced spreading and altered morphology on 3D PCL scaffolds,

reflecting their tumor-promoting behaviour and interaction with an ECM-like environment.

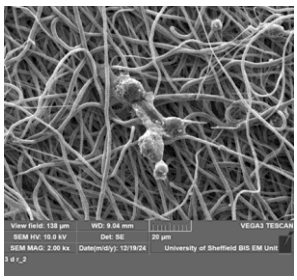

Figure 6 (SEM) image of BJ-RAS cells cultured on a 3D polycaprolactone (PCL) scaffold. The image shows BJ human fibroblasts transformed with oncogenic RAS (BJ-RAS) interacting with the fibrous PCL scaffold.

Quantitative PCR (qPCR)

Our results revealed a significant upregulation of several proliferation- and survival-related genes in BJ-RAS cells compared to BJ-hTERT controls, as illustrated, for example, in figure 5. In contrast, genes linked to cell cycle regulation and apoptosis were downregulated following Ras activation. These findings suggest that Ras transformation induces widespread transcriptional reprogramming, promoting a more proliferative and survival-favored phenotype.

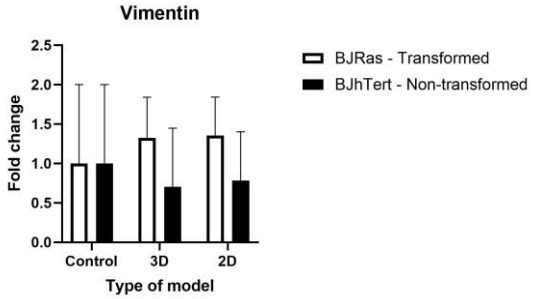

Figure 5 Vimentin expression in BJhtert and BJ-Ras cells across control, 3D, and 2D models. Quantitative PCR analysis of Vimentin expression showed an increase in BJ-Ras cells cultured in 3D and 2D models compared to BJhtert cells. Fold change values are normalized to control conditions. Error bars indicate standard deviation (SD) from biological replicates, reflecting variability in expression patterns.

Discussion

The cell model is based on newborn fibroblasts, and the most relevant physiological cancer is neonatal fibrosarcoma, a fatal and mutilating infant disease. The model system is also particularly relevant for all cancer types based on cells that express the cytoskeletal, mesenchymal marker protein vimentin and exhibit mesenchymal characteristics, which include sarcomatous

tumours like carcinosarcoma, fibrosarcoma, and mesothelioma (Sun, et al 2005)[6].

PCL contact angle was measured as seen in (Figure 1). PCL surface contact angle is critical in determining wetting behaviour and interactions with other substances (Li et al. 2019[4]). In addition, the roughness level was estimated, as shown in (figure 2). The roughness of PCL surfaces is a crucial property that can have a major impact on its qualities and uses.

Quantitative PCR analysis showed that transformation with Ras led to subtle transcriptional changes rather than dramatic shifts in gene expression for Fibronectin, Vimentin, and ACTA2 across different culture conditions. BJ-Ras cells tended to maintain or slightly upregulate mesenchymal markers (such as Vimentin and Fibronectin) under 3D and 2D conditions, suggesting that oncogenic Ras may contribute to maintaining a mesenchymal-like phenotype.

Acknowledgements

For financial support we thank the University of Sheffield and the Saudi Ministry of Education.

References

(1) Baker, B.M. et al. (2015) *Nature Materials*, 14(12), pp. 1262–1268.

(3) Hahn, W.C. et al. (1999) '*Nature*, 400(6743), pp. 464–468.

(4) Li, W. J., et al. (2019). *Journal of Biomedical Materials Research Part A*, 107(4), 776–785.

(5) Rezk, R., Marín-García, R. and Gad, A.K.B. (2021). *Engineering*, 7(10), pp. 1375–1380.

(6) Sun, B. et al. (2005) '*Neoplasia*, 7(6), pp. 585–593.

Engineering ECM-Enriched 3D Hydrogels for Enhanced Osteogenic Differentiation of Bone Marrow Mesenchymal Stem Cells

Anbazhagan, B.[1*], Tsigkou, O.[1], Basu.B.[2]
[1] Department of Materials, School of Natural Science, Faculty of Science and Engineering, the University of Manchester, UK
[2] Laboratory for Biomaterials and Translational Center on Biomaterials for Orthopedic and Dental Applications, Materials Research Centre, Indian Institute of Science, India
*bhuvaneshwari.anbazhagan@postgrad.manchester.ac.uk and olga.tsigkou@manchester.ac.uk

Introduction

Mesenchymal stem cells (MSCs) migrate to the site of injury in response to biochemical signals, orchestrating bone tissue regeneration. Their functional behaviour is strongly influenced by the surrounding niche, which provides a dynamic combination of biochemical and physical cues[1]. Decellularised extracellular matrices (ECMs) provide biomimetic microenvironment to support MSC adhesion and differentiation; however, xenogeneic ECMs can be immunogenic, and recombinant systems often lack the functional complexity of native matrices[2]. Human bone marrow MSC-derived ECMs (C-ECMs) can provide specific signals and cues required for osteogenic differentiation in 2D, offering better control and simplicity[3]. To further harness these advantages, it is essential to unravel MSCs responses to C-ECM components in a 3D environment. As a first step, we evaluated the dose-dependent modulation and spatial homogeneity of MSC behavior using 2D models of C-ECM, aiming to translate these findings into oxidized alginate-based hybrid bioinks that could potentially recapitulate the cues that would induce osteogenic differentiation.

Materials and methods

Five 2D decellularised ECM models were developed: (1) undifferentiated ECM (DM-ECM), (2) intact differentiated ECM (OS-ECM), and (3) solubilised differentiated ECM at 10% (S-10), (4) 50% (S-50), and (5) 70% (S-70) concentrations, all compared against tissue culture plastic (TCP) as control. MSCs (PromoCell, UK) (2×10^6 cells) were seeded onto 15 cm petri dishes and treated with basal (DMEM +10%FBS +1%Penicilin/streptomycin) or osteogenic media (10nM dexamethasone + 10nM 1α, 25-dihydroxy vitamin D3 + 50μM L-ascorbic acid 2-phosphate + 10mM β-glycerophosphate) for 7 days. At day 7 decellularisation was performed using 20 mM NH_4OH, 0.5% Triton X-100 and DNase I (20 U/ml) (all from Sigma, UK) extraction buffer. The C-ECM was scraped and sonicated on ice using pulsed cycles. ECM suspensions were coated on coverslips.

Metabolic activity, cell attachment, morphology and osteogenic differentiation were assessed.

Results

BMSCs were seeded on OS-ECM, DM-ECM, S-10, S-50, S-70, and TCP and cultured for 21 days in osteogenic differentiation media. On day 21, biomineralization was assessed using Von Kossa staining and calcium deposition was analyzed with Alizarin Red. Results demonstrated that MSCs seeded on OS-ECM and S-70 ECM exhibited significantly enhanced osteogenic differentiation compared to the control group, with higher levels of calcium deposition and mineralization as seen in Figure 1. In contrast, MSCs on DM-ECM showed reduced calcium deposition and less biomineralization. Additionally, increasing the concentration of solubilized ECM (S-10, S-50, S-70) resulted in a gradual increase in osteogenic differentiation potential, as confirmed by both Alizarin Red and Von Kossa staining.

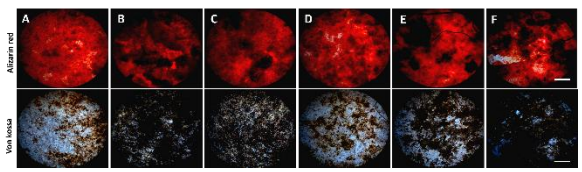

Figure 1. Alizarin red and Von kossa staining for the assessment of osteogenic differentiation of the BMSCs seeded on ECM for 21 days under osteogenic differentiation media. BMSCs seeded on (A) TCP, (B) OS-ECM, (C) DM-ECM, (D) S-10, (E) S-53, (F) S-70. Scale bar 200μm. n=3.

Discussion

This study elucidates the multifaceted role of MSC-derived ECM in guiding MSC behavior and osteogenic differentiation, offering valuable insight into their use in the design of 3D biomimetic constructs for tissue engineering applications. Novel data on the effect of solubilised ECM incorporated within 3D hydrogels on cell attachment and differentiation will also be presented.

Acknowledgements

We acknowledge the Henry Royce Institute for Advanced Materials (grant no. EP/R00661X/1, EP/S019367/1, EP/P025021/1, and EP/P025498/1) for support and equipment use.

References

1) A. R. Pereira, D. Trivanović, M. Rudert and M. Herrmann, *J. Tissue Eng*., 2022, **13**, 20417314221074453.158.

2) M. S. Carvalho, J. C. Silva, J. M. S. Cabral, C. L. Silva and D. Vashishth, J. *Tissue Eng. Regen. Med*., 2019, **13**, 291–301.269.

3) B. Antebi, Z. Zhang, Y. Wang, Z. Lu, X.-D. Chen and J. Ling, *Tissue Eng. Part C Methods,* 2015, **21**, 171–181.37.

Physio-mechanical Characterisation of Olive Stone Powder-Tapioca Starch Biocomposites for Sustainable Food Packaging

Ashimi, M.O. [a], Chisenga, S.M [b], Liu, H. [a, *]

[a] School of Engineering and Materials Science, Queen Mary University of London, London, E1 4NS, UK
[b] Department of Soil Science, University of Zambia, P. O. Box 32379, Lusaka, Zambia

* Correspondence to: Dr Haibao Liu, email: haibao.liu@qmul.ac.uk

Abstract

This study examines the properties of biocomposites made from olive stone powder and tapioca starch for sustainable packaging. Biocomposite films were created using solution casting with varying amounts of olive stone powder and tapioca starch, utilising distilled water as a solvent and sorbitol as a plasticiser. Transparency and colour were assessed with a spectrometer, particle volume fraction, density were measured through weighting, and film thickness was measured with a micrometre.

Mechanical properties were evaluated using a universal testing machine, and tensile and flexural characteristics such as Young's modulus, tensile strength, elongation at break, and bending strength were tested. Results showed that olive stone powder significantly increased tensile strength and stiffness, and the addition of sorbitol enhanced flexibility and shear strength. This highlights the potential of these biocomposites as cost-effective, biodegradable alternatives to traditional plastic packaging.

Introduction

The extensive use of conventional plastic packaging has led to an environmental crisis, with food packaging contributing to about 40% of global plastic production (UNEP, 2023). These petrochemical plastics can persist in ecosystems for centuries, with 25 million tons ending up in landfills yearly and significantly worsening marine pollution (Mahmud et al., 2024). Current recycling efforts are insufficient, with less than 9% of plastic waste being efficiently recycled globally (Gregory et al., 2021).

Figure 2 Plastic Pollution. UNEP/ Ollivier Girard.

It is essential to create innovative, high-performance, fully biodegradable alternatives to conventional food packaging. This study examines the physio-mechanical properties of olive stone powder and tapioca starch biocomposites by conducting comprehensive material characterisation and performance evaluation.

Materials and methods

The biocomposite films were developed using olive stone powder (60 µm) as a reinforcing filler and native tapioca starch powder (15 µm) as the matrix. Sorbitol (ACS grade-98%) acted as the plasticiser, and distilled water was used as the solvent. The solution casting method involved dissolving 50% (w/w) sorbitol in distilled water, followed by the addition of tapioca starch and varying percentages of olive stone powder (5%, 10%, 15%, 20%, and 25% w/w of starch). The mixture was heated to achieve gelatinisation and then poured into 14 mm-by-14 mm moulds to dry. The 100% tapioca starch films dried faster within ~30 hours, while the composites took ~4-5 days to dry, depending on the olive stone powder inclusion.

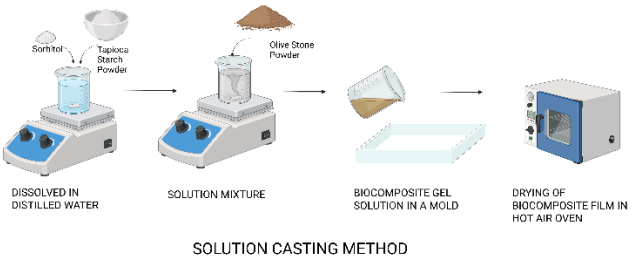

Figure 3 Solution Casting of Olive Stone-Tapioca Starch-Based Biocomposite Films

Results

Through the experiments, it was found that the tensile strength increased with the inclusion of olive stone powder. Fourier Transmission Infrared spectroscopy also showed that including olive stone powder reduces the presence of the hydroxyl group compared to 100% tapioca starch, thereby reducing the hydrophilic properties of tapioca starch. The biocomposite films' thickness and transparency/colour also varied as the percentage of olive stone powder increased.

Figure 4 Image of pure tapioca starch film (left) and tapioca starch film with 5%(w/w%) olive stone powder (right).

Discussion

The results from the physical and mechanical tests show that olive stone powder is a viable biobased material that can enhance the hydrophobicity and mechanical properties of tapioca starch to foster a scalable, cost-effective biobased film for sustainable food packaging and other applications due to its high stability, durability, and lightweight properties.

Acknowledgements

The authors would like to sincerely thank the Royal Society for the financial support for this work.

References

[1] UNEP. UN Environment Program's Annual Report UNEP. 2023

[2] Mahmud, M. Z. al, Mobarak, M. H., & Hossain, N. Emerging trends in biomaterials for sustainable food packaging: A comprehensive review. *Heliyon*. 2024, 10(1).

[3] Gregory D.A., L. Tripathi, A.T. Fricker, E. Asare, I. Orlando, V. Raghavendran, I. Roy. Bacterial cellulose: a smart biomaterial with diverse applications. *Mater. Sci. Eng. R Rep.* 2021, 145 100623.

Effect of poly-γ-glutamic acid molecular weight on the properties of whey protein isolate hydrogels.

Daniel K. Baines[a], Zuzanna Pawlak-Likus[b], Nikoleta N. Tavernaraki[c], Varvara Platania[c], Mattia Parati[d], Timothy N. Wong Wong Cheung[a], Iza Radecka[d], Patrycja Domalik-Pyzik[e], Maria Chatzinikolaidou[c], and Timothy E.L. Douglas[1]*

[a] School of Engineering, Lancaster University, Biomedical and Life Sciences, U.K.

[b] Department of Biocybernetics and Biomedical Engineering, Faculty of Electrical Engineering, Automatics, Computer Science and Biomedical Engineering, AGH University of Krakow, Poland

[c] Department of Materials Science and Engineering, University of Crete, Greece

[d] Faculty of Science and Engineering, School of Life Sciences, University of Wolverhampton, U. K.

[e] Department of Biomaterials and Composites, Faculty of Materials Science and Ceramics, AGH University of Krakow, Poland

Institute of Electronic Structure and Laser, Foundation for Research and Technology Hellas, Greece

* Corresponding author: t.douglas@lancaster.ac.uk

Introduction

Osteo-related pathologies effect over 200 million people [1]. Current gold standard treatments demonstrate limitations [2], suggesting a requirement for scaffolds for osseous regeneration. Whey protein isolate (WPI), in the form of hydrogel has demonstrated potential as osseous scaffolds. WPI hydrogels have been loaded with hydrophobic and hydrophilic molecules, demonstrating the cellular proliferation, differentiation and functioning of pre-osteoblasts [3,4]. Similarly, hydrophilic poly-γ-glutamic acid (γ-PGA), has demonstrated potential in tissue regeneration by demonstrating the proliferation of SaOs-2 osteosarcoma cells [5]. Therefore, WPI/γ-PGA hydrogels were synthesised and analysed physio-chemically and biologically, to evaluate any potential for use as tissue regeneration scaffolds.

Materials and methods

WPI-γ-PGA hydrogels were synthesised to 40% (w/v) with an additional 2.5%, 5%, 7.5% and 10% γ-PGA. The γ-PGA molecular weights were 10 kDa, 700 kDa and 1100 kDa. Homogenised solutions were de-gassed, and gelation was heat

induced at 70ºC. SEM and FTIR was utilised to determine successful synthesis of WPI-γ-PGA. Swelling and enzymatic degradation introduced 1 g WPI-γ-PGA hydrogels to 5mL PBS and proteases, incubated for 5 days at 37ºC. Mechanical, compression analysis was performed with 1 cm x 8 mm hydrogels. Cellular viability analysis was performed with Dental pulp mesenchymal stem cells incubated at 37ºC for 3 and 5 days. SEM was performed to image cell morphology.

Results and discussion

Scanning electron microscopy (SEM) and Fourier transform infrared spectroscopy (FTIR) demonstrated the incorporation of γ-PGA. The addition of γ-PGA improved the hydrogel swelling potential and supressed protease induced mass loss. However, mechanical strength was weakened with the addition of γ-PGA, for all assessed variables. Cell viability assays demonstrated that the hydrogels supported cellular proliferation from day 3 to 5 Figure 1a. All γ-PGA-containing scaffold compositions promoted cell adhesion as demonstrated by dense cellular layers, Figure 1b.

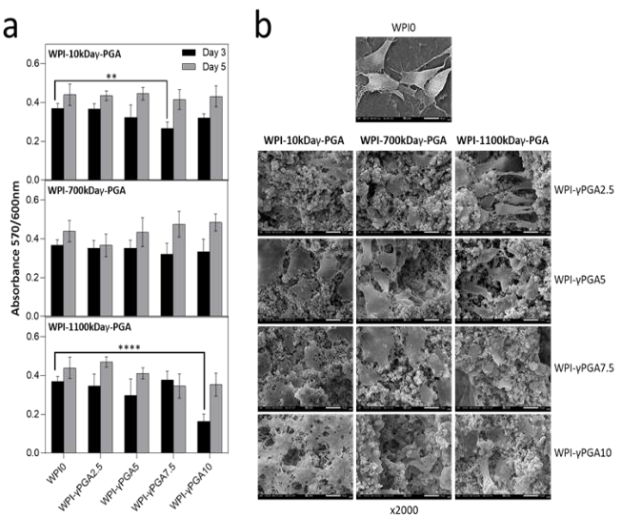

Figure 1 a and b. a, results from cell viability assays with DPSC's and b, SEM images of cellular morphology.

Conclusion

This work demonstrates the potential of WPI-γ-PGA hydrogel as tissue scaffolds. Although still preliminary the results suggest the potential of predictive degradation and demonstrates a potential route to manipulate mechanical strength. Additionally, the formation of vesicle like spheres could potentially develop a route for further drug encapsulation.

Acknowledgements

D.K.B. - The Faculty of Science and Technology, Lancaster University.
M.C., V.P. and N.N.T. - The Hellenic Foundation for Research and Innovation.

Z.P.L. - Excellence Initiative – Research University for the AGH University of Krakow.

References

1) Reginster, J.Y., et al. Bone. 2006, 38 (2), 2–9.
2) Zhang, Y.Y., et al. Small. 2021, 17,14.
3) Platania, V., et al. Mater Sci Eng C 2021, 129, 112412.
4) Baines, D.K., et al. Gels, 2023, 10 (1), 18
5) Poologasundarampillai, G., et al. Soft Matter. 2012, 8, 4822–4832

Effects of LDH-treated surfaces on biofilm formation.

Delle Fave, F. [a,*], Medaglia, P.G. [a], Froio, M. [a], Cisternino, D. [a], Giorgi, F. [b]

[a] University of Rome Tor Vergata, Italy.

[b] University of Liverpool, England.

* Corresponding author(s) e-mail(s): Francesco.Giorgi@liverpool.ac.uk

Introduction

Antibiotic resistance occurs when bacteria evolve mechanisms to survive exposure to medications designed to kill them. This phenomenon threatens the effectiveness of treatments for a wide range of infections. Reducing misuse and overuse of antibiotics is crucial to slowing the spread of resistant strains and preventing biofilm formation on surfaces. Suspensions of Layered Double Hydroxides (LDH) demonstrated their effectiveness in antimicrobial applications[1–5], however little progress has been made towards antimicrobial impact of LDH-treated surfaces.

Layered Double Hydroxides (LDH) Layered double hydroxides (LDHs) are ionic lamellar nanomaterials. Their simple synthesis method and possibility to host complex molecules in the interlamellar space makes them perfect for biological applications. Notably, the most used LDH types are MgAl based and ZnAl based, with different additives to aid in the antibacterial activity, such as lysozimes[6], p-hydroxybenzoic[7] and eucalyptus oil[8]. Moving towards LDH-treated surfaces, which topology plays a crucial role in antimicrobial mechanisms[9], A novel method of synthesizing an LDH-treated surface for antimicrobial assay is proposed.

Materials and methods

MgAl-NO_3 LDH, MgAl-Cl_2 LDH, ZnAl-NO_3 LDH, and ZnAl-Cl_2 LDH were synthesized by coprecipitation using aluminium nitrate nonahydrate or aluminium chloride hexahydrate as aluminium sources, and magnesium or zinc precursor salts[10–14]. Metal and aluminium salts were dissolved in DI water, and NaOH was added dropwise to adjust pH to 10–11. The precipitate was washed, centrifuged, and dried at 60°C for 24 hours to obtain LDH powders, which were suspended in DI water (100 mg/10 mL). Glass microscope slides, etched with 37% hydrofluoric acid, served as substrates. A 3D printed mask guided application of 150 µL LDH suspension, and slides were dried and annealed at 300°C. For bacteria assays, E. coli, S. aureus, and P. aeruginosa were cultured to 10^6 CFU/mL and incubated with the LDH-coated slides

for 24 hours at 37°C. Biofilms were detached via sonication, serially diluted, plated on agar, and colonies were counted after further incubation.

Results and discussion

Preliminary results are shown in Figure 1, in which an overall decrease in mean CFU/mL is observed when LDH is present. Notably, ZnAl-NO3 LDH seems to be the most effective on all bacteria types, causing approximately a 1-log decrease in cell viability for E. Coli and S. Aureus and a 2-log decrease for P. aeruginosa. This is expected since zinc's antimicrobial properties are widely known in literature[15]. MgAl-NO_3 LDH seems to perform worse than the S. aureus control, causing almost a 1-log increase in cell viability. More experiments are needed to consolidate the data obtained.

The antimicrobial mechanism exhibited from the preliminary results can be either topographical, due to the lamellar nanostructrure of the LDH (Figure 2), or chemical, due to the presence of antimicrobial elements like zinc. A control experiment using etched microscope slides not treated with any LDH can be used to point at the possible mechanism in place.

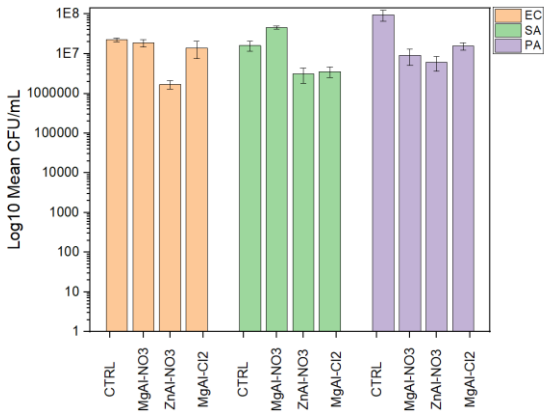

Figure 5. Mean CFU/mL for each LDH type, divided by bacteria type. Standard deviation bar for 4 samples.

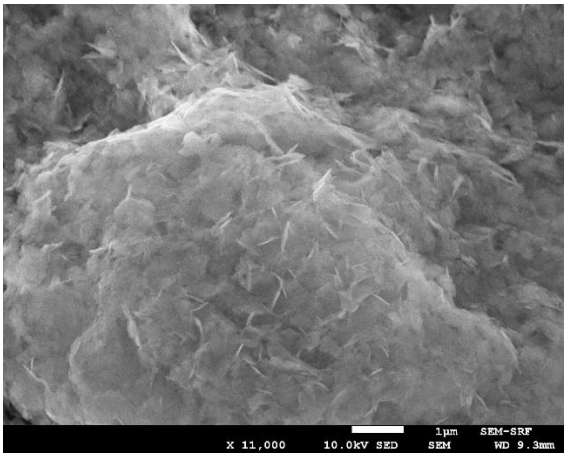

Figure 6. SEM of LDH structure on etched slide

Conclusions

Although more testing needs to be performed to consolidate the data obtained from those preliminary experiments, the advantage of a scalable synthesis of LDH-treated planar surfaces lies in their potential for widespread application in antimicrobial coatings, offering a cost-effective and

adaptable platform for surface functionalization in healthcare and environmental settings

References

1 C. Forano, F. Bruna, C. Mousty and V. Prevot, *Chem. Rec.*, 2018, **18**, 1150–1166.

2 R. E. K. Billah, Z. Azoubi, E. A. López-Maldonado, H. Majdoubi, H. Lgaz, E. C. Lima, A. Shekhawat, Y. Tamraoui, M. Agunaou, A. Soufiane and R. Jugade, *ACS Omega*, 2023, **8**, 10051–10061.

3 M. Kiani, M. Bagherzadeh, A. M. Ghadiri, P. Makvandi and N. Rabiee, *Sci. Rep.*, 2022, **12**, 9461.

4 M. Li, Z. P. Xu, Y. Sultanbawa, W. Chen, J. Liu and G. Qian, *Colloids Surf. B Biointerfaces*, 2019, **181**, 585–592.

5 A. M. Cardinale, S. Vecchio Ciprioti, M. Fortunato and M. Catauro, *J. Therm. Anal. Calorim.*, 2023, **148**, 1523–1532.

6 Q.-Z. Yang, Y.-Y. Chang and H.-Z. Zhao, *Water Res.*, 2013, **47**, 6712–6718.

7 Y. Yang, L. Xiong, X. Huang, Q. Shi and W.-D. Zhang, *Compos. Commun.*, 2019, **13**, 112–118.

8 M. Lobo-Sánchez, G. Nájera-Meléndez, G. Luna, V. Segura-Pérez, J. A. Rivera and G. Fetter, *Appl. Clay Sci.*, 2018, **153**, 61–69.

9 J. Awassa, S. Soulé, D. Cornu, C. Ruby and S. El-Kirat-Chatel, *Nanoscale*, 2022, **14**, 10335–10348.

10 D. Scarpellini, C. Falconi, P. Gaudio, A. Mattoccia, P. G. Medaglia, A. Orsini, R. Pizzoferrato and M. Richetta, *Microelectron. Eng.*, 2014, **126**, 129–133.

11 K. Abderrazek, N. Frini Srasra and E. Srasra, *J. Chin. Chem. Soc.*, 2017, **64**, 346–353.

12 A. A. A. Ahmed, Z. A. Talib, M. Z. Bin Hussein and A. Zakaria, *J. Solid State Chem.*, 2012, **191**, 271–278.

13 S. (Grace) Intasa-Ard, S. Bureekaew and M. Ogawa, *J. Ceram. Soc. Jpn.*, 2019, **127**, 11–17.

14 N. Gerds, V. Katiyar, C. B. Koch, J. Risbo, D. Plackett and H. C. B. Hansen, *Appl. Clay Sci.*, 2012, **65–66**, 143–151.

15 R. Kumar, A. Umar, G. Kumar, and H. S. Nalwa, *Ceram. Int.*, 2017, **43**, 3940–3961.

Mucoadhesive Hydrogel-Nanofiber Composites for Sustained Ocular Chemotherapy in Conjunctival Melanoma

Desai, N. [a], Robinson, D. E. [a], Colley, H. E. [b], Krishna, Y. [a,c], Bosworth, L. A. [a], Kearns, V.R. [a,*]

[a] Department of Eye and Vision Science, Institute of Life Course and Medical Sciences, University of Liverpool, Liverpool L7 8TX, United Kingdom.

[b] School of Clinical Dentistry, University of Sheffield, Sheffield S10 2TA, United Kingdom.

[c] National Specialist Ophthalmic Pathology Service, Liverpool Clinical Laboratories, University Hospitals of Liverpool Group, Liverpool L7 8YE, United Kingdom

* Corresponding author(s) e-mail(s): Vkearns@liverpool.ac.uk

Introduction

Conjunctival melanoma (Co-M) is a rare but aggressive ocular malignancy associated with high recurrence and metastasis[1]. Current topical mitomycin C (MMC) treatments are limited by poor retention, epithelial toxicity, and dosing burdens[2]. With this study, we aim to develop a bioengineered, mucoadhesive composite consisting of poly(ε-lysine)-based hydrogels (PeK/PeK-MA) integrated with electrospun PCL nanofibers to enable sustained and localized ocular drug delivery[3,4].

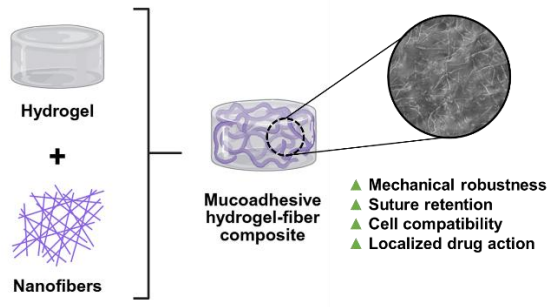

Figure 1. Schematic representation of the engineered mucoadhesive hydrogel-fiber composite formed by integrating electrospun nanofibers within a poly(ε-lysine)-based hydrogel matrix. The composite combines the structural and drug-loading advantages of nanofibers with the conformability and bioadhesion of hydrogels, offering a platform for sustained and localized ocular drug delivery.

Materials and methods

PeK and PeK-MA hydrogels were synthesized via carbodiimide and methacrylate crosslinking, respectively, and characterized using FTIR, NMR, and compression testing. Electrospun PCL nanofibers were fabricated and surface-modified using NaOH or plasma to enhance hydrophilicity. Composites were formed by embedding nanofibers

into the hydrogel matrix and assessed by SEM for structural integrity. Mucoadhesive and physicochemical properties were evaluated via swelling, zeta potential, and wettability assays. Cytocompatibility was tested using human conjunctival epithelial (HCjE) and melanoma cell lines (CRMM1, CRMM2, CM2005.1). MMC IC_{50} values were determined to guide future drug loading.

Results

PeK-MA hydrogels showed successful methacrylation and a compressive modulus of ~0.14 MPa. Incorporation of nanofibers increased composite stiffness to ~7.5 MPa, improving mechanical robustness. Water contact angle measurements (~39°) confirmed enhanced surface wettability compared to untreated PCL nanofibers and hydrogel-only controls. Cytocompatibility studies showed significantly higher HCjE proliferation on composites compared to hydrogel-only controls at day 21. MMC exhibited IC_{50} values of 0.32–0.58 μg/mL across Co-M cell lines, with sustained cytotoxicity observed up to 72 hours post-treatment.

Discussion

The composite design addresses key limitations of standalone hydrogels by improving structural stability, surface properties, and cellular response. The extended cytotoxic effect of MMC supports the feasibility of sustained delivery, offering a promising solution to reduce dosing frequency and improve treatment efficacy in ocular oncology by enabling more precise targeting and localized therapeutic effect.

Acknowledgements

This research was supported by the MRC through the DiMeN Doctoral Training Partnership (MR/W006944/1) and by the EPSRC under grant number EP/Y001656/1.

References

1 C. L. Shields, A. M. V. Silva, A. Laiton, N. E. Kalafatis, E. Schiller, S. E. Lally, J. M. Grant-Kels and J. A. Shields, *Clin Dermatol*, 2024, 42, 46–55.

2 K. Butt, R. Hussain, S. Coupland and Y. Krishna, *Cancers (Basel)*, 2024, 16, 3121.

3 L. A. Bosworth, L.-A. Turner and S. H. Cartmell, *Nanomedicine*, 2013, 9, 322–335.

4 M. Zhang, S. Xu, R. Wang, Y. Che, C. Han, W. Feng, C. Wang and W. Zhao, *J Mater Sci Technol*, 2023, 162, 157–178.

Resonant cavity enhanced photodetectors for non-invasive glucose detection

Fletcher, J.E.[a]*, Davis, S.L.[a], Bunyan, J.A.[a], Castaño, F.J.[b], Marshall, A.R.J[a]

[a]Physics Department, Lancaster University, Lancaster, United Kingdom, LA1 4YB

[b]ams-osram AG, Technology R&D, Tobelbader Strasse 30, 8141 PremstaeHen, Austria

*e-mail: J.Fletcher6@lancaster.ac.uk & a.r.marshall@lancaster.ac.uk

Introduction

Diabetes is a serious, life-threatening disease that is projected to impact a staggering 700 million people globally by 2045 [1]. Current techniques for monitoring blood glucose rely on painful and invasive methods, which are well known to reduce patient uptake [2]. Instead, infrared spectroscopic sensing could enable the non-invasive and high accuracy monitoring of blood glucose. To achieve this, infrared sensors must both discriminate between incident wavelengths as well as sense with high signal-to-noise ratios. Obviously, they must also fit into a tiny form factor and consume minimal energy, which prohibits the use of cooling to boost performance, and large optics to disperse wavelengths. This paper reports on the exciting advancement of Resonant cavity enhanced photodetectors (RCE-PDs) with InGaAsSb absorbers. Because the resonance condition allows for the precise tuning of the spectral response to a narrow band of wavelengths, the need for large dispersive optics is eliminated. Moreover, the InGaAsSb material system allows for the sensing of the stronger and more defined spectral features in the e-SWIR band [3], allowing measurements of biologically relevant glucose concentration with high accuracy.

Materials and methods

This work firstly presents simulations that study the RCE-PD photo-response induced by a change in glucose concentration. By varying the RCE-PD centre peak wavelength (CPW) and full width at half maximum (FWHM), the optimal RCE-PD parameters that maximise the photo-response change (in response to a change in glucose concentration) were identified. Informed by the simulations, an RCE-PD was epitaxially grown on an n-GaSb substrate using a Veeco GenXplor MBE reactor. The epitaxial structure consisted of a GaSb/AlAsSb distributed Bragg reflector input mirror and an optical cavity consisting of an InGaAsSb absorption layer. Standard lithography and etching techniques were then used to fabricate mesas and deposit a Ni/Au output mirror. Devices were subsequently wire bonded to a header and mounted onto an optical bench containing a

Thorlabs Tungsten-Halogen light source and a liquid cell with an adjustable path length. The photo-response was then measured for various glucose concentrations using a Keithley 2400 source measurement unit.

Results

The photo-response change induced by a change in glucose concentration has a complex dependence on, wavelength, temperature and water displacement effects. At a CPW of ~2125 nm, the photo-response is maximised, but strongly depends on the FWHM. At wavelengths smaller than ~2075 nm, the water displacement factor becomes larger than the molar absorptivity of glucose, causing the infrared absorption by the solution to decrease as the glucose concentration increases. Therefore, as the FWHM increases, the photo-response becomes correlated to portions of the spectrum that have opposite dependencies on glucose concentration, reducing the overall change in photo-response. The photo-response change of an RCE-PD with a CPW targeted 2125 nm was measured across a wide range of glucose concentrations. The photo-response demonstrates a strong dependence on glucose concentration up to clinically relevant concentrations and yields excellent agreement with the simulations.

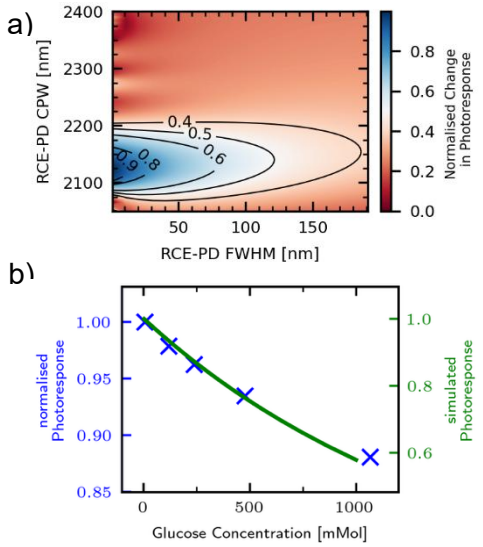

Figure 1 a) Simulation results demonstrating the optimum RCE-PD parameters to target for glucose sensing. b) Measured photocurrent for different glucose concentration, compared to simulation results.

Discussion

The work demonstrated here illustrates the advantages of using RCE-PDs for spectral sensing of glucose. Due to the complex and strong wavelength dependence on the absorption of infrared light by glucose solution, this work has illustrated the importance of targeting appropriate wavelengths to ensure strong correlations between the photo-response and the glucose concentration. Furthermore, an RCE-PD grown through Molecular beam epitaxy yielded a strong correlation

between the photo response across a wide range of glucose concentrations.

References

[1] Saeedi P, *et al*. Diabetes Research and Clinical Practice. 2019 Nov 1;157:107843.

[2] Ong WM, *et al*. *Patient Preference and Adherence*. 2014 Feb 15:237-46.

[3] Amerov AK, *et al. Applied Spectroscopy*. 2004 Oct 1;58(10):1195-204.

Development and Characterization of Multi-Material Hydrogels for Mimicking Skin Layers

Mete Gunaydin, H. [a,*], Metcalfe, A. [a] , Grover L.M. [a]

[a] School of Chemical Engineering, University of Birmingham, Edgbaston, UK.

* hxm304@student.bham.ac.uk

Introduction

Natural-synthetic composite hydrogels are widely used in the biomedical field due to their tunable properties to mimic skin. [1] Full-thickness skin substitute- including the epidermis, dermis, and hypodermis—should ideally replicate the mechanical properties of each corresponding skin layer. Given that skin demonstrates complex mechanical behavior due to the strain-stiffening properties of collagen and elastin fibers, leading to an exponential stress-strain relationship. Additionally, skin exhibits viscoelastic characteristics, showing time and rate-dependent responses, particularly during compression tests at higher strain rates. The diverse mechanical properties of skin stem from its multilayered structure, comprising the epidermis and dermis, with fiber orientation contributing to its heterogeneous nature.[2] This study aims to develop and characterize a multi-material hydrogel system fabricated via SLAM to replicate the mechanical behavior of layered skin using advanced hyperelastic modeling.

Materials and methods

Hydrogel Formulation and Fabrication:

Alginate (2–4% w/v) was gradually mixed with gelatin (1–2% w/v) at a 1:1 (v/v) ratio under continuous stirring. PEGDA (2–12% w/v) and 0.5% (w/v) photo-initiator were added, followed by $CaCO_3$ and GDL powders at 1:2 molar ratios. The mixture was poured into molds and incubated at 37°C, 5% CO_2 for 15 min for initial ionic crosslinking, then UV-exposed (360–420 nm) for 2 min to complete gelation, followed by overnight incubation.

3D Printing**:** The suspended layer additive manufacture (SLAM) technique was used to print the hydrogels. Its capability to operate at low viscosities enabled the precise fabrication of anisotropic structures that closely mimic real skin.[3] Furthermore, SLAM allowed for controlled, layer-by-layer construction of hydrogel formulations with directional mechanical properties.[4]

Mechanical Testing and Validation:

The mechanical properties of GAP hydrogels with varying concentrations were

evaluated using uniaxial compression tests on cylindrical samples. The resulting stress–strain curves exhibited nonlinear elastic behavior, resembling the mechanical response of human skin. Porcine skin was used as a biological reference model and subjected to the same testing protocol to provide comparative data. Experimental results were fitted to various hyperelastic models, including Ogden, Gasser-Ogden-Holzapfel (GOH), Mooney-Rivlin, Neo-Hookean and Fung models. [5] The mechanical behavior of GAP hydrogels was then characterized and compared with both native skin tissue and existing literature values. [2,6]

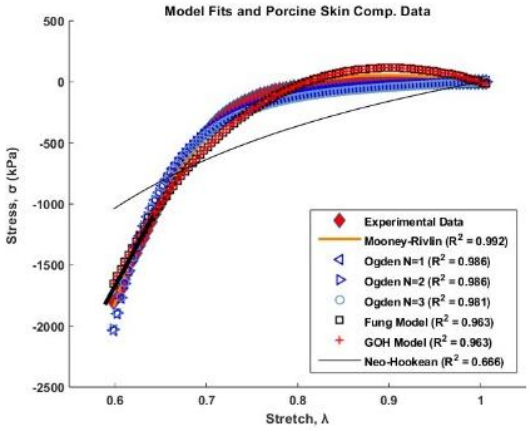

Figure 1. Fit of constitutive models to uniaxial compression data of porcine skin until failure

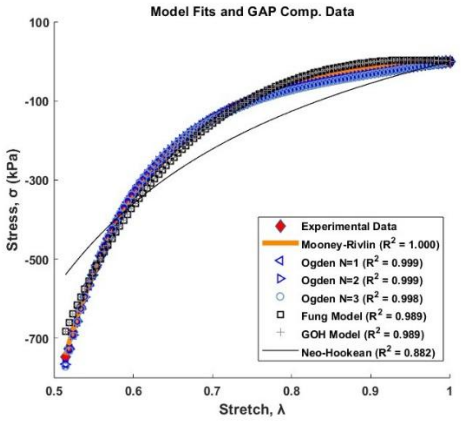

Figure 2. Fit of constitutive models to uniaxial compression data of GAP hydrogel until failure.

Results and Discussion

Full-thickness porcine skin displayed nonlinear elastic behavior, with a low-strain modulus below 100 kPa and high-strain modulus reaching 1.72 × 10⁴ kPa. The Mooney-Rivlin model provided the best fit (R^2 = 0.992) as shown in Fig1. GAP hydrogels showed a perfect Mooney-Rivlin fit (R^2 = 1.000) and closely matched target layer mechanics. The Ogden models also show higher accuracy with R^2 values of 0.999 for N=1 and N=2, and 0.998 for N=3, confirming suitability for modeling anisotropic behavior (Fig2.).

Experimentally, one formulation of the GAP hydrogel exhibited a low-strain modulus of 221.7 ± 46.3 kPa, indicating a compliant initial response. Under high-strain conditions, the modulus increased

significantly, reaching 5.65±1.33 MPa, consistent with the nonlinear stiffening behavior typically observed in soft anisotropic materials. These values align with the target mechanical ranges reported for dermal tissues, with low-strain moduli between 0.073–0.103 MPa and high-strain moduli ranging from 4.145–11.471 MPa, suggesting the hydrogel's suitability for soft tissue applications.[2]

While full-thickness skin mechanics are not yet fully replicated—expected for a single-layer hydrogel—the results are promising. Future work will explore SLAM-based multi-layer formulations with enhanced interlayer adhesion and mechanical strength. Incorporating three-layer printing and cellular components may better replicate native skin properties.

Conclusion

SLAM fabrication allows for efficient 3D printing of anisotropic structures similar to skin layers. Hyperelastic, 3D printable, shear-thinning, and balanced swelling hydrogels were formulated to mimic the skin layers. The hydrogels closely matched the target tissue mechanics, exhibiting nonlinear elastic responses and moduli within the physiological range of dermal tissues. Constitutive modeling with Mooney-Rivlin and Ogden formulations confirmed the material's suitability for mimicking soft anisotropic tissues, with excellent goodness-of-fit values.

Acknowledgements

The author thanks the Ministry of National Education of the Republic of Türkiye (YLSY program) for supporting tuition and living expenses, and the host institution for covering research-related costs.

References

1 K. Fetah, P. Tebon, J. Marcus, I. D. Derman, T. Rivera, L. G. Cerda and Y. P. Singh, *International Journal of Extreme Manufacturing*, DOI:10.1088/2631-7990/ad878c.

2 H. Joodaki and M. B. Panzer, *Proc Inst Mech Eng H*, 2018, **232**, 323–343.

3 M. E. Cooke and D. H. Rosenzweig, *APL Bioeng*, DOI:10.1063/5.0031475.

4 R. J. A. Moakes, J. J. Senior, T. E. Robinson, M. Chipara, A. Atansov, A. Naylor, A. D. Metcalfe, A. M. Smith and L. M. Grover, *APL Bioeng*, DOI:10.1063/5.0061361.

5 A. Pissarenko and M. A. Meyers, *Prog Mater Sci*, 2021, **120**, 100816.

6 S. A. Muslov, S. S. Pertsov, E. A. Chijmakov, N. B. Astashina, V. N. Nikitin

and S. D. Arutjunov, *Russian Journal of Biomechanics*, 2023, **27**, 67–79.

Development of an Antifungal Smart Biomaterial with Engineered Microenvironments for Corneal Regeneration

Ortega Asencio, I. [a], Claeyssens, F. [b], Shepherd, J. [a], Gunen, M. [a,*]

[a] School of Clinical Dentistry, The University of Sheffield, United Kingdom.

[b] School of Chemical, Materials and Biological Engineering, The University of Sheffield, United Kingdom.

* Corresponding author(s) e-mail(s): mgunen1@sheffield.ac.uk

Introduction

Corneal blindness, often resulting from limbal stem cell deficiency, remains a pressing global health concern. Simple limbal epithelial transplantation (SLET) offers a viable treatment by affixing limbal explants onto an amniotic membrane (AM) with fibrin glue. However, AM use is limited by infection risk, ethical issues, and scarce availability, while fibrin glue may inhibit cell proliferation. Based on clinical feedback, this study aims to develop a smart, ring-shaped corneal device made of adhesive, antimicrobial polymers, eliminating the need for AM and fibrin glue.

Materials and methods

Reagents including PEG (400 Da), PLGA (44,000 Da), and natamycin were obtained from commercial suppliers. The artificial limbal ring was fabricated from a slow-degrading PCL-based polyHIPE featuring engineered microenvironments, as detailed in [1]. Its cover was electrospun using PLGA-PEG blends dissolved in a DCM-DMF solvent system with natamycin. Electrospinning was conducted at flow rates of 1 mL/h and voltages of 19 kV. 3D-printed models with retentive geometries were evaluated under dynamic conditions (645 rpm, 6° tilt, 6 h). Scaffold characterisation included SEM, EDS, profilometry, tensile testing, and contact angle measurement. Antifungal activity was assessed via UV-visible spectroscopy and disc diffusion assays. Porcine corneal models were used for ex vivo studies.

Results

Natamycin was effectively encapsulated within electrospun nanofibers (2–4 μm) with minimal bead formation and no adverse effects on mechanical properties. Higher polymer content enhanced rigidity but reduced porosity, while PEG concentration influenced transparency and fibre morphology. Optimised PEG content yielded a nanofibrous, transparent membrane. A PCL-based polyHIPE (82% internal phase) formed a highly

interconnected structure. Flow assays showed 88% retention of explants in microenvironments. Antifungal tests against *Candida albicans* confirmed robust activity of natamycin and essential oils (diffusion zones: 120–160 mm). Preliminary results on air-liquid interface corneal models showed effective fungal response and wound healing potential.

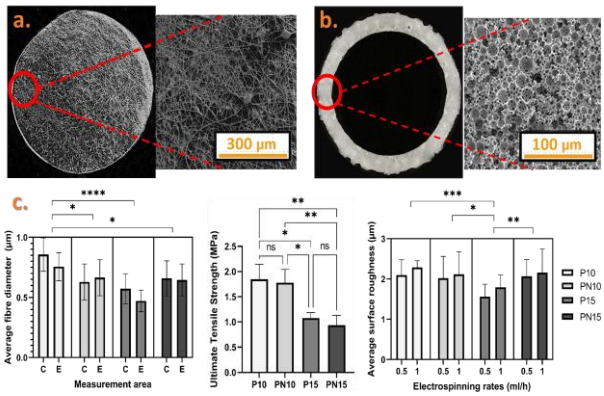

Figure 1. (a) Electrospun PLGA-PEG membrane including natamycin with optimal transparency. (b) PCL polyHIPE with its interconnected porous structure. (c) Fibre diameters and mechanical properties.

Discussion

Controlled pore distribution is key to scaffold performance: micro-pores (<5 µm) support fibroblast adhesion, medium pores (5–250 µm) allow cell infiltration, and macro-pores (>250 µm) promote vascularization [2,3]. Interconnected architectures enhance nutrient exchange and ECM formation. PEG400, a plasticizer, improves flexibility by reducing polymer chain entanglement [4]. Its hydrophilicity and compatibility with PLGA contribute to smoother fibers and lower light scattering, aided by the materials' matched refractive indices (~1.46), ensuring optical clarity. These properties support the suitability of the selected materials for ocular applications.

Conclusion

This work demonstrates the fabrication of porous PCL polyHIPEs and transparent, adhesive PLGA-PEG membranes incorporating antifungal agents. The resulting corneal device facilitates cell integration and microbial protection, offering a viable alternative to AM and fibrin glue in SLET.

References

1) B. Aldemir Dikici, et. al, *Polymer*, 2019, **175**, 243-254.
2) K. Zhang, et. al, *Regenerative Biomaterials*, 2018, **5**, 115-124.
3) B. Vagaská, et. al, *Physiological Research*, 2010, **59**, 309-322.

4) T.E. Paterson, et. al, *ACS Applied Bio Materials*, 2021, **4**, 5638-5649.

Advanced 3D Printing of PEKK/hydroxyapatite Composites via Fused Filament Fabrication (FFF) for Medical Implants

Hasson, F.*[1], Boyd, A.[1], Krzysztof, R.[1], Ward, J.[1], McIlagger, A.[1]

[1] Ulster University, United Kingdom

*hasson-f3@ulster.ac.uk

Introduction

Polyetherketoneketone (PEKK) is a high-performance thermoplastic polymer[1] from the PAEK family of polymers[2]. It is a novel biomaterial that is of particular interest for replacing metallic implants due to its excellent biocompatibility and mechanical properties. Fused filament fabrication (FFF) 3D printing provides an opportunity to create novel and customised PEKK implant solutions; however, anisotropic properties may result. This effect can be reduced by tailoring the print parameters to suit the material, as polymer crystallisation is driven by temperature[4]. When printing temperatures are high the polymer may crystallise more rapidly, causing shrinkage, warping, and weak inter layer bonding due to the thermal shield created by the spherulites during crystallisation. A lower temperature causes the polymer to crystalise more slowly, allowing material deposition onto an amorphous layer resulting in good inter layer bonding and improved mechanical properties[4]. It is crucial that suitable processing parameters are implemented during printing to ensure good mechanical and chemical properties of the part[5]. This study proposes a method of FFF which allows the mechanical properties to be tailored due to the ability to print crystalline, amorphous, and in-situ crystallised 3D printed parts.

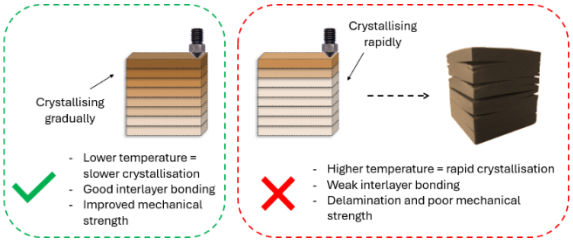

Figure 1 - The effect of temperature on crystallisation of 3D printed PAEK parts.

- Good interlayer bonding
- Improved mechanical strength
- Weak interlayer bonding
- Delamination and poor mechanical strength

Figure 1 - The effect of temperature on crystallisation of 3D printed PAEK parts.

However, PEKK is non-biodegradable and bioinert, which may lead to fibrous encapsulation of the implant and weak osteointegration at the bone-implant interface[5,6]. The main strategy implemented in this study to improve the osteointegration of PEKK is the addition of a hydroxyapatite (HA), which acts as a bioactive filler[5]. HA is chemically similar to the mineral component of bone and is

therefore osteoconductive and promotes osteointegration with the implant[7]. However, the challenge lies within identifying the precise quantity of HA that strikes a balance between preserving the mechanical properties of PEKK while simultaneously promoting bone growth[8]. Furthermore, confirming the presence of HA on the uppermost surface of the material is highly important.

Materials and Methods

The filaments for the study were produced by twin-screw extrusion using a co-rotating twin-screw extruder (Thermo Fischer Rheomex). CAPTAL®R hydroxyapatite filler (Plasma Biotal) was added to the KEPSTAN® PEKK 7003 (Arkema) polymer matrix at various weight percentages (0wt%-20wt%). The samples for the study were produced using fused filament fabrication (FFF) on a New Dimension OP Series 3D printer. For the first phase of the study, the parameters were adjusted to print samples at high temperature (HT), low temperature (LT), and a middle-ground 'adaptive' (A) approach.

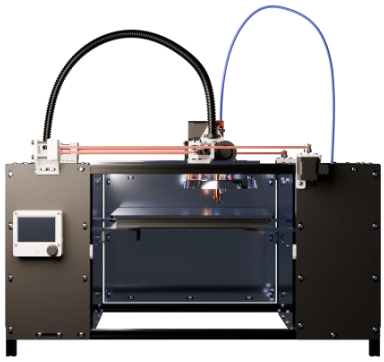

Figure 2. OP Series 3D Printer used to print specimens

For the second phase of the study, the samples were abraded with P240 silicon carbide paper. The 'as received' and 'abraded' 3DP samples were then assessed to observe any increase in HA on the surface. A range of analytical characterisation methods were employed in this study to assess polymer crystallinity: Scanning Electron Microscopy (SEM), X-Ray Diffraction (XRD), and Differential Scanning Calorimetry (DSC). To assess the presence of HA on the surface the following techniques were used: Thermal Gravimetric Analysis (TGA), Scanning Electron Microscopy with Energy Dispersive X-ray analysis (SEM-EDX), Fourier Transform Infrared Spectroscopy (FT-IR), and X-ray photoelectron spectroscopy (XPS). Additionally, the 'as received' and 'abraded' samples were immersed in SBF for a period of 7 days. Following this, apatite formation was analysed via EDX and FTIR to

determine the bioactivity. The in-vitro capability of the samples was determined – cell attachment was observed via SEM, and cellular metabolic activity was assessed using a Resazurin Reduction assay.

Results

SEM analysis revealed polymer spherulites indicative of the 3D printing conditions utilised. The XRD data is consistent with these images, reflecting the amorphous or semicrystalline nature of the samples. Furthermore, the % crystallinity was calculated from the XRD spectra at 27.20%, 0%, and 25.69% for the HT, LT and A samples respectively.

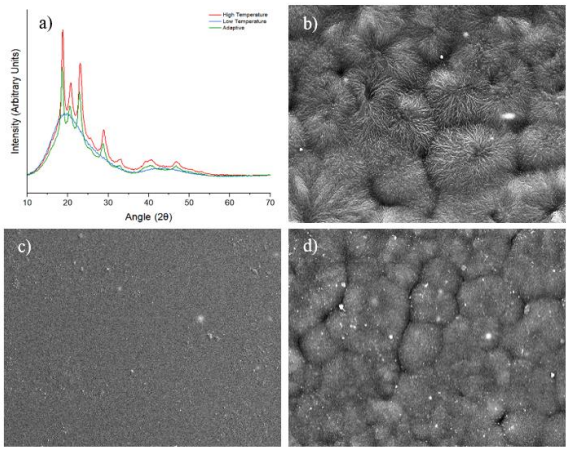

Figure 3. a) XRD spectra of high temperature, low temperature, and adaptive 3DP samples, b-d) SEM images of high temperature, low temperature, and adaptive 3DP samples respectively.

The crystallisation kinetics of the polymer were investigated via DSC and revealed fastest crystallisation around 230°C. Higher printing temperatures also shifted the glass transition towards higher temperatures.

TGA confirmed the expected wt% of filler in each sample. FTIR analysis revealed the presence of increasing PO_4^{3-} peaks between 900-1150 cm^{-1} with increasing wt% of HA, which is agreeable with the TGA results. However, the XPS spectra revealed negligible levels of Ca2p and P2p on the surface of the 'as-received' samples. The XPS spectra of the abraded samples showed a significant increase in the Ca2p and P2p peaks, confirming the presence of HA on the uppermost surface of the samples. These findings are supported by SEM-EDX analysis, which confirmed the homogeneous presence of calcium (Ca) and phosphate (P) elements on the surface of the abraded samples.

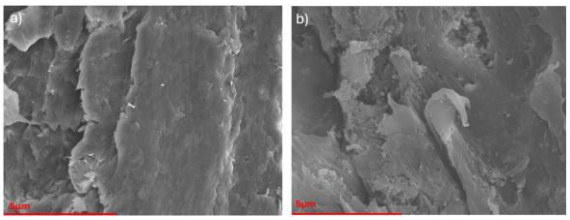

Figure 4. SEM images of a) PEKK-HA 20wt% 'as received' and b) PEKK-HA 20wt% abraded after immersion in SBF for 7 days, showing apatite formation on the abraded sample only.

The SBF study revealed that the ‘as-received’ samples were not bioactive, while apatite formation was observed on the abraded samples after 7 days.

Discussion

This study has confirmed the theory that during FFF the material must be deposited onto an amorphous layer, not a semi-crystalline layer, to achieve improved mechanical properties. Additionally, this study confirmed the presence of bioactive HA in the bulk of PEKK-HA composite 3D printed samples. However, the analysis suggests that the expected quantity of HA is not available on the uppermost surface of the samples, and that some post processing is required to achieve this. The abraded PEKK-HA samples formed a hydroxyapatite like layer, which may indicate that this material has bone-building potential. More investigation is required regarding different surface treatment methods, such as grit blasting. Furthermore, it may be beneficial to dope the HA with bioactive ions such as strontium (Sr) to further functionalise the surface and improve the bioactivity of the implant.

References

1) Alqurashi, H. et al. J Adv Res, (2021).
2) Lee, W. F. et al. Polymers (Basel), (2022).
3) Petersmann, S. et al. Journal of Materials Research and Technology, (2023).
4) Rodzeń, K. et al. Macromol Mater Eng, (2023).
5) Rodzeń, K. et al. Polymers, (2021).
6) Yuan, B. et al. Biomaterials, (2018).
7) Zheng, J. et al. Materials Science and Engineering C, (2021).
8) Li, S. et al. Composites Communications, (2021).
9) Manzoor, F. et al. J Mech Behav Biomed Mater, (2021).

Dual-Action Adenosine-Functionalized Scaffolds for Macrophage Reprogramming and Thyrocyte Support

Heim, M.[a, b], Handley, E.L.[a], Grant, D. [a] Hegarty, L.[b, c] Emmerson, E.[b] Callanan, A.[a]

[a] Institute of Bioengineering, School of Engineering, University of Edinburgh, UK.

[b] Centre for Regenerative Medicine, Institute for Regeneration and Repair, University of Edinburgh, UK.

[c] Centre for Inflammation Research, Institute for Regeneration and Repair, University of Edinburgh, UK.

* Corresponding author(s) e-mail(s): m.heim@ed.ac.uk

Introduction

92% of patients experience radiation-induced hypothyroidism (RIHT) following head and neck radiotherapy[1]. While the aetiology is unknown, oxidative stress and fibrosis are thought to be major contributors[2,3]. Current treatment relies on lifelong hormone replacement, which fails to restore native thyroid function[4]. Given their role in tissue repair and immune regulation, macrophages (Mφ) represent a compelling therapeutic target. This study explores adenosine-functionalized electrospun scaffolds as a dual-action platform to reprogram Mφ toward a reparative phenotype while supporting thyrocyte viability and antioxidant response.[4-10]

Materials and methods

Thyroid-resident Mφ subtypes were characterized in healthy murine tissue using flow cytometry and immunofluorescence. Reactive oxygen species (ROS) and fibrotic markers were assessed in a murine model of thyroid irradiation injury. Electrospun polycaprolactone (PCL) scaffolds incorporating 0.5%, 1%, 3% and 4% adenosine were fabricated and assessed for physical and mechanical properties. Nthy-ori 3-1 thyroid cells and THP-1-derived Mφ were cultured on scaffolds for 14 days to evaluate cellular responses.

Results

Two CSF1R-dependent resident Mφ subsets ($CD206^{+}CD11c^{-}$ and $CD206^{-}CD11c^{+}$) were identified in the healthy thyroid. An accumulation of nuclear ROS and upregulation of fibrotic marker (KRT8) was found in the irradiated thyroid, indicating underlying mechanisms of tissue damage. Scaffolds with up to 3% adenosine-maintained fibre integrity and provided controlled release profiles. The 1% scaffold most effectively supported Nthy-ori 3-1 proliferation, epithelial marker expression (ECAD, ZO-1), and thyroid-specific genes (TPO, NKX2.1). GPx1 and

CAT expression was elevated in both 1% and 3% groups, suggesting enhanced oxidative stress defence. mTHP-1 cells cultured on 1% and 3% scaffolds exhibited increased CD206 and CD163, reduced CD86 and TNF-α, and elevated IL-10 expression, indicating a shift toward a reparative Mφ phenotype.

Discussion

Adenosine-functionalized scaffolds show strong potential to modulate the irradiated thyroid microenvironment through immune reprogramming and antioxidant enhancement. The 1% scaffold offered the most balanced effect, improving thyroid cell function while promoting Mφ-driven tissue repair. This approach may serve as a future implantable therapy for RIHT, targeting the underlying pathology rather than just replacing hormones.

Acknowledgements

For financial support we thank UKRI Engineering and Physical Sciences Research Council (EPSRC) (EP/T517884/1), the Medical Research Council (MR/L012766/1 and MR/X018733/1) and the Wellcome Trust Institutional Strategic Support Fund (ISSF).

References

1) L. Zhou, et al., *J Cancer*, 2021, 12, 451.

2) S. Chakraborti, B. K. Ray and S. Roychoudhury, Handbook of Oxidative Stress in Cancer: Mechanistic Aspects, *Springer Nature*, 2022, vol. 1.

3) S. Wongwattananard, et al., 2022, preprint, DOI: 10.21203/rs.3.rs-1956532/v1.

4) M. Heim, et al., *Front Endocrinol*, 2022, 5;13:997288

Development of an in vitro wound healing model for large conjunctival defects

Hollett, J.A. [a*], Citro, V. [a], Tang, G. [a], Bosworth, L.A. [a*]

[a] Department of Eye and Vision Science, University of Liverpool, United Kingdom.

* Corresponding author(s) e-mail(s):

jessica.hollett@liverpool.ac.uk; lucy.bosworth@liverpool.ac.uk

Introduction

The conjunctiva is a translucent, mucosal membrane which lines the sclera of the eye and the inside of the eyelids.[1] In some conditions, the conjunctiva can become damaged to an extent in which the tissue cannot repair itself without excessive scarring or loss of function.[2] In these circumstances, amniotic membrane (AM) is widely used in practice. While AM is an effective treatment option, it is associated with increased risk of infection and keratitis, and there are ethical concerns around its use.[3] For this reason, there is a drive to develop synthetic materials for conjunctival transplantation. However, these materials are often escalated quickly to rabbit models, as the current in vitro testing does not effectively replicate the wound environment that would be encountered clinically.

We endeavoured to develop an in vitro model, using an immortalised human conjunctival epithelial cell line (HCjE) and electrospun poly(ε-caprolactone) (PCL) membranes, to mimic a large conjunctival defect and allow assessment of conjunctival substrates for transplantation.

Materials and methods

Model assembly: The model comprised a 3D printed polylactic acid (PLA) tube, with an electrospun membrane affixed to one end using silicone glue (**Figure 1**). Membranes were fabricated from a 10%w/v PCL in 1,1,1,3,3,3-hexafluoroisopropanol solution, spun onto a static collector plate with a 21cm needle-collector distance, 400 µL/h flow rate, +30kV applied voltage at the needle and -4kV at the collector, in 50% relative humidity, 23°C for 1 hour. The assembled model was irradiated with ultraviolet light (20 minutes per side) and disinfected in 70%v/v ethanol. The membrane was washed with phosphate buffered saline (PBS) and soaked in conjunctival medium for 60 minutes.

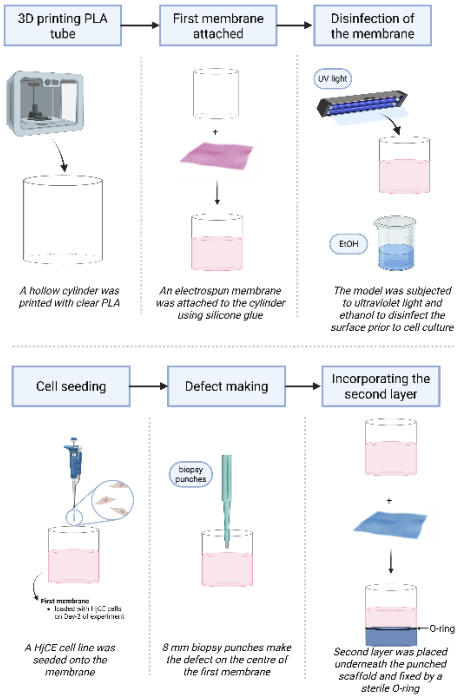

Figure 1. Experimental set up of the conjunctival defect model.

HCjE cells were seeded at a density of 25,000 cells/cm^2, incubated at 37°C, 5% CO_2 for 30 minutes, and then topped up with media. After 24 hours, the membrane was punctured with a biopsy punch, to generate a controlled defect with an 8mm diameter. Using an O-ring, a second "treatment" layer of fibres was attached to the model, ensuring contact with the "injured" cell layer. Negative controls did not receive a second membrane, and treatment groups were either coated with laminin-322 or left uncoated. At Days 1, 3 and 7, samples were analysed by PicoGreen assay (to quantify DNA content) and scanning electron microscopy (SEM) (to assess morphology and distribution of cells).

PicoGreen: Membranes were removed from the PLA tube and placed in sterile microcentrifuge tubes with 1mL lysis buffer. Samples were vortexed and freeze/thawed before adding PicoGreen working reagent and read on a plate reader.

SEM: Samples were fixed in 1.5%v/v glutaraldehyde in PBS for 30 minutes at 4°C. Samples were washed 2X with PBS, dehydrated in ascending concentrations of ethanol, and chemically dried in hexamethyldisilane. Samples were gold sputter coated and imaged.

Results

PicoGreen: samples at Day 1 and Day 3 showed a significant difference between DNA content on the negative control compared to both of the treatment options. For Day 1, the negative control had a DNA content of 0.27 ± 0.03 µg/mL, compared to 0.54 ± 0.09 µg/mL and 0.56 ± 0.05 µg/mL for samples with laminin and without laminin respectively. At Day 3, the negative control had a DNA content of 0.92 ± 0.38 µg/mL compared to 1.67 ± 0.05 µg/mL and 1.54 ± 0.17 µg/mL for samples with and without laminin respectively. There was no

significant difference between samples ± laminin coating.

SEM: at Day 1, no cells appear to be established on the second membrane, but areas around the defect show cells beginning to grow into the defect (Figure 2). At Day 3, few cells can be observed on the second membrane.

Discussion

The increase in DNA content from the negative controls to the treated samples implies that the cells are proliferating into the defect region when a second membrane is applied, as predicted. This confirms that the second membrane can support cell proliferation following a controlled injury to the monolayer. However, these results are not reinforced by the SEM images, which show very few cells growing into the defect area. We theorise that the SEM sample preparation might dislodge less established cells when the membrane is dehydrated as the layer of fibres appears to roll back (Figure 2). These results have provided preliminary, proof of concept data to support further development of the model, with a view to progress to a more complex conjunctival epithelial model which could aid in early testing of biomaterials for conjunctival transplantation.

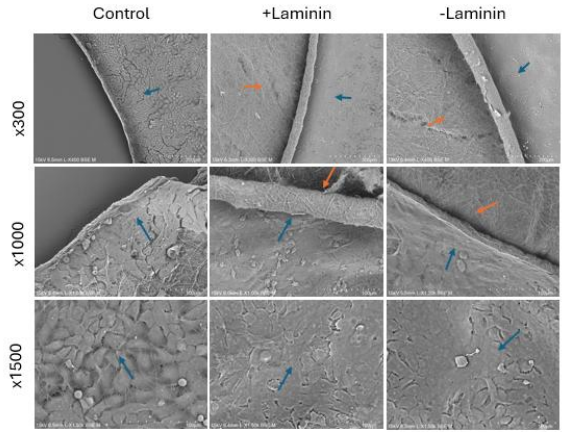

Figure 2. SEM images of Day 1 Samples showing the initial cell layer (blue arrow) and the added treatment layer (orange arrow).

Acknowledgements

This work was funded by the Faculty of Health and Life Sciences, University of Liverpool.

References

1) C.L. Shumway, M. Motlagh and M. Wade, StatPearls, 2023, PMID: 30137787.

2) A.G.Y. Chiou, G. Florakis and M. Kazim, Survey of Ophthalmology, 1998, 43, 19-46

3) I. Rahman, D.G. Said, V.S. Maharajan and H.S. Dua, Eye, 2009, 23, 1954-1961

Decalcifying and antibacterial bilayer grafts for vascular tissue engineering

Hood, R.M. [a], Claeyssens, F. [a,b], Green N. [a,b]

[a] Kroto Research Institute, Department of Chemical, Materials and Biological Engineering, University of Sheffield, UK

[b]Insigneo Institute for in Silico Medicine, Department of Chemical, Materials and Biological Engineering, University of Sheffield, UK

* Corresponding author(s) e-mail(s): rhood1@sheffield.ac.uk & f.claeyssens@sheffield.ac.uk

Introduction

The number of people living with cardiovascular disease (CVD) has doubled to an estimated 640 million people globally since 1993. [1] Saphenous vein autografts remain the gold standard for vascular replacement, but for patients lacking implantable vessels synthetic, bioinert alternatives based on non-biodegradable polymers are used. These often fail at smaller diameters due to thrombus formation and compliance mismatch.[2] Citric acid, a naturally occurring reagent in the Krebs cycle, has the potential to reduce post operative infections and both atherosclerotic calcium deposits and thrombus formation through the chelation of calcium ions in solution. [3,4] This work aims to create bilayer vascular grafts composed of a citrate-eluting inner sheath and porous polymerised high internal phase emulsion (polyHIPE) outer layer. Through extended cell culture and decellularisation, extracellular matrix proteins will be deposited leaving a biomimetic graft that possesses the potential for in situ treatments.

Materials and methods

Here previously developed poly(glycerol sebacate) (PGS) was functionalised with different ratios of citric acid (5-10 mol%). The resulting polymers were characterised with Fourier transform infrared spectroscopy (FTIR), ^{1}H nuclear magnetic resonance spectroscopy (NMR) and gel permeation chromatography (GPC), before analysis into the effect of composition on the mechanical properties and biocompatibility. Degradation and citrate elution of the material has been studied, confirming favourable properties for the graft. The outer layer has been synthesised from porous polyHIPE scaffolds of PGS-methacrylate and optimised for ideal pore size and interconnectivity. Human dermal fibroblasts were cultured for 28 days, and a comparison of cell proliferation and infiltration was completed. This highlighted

the best compositions to have pore diameters greater than 30 microns and interconnects larger than 10 microns.

Results

FTIR, NMR and GPC confirmed the production of different compositions of PGS-citrate. Altering the proportions of citrate leads to changes in polymer chain structure and hence leads to tunability of the material's tensile and compliance properties, fundamental for vascular tissue engineering. Cytotoxicity testing has proved that both PGS-based materials sustain cell proliferation. Histological staining highlighted the production of collagen during a 28-day culture period and optimum internal morphologies have been selected for use in extended bioreactor culture. This aims to encourage further infiltration of the cells and deposition of native extracellular matrix proteins like collagen and elastin. Decellularisation protocols will be optimised to leave a non-immunogenic graft.

Discussion

Citrate containing elastomers have been synthesised and characterised to show promise in the field of vascular tissue engineering. The combination of porous outer sheath embedded with native proteins and citrate eluting inner sheath will lead to a novel biomimetic bilayer vascular graft that can provide in situ treatment and mitigate the common failure factors associated with TEVGs.

Acknowledgements

The authors would like to thank the ESPRC funded CDT in Advanced Biomedical Materials grant for funding this work.

References

1. M. Lindstrom et al., *Journal of the American College of Cardiology*, 2022, **80**:25, pp. 2372–2425, doi: 10.1016/j.jacc.2022.11.001.

2.K. M. Naegeli, et al, *Circulation Research*, 2022 **131**:1, pp. 109–126, doi: 10.1161/CIRCRESAHA.121.319984.

3. L.-C. Su et al, *Frontiers in Bioengeering and Biotechnology*, 2014, **2**, p. 23, doi: 10.3389/fbioe.2014.00023.

4. L. F. Machado-Silveiro et al, International Endodontic Journal, 2004, **37**: 6, pp. 365–369, doi: 10.1111/j.1365-2591.2004.00813.x.

Testing a GDNF-eluting conduit in a mouse model of nerve injury

***LDV. Johnson[1,3], H. Gregory[2], JB. Phillips[2], F. Boissonade[3], F. Claeyssens[1]**

[1] Kroto Research Institute, School of Chemical, Materials and Biological Engineering, University of Sheffield, UK, [2] School of Pharmacy, University College London, UK, [3] School of Clinical Dentistry, University of Sheffield, UK

* Corresponding author(s) e-mail(s): ljohnson15@sheffield.ac.uk & f.claeyssens@sheffield.ac.uk

Introduction

Peripheral nerve injuries are a frequent consequence of severe trauma, yet existing surgical repair techniques often fail to restore full sensory and motor function. This study explores the extent to which an innovative biomaterial scaffold that incorporates a glial cell line-derived neurotrophic factor (GDNF)-eluting aligned nanofibrous structure and a fibrinogen/thrombin hydrogel can facilitate axonal regeneration. This multi-faceted design aims to promote cell integration and nerve repair outcomes.

Materials and methods

The scaffold was created using emulsion electrospinning, encapsulating GDNF within aligned polycaprolactone (PCL) nanofibres. Primary rat neurons were cultured on the substrates. A tri-layer configuration (aligned/random/aligned fibres) was formed into a conduit and stabilised with a fibrinogen/thrombin hydrogel to support cellular integration and structural integrity. The scaffold's effectiveness was assessed in vivo using a 3 mm sciatic nerve gap model in THY-1-YFP-H mice with a recovery period of 21 days.

Results

The aligned topography significantly enhanced and directed the outgrowth of primary rat neurons. Immunohistochemistry revealed that the scaffold effectively bridged a 3 mm sciatic nerve gap. Schwann cells were abundant throughout the constructs, and transverse sections revealed axonal growth along the aligned fibres within the conduit.

Discussion

Our results show the potential of this scaffold as a biomaterial for the repair of nerve gap injuries. Future work could utilise a model of chronic nerve injury in which the natural transient upregulation of neurotrophic factors such as GDNF has subsided. In such cases, spontaneous nerve healing is not observed. Further, previous research compared astrocyte activation within the spinal cord, as a

marker of neuropathic pain following nerve repair [1]. Some evidence suggests an analgesic effect of GDNF in neuropathic pain [2]. Thus, the activation of glial cells in the L4 region of spinal cords is currently analysed in an ongoing study.

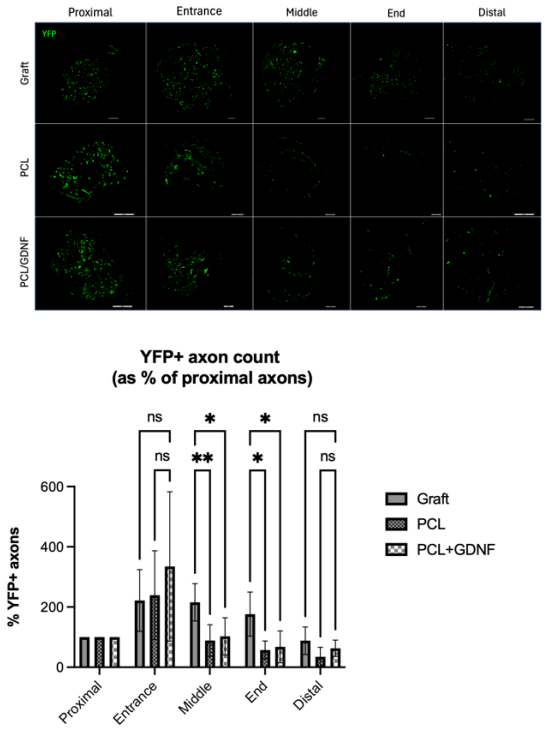

Figure 1. Transverse cross sections of aligned nanofibrous construct showing regenerating YFP+ axons within. Scale bar: 200 μm. % of axons was not significantly different from the grafts to the PCL or PCL/GDNF constructs.

Acknowledgements

The authors would like to thank the EPSRC funded Centre for Doctoral Training in Advanced Biomedical Materials grant reference EP/S022201/1 for funding this work.

References

Singh, A. J. Harding, E. Albadawi, F. M. Boissonade, J. W. Haycock, and F. Claeyssens, “Additive manufactured biodegradable poly(glycerol sebacate methacrylate) nerve guidance conduits,” *Acta Biomater*, vol. 78, pp. 48–63, Sep. 2018, doi: 10.1016/J.ACTBIO.2018.07.055.

[2] T. J. Boucher, K. Okuse, D. L. H. Bennett, J. B. Munson, J. N. Wood, and S. B. McMahon, “Potent analgesic effects of GDNF in neuropathic pain states,” *Science (1979)*, vol. 290, no. 5489, pp. 124–127, Oct. 2000, doi: 10.1126/SCIENCE.290.5489.124/SUPPL_FILE/1054233.XHTML.

Novel Electrospun Materials for the Advancement of Lateral Flow Diagnostics

[1]Nicola Kelly, [1]Dr Julia G Behnsen, [2]Dr Alex Ciupa, [3]Dr Lucy Bosworth, [1]Dr Riaz Akhtar, [1]Dr Jenny Aveyard*

[1]Centre of Materials and Structures School of Engineering, University of Liverpool, UK. [2] Materials Innovation Factory, University of Liverpool, UK [3] Institute of Life Course & Medical Science, University of Liverpool, UK.

* Corresponding author(s) e-mail(s): zippy78@liverpool.ac.uk

Introduction

First developed in the 1980s, lateral flow tests (LFTSs) are membrane-based diagnostics devices that are simple to use, cheap, robust, and accessible. However, their true potential was not recognised until more recently during the COVID-19 pandemic which saw LFTs used on an unprecedented scale globally with over 20 million tests used within the UK in 12 months, allowing diagnosis and monitoring to occur beyond healthcare settings[1]. Despite this, LFTs are fraught with issues relating to sensitivity and selectivity.

Currently, casted nitrocellulose membranes are the industry standard for LFT membranes due to their low cost, mechanical strength, and high protein binding. However, nitrocellulose membranes also have shortfalls, such as sensitivity to environmental factors that affect their mechanical strength, highly flammable behaviour, and batch-to-batch variation due to the manufacturing method. By reconsidering the materials and production method, the membrane design could significantly change LFT performance.

Manufacturing techniques such as electrospinning allow the fabrication of nanofibrous polymer materials with high porosity, interconnected porous networks, and a high surface-to-volume ratio. The membrane's porosity governs the capillary flow of a sample/reagent through the LFT, which in turn governs the LFT's sensitivity.

Materials and methods

The morphology of the commercial and electrospun membranes were characterised using SEM and MicroCT. Alongside this, MicroCT was performed to calculate the porosity and pore size distribution of the membranes and was compared to data acquired using BET which also provided

surface area data. Protein binding was calculated both in static and dynamic form using UV-Vis and HPLC respectively.

Results

Electrospun membranes displayed fibre uniformity, increased pore interconnectivity, and variable porosities when analysed using microCT and BET analysis. Polymer one displayed an increase in surface area compared to polymer 2. Protein binding was characterised using HPLC which displayed an increase in protein binding range compared to commercial nitrocellulose which could be linked to the surface area of the electrospun material.

Discussion

This project facilitates a step change in materials and manufacturing techniques in LFT production by investigating the use of electrospinning to fabricate polymer membranes with superior properties that will improve the sensitivity and selectivity of membrane-based diagnostics. This approach has the potential to address existing challenges and further expand the application of LFTs in point-of-care testing.

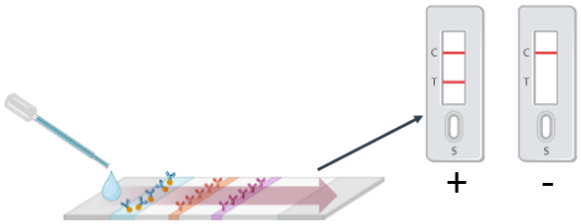

Figure 1. Schematic of a lateral flow test showing how a sample flows through via capillary action to produce either a positive test, or a negative test.

Acknowledgements

For financial support we thank The Royal Society.

References

1. Land, K.J., Boeras, D.I., Chen, XS. *et al.* REASSURED diagnostics to inform disease control strategies, strengthen health systems and improve patient outcomes. *Nat Microbiol* **4**, 46–54 (2019). https://doi.org/10.1038/s41564-018-0295-3

Optimising host response biology to advance wound dressing efficacy

Kiziloz, S. [a*], Hawthorne, D. [a], Sinha, A. [a], Sarker D. [a], Crua, C. [b], Sandeman, S. [a*],

[a] University of Brighton, United Kingdom.

[b] University of Sussex, United Kingdom.

* Corresponding author(s) e-mail(s):

s.kiziloz1@uni.brighton.ac.uk

s.sandeman@brighton.ac.uk

Introduction

Chronic wounds are marked by sustained inflammation, impaired fibroblast and keratinocyte function, and delayed re-epithelialisation, making them a significant clinical challenge.[1,2] Emerging strategies in wound care focus on bioactive materials that can modulate the wound environment, suppress inflammatory signalling, and promote cellular repair.[3] Here, we present the development of a bioactive wound dressing system incorporating $Ti_3C_2T_x$ MXene, a two-dimensional nanomaterial with known anti-inflammatory and conductive properties, alongside glycine betaine (GB), a small osmoprotective molecule with osmoprotective and anti-inflammatory effects.[4]

Materials and methods

To assess cellular responses relevant to wound healing, HaCaT keratinocytes and 1BR3 human dermal fibroblasts were cultured under osmotic stress conditions. A scratch assay using HaCaTs was conducted to evaluate the impact of hyperosmotic stress on epithelial wound closure dynamics. Inflammatory cytokine expression (NF-kB, IL-6, IL-1α, IL-1β, CXCL1, and CXCL8) was quantified in both cell types following exposure to osmotic challenge and bacterial lipopolysaccharide (LPS) stimulation. Actin cytoskeletal reorganisation was visualised via phalloidin staining to assess morphological changes and stress fibre formation. To enable controlled delivery of GB, an acrylate-based microgel was synthesised containing a cationic betaine ester (tBu-GB). This formulation enabled sustained release of the active osmoprotectant via hydrolysis. The microgels were subsequently incorporated into a $Ti_3C_2T_x$ MXene-functionalised dressing, combining small-molecule delivery with nanomaterial-enhanced bioactivity.

Results

Osmotic stress impaired keratinocyte migration and delayed wound closure without causing cytotoxicity. Treatment with $Ti_3C_2T_x$ MXene coatings effectively restored migratory capacity, while GB exposure enhanced migration further. The combination of MXene and GB led to complete closure in the *in vitro* scratch model (Fig 1a). Osmotic stress also upregulated pro-inflammatory cytokine expression, an effect that was further amplified in the presence of LPS. Both MXene coatings and MXene + GB treatments significantly suppressed inflammatory marker expression in keratinocytes and fibroblasts (Fig 1b). Improvements in actin cytoskeletal organisation were observed following treatment, indicating enhanced cellular integrity and migration potential.

The tBu-GB-loaded microgel demonstrated sustained release of the osmoprotective agent over 48 hours, supporting its suitability for incorporation into bioactive dressings aimed at improving outcomes in stress-compromised wound environments.

Figure 1. (top) Scratch assay showing reduced keratinocyte migration under mannitol-induced hyperosmotic stress. Treatment with $Ti_3C_2T_x$-coated surfaces and GB preserved migratory capacity and significantly enhanced wound closure. (bottom) ELISA quantification of IL-6 production in keratinocytes exposed to LPS and mannitol (550 mOsM), with or without $Ti_3C_2T_x$ and GB (10 mM) treatment, showing suppressed inflammatory response following treatment.

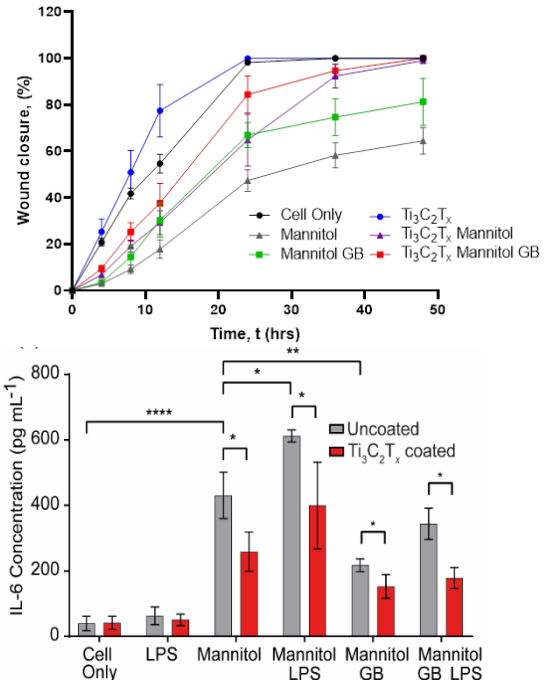

Discussion

This study demonstrates that hyperosmotic stress plays a key role in delaying wound healing by hindering

keratinocyte migration and initiating inflammation. Coatings of $Ti_3C_2T_x$ effectively restored cell migration and reduced the expression of major inflammatory cytokines, supporting their potential use in advanced wound dressings. GB improved cell migration on its own, and its combination with $Ti_3C_2T_x$ produced a synergistic effect, helping to promote healing while also lowering inflammatory signalling. The creation of a sustained-release tBu-GB microgel ensures extended osmoprotective action, reducing the frequency of dressing changes and helping to maintain a favourable wound environment.

Acknowledgements

University of Brighton authors acknowledge the EPSRC grant MyDress (EP/W023164/1).

References

1) J. F. Guest, G. W. Fuller and P. Vowden, *BMJ Open*, 2020, 10, e045253

2) H. Deng, B. Li, Q. Shen, C. Zhang, L. Kuang, R. Chen *et al.*, *J. Diabetes*, 2023, 15, 299–312.

3) Y. Hu, F. Wang, H. Ye, J. Jiang, S. Li, B. Dai *et al.*, *NPJ Flex. Electron.*, 2024, 8, 30.

4) S. Kiziloz, E. J. Ward, D. Hawthorne, A. Sinha, G. Cooksley, D. Sarker, C. Crua, A. Lloyd, C. E. Shuck, Y. Gogotsi and S. Sandeman, *Nanoscale*, 2025, 17, 12758-12774.

A Passive Nanorheological Tool to Characterise Hydrogels.

Lorenzo López, Moira [a, b] *; Kearns, Victoria [b]; Patterson, Eann [a]; Curran, Jude [a].

[a] School of Engineering, University of Liverpool, UK.

[b] Department of Eye and Vision Science, University of Liverpool, UK.

* M.Lorenzo-Lopez@liverpool.ac.uk

Introduction

The high-water content of hydrogels and the ability to tune their physical properties at the sub-micron scale makes them a highly versatile tool in biological applications. Differences in mechanical and morphological properties at the micro/ nanoscale can be controlled to optimise their potential in numerous fields including synthetic tissue analogues, drug delivery and regenerative medicine. Current techniques to characterise hydrogels usually focus on bulk properties and are limited to identifying macroscopic properties, providing little information about local variations and heterogeneity at the micron/nano scale, or fail to provide insight into real-time dynamic responses to external stimuli.[1] These limitations are increased when characterising soft hydrogels. Here, we present a passive nanorheological tool to indirectly characterise soft hydrogels at the micro/nanoscale by tracking nanoprobes through a hydrogel with a label-free optical microscopy technique.

Materials and methods

Gold nanoparticles (AuNP) of 100 nm of diameter were use as nanoprobes; these were added in each of the solutions/hydrogels to reach a constant concentration of 10^7 particle/mL. Simple, Newtonian fluids (different glycerol solutions and silicone oils) were used to validate the nanorheological platform, correlating nanoparticle's experimental diffusion coefficient to the experimental values of viscosity of the media. Once validated, the nanoprobes were used to i) characterise local viscosities in heterogeneous hydrogels based in agar-hyaluronic acid as in vitro vitreous humour models and to ii) characterise the phase temperature transition in Pluronic F127 (20% w/v) a thermosensitive hydrogel for drug delivery purposes. The nanoprobes were tracked over time using a label-free technique, based on the optical phenomena of caustics, on an inverted optical microscope.[2] The tracking data was analysed with the ImageJ TrackMate plugin to obtain experimental values of the diffusion coefficient.

Results

A strong linear negative relationship was obtained between the logarithm of the AuNPs experimental values of diffusion and the logarithm of the viscosity of the media with a correlation coefficient of 0.99, validating the relationship between both quantities. To map the intrinsic heterogenicity of the in vitro vitreous analogues AuNPs were used as nanoprobes, uncovering wide ranges of viscosity from near water values (0,001 Pa s) to values in the range of high viscous silicone oils (5 Pa s) for different localised micro/nano environments. Furthermore, the tracking of the nanoprobes at specific temperatures (ranging from 20˚C to 40˚C) in Pluronic F127 successfully characterized the $T_{sol\text{-}gel}$ transition at 28˚C, in agreement with rheological data as shown in **Figure 1**.

Discussion

The time-efficient, user-friendly, and inexpensive novel passive nanorheological platform has proven useful in the characterisation of hydrogel properties, from localised viscosity, heterogeneity and phase transition at the micro/nanoscale. This technique is presented as a solution to empirically identify soft materials features at the micro/nano scale in a real time on dynamic events.

Figure 1. Phase transition temperature of Pluronic shown using the storage modulus, G' (turquoise squares) and the diffusion coefficient for 100 nm nanoprobes (grey circles) showing that both methods indicate the same transition temperature of 28 ˚C.

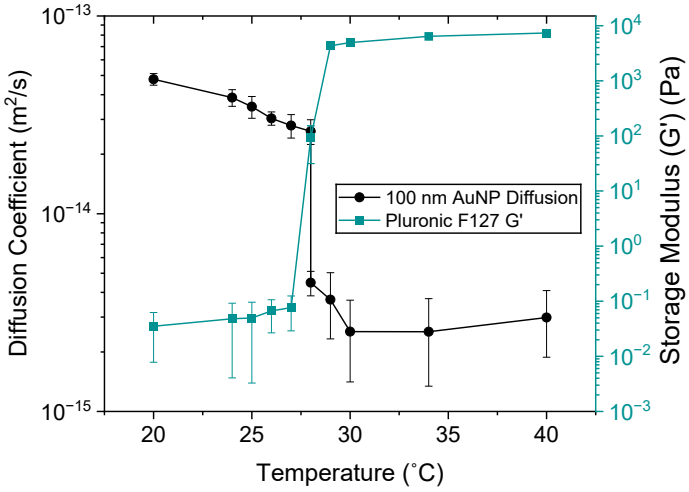

Acknowledgements

For financial support we thank the Doctoral Network in Technologies for Healthy Aging, and the Engineering and Physical Sciences Research Council.

References

1) A. S. Priya, R. Premanand, I. Ragupathi, V. R. Bhaviripudi, R. Aepuru, K. Kannan and K. Shanmugaraj, *Journal of Composites Science*, 2024, **8**, 457.

2) E. A. Patternson and M. P. Whelan, *Nanotechnology*, 2008, **19**,10.

Replicating the tendon-to-bone interface through the creation of electrospun scaffolds with chemical and mechanical gradients.

Lu, M.[1] Barker, E.[1] Paterson, T, E.[1, 2] Miller, C, A.[1, 2] and Asencio, O, I.[1,2]*

[1] School of Clinical Dentistry, University of Sheffield, Sheffield, UK

[2] Insigneo Institute for In Silico Medicine, University of Sheffield, Sheffield, UK

*e-mail: i.ortega@sheffield.ac.uk and c.a.miller@sheffield.ac.uk

Introduction

The reattachment of bone to tendon presents a persistent clinical challenge, particularly in cases where the enthesis, the specialized connective tissue at the tendon-bone junction, has been compromised. Increasing evidence indicates that the spatial gradients inherent to the enthesis are critical for modulating local cellular responses and ensuring the structural and functional integrity of the bone-tendon interface. Emulating these intricate gradient architectures holds significant potential for the development of advanced therapeutic strategies in joint repair[1,2]. The present study examines the utilization of microfabrication techniques to engineer scaffolds with spatially graded mechanical and chemical properties, with the objective of recapitulating the native tendon-to-bone interface.

Materials and methods

Spin-coated (SC) and electrospun (ES) scaffolds were fabricated using polycaprolactone (PCL, Mn ≈ 60,000). Single and multi-layered scaffolds were produced with varying concentrations of hydroxyapatite (HA, 1 - 20% w/w, particle size: Dv (50) = 3.39 μm). Structural and surface characteristics of the PCL and PCL+HA scaffolds were analysed using scanning electron microscopy (SEM), wettability testing, surface roughness assessment (profilometry), porosity measurements (mercury porosimetry), and tensile testing. Bone-derived MG-63 cells were used to evaluate cell viability, differentiation, and distribution across the scaffolds. Additionally, preosteoblast MC-3T3 cells were cultured to assess scaffold-induced differentiation following hydrolysis treatment. Biological evaluations included DAPI-Phalloidin staining, PrestoBlue™ assay, MTT assay, quantitative PCR (qPCR), ALP assay, PicoGreen assay, and SEM imaging.

Results

Initially, a notable decrease in tensile strength was observed in SC and ES scaffolds when HA was added ($P<0.05$).

SEM imaging and DAPI-Phalloidin staining assay demonstrated that HA improved cell adhesion, with cells in the 10–20% w/w HA scaffold groups transitioning from a circular to an elongated morphology by day 6. Biocompatibility and cell differentiation assays indicated that HA concentrations exceeding 5% w/w promoted enhanced cell survival, proliferation and osteogenic differentiation. Subsequently, multilayered scaffolds with graded HA concentrations were successfully fabricated using a layer-by-layer electrospinning approach and imaged by SEM. To better mimic the native enthesis gradients, we developed a three-layered scaffold with increasing HA concentrations (0-20% w/w) and a combination of manufacturing strategies involving electrospinning (ES) and Spin-coating (SC). The first layer consisted of 0% HA and 15% PCL fabricated via electrospinning (ES), the second layer contained 10% HA and 15% PCL (ES), and the final layer incorporated 20% HA, and 15% PCL fabricated via spin-coated (SC).

Discussion

Incorporating HA gradients into ES and SC polymeric scaffolds helps support cell growth and attachment, making the scaffold more native-like. However, higher levels of HA can weaken the scaffold's strength, creating a trade-off between making it more biologically active and keeping it mechanically strong. This balance is especially important for areas that need to handle physical stress. The layer-by-layer electrospinning method helps solve this problem by allowing precise control of HA distribution, creating structures that closely mimic the natural transition from tendon to bone. This approach supports native-like cell responses while keeping the scaffold strong, making it a promising option for repairing tissues at this interface.

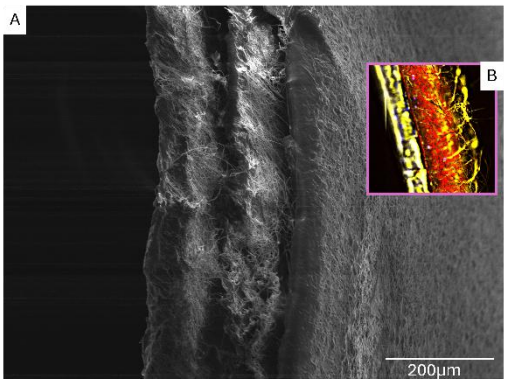

Figure 1. A: SEM image of the prototype multi-layered scaffold; B: optical image stained by food dyes. White, red and yellow layers show increasing concentrations of HA (0-20%) and combination of fibrous and non-fibrous materials.

Acknowledgements

For financial support we thank China Scholarship Council and University of Sheffield. CSC NO. 202208440124

References

1) Y. Chen, Y. Li, W. Zhu and Q. Liu, *Biofabrication*, 2024, **16**, 032005.
2) A. Aponte-López, J. Enciso, S. Muñoz-Cruz and E. M. Fuentes-Pananá, International Journal of Molecular Sciences, 2020, 21, 5293.

United Kingdom Society for Biomaterials Annual Conference 2025

Impact of Corrosion Study Parameters on the Degradation Rate of Magnesium Alloy

McCallion, A. [a*], Acheson, J. [a], Brown, B. [a], Ward, J. [a]

[a] School of Engineering, Ulster University, Belfast, UK.

* Corresponding author(s) e-mail(s): mccallion-a22@ulster.ac.uk and je.ward@ulster.ac.uk

Introduction

Resorbable implants have gained interest within the orthopaedic field as temporary fixation devices, to reduce the need for secondary surgeries[2]. Magnesium (Mg) alloys are a popular material choice for these implants, due to advantages including a similar elastic modulus (~45 GPa) and yield strength (modulus 5-23 GPa) to cortical bone[3], leading to a reduction of stress shielding[4]. However, Mg has a low corrosion resistance within electrolytic and aqueous environments, accelerating its corrosion rate *in vivo*. Therefore, it is of high importance to accurately measure the degradation rate of the material.

Corrosion studies are a necessary part of biomaterials testing as they provide insight into the degradation profile of the material within specific conditions. Variations in these studies are present from author to author[7], leading to ambiguity in the results as *in vivo* conditions are not always accurately represented. Standardisation of these studies is required to allow *in vivo* conditions to be replicated as best as possible, providing reliable degradation profiling and corrosion rate calculations.

This study investigates the influence of gas exchange and media composition on the corrosion rate of WE43 Mg alloy.

Materials and Methods

Five immersion media were utilised in this study: de-ionised water, phosphate buffered saline solution (PBS), simulated body fluid (SBF), McCoy's 5A cell culture media (McCoy's 5A) and McCoy's 5A with foetal bovine serum (FBS).

Extruded WE43 samples (12.7 x 12.7 x 4mm, Luxfer MEL Technologies) were marked with an indent in the top right-hand corner to ensure correct orientation in pre- and post-characterisation. Three samples were placed into each media within the closed system (no gas exchange) and open system (gas exchange) (Figure 1), creating a sample set of 30. All other variables were controlled across both systems to provide a fair comparison. Volume of media: 105.16ml (ASTM G31-72)[5], temperature: 37°C, and length of study: 14 days.

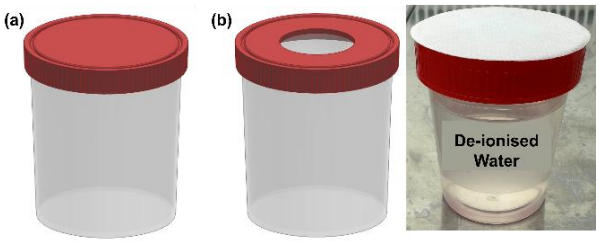

Figure 7- (a) CAD Model of Closed System, (b) CAD Model of Open System and Picture with Hydrophobic Filter Paper.

Results

Weight loss was used to calculate the mean corrosion rate for each set of samples. Figure 2 illustrates these corrosion rates for each media in both systems. When measuring weight loss, it was noted that the closed system had a much greater standard deviation between each sample set, than the open system with the exception of McCoy's 5A. Both SBF and de-ionised water demonstrated a significantly higher corrosion rate within the open system ($p<0.05$), whereas other immersion medias showed no significant difference under gas exchange conditions.

Post corrosion, pH measurements were taken, and it was observed that the open system maintained a pH ~7 with some outliers, while the closed system was more alkaline (pH 8+).

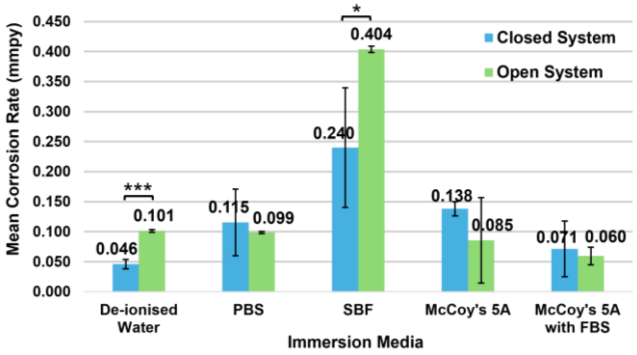

Figure 8- Mean Corrosion Rate within the Closed and Open System.

Discussion

Of the five immersion medias McCoy's 5A with FBS is the most physiologically relevant as it contains proteins such as albumin which are present *in vivo*. These adsorb onto the surface of the sample, slowing the rate of corrosion in both systems. CO_2 is highly soluble in water, creating carbonic acid and providing an explanation for the pH remaining ~7 in the open system while in the closed system it is more alkaline. A pH of 7-7.4 (open system) is comparable with *in vivo* conditions, and within this system McCoy's 5A with FBS possesses a significantly lower corrosion rate ($p<0.05$). Therefore, both the open system and McCoy's 5A with FBS variables will be utilised in future studies when investigating the impact of other corrosion variables, such as degradation kinetics and surface area-to-volume ratio. Additionally, protein adsorption and carbonic acid presence will be explored.

Acknowledgements

For financial support we thank the Department for the Economy (DfE), for funding this PhD research project.

References

1) V. Tsakiris (*et al*), Journal of Magnesium and Alloys, 2021, 9 (6): 1884–1905.

2) D. Bairagi (*et al*), Journal of Magnesium and Alloys, 2022, 10 (3): 627–669.

3) A. Bandyopadhyay (*et al*), Progress in Materials Science, 2023, 133:101053.

4) M. Esmaily (*et al*), Progress in Materials Science, 2017, 89:92–193.

5) ASTM G31-72(2004): Standard Practice for Laboratory Immersion Corrosion Testing of Metals.

United Kingdom Society for Biomaterials Annual Conference 2025

Enhancing Corrosion Resistance of WE22 Magnesium Alloy with Calcium Phosphate Coatings for Resorbable Bone Fixation Applications

McIlhatton, E.[1], Boyd, A.[1], O'Connor, J.[1] , Ward, J.[1], Acheson, J.[1]

[1] School of Engineering, Ulster University, Belfast, Northern Ireland

* Corresponding author e-mail: Mcilhatton-e2@ulster.ac.uk and je.ward@ulster.ac.uk and ar.boyd@ulster.ac.uk

Introduction

Gold-standard materials used for bone fixation devices, such as stainless steel and titanium alloys, often require subsequent removal, leading to patient discomfort, increased surgical risks such as infection, and heightened healthcare costs[1]. Additionally, implants made from these materials can cause stress shielding, a phenomenon in which the implant bears too much of the mechanical load that normally stimulates the surrounding bone, leading to bone resorption and eventual loss of bone density over time[2]. Resorbable implants offer a promising alternative, eliminating the need for secondary surgeries and providing the possibility for gradual load transfer to the healing bone[3]. Magnesium is an attractive material for this application because it possesses mechanical properties similar to natural bone and is biocompatible; however, its rapid corrosion rate limits its clinical applicability[4]. To overcome this limitation, surface modifications, such as protective coatings, are being explored to enhance corrosion resistance and promote osteoinduction. Calcium phosphate (CaP) coatings and ion-doped variants have emerged as a promising solution for controlling corrosion while enhancing bioactivity[5]. Recent studies demonstrate that incorporating elements such as strontium, zinc, silver, and silicon into CaP coatings can improve osteoinduction, and provide antimicrobial benefits[6,7].

Materials and methods

Magnesium alloy WE22 coupons (10 mm Ø x 1 mm) were polished on all sides using P240 and P1200 grade SiC papers. Both uncoated and CaP-coated samples were prepared. The CaP coatings were deposited using RF magnetron sputtering. Each sample was immersed in 40 mL of simulated body fluid (SBF) at 37 °C for seven days, with the SBF replenished daily. Corrosion testing was carried out in accordance with ASTM G31-21 and ASTM G01-03 standards. Gravimetric analysis was used to determine corrosion rates based on mass loss over the immersion time. Characterisation techniques including

optical microscopy, scanning electron microscopy (SEM), and micro-computed X-ray tomography (μCT) were used to examine surface morphology and assess the extent of corrosion (**Figure 9**).

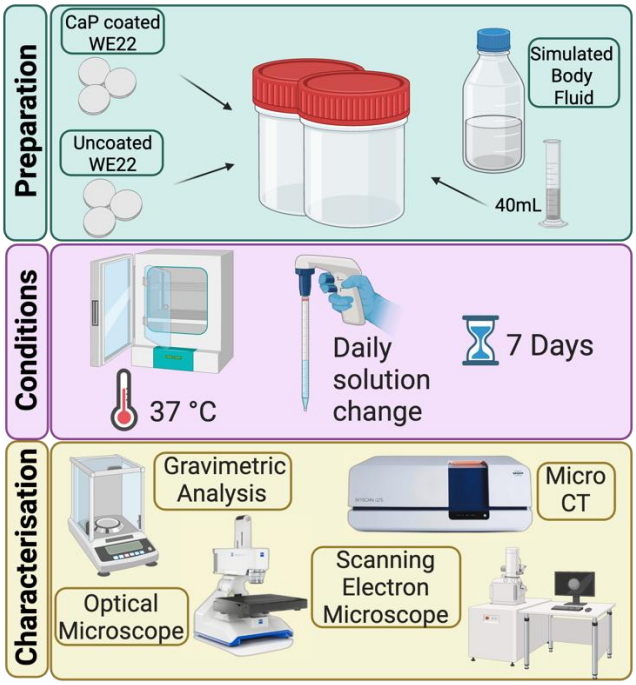

Figure 9. Schematic summary of method and materials used.

Results

Following seven days of immersion in SBF, uncoated WE22 magnesium alloy samples exhibited notable surface corrosion, characterised by visible pitting and progressive mass loss. Gravimetric analysis revealed an average corrosion rate of 0.581 mmpy for uncoated samples (**Figure 10**). SEM imaging further confirmed extensive surface corrosion (**Figure 11**). In contrast, the CaP-coated samples demonstrated a significantly lower average corrosion rate of 0.384 mmpy, indicating enhanced corrosion resistance (**Figure 10**). SEM analysis confirmed that the CaP coating effectively enhanced corrosion resistance, with significantly fewer surface defects observed when compared to uncoated samples (**Figure 11**). These results highlight the potential of CaP coatings for improving the corrosion resistance of WE22 in physiological environments.

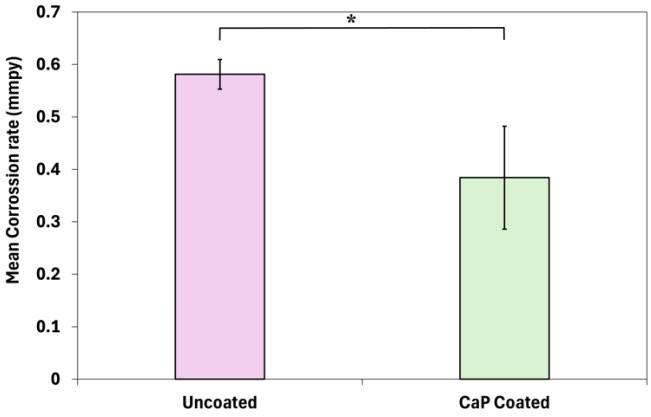

Figure 10. Average corrosion rates of WE22 samples after 7 days in SBF at 37 °C. * = p-value < 0.05.

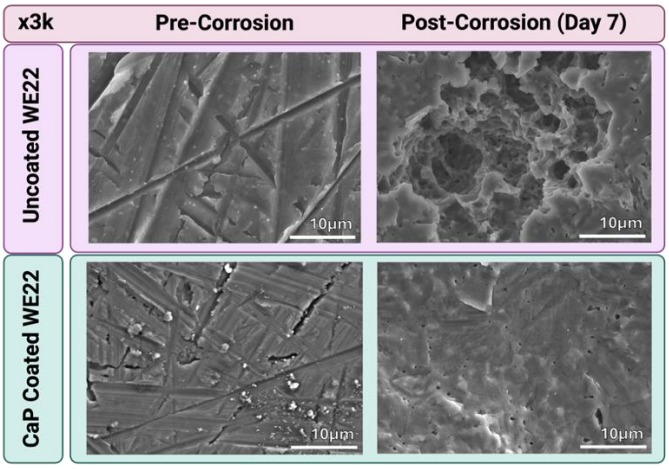

Figure 11. SEM images of WE22 samples pre-corrosion and post-corrosion (Day 7).

Discussion and Conclusion

These findings highlight the effectiveness of CaP coatings in improving corrosion resistance of magnesium alloys, reinforcing their potential in enhancing the performance of resorbable orthopaedic implants. By enabling controlled corrosion while maintaining biocompatibility, these coatings promote resorption that aligns with the natural rate of bone regeneration. This ensures the maintenance of mechanical strength during the critical early phases of bone healing. These results demonstrate the value of surface modification techniques, specifically RF magnetron sputter-deposited CaP coatings, in advancing next-generation bioresorbable biomaterials tailored for safe and effective clinical applications.

Future Work

Future research will aim to enhance the multifunctionality of these coatings by incorporating therapeutic ions, such as silver and strontium, to further promote osteointegration and introduce antibacterial properties. Ion release profiles will be investigated using atomic absorption spectroscopy to quantify the dissolution of the incorporated ions over time. This data will support future efforts to correlate ion release with biological responses. Additionally, antimicrobial analysis will be performed to assess the individual and combined antibacterial effects of the incorporated ions within the CaP coatings. This will provide insight into optimal ion combinations for maximal antibacterial efficacy. Future studies will also explore and compare different annealing methods for CaP coatings, such as flash-annealing using an infrared source and solvo-thermal annealing, to investigate their effects on coating crystallinity, adhesion, and dissolution behaviour.

Acknowledgements

This work was supported by the Engineering and Physical Sciences

Research Council (EPSRC) [grant number EP/X038408/1].

References

1.Onche, I. I. *et.al.*, *J West Afr Coll Surg* **1**, 101–112 (2011).

2. Liverani, E. *et.al., J Mech Behav Biomed Mater **121**, 104608 (2021).*

3.Amini, A. R., *et.al.*, *Long Term Eff Med Implants* **21**, 93–122 (2011).

4.Sezer, N., *et.al.*, *Journal of Magnesium and Alloys* **6**, 23–43 (2018).

5.Acheson, J. G., *et.al.*, *Materialia* **6**, 100291 (2019).

6.Fosca, M., *et.al., Journal of Functional Biomaterials* **14**, 250 (2023).

7.Acheson, J. G. *et.al.*, *Surface and Coatings Technology* **421**, 127446 (2021).

3D Printing of Polyaryletherketone (PAEK)/Apatite composites for lattice structures for orthopaedic implants

McMullan, R[1], Salma-Ancane, K[2], Ward, J[1] Golbang, A[1] and Boyd, A R[1]
[1] School of Engineering, Ulster University, York Street, Belfast. BT15 1ED (UK).
[2] Riga Technical University, Latvia
*e-mail: Monachan-R@ulster.ac.uk and ar.boyd@ulster.ac.uk

Introduction:

Neck and lower back pain is commonly caused by injuries or spinal disorders like degenerative scoliosis and disc disease, leading to many hospital visits globally. Spinal fusion surgery is a treatment option for these conditions. [1]. The spinal implants market was valued at $13.3 billion in 2023, with a projected 5.4% growth to 2030. [2]. While metallic implants are used for spinal fusion due to their mechanical strength, they can cause complications like stress shielding and imaging artefacts in CT scans. Polyaryletherketone (PAEK) offers a promising alternative, as it is biocompatible, strong, and can be sterilised making it a perfect candidate for healthcare applications, especially orthopedics [3]. Polyetheretherketone (PEEK) and Polyetherketoneketone (PEKK) are considered as bioinert, but Rodzen *et al.* demonstrated that adding bioactive agents such as hydroxyapatite (HA) into the matrix solves this problem and can help with aiding direct bone apposition [3]. In addition, by utilising lattice structures for orthopaedic implants this can alleviate stress-shielding, provide for enhanced surface area for the release of bioactive agents (or antimicrobial materials), and reduce imaging artefacts compared to simple solid metal implants. The aim of this work is to produce 3D printed lattice structure containing bioactive HA to enhance direct bone apposition.

Materials and Methods:

A commercial printer CreatBot (Fused Filament Fabrication) was used to print the solid samples and simple lattice structures from PEEK and PEKK. Composite samples were also 3D printed with different amounts of

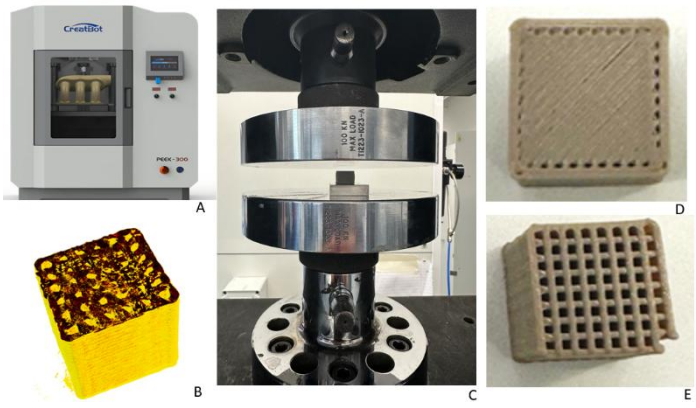

Figure 1. A) CreatBot 3D printer B) MicroCT scan C) Compression testing on the cube D) Basic 3D printed Solid Structure E) Basic 3D printed Lattice Structure

hydroxyapatite (HA) to try an enhance the potential bioactivity of the samples. The samples were then characterised using a range of techniques including XRD, FTIR, SEM/EDX, Micro CT, Digital Microscopy and mechanical testing. The samples were also tested for potential bioactivity testing using Simulated Body Fluid (SBF).[4]

Results and Discussion

Compression testing highlights the difference between the solid structure and different lattice structures. Digital Microscopy shows how the lines were printed on the 3D printer for different lattice structures and shows that the more crystalline materials are less well fused together. XRD and FTIR characterization highlighted that the overall chemistry of the materials did not change significantly when compared with the raw materials and filaments. Typically, the PEEK materials are semicrystalline in nature (30-45%), whereas, the PEKK can have a range of crystallinities (0-30%) depending upon the chamber temperature in the 3D printer. MicroCT results highlight the porosity, density, and morphology of the different 3D printed lattice structures. Preliminary results indicate that the 3D printing conditions utilised have a significant influence on the PEEK or PEKK printed materials, namely differences in crystallinity because of the chamber temperature in the printer, which affects layer adhesion and ultimately the mechanical properties of the samples. If a material is too crystalline the layer adhesion can be lowered when compared to materials that were printed to be amorphous. In addition, the application of HA into composite materials can influence crystallinity also and the overall mechanical properties of the samples. Testing of the samples using SBF has shown the deposition of apatite crystals on the surface, indicating that the samples, in particular those composite

materials containing HA are bioactive in nature.

Conclusion:

These experiments show how 3D printing of PAEK/HA composites can be achieved and show significant promise. Further studies need to be conducted to understand further their mechanical, chemical and physical nature along with targeted *in vitro* characterisation.

References:

1.D. I. Rubin *Neurol Clin*, vol. 25, no. 2, pp. 353–371, May 2007, doi: 10.1016/J.NCL.2007.01.004.

2.“Spinal Implants & Devices Market Size, Share & Trends Analysis Report By Product, By Technology, By Surgery Type, By Procedure Type, And Segment Forecasts, 2022 - 2030,” *Report ID: GVR-1-68038-031-6*.

3.K. Rodzeń *et al.*, *Polymers (Basel)*, vol. 13, no. 18, p. 3117, Sep. 2021, doi: 10.3390/POLYM13183117.

4.(ISO/PRF 23317 - Implants for Surgery — Materials — Simulated Body Fluid (SBF) Preparation Procedure and Test Method to Detect Apatite Formation in SBF for Initial Screening of Bone-Contacting Implant Materials, n.d.)

Material Characterisation of Electroactive (AMPS-co-PEGDA) hydrogels.

Mikalef G[1], Schofield Z[1], Grover L,M[1*]

[1] Healthcare Technologies Institute, University of Birmingham, United Kingdom

* Corresponding author(s) e-mail(s):

l.m.grover@bham.ac.uk, GXM034@student.bham.ac.uk, s.zoe@bham.ac.uk

Introduction

Electroactive hydrogels have been described as stimuli-responsive materials capable of changing shape upon exposure to an electric field. These polyelectrolyte gels have been shown to swell asymmetrically due to changes in osmotic pressure, resulting in bending toward the cathode. As a result, they have attracted considerable interest within the biomedical science community. Herein, an electroactive hydrogel was synthesised using 2-acrylamido-2-methylpropane sulfonic acid (AMPS) and poly(ethylene glycol) diacrylate (PEGDA, Mn 700) as the secondary monomer to produce a material capable of actuation at 100 mA and 5 V.

Materials and methods

2-acrylamido-2-methylpropane sulfonic acid (AMPS) was polymerised onto Poly(ethylene) Glycol Diacrylate (PEGDA, Mn 700) via free radical polymerisation at 365 nm^{-1} using ketoglutaric acid (KGA) as the photoinitiator. The resulting material was injected in a rectangular mould (20 mm x 50 mm x 4 mm) and max uniaxial compressive testing was performed to characterise its mechanical properties (2). Fourier-transform infrared (F-TIR) spectroscopy was used to evaluate the degree of monomer conversion. Actuation testing was conducted by cutting the (AMPS-co-PEGDA) polymer into uniform segments (45 mm x 10 mm), placing them in parallel between two copper electrodes, measuring the degree and speed of bending under 100 mA and 5 V. The material was successfully 3D printed using Suspended layer Additive manufacturing (SLAM) technique (3). Finally, indirect cytotoxicity testing was carried out to assess the polymer's effect on the metabolic activity of neonatal human dermal fibroblasts.

Results

S=O and N-H peaks were identified as AMPS monomer consumption whilst, C=O and C=C peaks were identified as PEGDA consumption. PEGDA was found to have the greatest influence on the mechanical properties of the material. Increased UV

exposure resulted in a stiffer material and a higher degree of bending. SLAM printing produced a softer material that exhibited faster and greater degree of bending. Finally, cell viability assays revealed no significant difference between treated and untreated samples.

Discussion

PEGDA was found to have a greater influence on mechanical properties than AMPS. UV exposure affected the mechanical properties by producing a stiffer, though more brittle, material. This effect was attributed to increased radical formation and a higher degree of cross-linking. UV exposure also resulted in greater bending, likely due to enhanced AMPS incorporation into the polymeric chain. SLAM printing produced a softer material with an increased degree of bending. Finally, cell viability assays indicated that the polymer had no significant effect on cell health, suggesting its potential suitability for use in implantable devices.

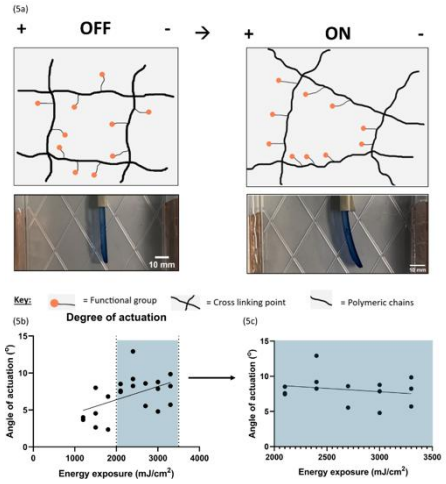

Figure 1. Illustration of the mechanism of actuation and the material actuating upon exposure to an electric field. 5b: Degree of actuation against different energy exposures showing a linear relationship between energy exposure and degree of actuation. R2 = 0.2315, P = 0.0272, slope is significantly non-zero Gradient = 1.799*10-3 5c: Degree of actuation against energy exposures ranging 2000-3500. R2 = 0.04585 P = 0.4623, slope is not significantly non-zero

Acknowledgements

This work was funded by UK Research and Innovation under the UK government's Horizon Europe funding guarantee [grant number 101092242]. Views and opinions expressed are however those of the author(s) only and do not necessarily reflect those of the European Union.

References

1) T. Shiga, T. Kurauchi, Deformation of polyelectrolyte gels under the influence of electric field, 1990.
2) Yang, W. Wang, C. Yao, R. Xie, X. Ju, Z. Liu, L. Chu, Hydrogel Walkers with Electro-Driven Motility for Cargo Transport, 2015.
3) S. Moxon, M. Cooke, S. Cox, M. Snow, L. Jeys, S. Jones, AM. Smith, L. Grover, Suspended manufacture of biological structures, 2017, Vol 29, Issue 13

A polyHIPE dermal scaffold featuring rete ridges for full-thickness wound healing

Morgan, A. [a,b]*, Claeyssens, F. [b], Shepherd, J. [a], Ortega Asencio,Í. [a]

[a] The School of Clinical Dentistry, University of Sheffield, UK.

[b] School of Chemical, Materials and Biological Engineering, University of Sheffield, UK.

* Corresponding author(s) e-mail(s): amorgan14@sheffield.ac.uk and f.claeyssens@sheffield.ac.uk

Introduction

Full thickness wound healing caused by chronic ulcers, traumatic injuries and cancer excisions is a major clinical challenge. While autologous skin grafts are the gold standard treatment, their various limitations have prompted the design of 'off-the-shelf' alternatives that support neo-dermis formation. However, existing products do not directly mimic the skin's native architecture, particularly the rete ridges at the dermal-epidermal junction that act as stem cell niches for epidermal regeneration. In this project, artificial rete ridge topography is created on the surface of polymerised high internal phase emulsion (polyHIPE) scaffolds via a conventional moulding technique, with the aim of stimulating correct cell positioning into niches.

Materials and methods

Ridged silicone moulds are made using a stereolithography (SLA)-printed template. Methacrylated polyglycerol sebacate (PGS-M) is synthesised in-house according to a previous method published by the group[1] and used as the oil phase in the manufacture of HIPE. Emulsion parameters such as stir speed and water bath temperature are varied to tune porosity. The HIPE is cast into ridged moulds, UV cured to form polyHIPE and demoulded to reveal surface ridges. PolyHIPE morphology is assessed by SEM imaging. Immortalised human dermal fibroblasts (HDFs) are cultured on the scaffold to assess the scaffold's ability to support neo-dermis formation. HDF infiltration is measured using H&E staining and cell patterning at the surface visualised by DAPI and Phalloidin-TRITC staining.

Results

The moulding technique imparts defined, near-native-size ridges on the polyHIPE surface, measuring 300-400 μm in width and 115-150 μm in height (**Figure 1**). Scaffold thicknesses of 1000 μm are achievable by emulsion casting. A stir speed of 300 rpm at 37°C yields mean

Figure 1. SEM images of (A) top view of ridged polyHIPE and (B) a cross-section

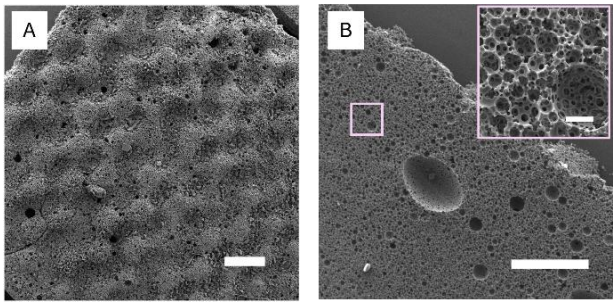

showing polyHIPE porosity. Scale bars = 500 μm. Inset scale bar = 20 μm.

pore and window diameters of 29.0 ± 11.0 μm and 5.8 ± 2.1 μm, respectively. A porosity of 84% confirms a 'high' internal phase, as measured by mercury porosimetry. HDF infiltration after 21 days is not significantly different between top-down and bottom-up seeding at 410 ± 237.0 μm and 320 ± 95.5 μm, respectively (**Figure 2A**). Fluorescence imaging with DAPI/Phalloidin-TRITC reveals HDFs patterning, influenced by pseudo-ridges (**Figure 2B**).

Discussion

'Off-the-shelf' dermal matrices are intended to support neo-dermal regeneration in full thickness wound beds. The PGS-M polyHIPE herein demonstrates this potential, with the versatility of emulsion templating lending itself to pore optimisation for cellular population.

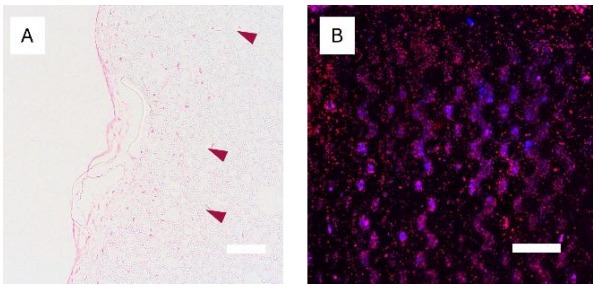

Figure 2. (A) H&E cross-section of seeded polyHIPE. Scale bar = 100 μm. (B) DAPI/Phalloidin-TRITC stained HDFs patterned on the surface. Scale bar 1000 μm.

Good biocompatibility up to day 21 is shown and HDF infiltration depth equals or surpasses dermal thickness in many regions of the body. HDFs herein can infiltrate the bulk of the ridges and arrange on the surface which is ultimately beneficial for HDFs and keratinocyte signalling. Further investigation is planned into the effects of the pseudo-rete ridges on keratinocyte key marker expression.

Acknowledgements

The author acknowledges the Advanced Biomedical Materials CDT (EPSRC) for funding this project.

References

1) S. Pashneh-Tala, et al., *Frontiers in Physics*, 2018, **6**.

Fabrication of Antibacterial NO Releasing Cellulose Acetate Nanofibers for Wound Healing Applications

Cadhan O'Garra[a], Jenny Aveyard[a], Daniel G Metcalf[c], Kevin J Hamill[b], Raechelle A D'Sa[a],

[a]*School of Engineering, University of Liverpool, Liverpool UK*

[b]*Department of Eye and Vision Science, Institute of Ageing and Chronic Disease. University of Liverpool, Liverpool, UK*

[c]*Convatec Ltd, Deeside**

Corresponding author(s) e-mail(s): cadhan97@Liverpool.ac.uk and R.Dsa@liverpool.ac.uk

Introduction

Chronic wounds represent a major problem for the quality of life of patients and healthcare systems.[1] Infection is one potential reason the major reasons that wounds fail to heal or turn chronic.[1] Treating chronic wounds is problematic, given the rise in multidrug resistant bacteria and hence there is an urgent need to develop alternatives to antibiotics. Nitric oxide (NO) is a promising alternative to antibiotics because it has a multimechanistic way of killing bacteria and therefore there is a low chance of the bacteria developing resistance.[1] As NO is a gas, the delivery of NO to the site of the infection can be challenging.

Electrospinning is a cost effective and easily scalable manufacturing method of which can fabricated nanofibrous mats of high porosity and surface-to-volume, ideal for wound dressing materials and can be modified with NO releasing compounds.[2] In this study we report on the fabrication and characterisation of NO-doped functionalised cellulose acetate acrylate (CAA) electrospun nanofiber mats and their antimicrobial efficacy against both gram negative and gram positive bacteria.

Materials and methods

CA was partially acrylated to give CAA, the resulting polymer was electrospun into nanofibrous mats and subsequently underwent a thio-Michael click reaction to introduce dithiols. The chemistry and the morphology of the of the nanofibers were assessed by Fourier-Transform infrared spectroscopy (FT-IR) and scanning electron microscopy (SEM). Chemiluminescence was used to study the payload and release of NO. The antimicrobial efficacy of the fibres tested over 24 hours against Staphylococcus aureus and Pseudomonas aeruginosa. The cell viability was investigated on WS1 cells.

Results and Discussion

The morphology of CA nanofibers were analysed by SEM and were between 378±300nm and 400±200nm. Tethering of the NO donors onto the CAA nanofibers did not affect the morphology or the diameter.

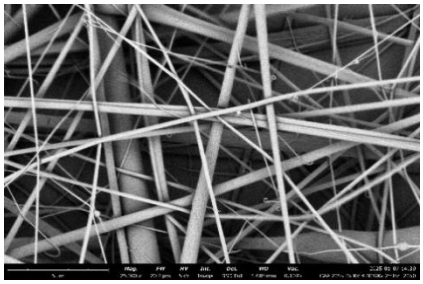

Figure 12. SEM micrographs of images of a CAA: NO donor nanomat spun with the following conditions: 25 kV, 1.0 mL/min, 20 °C, 50%RH, 15 cm needle to collector distance.

The chemical composition of the CA nanofibers were investigated before and after NO donor loading. Inclusion of the NO donor was confirmed by the presence of peaks in the FTIR representative of N-O stretching at 1550cm^{-1}.

Chemiluminescence was used to analyse the release of NO from the fibres. An initial burst was seen, followed by sustained release over 40 hours.

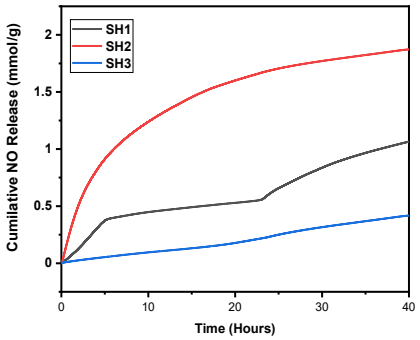

Figure 13. Chemiluminescence Nitric Oxide Releasing Profile with varying NO donor.

Antimicrobial testing demonstrated that NO-releasing nanofibers were able to effectively reduce bacterial populations of S aureus and P aeruginosa at 4 hours and 24 hour time points. The nanofibers were found to be non-cytotoxic to WS1 Fibroblasts.

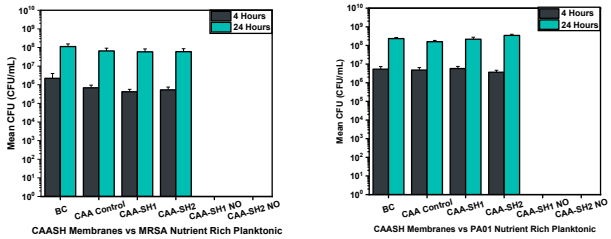

Figure 14. Remaining culturable bacteria after 4 and 24 hours incubation, where Blank = bacteria without membrane, Control = bacteria incubated with 2x2 cm control electrospun **CAA**, and **CAA:NO** = bacteria incubated with 2x2 cm electrospun CAA:NO membrane.

Acknowledgements

This work was supported by EPSRC Doctoral Training Network in Healthy Ageing and Convatec Ltd.

References

1 Riccioand (et al.) ,Chem.Soc.Rev.,41,3731–3741. 2012.

2 Teo (et al.), Nanotechnology,17,R89–R106, 2006.

2D and 3D Printed Cobalt Phosphate Bioactive Glass-Polycaprolactone (CoPBG-PCL) Scaffolds for HIF-1α directed Diabetic Bone Regeneration.

Proctor, C[1,*] Radu, AM[1], De Vega, B[1] Brauer, D[2], Jell, G[1]

1) University College London, UK

2) Otto Schott Institute of Materials Research, Friedrich Schiller University Jena, Germany.

Emails: connor.proctor.24@ucl.ac.uk & g.jell@ucl.ac.uk

Introduction

Diabetic patients have an increased need for bone regeneration, and have orthopaedic implant failure rates(1). Diabetic patients also have an inhibited response to hypoxia, by an impaired HIF-1α pathway. Previous studies have shown that Co can artificially stabilise the HIF-1α pathway and restore diabetic inhibited bone regeneration (Rezaei paper). This multi-functional approach not only enhances biological performance but also enables fabrication of scaffolds via 3D printing. Importantly, 3D printing allows to produce patient-specific implants tailored to defect size, improving the conventional, one-size-fits-all grafts.

Materials and methods

Cobalt-phosphate bioactive glass (Co-PBG, molecular formula) were kindly donated by Prof. D. (particle size <32 microns) and combined with polycaprolactone (PCL) scaffolds. at a w/w % (BG/PCL) of 10, 30, and 50. Co-PBG were fabricated using a solvent-based method with chloroform; phosphate bioactive glass (PBG) was used as a control. Physicochemical characterisation of the scaffolds was assessed by mechanical (compression testing), surface (SEM, contact angle, rheology), and biochemical (EDX, FTIR, TGA, DSC). Biological evaluation with BM-MSCs included degradation analysis, live/dead assay, DNA quantification, adhesion (phalloidin), metabolic activity (Presto Blue), and TRAP-based osteoblast activity.

Results and Discussion

CoPBG-PCL materials were manufactured for the first time. The incorporation of PBG had a concentration dependent effect on surface chemistry (Fig. 1a) and the BG particles appeared to be even distributed within the scaffold. The degradation, release of ions and cellular interaction will be reported at the meeting.

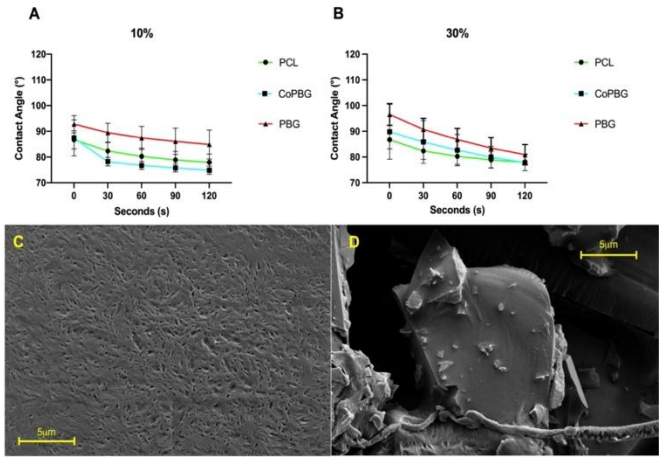

Figure 15. Characterisation of CoPBG-PCL and PBG scaffolds. An increase overtime of hydrophilicity demonstrating incorporation of PBG and PCL scaffold (BSEM demonstrated homogenous incorporation of CoPBG into the PCL Image (C) shows many small pores in the top surface layer of the 2D scaffold at 2000x.

The development of 3D printed CoPBG-PCL scaffolds presents a promising approach for diabetic bone regeneration by combining bioactivity with structural customisation. Cobalt incorporation may enhance cell response by stabilising the HIF-1α pathway, which is impaired in diabetes. Although these results suggest potential for improved healing, this effect is not yet confirmed, and further evidence is required to validate HIF-1α activation and long-term regenerative outcomes. Continued in vitro and in vivo studies will be critical to fully establish clinical relevance.

Acknowledgements

This work was supported by colleagues in the UK and Germany.

References

1) Wagner, J., Spille, J.H., Wiltfang, J. et al. Systematic review on diabetes mellitus and dental implants: an update. Int J Implant Dent 8, 1 (2022). https://doi.org/10.1186/s40729-021-00399-8
2) Rezaei A, Li Y, Turmaine M, Bertazzo S, Howard CA, Arnett TR, Shakib K, Jell G. Hypoxia mimetics restore bone biomineralisation in hyperglycaemic environments. Sci Rep. 2022 Aug 17;12(1):13944. doi: 10.1038/s41598-022-18067-1. PMID: 35977987; PMCID: PMC9385857.

United Kingdom Society for Biomaterials Annual Conference 2025

Optimisation of Bioresorbable Implant Degradation with Machine Learning

Rees, S. [a,*]

[a] Department of Physics, University of Aberystwyth, Wales.

* Corresponding author e-mail: jar77@aber.ac.uk

Introduction

Traditional metallic implants often involve secondary complications such as corrosive release of cytotoxic metal ions, fatigue, and failure over decades of use.[1] This necessitates undesirable secondary surgery, each subsequent revision required sooner (from 15 to 3 years in hip replacements), straining patients and healthcare systems.[2] Bioresorbable implants are a developing alternative, in which the implant acts as a scaffold loaded with materials that cell ingression, vascularization and ossification processes can utilise to 'regenerate' the affected part.[3] In other cases such as cardiac stents the implant is only needed for a certain amount of time, such as to act as a drug delivery platform, and must only break down after completion.[4] The resorption (or degradation) rate of these implants have proven difficult to control – for example, Fe and Zn are mechanically desirable but intolerably slow – without sacrificing other key factors such as yield strength or porosity.[5] Machine Learning (ML) is well-suited to optimisation and correlation tasks from large and nonlinear datasets, and we demonstrate a method to facilitate selection of an optimal parametric setup.

Machine Learning (ML)

ML finds connections within data and interpolates from them based on which transformations from input (e.g. porosity, composition) to output functions (resorption rate) give the lowest errors ("loss"). The model learns to do so in a "gradient" of improvement until errors are ≈ 0 - giving the most statistically probable outcome. An experimental dataset would be split into training (70%), validation (10%) and testing (20%) sets, which respectively allow the model to learn connections, ensure that patterns rather than noise are being learned, and assess performance on unseen data.[6] In general, the more training data available, the better it performs on unseen tasks, such as new experimental data.

Gradient Boosting Method (LGBM)

"Gradient improvement" involves differentiating the input function and minimising error as far as possible.

However, this may stop too early and cut the improvement gradient. *LightGBM* (LGBM) instead dismantles and recreates the gradient at every epoch to avoid differential chain issues, with the first epochs capturing broad connections and subsequent epochs filling in missing ones until the most accurate transformation occurs. As **Figure 1** below shows, this allows a predictive interpolation to be made; if time is recorded, one can generalise how, for example, resorption rate is inhibited or encouraged by porosity. *Seaborn Correlation Matrices* also visualise covariance but underestimate small variations or timescales.

Genetic Algorithm (NSGA3)

Genetic Algorithms like the NSGA3 model are multiparametric optimisation tools that emulate natural selection, with the set of values that most closely fit specified demands (e.g. maximal degradation rate and porosity for minimum Fe%) within specified constraints (e.g. $\leq 50\%\ Fe$) that are enforced by a "penalty" function (e.g. $\forall\ Fe < 50, Penalty = 1000$); those with the lowest penalty progress to the next round until left with a "Pareto Front", i.e. best-of-the-best selection. Some variants such as *PyMoo* allow more than three 'demands', but this can lead to an "overdetermined system" – i.e., has no consistent viable solution.

Synthetic Demonstration

A synthetic dataset of $n = 10000$ experiments was generated for demonstration, with each parameter (e.g. elastic moduli) assumed to follow a Gaussian distribution about their "ideal" values (e.g. $17900 \pm 3900\ MPa$). We stress that real experimental data may deviate from this. The parameters used were porosity, elastic modulus, bioalloy (Fe, Mn, Zn, Li, Mg) and additive (Cu, Si, Sr) fractions, degradation (resorption) rate as a change in volume, and time.

Figure 1 demonstrates that LGBM can interpolate the likely degradation rate for every porosity from 0-40%, from which 10%, 22-25% and 35% lead to the highest degradation rates ($\approx 0.74\%/wk = 2.6yr$). However, 10% may be too low and 35% too high for efficient ingression; the delay in using a moderate 20% ($0.65\%/wk = 3.1yr$) can then be judged.

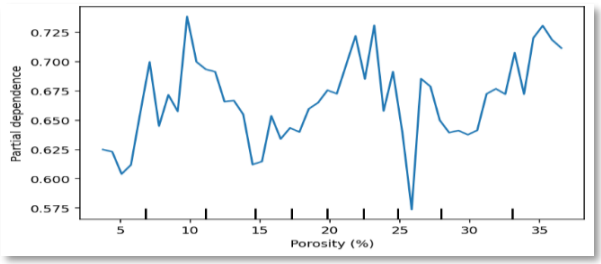

Figure 1. LightGBM predicted plot of degradation per week (y) against porosity level (x).

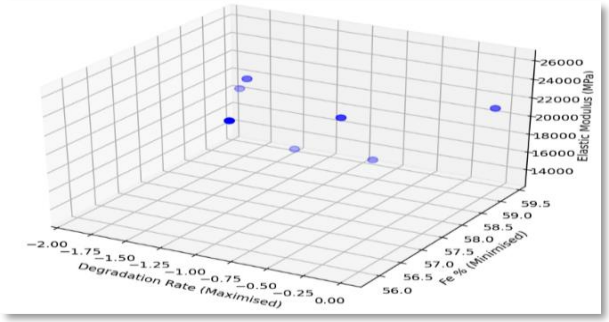

Figure 2. 3D plot of the NSGA3 model.

	Li_%	Mg_%	Cu_%	Si_%	Sr_%	degradation_rate	\
0	1.162241	2.645508	0.575658	0.457941	0.324062	1.447938	
1	1.017320	1.729580	0.487927	0.149005	0.166200	0.861172	
2	1.085804	2.619594	0.604919	0.688778	0.147171	0.589169	
3	0.886236	2.502975	0.598888	0.585227	0.312619	1.903366	
4	1.827523	2.164918	0.322588	0.194948	0.112791	0.825550	
5	0.698698	2.684965	0.507433	0.394024	0.153804	0.000000	
6	0.751670	2.640993	0.838381	0.226027	0.160500	1.493814	

	duration_hours	obj_degradation	obj_Fe_pct	obj_penalty
0	165.155880	-1.447938	59.268336	949.11282
1	206.545571	-0.861172	59.262938	598.58187
2	239.559088	-0.589169	57.529951	3032.78786
3	219.949976	-1.903366	59.399084	0.00000
4	239.067743	-0.825550	55.835092	6152.44702
5	298.321431	1001.150000	59.233777	1511.02629
6	147.812318	-1.493814	58.300840	3146.22016

Figure 3. Pareto Front value combinations.

As viable ranges can be specified in NSGA3, more specific tradeoffs are found. Resorption rate was constrained to $2.0 - 0.6\%/\mathrm{wk} \approx 1 - 3\mathrm{yr}$, the elastic modulus $14000 - 20000\ \mathrm{MPa}$, and $\mathrm{Fe}\%$ to be minimised for its slow degradation behaviour[3].

Figure 2 maps out these tradeoffs; the fastest degradation rate $(2\%/wk)$ can be obtained but then would require substandard elastic modulus $(14000\ MPa)$ and higher Fe (59%); conversely, a higher elasticity $(17000\ MPa)$ halves degradation. **Figure 3**'s Pareto Front justifies these choices by displaying the relative penalty values and values (including unconstrained) required for this outcome. In this case, set 3 might be optimal. In real data, even a lower-penalty combination may be unacceptable; however, NSGA3 will at least show which are the *most* viable. LGBM should track single experiments with time, while NSGA3 is best for multi-experiment interpolation. All Python code used will be made available here.[8]

References

1) P. Lemoine *et al*, *J. Mech. Behav. Biomed. Mat.,* 2022, **133,** 105306. 2) K. Deere *et al*, *Lancet Rheumatol.,* 2022, **4(7),** e468-479**.** 3) R.G. Estrada *et al*, *JOM,* 2025, **77,** 4445-4455. 4) M. Seguchi *et al, EuroIntervention,* 2023, **19(2)**, 10.4244/EIJ-D-22-00718. 5) M. Hussain *et al, Heliyon,* 2024, **10(12)**, e32713. 6) L. Yang, A. Shami, *ArXiv,* 2020, preprint, ArXiv: 2007.15745,

https://doi.org/10.48550/arXiv.2007.15745.
7) D.T. Reilly, A.H. Burstein, *J. Biomech.,* 1975, **8,** 393-396. 8) Rees, S., https://drive.google.com/drive/folders/1-C7fbwRNTfC0g0F2u1yd99m9PRi-s751?usp=sharing , (accessed May 21, 2025).

Real-time label-free exploration of the dynamics and interactions of bacteriophages

Ritchie, G.*, Curran, J., Giorgi, F.
School of Engineering, University of Liverpool, The Quadrangle, Liverpool, L69 3BX, UK
*e-mail: hlgritch@liverpool.ac.uk and J.Curran@liverpool.ac.uk

Introduction

Bacteriophages (phages) play a key role in bacterial ecology and are increasingly explored as tools for therapeutic and diagnostic applications, particularly in light of rising antimicrobial resistance [1]. A comprehensive understanding of phage-host dynamics is critical for the development of responsive biomaterials and infection-controlling technologies. Traditional methods for visualising phages, such as electron or fluorescence microscopy, often require invasive sample preparation or labelling, which can alter biological behaviour and preclude real-time observation [2, 3]. In this study, we present a novel label-free, caustics-based optical microscopy approach to dynamically monitor phage movement and interactions in solution. Caustics—optical phenomena resulting from the focusing of light—can be manipulated in a modified microscope to amplify the optical signatures of nanometric particles like phages [4]. This technique enables the real-time tracking of phages and their interactions with bacteria under standard laboratory conditions, with minimal sample alteration. The approach holds promise for advancing infection-related biomaterial testing, phage therapy development, and microbial diagnostics.

Materials and methods

Three bacteriophages were investigated: Pseudomonas aeruginosa phages pelp20 and phiKZ, and a novel Escherichia coli phage (EcoLiv25). Phages were isolated, amplified, and purified using standard plaque assay protocols. Transmission electron microscopy (TEM) was employed for morphological confirmation. Phage caustics were generated using an inverted optical microscope (Axio Observer.Z1, Zeiss) equipped with a monochrome camera and a stage-top incubation system to maintain biological temperatures. Kohler illumination narrowed condenser aperture, and a 546 nm narrowband filter were used to generate caustic patterns [4]. To validate caustic-generated signatures, phages were also stained with SYTO9 and imaged under fluorescence. Single-phage dynamics were tracked using ImageJ's TrackMate plugin. For preliminary host interaction studies, a non-flagellated E. coli strain (ATCC 10536)

was exposed to EcoLiv25 phages, and interaction events were recorded and compared to control (non-infected) cells.

Results

Caustic microscopy reliably produced distinct optical signatures for each phage strain, with visible caustics ranging several microns—far exceeding the physical size of the phages (Fig 1a). Cross-validation with fluorescence microscopy confirmed the one-to-one correlation between caustics and labelled phages, supporting the accuracy of the method (Fig 1b).

Phage movement exhibited classic Brownian motion, with calculated mean square displacement (MSD) curves following a linear trend consistent with random walk dynamics (Fig. 1c). Morphology-dependent variations in caustic shapes were noted, though further work is needed to establish robust classification based on morphology alone.

Preliminary experiments demonstrated detectable differences in optical signatures between phage-exposed and control bacterial populations. Observations included possible phage attachment and membrane damage, suggesting the potential to distinguish infection stages and phage-host interactions in real time (Fig. 2).

Discussion

This study demonstrates the potential of caustics-based optical microscopy as a powerful, label-free platform for real-time monitoring of bacteriophage dynamics and interactions. By eliminating the need for fluorescent labels or invasive preparation, this method allows the observation of individual phages in physiologically relevant conditions and supports the exploration of their interactions with bacterial hosts. The ability to track infection events and distinguish bacterial responses at early stages provides a novel tool for evaluating antimicrobial biomaterials, phage therapy efficacy, and host-pathogen dynamics in engineered environments. This technology offers a significant step forward in bridging fundamental virology with applied biomaterials science and clinical diagnostics.

References

[1] Clokie, M.R., et al. (2011). Phages in nature. Bacteriophage, 1(1), 31–45.

[2] Liu, S.L., et al. (2020). Single-Virus Tracking: From Imaging Methodologies to Virological Applications. Chem. Rev., 120(3), 1936–1979.
[3] Jensen, E.C. (2012). *Use of fluorescent probes: their effect on cell biology and limitations*. Anat. Rec., 295(12), 2031–2036.
[4] Patterson, E.A., & Whelan, M.P. (2008). Tracking nanoparticles in an optical microscope using caustics. Nanotechnology, 19(10), 105502.

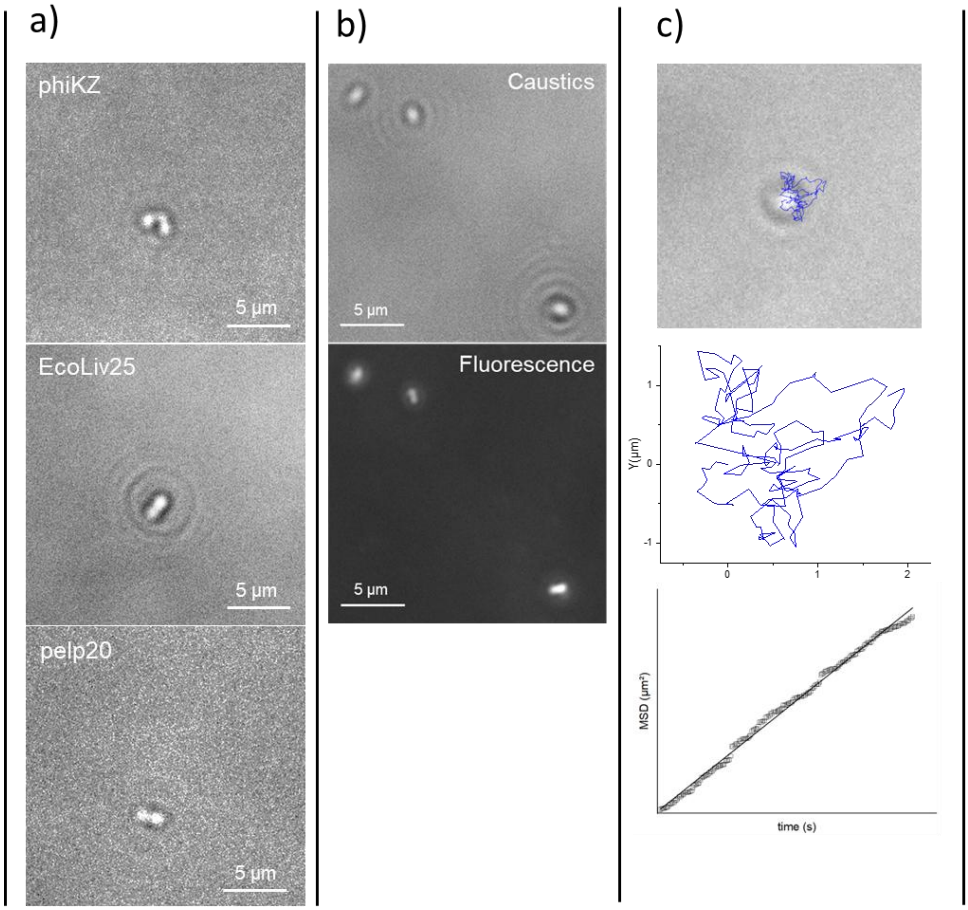

Figure 16. Real-time label-free monitoring of bacteriophage dynamics using optical caustics. Column A: Caustics produced by label-free phages tested in this study. The optical signatures generated are significantly larger than the physical size of the phages, enabling their visualization and tracking without the need for fluorescent labeling. Column B: Direct comparison between EcoLiv25 phage populations imaged under fluorescence mode (left) and caustics mode (right) using an inverted optical microscope. The overlapping visual profiles validate the reliability of caustics-based detection. Column C: Dynamic tracking of a pelp20 bacteriophage. Top: 2D random trajectory over 5 seconds. Middle: Plot of the same trajectory.

Bottom: Mean square displacement (MSD) of the random walk, with square data points and a linear fit (black line), confirming Brownian motion behavior.

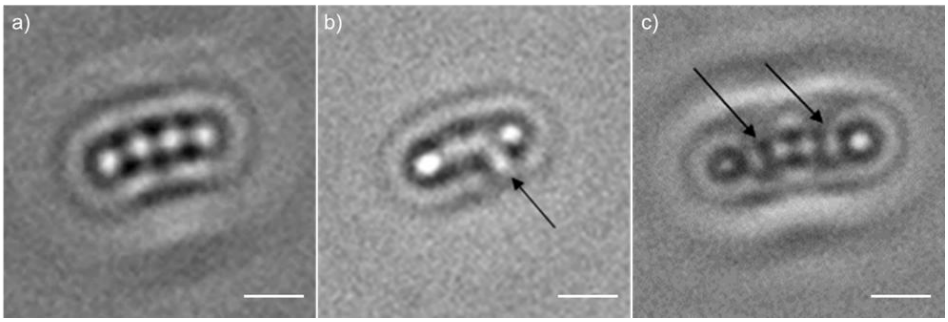

Figure 2. Details of E. coli bacteria: a) not exposed (reprinted from [17]), b) and c) exposed to a population of EcoLiv25 phages in solution. In figure b), the arrow points at the supposed presence of a phage attached to the bacterium's external membrane, while in figure c), the arrows point at the compromised sections of the bacterium's external membrane as a result of phage infection. Scale bars are 2 μm.

Shape Memory Polymer-Enabled Minimally Invasive Blood Pressure Sensor: PCL-PDMS Polyurethane Integration via Photolithographic Microfabrication

Sall, A [a,*], Schofield, Z. [a], Grover, L.-[a]
[a] University of Birmingham, United Kingdom.
* Corresponding author(s) e-mail(s): axs2196@student.bham.ac.uk

Introduction

Hypertension is becoming a global problem, highlighted by a recent report from the WHO[(1)], being a major factor in the diagnosis of cardiovascular disease and a rise in mortality[(2)]. As a result of this it is critical that the presence of hypertension in patients is identified at an early stage. Current methods of blood pressure measurement such as in a clinical setting or electronic monitors at home are subject to fluctuation or can only take single measurements[(3,4)]. Reported here is the potential for the combination of two technologies. Shape memory polymers (SMP), in the form of a polycaprolactone (PCL) – Polydimethylsiloxane (PDMS) shape memory polyurethane (SMPU), which is being developed, and the photolithographic microfabrication of a capacitive blood pressure sensor. The integration of the blood pressure sensor with the shape memory polymer will allow its minimally invasive implantation into the patient's wrist.

Materials and methods

The PCL-PDMS SMP was synthesised by first dissolving both PCL-diol and PDMS-diol at mass ratios of 4:1, 3:2, 3:2 and 2:3 in 25mL anhydrous toluene at 60ºC. Once a homogeneous mixture was achieved 290µl of hexamethylene diisocyanate and 2µl of dibutyltin dilaurate were added to the mixture. The mixture was reacted under argon at 110ºC, then precipitated in n-hexane and filtered under reduced pressure to produce a solid product[(5)]. Variations to this synthetic process were trialled, including, the increase of the toluene volume to 50ml, 75ml and 100ml. Also, the removal of the precipitation step and casting samples using the raw reaction mixture. Fourier transform infrared (FTIR) spectroscopy was used to characterise the polymer structure; differential scanning calorimetry (DSC) was used to characterise the polymer's thermal properties. The mechanical properties have been tested by first solvent casting the SMP, using chloroform, into circular disk specimens that undergo cyclic compressive test where samples are compressed for 10,000 cycles at 20% strain and a frequency of 1Hz. Specimens were also cast into sheets which were used for shape memory testing.

The fabrication of the blood pressure sensors was done under clean room

conditions, using a multilayered approach involving spin coating, photolithography and physical vapour deposition (PVD), in collaboration with the Engineering Clean Room Facility at the University of Birmingham.

Results

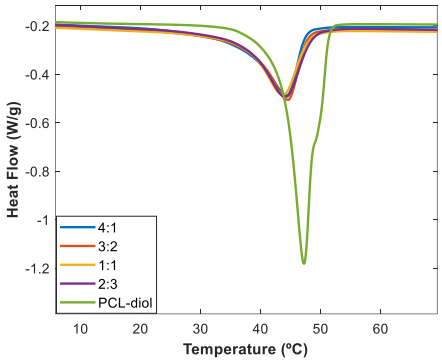

Figure 1. Variation of PCL:PDMS Ratio.

The DSC results showed a slight depression of the melting temperature when comparing the PCL-PDMS SMP to pure PCL-diol moving from 47°C to 44°C. Although when looking at the different ratios no significant difference was seen. The same can be said when the toluene volume was varied.

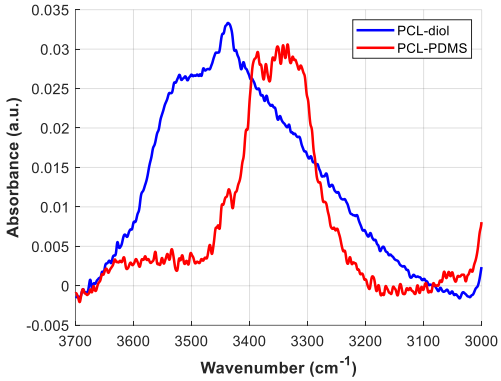

Figure 2. Validation of PCL-PDMS polymerisation via FTIR.

The FTIR spectra of the PCL-PDMS SMP when compared to that of the pure PCL-diol showed successful polymerisation as seen in figure 2 from the sharpening of the broad -OH peak in PCL-diol to the sharp N-H stretch. The PCL-PDMS SMP showed lower compressive strength compared to the PDMS, although it had greater elasticity, and a more appreciable hysteresis loss in the 3:2 variant. The shape memory performance of the SMP was found to be good with average shape recovery of 99.03% and a quick recovery time.

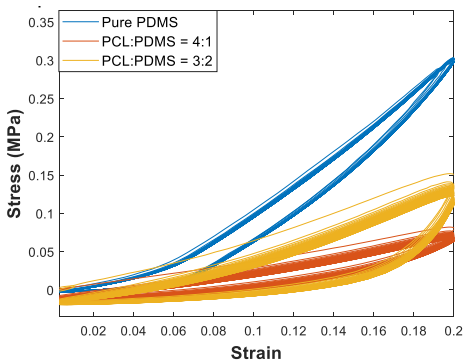

Figure 3. Stress vs Strain Comparison of PCL-PDMS SMP and pure PDMS. Sensors were successfully fabricated using the techniques stated.

Discussion

The results showed that a shape memory polyurethane has been successfully produced and that a microfabrication process for the sensor fabrication has been validated. One aspect that is called for optimization is the melting temperature of the SMPU so that the polymer will actuate at body temperature. The next challenge is to bring these two processes together as currently the sensor is encapsulated with PDMS. The hope is that the SMPU can replace the PDMS allowing the shape of the sensor to be changed to an implantable geometry and return to its intended shape when implanted.

Acknowledgements

This work was funded by UK Research and Innovation under the UK government's Horizon Europe funding guarantee [grant number 101092242]. Views and opinions expressed are however those of the author(s) only and do not necessarily reflect those of the European Union.

References

1) World Health Organisation. Global report on hypertension: the race against the silent killer. Geneva; 2023.

2) Kario K, Okura A, Hoshide S, Mogi M. The WHO Global report 2023 on hypertension warning the emerging hypertension burden in globe and its treatment strategy. Vol. 47, Hypertension Research. Springer Nature; 2024. p. 1099–102.

3) Ogedegbe G, Pickering T. Principles and Techniques of Blood Pressure Measurement. Vol. 28, Cardiology Clinics. 2010. p. 571–86

4) Turner JR, Viera AJ, Shimbo D. Ambulatory blood pressure monitoring in clinical practice: A review. Vol. 128, American Journal of Medicine. Elsevier Inc.; 2015. p. 14–20.

5) Hsieh CH, Razali NAM, Lin WC, Yu ZW, Istiqomah D, Kotsuchibashi Y, et al. Development of thermo-responsive polycaprolactone–polydimethylsiloxane shrinkable nanofibre mesh. Nanomaterials. 2020 Jul 1;10(7):1–13.

Formulating *L*-alanine-based poly(ester amide) inks for 3D printing and scaffold-guided tissue regeneration

Santos, P.[a,b], Alves B.[a], Inocêncio S.[a], Nunes P.[a], Richardson, S.[c], Gloria A.[d], Serra, A.[a], Fonseca, A.[a]*, Domingos M.[b]*

[a] CEMMPRE, ARISE, Department of Chemical Engineering, University of Coimbra, 3030-790, Coimbra, Portugal

[b] Department of Mechanical and Aerospace Engineering, School of Engineering, Faculty of Science and Engineering & Henry Royce Institute, The University of Manchester, M13 9PL, Manchester, United Kingdom

[c] Division of Cell Matrix Biology and Regenerative Medicine, School of Biological Sciences, Faculty of Biology, Medicine and Health, The University of Manchester, Manchester M13 9PL, UK

[d] Department of Industrial Engineering, University of Naples Federico II, P.le Tecchio 80, 80125, Naples, Italy.

* Corresponding author(s) e-mail(s): marco.domingos@manchester.ac.uk

Introduction

The combination of biocompatibility, biodegradability, and thermomechanical stability makes polyester materials highly attractive for use as 3D printed scaffolds in tissue engineering. However, their low bioactivity, acidic degradation products, and hydrophobicity still limit their wider use. α-Amino acid-based poly(ester amide)s (AAA-PEAs), combining the biocompatibility and degradability of polyesters with the superior mechanical properties of polyamides, have emerged as a promising alternative. These materials can be synthesized with various structures, allowing for precise tuning of properties like stiffness, wettability, and degradability. On the other hand, thermal processing of AAA-PEAs remains challenging and largely unexplored. Here we formulate a new library of AAA-PEA inks with tuneable physicochemical properties and demonstrate its applicability in tissue engineering by printing

3D scaffolds and evaluating their thermal, mechanical, chemical and biological performance in vitro (**Figure 1**).

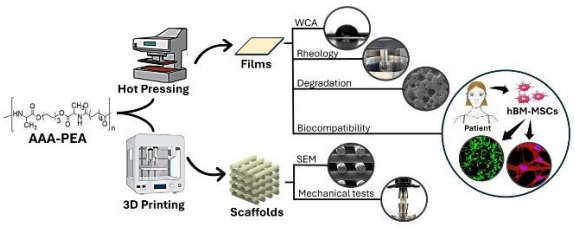

Figure 1. Graphical abstract.[1]

Materials and methods

The synthesis AAA-PEAs based on L-alanine (PEA-ala), L-alanine/glycine (PEA-ala-gly(75:25)) and L-alanine/glycine/jeffamine (PEA-ala-gly-jeff

(50:25:25)) was confirmed using Nuclear Magnetic Ressonance (NMR) and Fourier Transform Infrared Spectroscopy (FTIR). Differential Scanning Calorimetry (DSC) and Thermogravimetric analysis (TGA) were conducted to evaluate thermal properties. Processability was assessed through oscillatory rheology, measuring viscosity changes with temperature. Hot-pressed, two-dimensional (2D) films of AAA-PEAs and poly(ε-caprolactone) (PCL) were used to study in vitro degradation, wettability, and nanoindentation properties. Morphology of 3D-printed scaffolds, produced by melt extrusion, was characterized using Scanning Electron Microscopy (SEM) and micro–Computed Tomography (μ-CT), with mechanical properties tested under static compression. Cell viability, metabolic activity and morphology of human bone marrow-derived mesenchymal stem cells (hBM-MSCs) seeded on 2D films of PCL and AAA-PEAs was determined with LIVE/DEAD™, Presto Blue™ and Rhodamine Phalloidin and Hoeschst 33342 stainings, respectively.

Results and Discussion

A library of AAA-PEAs with molecular weights of 60kDa to 70kDa (Đ≈1.50) and thermal stability (up to 370 ºC) suitable for melt-extrusion 3D printing was successfully created. Despite their relatively low Tg (approx.15ºC), AAA-PEAs displayed a gradual increase in viscosity during solidification, enabling their processing into 3D porous scaffolds with well-defined internal/external geometries and precise dimensions, as confirmed by SEM and μ-CT. Water Contact Angle (WCA) analysis revealed a more hydrophilic nature of the AAA-PEAs films compared to PCL ones. The addition of jeff accentuated this feature leading to a further increase in mass loss of the AAA-PEAs films under hydrolytic (from 2% to 6%) and enzymatic (up to 17%) conditions over a period of 4 weeks. Despite their softer nature and higher affinity to water, AAA-PEA materials did not yield significant differences in terms of cell viability, metabolic activity and morphology compared to PCL.

Conclusion

New formulations of AAA-PEAs were successfully developed and validated for melt-extrusion 3D printing, expanding the range of processable materials beyond the traditional polyester-based inks. Our results confirm the in vitro biocompatibility of AAA-PEAs and suggest that further structural modifications to the materials can be pursued, facilitating the fabrication of scaffolds with tailored physical and

chemical properties to support the guided regeneration of different human tissues.

Acknowledgements

For financial support we thank Portuguese National Science Foundation through the FCT scholarship 2021.05900.BD and Henry Royce Institute EPSRC grants EP/R00661X/1, EP/S019367/1, EP/P025021/1 and EP/P025498/1

References

2) P. Santos, B. Alves, S. Inocêncio, P. Nunes, Stephen M. R., A. Gloria, A. Serra, Ana C. Fonseca, and M. Domingos, *Journal of Materials Chemistry B*, 2025, **13**, 3049-3066.

Development of an experimental model for quantifying the effect of cell monolayers on nanoparticle dynamics

Schleyer, G.[a] *, Patterson, E. A. [b], Curran, J.M. [a]

[a] Department of Materials, Design & Manufacturing Engineering, University of Liverpool, UK

[b] Department of Mechanical and Aerospace Engineering, University of Liverpool, UK

* G.Schleyer@liverpool.ac.uk

Introduction

To optimise the efficiency of using nanocarriers to effectively deliver payloads to target sites or interfaces, it is essential to understand how the design of nanocarriers can be optimised to enhance delivery. Physiological environments are host to many biological solutions, the components of which interact with nanomaterials and potentially affect their dynamic behaviour.

Experimental regimes that can characterise the influence of changes in protein concentrations in localized environments on nanoparticle dynamics are needed to further our understanding of sub-micron entity transport in complex biological environments and therefore aid in the design of biomaterials of the future as well as increase current understanding of cellular processes. In this study an experimental model for the diffusion of nanoparticles through biological media in the presence of a cell monolayer has been developed. The motivation was the creation of a technology platform for *in-vitro* test systems to monitor the effect of the presence of a specified cell monolayer on the diffusion of sub-micron entities as they approach the cell monolayer.

Materials and methods

A label-free microscopy technique, based on the optical phenomenon of caustics, has been used. A standard inverted optical microscope was adjusted to produce near-coherent light to generate optical signatures of entities, or caustics signatures, as described by Patterson and Whelan [1]. To test the lower limitations of the technique, positively- and negatively charged gold particles as small as 50nm in diameter have been successfully visualized and tracked at defined heights above a cell layer (Figure 1). Particles were tracked diffusing at above a human mesenchymal stem cell monolayer

(hMSC) and the influence of time, particle charge, concentration and size on their dynamics in biological environments was investigated.

Results and Discussion

A protocol has been developed that allows nanoparticles to be tracked directly above a cell layer and their dynamics to be characterised as they approach the cell layer over time. Analysis of the values of the diffusion coefficients of the particles and the size of the convex hull enveloping their motion has shown that the local extracellular microenvironment of particles influences their diffusion. Significant changes in particle diffusion rate have been observed one hour after exposure to a cell layer and factors such as the presence of serum proteins, particle surface charge and cellular activity could potentially influence particle dynamics. The conventional understanding of the effect of particle size on diffusion is also challenged in this study (Figure 2).

Conclusion

Comprehensive models of diffusion have been developed which shed light on the effect that changes in local environment, due to cellular activity, have on particle dynamics. The caustics technique has also been demonstrated to be a powerful tool for the development of *in-vitro* testing regimes.

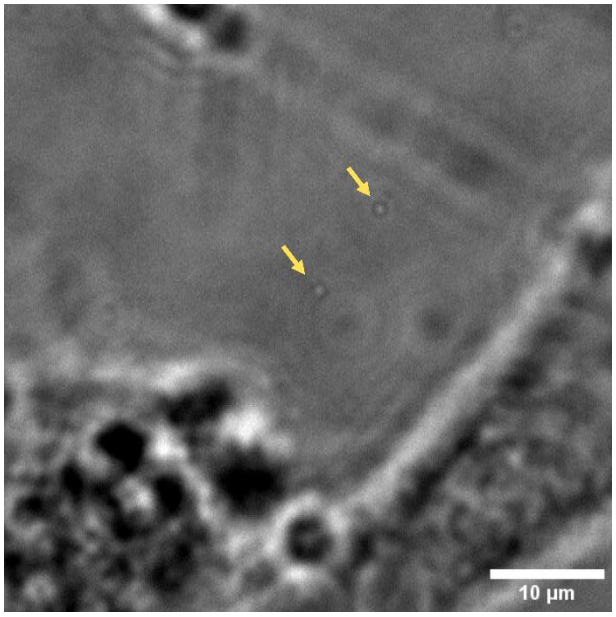

Figure 1. Caustic signatures produced by cell layer and 100nm gold nanoparticles (indicated by yellow arrows) 25µm from cell layer.

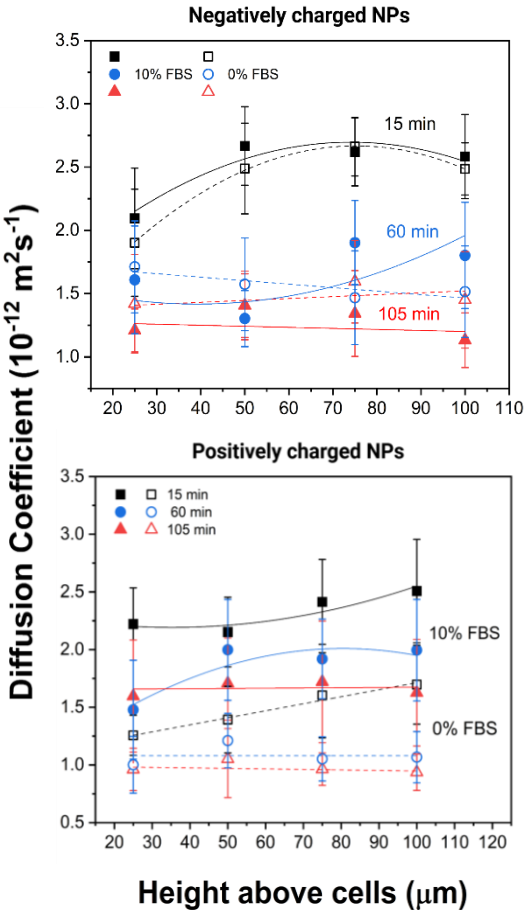

Figure 2: Experimental diffusion coefficient for gold negatively and positively charged nanoparticles with diameters of 100nm tracked at different distances from a cell layer over time with trend lines. Error bars are ±0.5 standard deviation.

References

1. Patterson, E. A. & Whelan, M. P. (2008) Optical signatures of small nanoparticles in a conventional microscope. *Small* **4 10**, 1703-1706

Tissue Engineered Vascular Grafts

Slavova, N.S [a], Prof Claeyssens, F. [a,b], Dr Green, N [a]

[a] Kroto Research Institute, School of Chemical, Materials and Biological Engineering, University of Sheffield, Broad Lane, Sheffield, S3 7HQ, United Kingdom

[b] School of Chemical, Materials and Biological Engineering, INSIGNEO Institute for in Silico Medicine, University of Sheffield, Sheffield, United Kingdom

nslavova1@sheffield.ac.uk

Introduction

Cardiovascular disease (CVD) is the most common cause of death worldwide, with disease incidence increasing annually [1]. Coronary bypass surgery is the current treatment for severe CVD cases, where the occluded vessel is bypassed using an autologous saphenous vein or a synthetic graft to revascularize the region [2]. However, autologous grafting is associated with, poor quality, lack of availability and donor site morbidity [2,3]. Synthetic grafts are routinely used for large vessel grafting [4] but poor patency and thrombosis, limit their use for small diameter applications (<6mm) [5,6]. To address these limitations, we propose a decellularised tissue engineered vascular graft (dTEVG) that harnesses the properties of porous biocompatible materials and the ability of fibroblasts to produce extracellular matrix in abundance, particularly collagen and elastin.

Materials and methods

The polymer scaffolds were manufactured via emulsion templating of poly(glycerol sebacate)-methacrylate (PGS-M) to produce photocurable, high internal phase emulsions (polyHIPEs). The PGS prepolymer is a result of a polycondensation reaction between glycerol and sebacic acid, which when functionalised with methacrylic anhydride, becomes photocurable. PGS-itaconate was also synthesised as a more sustainable alternative to PGS-M that is still photocurable. The polyHIPEs were created by the addition of water (internal phase) to the PGS-M polymer (external phase) with the use of emulsion stabilising surfactant. PGS-M grafts were produced from the polyHIPE using injection moulding. Immortalised human fibroblasts (BJ-5TA) were cultured on the PGS-M grafts. Macromolecular crowding (MMC) of cell culture media with carrageenan and

polyvinylpyrrolidone was employed to enhance collagen and elastin production.

Results

Scanning electron microscopy analysis and cell proliferation experiments were used to select a polyHIPE composition with median pore size of 30 microns, ranging between 10-100 microns. PGS-M grafts with internal diameter of 3.8 mm were successfully manufactured using the same polyHIPE composition via injection moulding. Immortalised fibroblast cells readily infiltrate the tubular scaffolds and deposit collagen and additional ECM proteins on them after 3-week cell culture period. PGS-M grafts were sterilised using medical grade ethylene oxide (EtO). We show that EtO sterilisation has no effect on the graft properties, and they are conducive of cell growth and proliferation. Using MMC to increase collagen production revealed a difference between the response to PVP or Carrageenan - primary fibroblasts increased their collagen production but immortalised fibroblasts did not.

Discussion

The generation of small-diameter cell-laden PGS-M grafts with good ECM deposition enables the next stages of the project. A complete ECM protein characterisation, decellularisation and mechanical testing being the next focus. Media crowding work suggests that this method to stimulate collagen production is highly cell type dependent and its use is being determined.

Acknowledgements

The authors would like to thank the EPSRC funded Centre for Doctoral Training in Biomedical Materials grant reference EP/S022201/1 for funding this work.

References

1) G. A. Roth, G. A. Mensah, C. O. Johnson, G. Addolorato, E. Ammirati, L. M. Baddour, N. C. Barengo, A. Beaton and E. J., *J. Am. Coll. Cardiol.*, 2020, **76**, 2982–3021.
2) S. Pashneh-Tala, S. MacNeil and F. Claeyssens, *Tissue Eng. Part B Rev.*, 2016, **22**, 68–100.
3) M. S. Conte, *J. Vasc. Surg.*, 2013, **57**, 8S–13S.
4) J. S. Soares, S. K. Saunders, F. Potere, S. Toldo and A. Abbate, *Appl. Eng. Sci.*, 2022, **12**, 100114.
5) S. L. M. Dahl, J. L. Blum and L. E. Niklason, *Trends Cardiovasc. Med.*, 2011, **21**, 83–89.
6) B. B. J. Leal, N. Wakabayashi, K. Oyama, H. Kamiya, D. I. Braghirolli and P. Pranke, *Front. Cardiovasc. Med.*, 2021, **7**, 592361.

Development of Delivery Platforms for RNA-Based Immunotherapy in Breast Cancer

Ziyue Su [a], Vahid Heravi Shargh [a], Jenny Hanson [a], Kai Ti Lin [b] and, Raechelle A D'Sa [a, *]

[a] Department of Materials, Design and Manufacturing Engineering, School of Engineering, University of Liverpool, Liverpool, United Kingdom.

[b] Institute of Biotechnology, National Tsing Hua University, Hsinchu, Taiwan.

* Corresponding author(s) e-mail(s): ziyuesu@liverpool.ac.uk

Introduction

Breast cancer is the most prevalent cancer among women worldwide. Conventional treatments, such as surgery, chemotherapy, and radiotherapy, are often associated with significant side effects, along with the risks of recurrence and metastasis. In recent years, RNA-based immunotherapy has gained more attention, particularly following the successful commercial application of COVID-19 mRNA vaccines. In addition to mRNA, RNA interference (RNAi) molecules, including small interfering RNA (siRNA) and microRNA (miRNA), which regulate gene expression post-transcriptionally by targeting specific mRNA sequences, also offer a promising therapeutic approach.

Several RNAi candidates have been identified with expression levels strongly correlated with breast cancer progression[1], suggesting their potential as therapeutic targets. However, the clinical translation of RNA-based therapies faces challenges due to the instability of naked RNA molecules in vivo. Therefore, low toxicity, biodegradable, and high transfection efficiency delivery systems are required for effective intracellular transportation. In this study, we aim to develop a lipid-based nanocarrier to enhance mRNA delivery into breast cancer cells and tissues in vitro and in vivo.

Materials and methods

mRNA-LNP formulation: The aqueous phase consisted of 1 mg/mL model mRNA (Poly A) in citric acid buffer. LNPs were formulated by rapid mixing of the lipid phase containing ionisable aminolipids Dlin-MC3-DMA, cholesterol, DSPC, and DMG-PEG2000 with the polyA aqueous phase and subsequently dialyzed against PBS. The liposomes were characterised by dynamic light scattering for particle size, zeta potential for charge, cryo-scanning electron microscopy for morphology.

Results and Discussion

The LNPs were formulated by mixing varying concentrations of the ionisable aminolipids and cholesterol together. The LNPs synthesis parameters were optimised to have an average particle size of ~ 100 nm with a narrow size distribution. The model mRNA poly A was added to LNP synthesis to generated mRNA-LNPs with an optimal size range (~ 100 nm) and near neutral surface charge (+2.77 mV), (**Figure 1**). The size and surface charge will allow for a prolonged circulation, thereby increasing the cellular uptake and tumour targeting (via the enhanced permeability and retention (EPR) effect)[2] potential. Future work will focus on the evaluation of encapsulation efficiency and in vitro transfection performance.

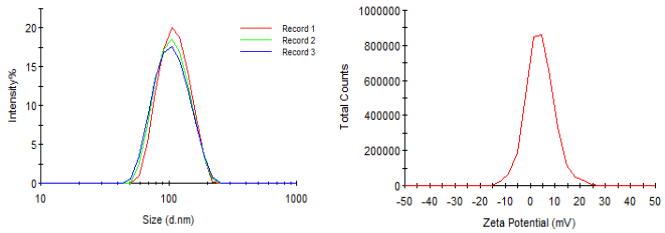

Figure 1. Particle size distribution (Left) and zeta potential (Right) of mRNA-LNPs.

Acknowledgements

This project was financially supported by University of Liverpool-National Tsing Hua University joint studentship.

References

1) X. Zhang, Q. He, L. Sun, Y. Zhang, S. Qin, J. Fan, and J. Wang. Disease Markers, 2019, **2019**, 6057280.
2) B. Belyaev, O. Y. Griaznova, A. V. Yaremenko, S. M. Deyev, and I. V. Zelepukin. Advanced Drug Delivery Reviews, 2025, **219**, 115550.

Engineering Magnetic nanobots for Boron Neutron Capture Therapy Applications

Ece Tezsezen[a], Moira Lorenzo Lopez [a] and Jenny Aveyard [a]

[a] Dept of Materials, Design and Manufacturing, School of Engineering, University of Liverpool, United Kingdom.

* Corresponding author(s) e-mail(s): zippy78@liverpool.ac.uk

Introduction

Boron neutron capture therapy (BNCT) is an innovative, non-invasive radiation treatment strategy that overcomes the shallow penetration of light, in other photon-induced binary cancer therapies, such as photothermal therapy (PTT) and photodynamic therapy (PDT). One key factor in performing successful BNCT is to accumulate a sufficient therapeutic amount of the isotope Boron-10 (B-10;>20 ppm) within cancer cells, which has been a long-standing challenge for small-molecule-based boron drugs. Another obstacle to overcome in BNCT is the nonspecific in vivo distribution of boron-containing compounds. As a result, it is necessary to develop a drug delivery system (DDS) with improved boron accumulation at cancer cells. Previous studies have emphasized the importance of DDS for higher solubility (1,2), low systematic toxicity (3), quantitative release of boron at the tumour microenvironment and intratumor retention (4,5).

Boron-containing nanoparticles (BNPs) have gained considerable attention as promising DDS for tumour-targeted BNCT. They exhibit selective and high tumour uptake, limiting toxicity, improve cellular stability and enable blood brain barrier (BBB) passage (6–11), however, drug delivery with BMPs in physiological environments is still challenging.

Controllable DDS, or nanobots, can be externally controlled by light, electric field, ultrasound or by chemicals but all these propulsion methods have limitations that can affect their use including lack of directionality or the generation of toxic chemicals during propulsion. Magnetically driven nanobots address most of the drawbacks associated with other propulsion principles, as they can be manipulated with low frequency magnetic fields in a non-invasive way, and they can penetrate biological tissues.

Magnetically driven nanobot DDS could address many of the challenges associated with BNCT by actively targeting cancerous cells, allowing accumulation of B-10,

subsequently reducing adverse effects and improving therapeutic efficacy.

Described herein is the synthesis and characterisation of magnetic nanobots. We investigate the effects of altering synthesis parameters such as reactant concentration, titration time, stir speed and temperature on the subsequent size, shape and properties of the resulting nanobots. The ability to control the nanobots in physiologically relevant solutions is also assessed using the caustics technique. Results demonstrate that monodisperse, magnetic nanobots with the requisite properties can be synthesised using a simple protocol and that these could be a promising DDS for BNCT.

Materials and methods

Materials

Ethanol, hydrochloride acid (HCl, 36–38%), sodium hydroxide (NaOH), ferric chloride ($FeCl_3 \cdot 6H_2O$), and ferrous chloride ($FeCl_2 \cdot 4H_2O$) were obtained from Sigma-Aldrich. Ultrapure water was obtained from a Millipore pure water system Ferric chloride hexahydrate ($FeCl_3 \cdot 6H_2O$, ≥98%;Sigma-Aldrich), poly(vinylpyrrolidone) (PVP40; Sigma-Aldrich), sodium acetate trihydrate ($NaAc \cdot 3H_2O$, ≥99%; Sigma-Aldrich), ethylene glycol (EG, ≥99.5%; Fluka), citric acid ($C_6H_8O_7$, ≥99.5%; Sigma-Aldrich), and agar (2%; Panreac) were obtained. All chemicals are of analytical-reagent grade and were used without further purification

Methods

Magnetic Iron Nanoparticles

Magnetic Fe_3O_4 nanoparticles were synthesised using a modified version of the previously described co-precipitation technique. Different stir speed, titration speed, beaker shapes were used to investigate the relationship between synthesis parameters and NP size dispersity.

25 ml of water was ultrasonically sonicated for 30 minutes to dissolve 19.2 mmol $FeCl_3 \cdot 6H_2O$ and 19.2 mmol $FeCl_2 \cdot 4H_2O$. Then, 0.85 ml of HCl (36–38 percent) was added. With constant stirring, 250 ml of NaOH aqueous solution (1. 5 mol l−1) was then added dropwise the resulting homogenous yellow solution. The mixture was then vigorously stirred at 700 rpm for one hour at room temperature. Using a magnet, the black precipitates were gathered, repeatedly cleaned with ethanol and ultrapure water, and then vacuum-dried for 24 hours at 60 °C.

Magnetic Iron Nanoflowers

Magnetic Fe_3O_4 nanoparticles were synthesised using a modified version of the previously described co-precipitation technique. 2.62 mmol $FeCl_3 \cdot 6H_2O$ was dissolved with ultra-sound in 109 mL of ethylene glycol. Then, 140 mmol PVP40was added slowly under vigorous magnetic stirring (>1000rpm) and mild heating until completely dissolved. Then, 15.8−36.5 mmol $NaAc \cdot 3H_2O$ was added to the solution. The mixture was sealed in a Teflon-lined autoclave (125 mL) and maintained at 200 °C for 0.5−48 h for solvo-thermal crystallization, followed by cooling inside an oven. The precipitated solid product was washed with ethanol and distilled water through centrifugation several times

Characterization of Size, Morphology and Caustic effects

The hydrodynamic size distribution and zeta potential of the samples were measured using a Malvern Zetasizer dynamic light scattering (DLS) instrument. Surface morphology and microstructure were observed using a Desktop Scanning Electron Microscope (Thermo Fisher Scientific) operated at an acceleration voltage of 10kV. Caustic behaviours of the different size and shape nanoparticles such as nanoflowers and nanoparticles were observed under live microscopy. In an optical microscope, we visualize and investigated the movement and aggregation profiles, providing insights into their behaviour in various biological environments.

Results

SEM and DLS

Surface morphology and microstructure were observed using a Desktop Scanning Electron Microscope (Thermo Fisher Scientific) operated at an acceleration voltage of 10kV. As the reaction parameters changes, we observed different shape and morphological properties.

Caustics Effects

Caustic behaviours of the different size and shape nanoparticles such as nanoflowers and nanoparticles were observed under live optical microscopy. We investigated the movement and aggregation profiles with different ratios of glycerol/water for the variant viscosity. The nanoparticles showed movement towards to magnetic field and showcased and possible magnetic functionality for BNCT.

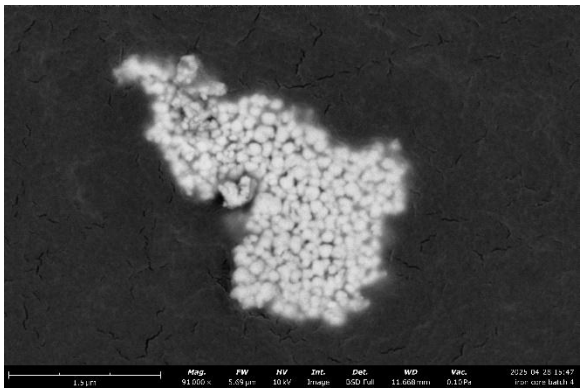

Figure 1. Magnetic Fe_3O_4 nanoparticles under 91,000 magnification and acceleration voltage of 10KV

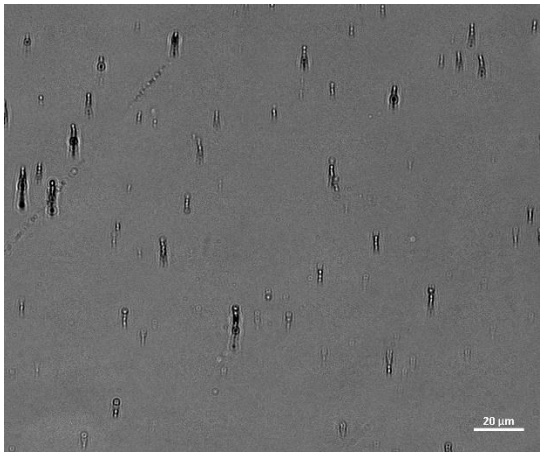

Figure 2. Magnetised Fe_3O_4 Nanoparticles under optical microscopy

Acknowledgements

We gratefully acknowledge funding from the UoL-NTHU dual funded PhD studentship programme.

References

1. Hirano F, et al Bioorganic Chem. 2024 Jan;142:106940. 2. Järvinen J et al; P Pharmaceutics. 2023 Nov 23;15(12):2663. 3.Skwierawska D, L et al. 2022 Jun 10;14(12):2865. 4. Wang M et al. Angew Chem Int Ed. 2025 Jan 10;64(2):e202413232. 5. Tsujino K, et al. Neuro-Oncol Adv. 2024 Jan 1;6(1):vdae062. 6. Fisher RS et al. CNS Drugs. 2002;16(9):579–93. 7. Lockman PR, Drug Dev Ind Pharm. 2002 Jan;28(1):1–13. 8. Ali F et al. Molecules. 2020 Feb 13;25(4):828. 9. Ailuno G, et al. Cells. 2022 Dec 13;11(24):4029. 10. Sumitani S et al. React Funct Polym. 2011 Jul;71(7):684–93. 11. Dymova MA et al. Cancer Commun. 2020 Sep;40(9):406–21. 12.Tamanoi F, et al. Int J Mol Sci. 2021 Feb 24;22(5):2251.

Development of Inhaled Therapeutic Polymeric Nanoparticles for the Treatment of Respiratory Infections

Imogen Walker*, Jenny Aveyard and Raechelle D'Sa
School of Engineering, University of Liverpool, UK
* Corresponding author e-mail: iw64@liverpool.ac.uk

Introduction

Respiratory diseases and infections are a significant global public health concern, ranking third and fourth among the leading causes of death worldwide (WHO). Lower respiratory infections were the leading communicable cause of death in 2019, resulting in 2.6 million deaths.[1] Treating bacterial respiratory infections has become increasingly problematic due to the rise of multidrug-resistant bacteria. Nitric oxide (NO) is a promising alternative to antibiotics due to its broad-spectrum antimicrobial activity. NO disrupts cellular functions through multiple mechanisms, making bacterial resistance unlikely. However, as a gas, delivering NO to infection sites is challenging. This project aims to develop polymeric drug delivery vehicles to encapsulate NO donors for inhalation.

Materials and methods

The two selected cationic polymers show low toxicity due to their degradable backbones. Both polymers were synthesized in anhydrous solvents to ensure high yield and purity. Reaction conditions were optimized to produce polymers with molecular weights of 10-30 kDa. The polymers were modified and nitrosylated using an in-house NO donor, enabling them to store high quantities of NO. Their planktonic and biofilm antimicrobial activity was tested against Staphylococcus aureus (S. aureus) and Pseudomonas aeruginosa (PA01). Cytocompatibility of the nitrosylated polymers was determined against NL20 (human lung epithelial cells).

Polymer characterization included ^{1}H, ^{13}C, ^{13}C DEPT, COSY, HSQC, HMBC nuclear magnetic resonance spectroscopy (NMR), FTIR, and gel permeation chromatography (GPC). NO release was measured in differing media (PBS, broth, BAL supernatant, artificial mucus) under varying conditions (light/dark, EDTA) using chemiluminescence.

Results

Both linear polymers exhibited high NO payloads, releasing 200 μM mg^{-2} over 24 hours.

Planktonic antimicrobial testing showed complete bacterial kill against both gram-positive and gram-negative bacteria. Linear polymer 1 achieved complete kill at for *S. aureus* a higher dose was needed for PA01. Polymer 2 showed complete kill at the lower dose for both strains. Under nutrient-poor conditions, both polymers eliminated bacteria at 2.5 mg. Biofilm antimicrobial testing showed complete kill for both polymers against both *S. aureus* and PA01 in nutrient rich conditions. In nutrient poor conditions complete kill was achieved at the lower dose for both polymers against both bacteria species.

Discussion

In summary, we synthesized two linear polymeric carriers tethered to NO donors, demonstrating controlled, sustained NO release and effective bacterial elimination. Future work will explore formulation optimisation, aerosolization and antimicrobial testing in various media ie BAL supernatant and artificial mucus.

Acknowledgements

The authors gratefully acknowledge the financial support of the Kitchner Fellowship, Munitions Fellowship, Mrs W M Horsman Endowment and Andrew Hamilton Endowment.

References

3) Health matters: Antimicrobial resistance (2015) GOV.UK. Available at: https://www.gov.uk/government/publications/health-matters-antimicrobial-resistance/health-matters-antimicrobial-resistance (Accessed: 23 April 2025).

Melt electrowriting of a bacterial polyester for shoulder tendon repair

Weber, L. [a], Domingos, M. [a], Roy, I. [b], Peach, C. [c]

[a] Department of Mechanical and Aerospace Engineering, School of Engineering, Faculty of Science and Engineering & The Henry Royce Institute, The University of Manchester, UK

[b] Department of Materials Science and Engineering, Faculty of Engineering, University of Sheffield, UK

[c] Manchester Shoulder and Elbow Unit, Manchester University Foundation NHS Trust, Manchester, UK

* Corresponding author e-mail: lukas.weber@manchester.ac.uk

Introduction

If you suffer from shoulder pain, there is a 40% chance that tears in the rotator cuff tendons are the cause. Surgery involving decellularized tissue grafts remains the most effective approach to re-establish the tendon-bone connection. Even though a range of grafts are commercially available, 10-70% of cases show incomplete healing.[1,2] Hence, there is an unmet need for constructs closely replicating the gradient nature of the native tissue.

Materials and methods

This study aims to engineer bioactive and mechanically stable scaffolds for tendon-bone repair. As the first part, the processing of medium-chain-length poly-(3-hydroxyalkanoate) (mcl-PHA), a biodegradable polyester, via melt electrowriting (MEW) is investigated. mcl-PHA was synthesized through microbial fermentation and characterized using differential scanning calorimetry and oscillatory rheology. The MEW process was monitored using microscopy (light, fluorescence, and scanning electron).

The effect of MEW patterns on the viability and alignment of seeded fibroblast and osteosarcoma cells was assessed *in vitro* using Calcein, Ethidium homodimer (EthD-1), and Hoechst 33342 staining.

Results

Compared to the gold standard polycaprolactone, mcl-PHA exhibited advantageous characteristics including a glass transition temperature of approximately –40 °C and low melt viscosities (200–570 Pa·s). These enabled processing at reduced temperature (40-60 °C) and pressure (< 200 kPa). Initial fibres were thick (80–220 µm) and fused, but multiparameter optimization improved

fibre fidelity, producing diameters close to 10 µm. Patterns with fibre spacings as low as 100 µm were printed and layered.

Fibroblasts preferentially aligned along parallel mcl-PHA fibres with the degree of alignment increasing with decreasing fibre spacing (**Figure 17** (top)). Meanwhile osteosarcoma cells seemed to spread more randomly on grids with larger pore size (bottom).

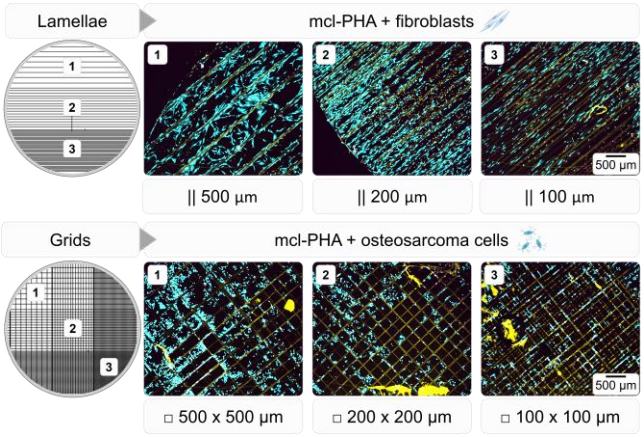

Figure 17. *Effect of different MEW patterns of mcl-PHA on cell alignment in fluorescence microscopy: (top) fibroblasts on lamellae with (1-3) varying fibre spacings, (bottom) osteosarcoma cells on grids with (1-3) varying pore sizes. All prints consist of 3 layers. Used stains: Calcein – cyan, EthD-1 – magenta, Hoechst 33342 – yellow.*

Discussion

This study demonstrates the processability of a novel bacterial polyester in MEW with high accuracy. Furthermore, the ability to control fibre morphology and mesh architecture allows for a customizable scaffold design of scaffolds that support cell alignment specific to the needs of the rotator cuff tendon tissue.

Acknowledgements

The authors would like to thank the EPSRC-funded Centre for Doctoral Training in Advanced Biomedical Materials grant EP/S022201/1 and the Henry Royce Institute EPSRC grants EP/R00661X/1, EP/S019367/1, EP/P025021/1, and EP/P025498/1.

References

1) H. Hinsley, C. Ganderton, N. K. Arden and A. J. Carr, *BMJ Open*, 2022, **12**, e059175.

2) A. Carr, C. Cooper, M. K. Campbell, J. Rees, J. Moser, D. J. Beard, R. Fitzpatrick, A. Gray, J. Dawson, J. Murphy, H. Bruhn, D. Cooper and C. Ramsay, *The Bone & Joint Journal*, 2017, **99-B**, 107–115.

Structural polymer as suspending media for lightsheet fluorescent microscopy.

Weightman, J.R.[a], White, P.C.[b], Moakes, R.J.A.[a], Robinson, T.E. [a], Mueller, F.[b] Grover, L.M.[a]

[a] Healthcare Technologies Institute, University of Birmingham, United Kingdom.

[b] Department of Cancer and Genomic Sciences, University of Birmingham, United Kingdom.

Email: l.m.grover@bham.ac.uk

Introduction

In recent years, the introduction of lightsheet fluorescent microscopy (LSFM) has provided an outlet to study a host of multidisciplinary areas, ranging from spatial cellular organisation to targeted cancer treatment. However, it is challenging to maintain 3D cell models long term for temporal imaging, due to the absence of suspension materials compatible with cell culture and imaging parameters[1]. In this study, we utilised gellan gum to create optically clear fluid gels, and investigated whether these materials could maintain both cell viability and material support necessary for long term 4D imaging.

Materials and methods

Gellan gum formulation

Low acyl gellan gum (Kelco) was dissolved at varying (1-2) w/v% in deionised water, supplemented with 5% PBS and 10 mM NaCl, by heating to 90 degrees and mixing until dissolved. The solution was then autoclaved for 1 hour at 121°C. The hot solution was cooled to 20 degrees under agitation to form the fluid gel, then stored at 4°C until use.

Lightsheet imaging

FUCCI-expressing colorectal cancer organoids encapsulated in gellan gum were imaged using the Z1 Zeiss lightsheet using lasers at 488 and 561nm. Images were processed through imageJ.

Rheometry

Temperature sweep rheological testing was performed on Malvern Kinexus Ultra+ rheometer using parralel plate surface finish geometry. To measure the dependence of the material properties on temperature, the fluid gels were heated from 25 to 40 at 1 deg/min.

Results

Temperature sweeps on varying Gellan gum formulations remained elastically dominant under increasing temperatures. Gellan-embedded organoid models showed continuous growth and retention of important morphological features. Additionally, gellan-embedding held organoids stable over a 2-week cell cycle

study, enabling continuous imaging of the same region over time.

Discussion

Through rheological sweep testing we were able to evaluate and alter the hydrogel microstructure and its response to deformation and temperature. This opens up the potential for gellan gum to be designed to sustain a variety of investigative models. Our initial research has found that gellan gum acts as a suitable medium to support live organoid growth and imaging up to 14 days, allowing for spatiotemporal fluorescent reporter tracking. Our next steps will determine cell viability, followed by expansion into *in vivo* imaging to explore tissue development.

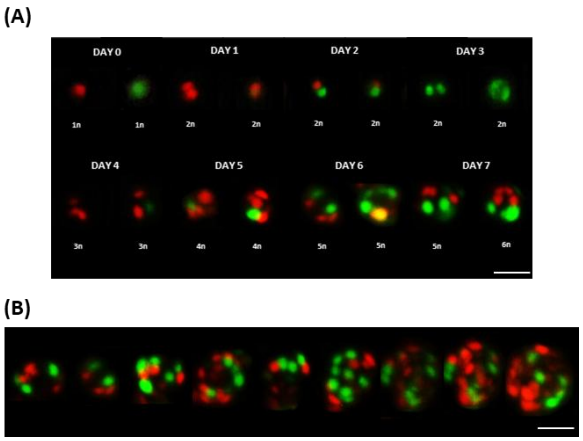

Figure 1. Cell cycle tracking of FUCCI organoid over 14 days. Fluorescent snapshots of nuclear expression of FUCCI fluorescent reporters in the same organoid over 14 days (Post seeding on day 0) using adapted long-term high-resolution imaging protocol in Zeiss Z1 lightsheet. Captured using selected lasers 488 and 561nm at 1.8 and 1.3 intensity and 219.71 millisecond (ms), scale 50 µm. (A) Tracking of cell divisions using both fluorescent reporters to distinguish cycle phase and number of nuclei. Same organoid imaged every 12 hours. (B) Same organoid imaged for days 8-14 showing loss of synchronicity and resolution of individual cellular changes.

Acknowledgements

This work was supported by Science Foundation Ireland **18/EPSRC-CDT/3583** and the Engineering and Physical Sciences Research Council **EP/S02347X/1**

References

1) M. Adams, A. Loftus and J. Fitzpatrick, *Curr Protoc Cytom.* **2015**, 1, 71.

Poster presentations

Development of a Smart EV-Loaded Multifunctional Membrane for Bone Regeneration

Alshammari, F. [a,b,*], Ortega Asencio, I. [a], Lambert, D.W. [a]

[a] School of Clinical Dentistry, University of Sheffield, UK

[b] Department of Dental Health, King Saud University, KSA

* Corresponding author e-mail: falshammari1@sheffield.ac.uk

Introduction

Musculoskeletal diseases and injuries affect millions of people every year, reducing quality of life and creating a burden for healthcare systems. Specifically, bone injuries may result from trauma, cancer, or long-term infections, and they are currently considered a major global problem in both Medicine and Dentistry.

Addressing clinical challenges like poor vascularisation and infection during biomaterial design is crucial for effective outcomes. A promising avenue of research involves extracellular vesicles (EVs), which have substantial promise in cell-free tissue engineering [1]. Our group has recently developed a new manufacturing route that has proven to be effective in incorporating EVs on fibrous membranes, as well as allowing their sustained release.

The aim of this project is to develop a novel multifunctional angiogenic and antimicrobial EV membrane for bone regeneration.

Materials and methods

A fibrous membrane composed of 10% poly (ε- caprolactone) (PCL) was fabricated using an upright electrospinning setup, with a flow rate of 1.5 mL/h, voltage of 21 kV, and a needle-collector distance of 17 cm. Scaffolds were characterised by scanning electron microscopy (SEM) to determine fibre diameter and by contact angle measurements to assess wettability.

Surface hydrophilicity was enhanced by air plasma treatment for 2 min at 10 W using a low-pressure plasma system (ZEPTO, Diener Electronics, Germany).

EVs were isolated from H357 cell line medium using size exclusion chromatography (SEC). Nanoparticle tracking analysis (NTA) was performed using a ZetaView PMX-120 (Particle Metrix, Germany) to assess EV size distribution and concentration. Samples were analysed across 11 positions and processed using ZetaView software (version 8.04.02, SP2).

Results

The electrospun PCL scaffolds exhibited a uniform structure with an average fibre diameter of 1.4 µm ± 0.7 µm. Initial wettability tests demonstrated a high hydrophobicity, with a water contact angle measured at 133.8° ± 6°. Plasma surface treatment significantly improved scaffold hydrophilicity, an essential modification for enhancing EV attachment and functionality.

Nanoparticle tracking analysis (NTA) using the ZetaView PMX-120 confirmed the successful isolation of extracellular vesicles with particle concentrations ranging from approximately 10^9 to 10^{10} particles/mL (**Figure 1**).

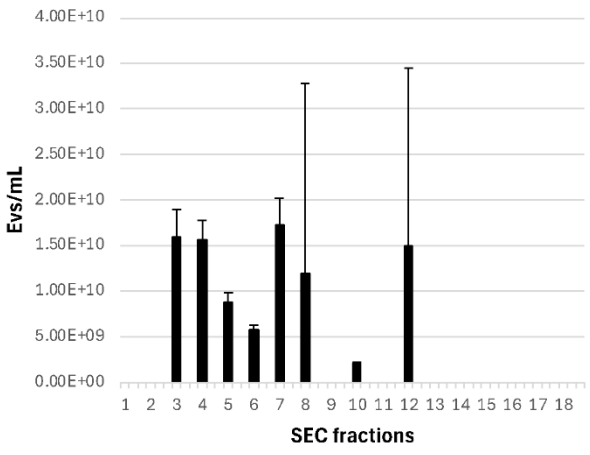

Figure 1. Nanoparticle tracking analysis (NTA) results showing extracellular vesicle (EV) concentrations across SEC fractions 1–18. Highest EV concentrations were detected in fractions 3–8 and 12, with particle counts ranging from approximately 10^9 to 10^{10} EVs/mL. Data are presented as mean ± standard deviation (SD).

Discussion

The structural properties of the developed PCL scaffolds are promising for applications in bone regeneration. Initial hydrophobicity was successfully addressed through plasma treatment, significantly improving scaffold hydrophilicity and creating a surface more conducive to EV attachment.

Extracellular vesicles (EVs) were successfully isolated and characterised by nanoparticle tracking analysis (NTA), confirming particle concentrations in the range of 10^9–10^{10} EV/mL in specific SEC fractions. These results validate the effective isolation and concentration of EVs suitable for scaffold functionalisation.

The functionalisation of plasma-treated PCL scaffolds with EVs is anticipated to enhance vascularisation and deliver antimicrobial activity, addressing two critical challenges in clinical bone healing. Future work will focus on optimising EV loading onto the scaffolds, exploring the use of ECM-derived EVs, modifying the EVs to enhance their

antimicrobial function, and assessing the regenerative performance of the constructs in vitro.

Acknowledgements

The author acknowledges the support of Prof. Dan Lambert and Dr. Ilida Ortega Asencio, and the sponsorship from King Saud University.

References

1) Alqurashi H, Ortega Asencio I, Lambert DW, Tissue Eng Part B Rev, 2021. **27(5):530-538**.

Advanced AFM Imaging and Analysis of Cellular and Tissue Samples: Innovations in Large-Area Mapping and Mechanobiology

Barner, J.[a,*], Körnig, A. [a], Dulebo, A. [a], Escolano J.C. [a], Henze, T. [a]

[a] BioAFM, Bruker Nano GmbH, Am Studio 2D, 12489 Berlin, Germany

* joerg.barner@bruker.com

Introduction

Atomic Force Microscopy (AFM) is a pivotal tool for nanoscale mechanical property mapping, providing high-resolution characterization of stiffness, adhesion, and viscoelasticity. This capability is crucial for understanding material behaviour in complex structures such as living cells, tissues, and biomaterials. These insights drive forward studies of cell behaviour, disease progression, and drug treatments. However, challenges such as sample roughness and limited lateral scanning range often hinder large-scale mechanical mapping, particularly for complex and heterogeneous specimens.

Materials and methods

To address these challenges, we developed a new concept for AFM imaging, incorporating SmartMapping technology. This technology coordinates AFM head motors and XYZ-piezo movement of the AFM stage, enabling continuous, high-resolution automated mapping over extensive areas without user intervention. This innovation enhances the precision and efficiency of AFM. Our research utilized this newly developed AFM technology to perform multi-compartment imaging with high reproducibility and throughput across multiple regions.

In our studies, we used Cytochalasin D treated 3T3 fibroblasts and compared them to non-treated controls. Additionally, we investigated highly corrugated 3D spheroid SKOV-3 model lines and zebrafish tumours, focusing on their structural and mechanical characteristics. We also mapped mouse brain tissue along the anterior-posterior axis to draw functional correlations between regional structural and mechanical differences and the underlying anatomical composition and architecture. Neuroblastoma tumours, embedded in low-melting agarose gels, were analysed despite their roughness, demonstrating the stage's capability to handle complex tissue samples.

Results

The application of SmartMapping technology in AFM imaging revealed significant time-lapse differences in mechanics, structure, and cytoskeletal organization between Cytochalasin D treated 3T3 fibroblasts and non-treated controls. For the 3D spheroid SKOV-3 model lines and zebrafish tumours, we observed detailed structural and mechanical characteristics, with the tumours exceeding 100 μm and 300 μm in height, respectively. The mapping of mouse brain tissue along the anterior-posterior axis highlighted functional correlations between regional structural and mechanical differences and the underlying anatomical composition and architecture. The analysis of neuroblastoma tumours, 600 μm thick, embedded in low-melting agarose gels, was successfully conducted, showcasing the stage's capability to handle complex tissue samples.

Discussion

The integration of SmartMapping technology within our innovative AFM stage underscores the potential for large-area imaging and mapping in mechanobiology. Our findings demonstrate the enhanced precision and efficiency of AFM imaging, enabling detailed analysis of complex and heterogeneous specimens. This advancement in AFM technology facilitates a deeper understanding of cellular and tissue mechanics, contributing significantly to the broader field of mechanobiology. Our work paves the way for future research and applications, advancing the study of cell behaviour, disease progression, and drug treatments.

Optimising Surgical Handling and Drug Release from Hydrogel/Fibre Composites for Treatment of Conjunctival Melanoma

Bhalla, M. , Desai, N. , Bosworth, L.A , Robinson, D.E. , Kearns V.R*

[a] Department of Eye and Vision Science, Institute of Life Course and Medical Sciences, University of Liverpool, Liverpool L7 8TX, United Kingdom.

* Corresponding author(s) e-mail(s): vkearns@liverpol.ac.uk

Introduction

Conjunctival melanoma is a fatal ocular malignancy. Although rare, accounting for 5% of all ocular melanomas (Butt et al., 2024), it is an aggressive and invasive cancer. Current treatment options for conjunctival melanoma are ineffective, resulting in high recurrence and metastasis. This study aimed to optimize the surgical handling properties of a hydrogel/nanofiber composite intended to deliver adjunct chemotherapy to the conjunctiva.

Materials and methods

Poly(ε-lysine) (PeK) hydrogels were manufactured via carbodiimide crosslinking (Lace et al., 2021) and subsequently combined with electrospun PCL nanofibers to make a composite. PCL fibres were pre-treated with NaOH or air plasma to enhance hydrophilicity. Surgical integrity and handling were assessed semi-quantitatively by passing a 8/0 Vicryl suture with a curved needle through hydrogel and composite samples. Mechanical properties of different composite compositions were measured using an Instron 68SC-5 uniaxial tester.

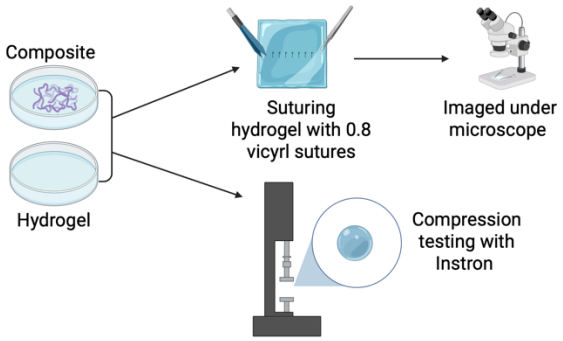

Figure 1. *Schematic overview of manufacture and mechanical testing of hydrogel and composites.*

Results

PeK hydrogels were initially handleable and tolerated suture passage; however, their structural integrity deteriorated over a week in solution, rendering them unsuitable for joining via suturing. In contrast, nanofibre – hydrogel composites remained suturable, highly handleable, and flexible, maintaining

mechanical integrity despite their reduced thickness. Mechanical testing supported these observations, with fibre-reinforced composites exhibiting significantly higher compressive strength, While the hydrogel had compressive strength of 0.15N, the composite material had compressive strength of 0.3N, a twofold increase.

Discussion

Composites exhibited improved mechanical properties compared to hydrogels alone, allowing for improved surgical handling. These findings suggest that fibre incorporation substantially enhances both the mechanical performance and practical usability of hydrogels for applications requiring suturability and durability.

Acknowledgements

For laboratory assistance, I would like to thank Rumana Hussain and Jessica Hollett.

For financial support, I would like to acknowledge Medical Research Council (MRC) [MR/Y019385/1], DiMeN Doctoral Training Partnership [MR/W006944/1] and Impact
Acceleration Account [MR/X502765/1], and Engineering and Physical Sciences Research Council (EPSRC) [EP/Y001656/1, EP/X525741/1].

References

Butt, K., Hussain, R., Coupland, S.E. and Krishna, Y. (2024). Conjunctival Melanoma: A Clinical Review and Update. Cancers, 16(18), p.3121. doi: https://doi.org/10.3390/cancers16183121.

Lace, R., Duffy, G.L., Gallagher, A.G., Doherty, K.G., Maklad, O., Wellings, D.A. and Williams, R.L. (2021). Characterization of Tunable Poly- ε -Lysine-Based Hydrogels for Corneal Tissue
Engineering. *Macromolecular Bioscience*, p.2100036. doi: https://doi.org/10.1002/mabi.202100036.

Bioinspired hierarchical scaffolds direct human conjunctival epithelial cell organization and distribution

Citro, V.[a], Liashenko I.[b], Dalton, P.D.[b], Hamill K.J.[a], Bosworth, L.A. [a,*]

[a] Department of Eye and Vision Science, Institute of Life Course and Medical Sciences, Faculty of Health and Life Sciences, University of Liverpool, Liverpool, UK

[b] Dalton Lab, Knight Campus for Accelerating Scientific Impact, University of Oregon, USA

* lucy.bosworth@liverpool.ac.uk

Introduction

The conjunctival matrix is a complex protein-polysaccharide network that ensures structural integrity and regulates cellular functions critical for ocular surface homeostasis[1]. Trauma and inflammation can compromise this matrix causing scarring and dysfunction[2]. Understanding its composition and structure is key to designing biomimetic scaffolds for functional tissue regeneration [3]. In this context, the integration of melt electrowriting (MEW) and electrospun fiber scaffolds presents a promising strategy for replicating diverse topographical features and modulating pore interconnectivity at multiple scales. This approach enables systematic investigation of how these architectural parameters influence cell-scaffold interactions, ultimately providing insights into the optimization of biomaterial design for tissue engineering applications.

Materials and methods

Hierarchical 3D scaffolds were fabricated by depositing electrospun polycaprolactone (PCL) fibers onto PCL MEW frameworks with box, hexagon, and decagon geometries to modulate pore interconnectivity. PCL electrospun fiber thickness varied with deposition times of 2, 5, 10, and 20 minutes. Immortalized human conjunctival epithelial cells were cultured up to 7 days, cell distribution and migratory pattern were analysed by SEM whereas immunofluorescence staining of vinculin and actin filaments enabled the assessment of focal adhesion dynamic and cytoskeletal organization in response to scaffold architecture.

Results

Electrospinning directly onto MEW scaffolds resulted in their conformation to the underlying microstructured geometry, thereby influencing cellular organization. At shorter electrospinning durations (2 and 5 minutes), the resultant electrospun layer remained sufficiently porous, allowing cells to infiltrate and align with the MEW fibre architecture. In contrast, prolonged electrospinning (10 and 20 minutes) resulted in a denser, more compact fibre

deposition, effectively restricting cellular penetration. Under these conditions, cells predominantly remained on the surface of the electrospun layer, forming a monolayer with minimal interaction with the MEW scaffold beneath (**Figure 1**).

Discussion

Electrospinning directly onto MEW scaffolds proved to be an effective strategy for modulating cellular organization by leveraging the pore interconnectivity. At shorter electrospinning durations (2–5 minutes), the deposited fibers conform closely to the underlying MEW geometry while maintaining sufficient porosity. This structural openness permitted cell infiltration and facilitated alignment along the MEW fibers.

However, with extended electrospinning times (10–20 minutes), the accumulation of fibers led to a denser, more compact layer. This increased fiber density impedes cellular infiltration, confining cells to the uppermost surface of the electrospun mat. As a result, a monolayer of cells formed on top of the construct, with minimal interaction with the MEW scaffold's microarchitecture. These findings underscore the importance of fine-tuning electrospinning parameters to balance scaffold permeability and guidance properties, enabling the design of hierarchical constructs that can direct cellular behaviour in a controlled manner.

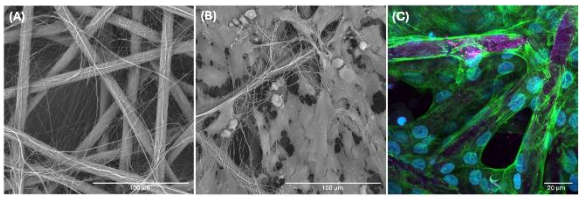

Figure 1. Images of hCjE cells cultured on composite scaffolds after 7 days. *(A) SEM image of decagon MEW with 2min electrospun fiber deposition (scale = 100□m). (B) SEM demonstrates cell attachment and network formation on this scaffold (scale = 100□m). (C) Fluorescence microscopy image of the same system, highlighting the cytoskeleton (green, actin filaments), nuclei (blue, DAPI), and vinculin (purple) (scale = 20□m).*

Acknowledgements

For financial support we thank EPSRC funding EP/Y001656/

References

1. Makuloluwa, A. K. *et al.* The conjunctival extracellular matrix, related disorders and development of substrates for conjunctival restoration. *Ocul Surf* 28, 322–335 (2023).
2. Dart, J. K. The 2016 Bowman Lecture Conjunctival curses: scarring conjunctivitis 30 years on. *Eye 2017 31:2* 31, 301–332 (2017).

3. Bosworth, L. A. *et al.* Material Characterisation and Stratification of Conjunctival Epithelial Cells on Electrospun Poly(?-Caprolactone) Fibres Loaded with Decellularised Tissue Matrices. *Pharmaceutics 2021, Vol. 13, Page 318* 13, 318 (2021).

Mechanochemical Optimisation of Carboxymethylcellulose (CMC) Hydrogels

Kaliyeva, A.M.,[a,b,*] Kalniyazov, D.F.[a]

[a] Asfendiyarov Kazakh National Medical University, Kazakhstan.

[b] Lancaster University, United Kingdom.

* Corresponding author e-mail: a.kaliyeva@lancaster.ac.uk

Introduction

Cellulose and its semi-synthetic derivatives have a range of applications across industries, including construction, print, textiles/clothing, foods, veterinary, cosmetics and pharmaceuticals. Cellulose ethers and cellulose esters have diverse physicochemical and mechanical properties and are commonly used in the formulation of dosage forms and healthcare products. Carboxymethylcellulose (CMC), a cellulose ether is biodegradable, non-toxic, and has low immunogenicity.[1-3] Here we present CMC-based hydrogels employing mechanochemistry as a key processing step to induce material transformations that ensure the colloidal stability of the formulations over time.

Materials and methods

Hydrogels were produced using CMC, glycerol (to improve textural stability and hydration) and ultrasonic treatment (UST), and characterized via rheological measurements (viscosity and yield point), pH and electrical conductivity.

Results

Increasing the content of CMC from 0.5 to 5%, the electrical conductivity and viscosity increased (**Figure 1**). Addition of glycerol significantly reduces the electrical conductivity and viscosity of the hydrogels. By varying the hydrogel composition (i.e., ratio of water, CMC, and glycerol), it is possible to obtain a system with medium viscosity and high electrical conductivity, i.e., with the desired rheological properties and high activity (for this study, the optimal composition was: 2% CMC, 18% glycerol, with the remainder being water. Subsequent UST of the gels leads to a slight decrease in the pH of the systems, but a significant change in their electrical conductivity and viscosity (**Figure 1**). It should also be noted that the viscosity values of the system have stabilized with a fairly significant range of glycerol content, while reducing glycerol to 10% leads to an increase in the electrical conductivity of the hydrogel system.

Discussion

Varying the composition of the hydrogels and their exposure to UST results in qualitative changes of the resulting

materials that can be directionally regulated. These changes are largely attributed to shock waves generated by bubble rebound, which accelerate suspended solid particles in the liquid, leading to changes in particle size distribution, morphology, and surface composition.[4] UST is an effective regulator of the viscosity of the hydrogels system, which is clearly shown in the graphical dependence of the viscosity on the content of CMC (from 0.1 to 5%) and subsequent exposure to UST (**Figure 1**), suggesting that UST is an effective tool to control cosmetic and pharmaceutical formulations.

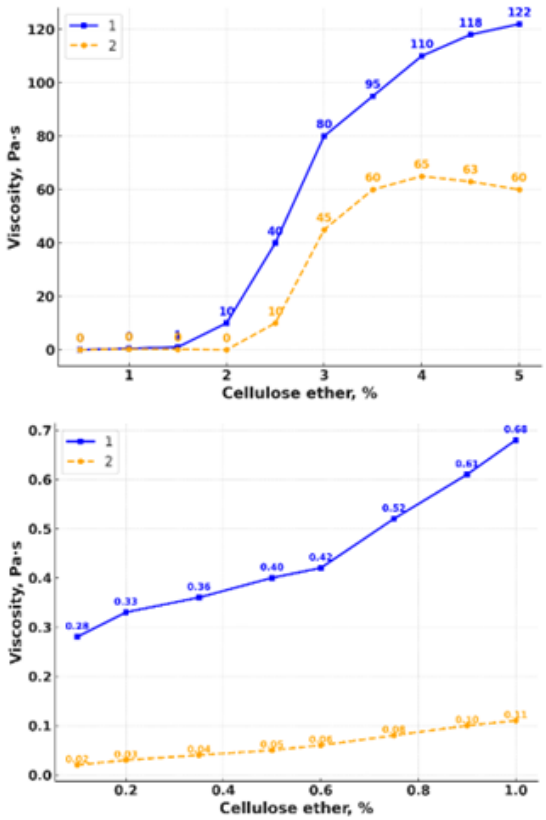

Figure 1. Change in the viscosity of the hydrogel system from the content of CMC in water (a) and water-glycerol (b) solutions before (1) and after UST (2).

Acknowledgements

financial support we thank the JSC "Center for the International Programs BOLASHAK", Ministry of Science and the Higher Education of the Republic of Kazakhstan.

References

1) H. Seddiqi et al *Cellulose,* 2021, **28**, 1893–1931.
2) I. Bravo, et al, *The Royal Society of Chemistry*, 2020, **10**, 7967–7975.
3) M.C. Cabua, et al, *ACS Applied Polymer Materials*, 2024, **6**, 6926–6936.
4) Kenneth S. Suslick. *The Royal Society of Chemistry*, Faraday Discuss., 2014, 170, 411–422.

Layer-by-layer antimicrobial electrospun polymeric dressings incorporating cellulose nanocrystals for diabetic foot ulcers

Khacharat, L. [a, *], Ramage, G. [b], and Lalatsa, A. [a]

[a] Strathclyde Institute of Pharmacy and Biomedical Sciences, University of Strathclyde, UK

[b] Health and Life Sciences, Glasgow Caledonian University, UK

* e-mail: lalita.khacharat@strath.ac.uk

Introduction

A third of the 500 million diabetics worldwide experience a Diabetic Foot Ulcer (DFU) at some point in their lives[1]. Seventy percent of DFU remain unhealed after 20 weeks of treatment, and 60% of them become infected, and of these, 20% end in different levels of amputation. Mortality rates following DFU range from 13.1% at one year to 76.9% at ten years, with cardiovascular disease and infection being leading causes of death. Treatment focuses on local wound care with surgical debridement, dressings promoting a moist wound environment, wound off-loading, vascular assessment, treatment of active infection, and glycaemic control and cost remains substantial ($25,000 per patient)[2]. Here, we aim to create a layer-by-layer antimicrobial dressing (antibacterial and antifungal) prepared by pharmaceutical-grade polymers and cellulose nanocrystals (CNC) capable of sustaining the release of the active antimicrobials for a period of 3-7 days and promote DFU healing.

Materials and methods

CNC were synthesized by sulfuric acid hydrolysis (45% v/v, 50 °C, 60 min)[3] of Western Hemlock cellulose (Cosmo 93-10, Cosmo Speciality Fibers Inc.). Gravimetric analysis of dried samples (60°C, 24h) was followed by FTIR and TEM. Crystallinity index of CNC was determined utilizing the Segal method[4]. Mixtures of PCL-PVAc-PEG (57:30:13 w/w, 90-140 kDa, BASF, Germany) and/or CNC (SM and SCNC) with tetracycline hydrochloride (T, ≥95%, Sigma Aldrich) or amphotericin B (AmB, ≥95%, China Pharmaceutical Huasheng Company) were subjected to electrospinning using the EF050 kit (20G needle, flow rate: 4.8 mL/h, distance from aluminium foil covered collection plate: 11.50 cm) (Leonardino Srl.) The antimicrobial activity was performed according to DIN EN ISO 20645 and antibiofilm activity was assessed using *Staphylococcus aureus* (ATCC 25923) and *Candida albicans* SC5314 (ATCC MYA-2876). Franz diffusion cell was used to evaluate the release of T or AmB. Cytotoxicity studies using HS27 Fibroblasts

(94041901, Public Health England) for dressings were also undertaken.

Results

CNC FTIR spectra (Figure 1A) exhibit distinct peaks at 896 cm^{-1} (v C-O-C, β-glycosidic linkage of cellulose), as well as asymmetrical S=O vibrations linked to the C-O-SO_3 group at 822 cm^{-1}. The distinctive XRD peaks of CNC were observed at 2θ values of 14.9°, 16.2°, and 22.8° (Figure 1B) and the calculated crystallinity index was 87.17. PCL-PVAc-PEG CNC (SCNC) dressings demonstrated an enhanced tensile strength [647.09 ± 95.76 g] compared to dressings without CNC [493.62 ± 203.80 g]. Dressings exhibited a cumulative drug release of 7.29% within the first 5 minutes (Figure 1C), and no significant cytotoxicity on fibroblast cells was observed at 5 µg/mL of dressings. Tetracycline (2%) and AmB (1%) loaded SCNC dressings exhibited significant antibiofilm efficacy, reducing biofilm biomass by approximately 80% and exhibiting significant inhibition zones against polymicrobial (*S. aureus* and *C. albicans*), measuring 34.33 ± 3.06 mm (Figure 1D).

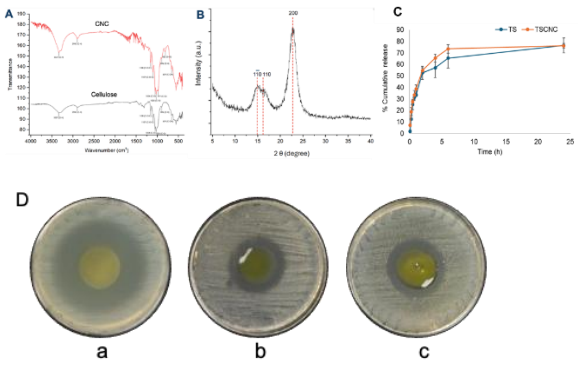

Figure 1. A: FTIR spectra (Cellulose, CNC), B: CNC XRD pattern, C: %cumulative drug release, and D: antimicrobial activity in *S. aureus* (a), *C. albicans* (b) and polymicrobial (c).

Discussion

Successful incorporation of CNC into PCL-PVAc-PEG dressings with improved mechanical strength. Antimicrobial layer-by-layer dressings provide enhanced efficacy against polymicrobial infection.

Acknowledgements

For financial support, we thank the Royal Thai Government Scholarship and KAPI.

References

4) D.G. Armstrong, A.J. Boulton, and S.A. Bus, *New England Journal of Medicine,* 2017, **376,** page. 2367-2375.

5) R. José Antonio, S. Jiménez, and J. L. Lázaro-Martínez. *Journal of Clinical Medicine,* 2020, **9**, page. 3009.

6) D. T. de Farias, J. Labidi and C. Pedrazzi, *Polymers,* 2024, 16, page. 3371

7) B. P. Rocky and A. J. Thompson, *The Journal of the Textile Institute,* 2021, **112**, page. 1295.

Controlling Transport of Colloidal Particles in Complex Fluids in Microfluidic Devices

Lad, N.[a], Singh, N.[a,*]

[a] School of Engineering, Lancaster University, Lancaster, LA1 4YW, United Kingdom.

* n.singh1@lancaster.ac.uk

Introduction

Recent developments in microfluidics and soft matter science have opened up new opportunities for the control of microparticles in complex fluidic environments. Complex fluids, such as polymer solutions and emulsions, exhibit distinctive rheological behaviours and interfacial effects that can significantly influence particle dynamics, presenting both challenges and opportunities beyond those seen in Newtonian fluids.[1,2] We aim to explore strategies for manipulating microparticles within non-Newtonian and multiphase fluids using microfluidic devices. Initial designs of microchannels fabricated using lithographic techniques integrate specific geometrical features to guide flow and promote particle localisation. Our focus is on harnessing phenomena such as viscoelasticity and interfacial tension gradients to achieve functionalities including particle focusing, separation, and trapping under continuous flow conditions. This investigation into particle manipulation in complex fluids expands the functional scope of lab-on-a-chip systems, offering promising avenues for applications in cell sorting, diagnostics, targeted delivery, and the study of biological and synthetic complex fluids.[3]

References

1) H. Lim, J. Nam and S. Shin, Microfluid Nanofluidics, 2014, 17, 683–692.

2) S. Saad and G. Natale, Soft Matter, 2019, 15, 9909–9919.

3) F. Tian, L. Cai, J. Chang, S. Li, C. Liu, T. Li and J. Sun, Lab Chip, 2018, 18, 3436–3445.

Supramolecular hydrogels for ambient storage and delivery of biological therapeutics

Marshall, L.J. [a,*], Gibson, M.I. [b], Adams, D.J.-[a,*]

[a] University of Glasgow, United Kingdom.

[b] University of Manchester, United Kingdom.

* libby.marshall@glasgow.ac.uk; dave.adams@glasgow.ac.uk

Introduction

As biological therapeutics become increasingly common, the challenge becomes finding energy-efficient ways of storing and transporting these products without compromising their activity. Such medicines generally rely on lyophilisation or and the cold chain to prevent loss of activity during distribution.[1] These requirements greatly increase the cost and reduce the accessibility of these medicines, particularly in countries with hot climates that may not have the infrastructure required for cold chain. To combat this, we have developed a supramolecular hydrogel that traps biological molecules within the gel network, preventing diffusion.[2] This delivers multiple benefits by preventing aggregation, a common mode of deactivation and immunogenicity,[3] and providing thermal protection, while maintaining the protein in a hydrated state.

The gels can be formed directly in a syringe. When the protein is ready to be used, the sample is extruded through a filter. The filter catches the extended supramolecular gel network, allowing the protein to pass through in a pure form (**Figure 1**).

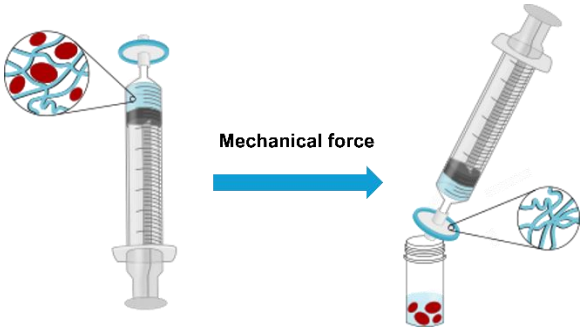

Figure 1. Schematic showing how gel formation in a syringe allows storage and release of pure therapeutic.

Supramolecular gelators are well suited for this application as they are synthetically pure and can be designed at the molecular level to have specific properties.

Materials and methods

All materials were purchased from Sigma Aldrich or Fisher and used as received. Gelators were synthesised as previously reported.[2] Rheological measurements were performed using an Anton Paar Physica MCR301 rheometer. A cup and vane (ST10-4V-8.8/97.5-SN42404) system was used for all measurements, with a measuring gap of 1.35 mm. Gels were prepared directly in

7 mL Sterilin vials, which were loaded on to the rheometer and measured *in situ* to ensure that no damage was carried out to the gels by transfer from vials. Rheological measurements investigating the effect of temperature on gel properties were recorded at a constant strain of 0.1% and a constant frequency of 10 s^{-1}.

Results

We have been investigating two structurally similar gelators: I and V. Both gelators maintain the gel state at elevated temperatures. Gelator I maintains the same mechanical properties up to ~35 °C where the network gradually loses stiffness whilst maintaining elasticity as temperature increases, before completely breaking at around 57 °C (**Figure 2 – black data**). The mechanical properties of gelator V fluctuate with increasing temperature but maintain the gel state at temperatures greater than 60 °C (**Figure 2 – blue data**). This exemplifies the potential of these gelators to protect therapeutics in temperature conditions likely to be experienced during global distribution.

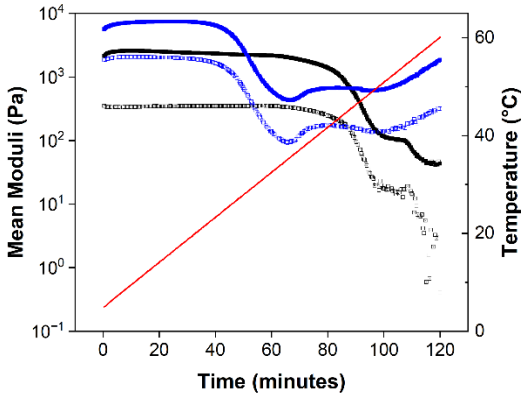

Figure 2. Rheological properties of gelators I (black) and V (blue) measured as the temperature was ramped from 5 °C to 60 °C.

Acknowledgements

This work was funded by Scottish Enterprise and the MedTech Innovation fund from the University of Glasgow. I would also like to acknowledge Dr Simona Bianco for her work pioneering this project and her input throughout.

References

1) Muralidhara, B.K. and Wong, M., *Drug Discovery Today*, 2020, **25**, 574-581.
2) Bianco, S., et al. Nature, 2024, **631**, 544-548.
3) Pham, N.B. and Meng, W.S., *International Journal of Pharmaceutics,* 2020, **585**, 119523.

Plasma CTHRC1: A Quantitative Correlate of Kidney Function Metrics.

Myngbay, A. [a]*

[a] NJSC "K.Zhubanov Aktobe regional university", Kazakhstan.

* Corresponding author(s) e-mail(s): askhat.myngbay@zhubanov.edu.kz

Introduction

Chronic kidney disease (CKD) is a multifactorial condition with diverse etiologies, complicating a complete understanding of its pathophysiology [1,2]. Hallmark features include elevated plasma creatinine, proteinuria, albuminuria, and reduced estimated glomerular filtration rate (eGFR) [3,4]. This study explores the potential of collagen triple helix repeat containing 1 (CTHRC1) as a novel plasma biomarker for CKD, complementing established indicators of disease progression [5,6].

Materials and methods

A prospective observational validation study was conducted with 26 chronic kidney disease (CKD) patients (stages 1–3) recruited from a hospital and 18 healthy volunteers from outpatient clinics. Participants were aged 18–65, clinically stable, and free from malignancies, autoimmune, cardiovascular, neuropsychiatric, or inflammatory diseases. CKD diagnosis was based on proteinuria levels (>300 mg/24h) and estimated glomerular filtration rate (eGFR) calculated by the CKD-EPI equation. Patients with severe CKD (GFR <15), pregnancy, diabetes, cancer, infections, or other inflammatory/autoimmune diseases were excluded.

Results

Median proteinuria was significantly higher in CKD patients compared to controls. CKD patients had significantly lower mean eGFR and higher creatinine levels. Significant differences were found in white blood cells (WBCs), particularly neutrophils and monocytes, as well as blood lipid levels between CKD and controls. ELISA tests showed no significant differences in TNF alpha, MMP2, and MMP9, but CTHRC1 levels were significantly elevated in CKD (Figure 1.).

Relationship between CTHRC1 and CKD Indicators

CTHRC1 plasma levels positively correlated with key kidney function markers and negatively correlated with eGFR. CTHRC1 showed stronger significance in differentiating CKD from controls than urea, eGFR, or creatinine. Similar correlations were observed when combining CKD and control groups, confirming CTHRC1's

association with kidney function markers. ROC curve analysis comparing patients with eGFR below and above 60 mL/min/1.73 m² showed that CTHRC1 has similar diagnostic accuracy (AUC) to traditional clinical markers (creatinine, urea, etc.) for identifying reduced kidney function.

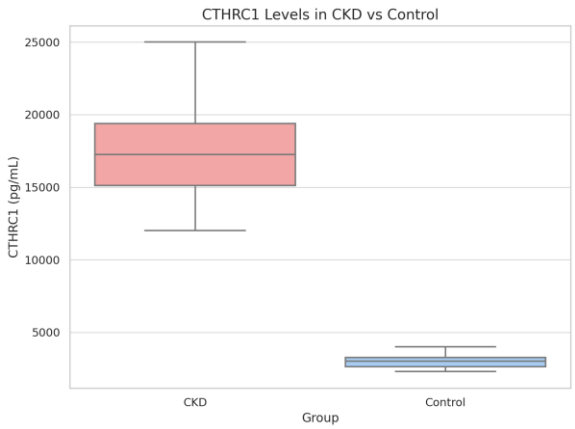

Figure 1. Bar plot comparing plasma CTHRC1 levels between CKD patients and healthy controls. It reflects the strong and statistically significant elevation of CTHRC1 in the CKD group ($p \leq 0.0001$).

Discussion

This pilot cross-sectional study investigates the role of CTHRC1, a protein previously linked to fibroblast migration and rheumatoid arthritis, as a potential blood-based biomarker for chronic kidney disease (CKD). Biologically, CTHRC1 interacts with TGFβ and Wnt signaling pathways involved in renal fibrosis and inflammation, suggesting a role in CKD pathogenesis [5].

Despite limitations due to sample size and study design, these findings highlight CTHRC1 as a sensitive and affordable marker for CKD, warranting further research to elucidate its functional role and validate its clinical application.

Acknowledgements

The study was funded by the Ministry of Science and Higher Education of the Republic of Kazakhstan grant AP26198667 for A.M.

References

1. Levey AS, Coresh J. *Lancet*. **2012**;379(9811):165-180.
2. Webster AC, Nagler EV, Morton RL, Masson P. *Lancet*. **2017**;389(10075):1238-1252.
3. Stevens PE, Levin A. *Ann Intern Med.* **2013**;158(11):825-830.
4. Inker LA, Astor BC, Fox CH, et al. *Am J Kidney Dis.* **2014**;63(5):713-735.
5. Tang L, et al. *Front Med.* **2021**;8:683936.
6. Baiken Y, et al. Elevated Levels of *Medicina.* **2023**; 59(4):651.

Supramolecular hydrogels with tunable stiffness to model 3D in vitro microenvironment of pancreatic cancer

Okesola, B. O.[1 *], Liu, Y.[2], Mata, A[3], Pearce O. M. [2,]

[1]School of Life Sciences, University of Nottingham, Nottingham, Nottingham, UK

[2]Barts Cancer Institute, Queen Mary University of London, London, UK

[3]School of Pharmacy, University of Nottingham, Nottingham, UK

* Corresponding author(s) e-mail(s): Babatunde.okesola@nottingham.ac.uk

Introduction

Pancreatic ductal adenocarcinoma (PDAC) is a highly aggressive and most deadly type of pancreatic cancers with 5-year survival rate less than 10%[1]. The microenvironment of PDAC is characterized with a dense and stiff network of nanofibers composed of molecular building blocks such as the extracellular proteins. This highly stiff environment drives tumour invasiveness, metastasis and drug resistance[2,3]. Ability to recreate PDAC 3D microenvironment will help us to identify key pathological pathways promoting PDAC progression and resistance to chemotherapy.

Self-assembling hydrogels are attractive class of hydrogels to recapitulate the nanoscale architecture, dynamic and mechanical properties of the native tumour microenvironments owing to their nanofibrillar structures and supramolecular nature. Considering these unique features of self-assembling hydrogels, we developed 3D self-assembling hydrogels with tuneable stiffness and nanofibrillar structure to model the tumour microenvironment in PDAC patients.

Results and Discussion

We designed a new peptide amphiphiles (PA-E3Y; $C_{15}H_{31}CO$-V3A3E3Y-amide) (**Figure 1A**). Then, we created hydrogels of PA-E3Y using divalent metal ions after an initial thermal annealing of the aqueous solutions. Using electron microscopy, we confirmed that the hydrogels are composed of sample-spanning nanofibers reminiscent of the native tumour microenvironment. By tuning the concentrations of the gelation trigger (calcium chloride), we created hydrogels with stiffness ranging from 1 – 90 kPa[4].

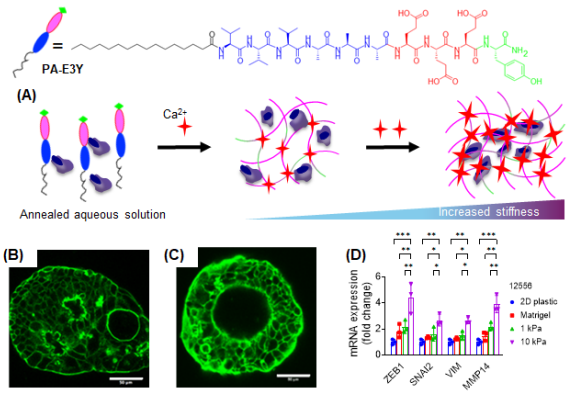

***Figure 18**. Schematic of PDAC cells encapsulated in PA-E3Y hydrogel nanofibers network with tuneable stiffness (**A**). Stiffness was tuned using low and high concentration of calcium ions. The PDAC cells self-organised into tumour ductal-like morphology in the stiff hydrogels (**C**) than in the soft hydrogels (**B**). Also, tumorigenic genes are more upregulated in the stiff hydrogels than soft hydrogels, Matrigel and on tissue culture plastics (**D**).*

This broad range of stiffness also spans the stiffness of soft (2.2 kPa), and stiff (10.5 kPa) tissues obtained from PDAC patients. We used flow cytometry to show that PDAC cells encapsulated in both soft and stiff PAs hydrogels maintained high viability (> 90%) and proliferation after 14 days in culture, which is comparable to results obtained in the gold standard Matrigel and a tissue culture plastic. PDAC cells encapsulated within the stiff (10 kPa) PA-E3Y hydrogels expressed high level of ECM (COL1A1 and FN1) and epithelial-mesenchymal transition (ZEB1, SNAI2, VIM, MMP14) related genes and proteins. These tumorigenic behaviours were not significantly expressed by PDAC cells encapsulated in soft (1 kPa) PA-E3Y hydrogels, Matrigel or TCP (**Figure 1B, C,D**). In addition, PDAC cells displayed an aggressive phenotype and high resistance to Gemcitabine and Abraxane in the stiff PA-E3Y hydrogels. The findings reveal how a stiff 3D environment renders PDAC cells more aggressive and therefore more faithfully recapitulates in vivo tumours.

Conclusion

We developed peptide amphiphiles based hydrogels with tunable stiffness to model PDAC 3D microenvironment. This hydrogel system enables us to investigate the effects of matrix stiffness on cancer cells behaviours. The wider range of hydrogel stiffness offered by PA-E3Y opens potential avenues of research in mechanobiology, such as examining the influence of matrix stiffness on stem cell expansion, organoid formation and its impact on adipogenesis in MSCs.

Acknowledgements

For financial support we thank the University of Nottingham for the Award of Nottingham Research Fellowship and Royal Society.

References

[1] V. Tonini, M. Zanni, *World J. Gastroenterol*. 2021, 27, 5851. [2] T. Brabletz, R. Kalluri, M. A. Nieto, R. A. Weinberg, *Nat. Rev. Cancer*. 2018, 18, 128. [3] L. Fattet, H. Y. Jung, M. W. Matsumoto, B. E. Aubol, A. Kumar, J. A. Adams, A. C. Chen, R. L. Sah, A. J. Engler, E. B. Pasquale, J. Yang, *Dev. Cell* 2020, 54, 302. [4] Y. Liu, B. O. Okesola, et al. *Adv. Healthcare Mater*. 2024, 2301941.

ELECTRICALLY CONDUCTIVE BIOMATERIALS FOR THE PRESERVATION AND REGENERATION OF SOFT TISSUE.

Leah Pomfret. [a,b,c,d], Hardy, J.G.[a,b,*] Mort, R.M.[c,*] Cheneler, D.[b,c,*]

[a] Department of Chemistry, Lancaster University, Lancaster, LA1 4YB, UK.

[b] Materials Science Lancaster, Lancaster University, Lancaster, LA1 4YB, UK.

[c] Division of Biomedical and Life Sciences, Lancaster University, Lancaster, LA1 4YQ, UK.

[d] Department of Engineering, Lancaster University, Lancaster, LA1 4YW, UK.

* Corresponding author(s) e-mail(s): l.pomfret@lancaster.ac.uk; j.g.hardy@lancaster.ac.uk; r.mort@lancaster.ac.uk; d.cheneler@lancaster.ac.uk

Introduction

Combat trauma results in severe, complex injuries involving multiple tissue types. There is growing evidence that an electrical stimulus applied to a wound can enhance tissue regeneration. Therefore, in early wound management it is important to optimise endogenous responses including the bioelectric current.

Materials and methods

In order to fabricate electroactive wound dressings, we have incorporated a network of the conductive polymer polypyrrole (Ppy) into non-biodegradable wound care products. We are also developing electrically controlled delivery methods using conductive polymers incorporated in the wound dressings for therapeutic use that enhance tissue preservation. In parallel we are investigating the migratory and proliferative properties of skin cell types and their response to electrical stimulation.

Results

Comparison of pristine wound dressings to Ppy coated wound dressing shows that foam, alginate and aquafiber based dressings are electrically conductive. Preliminary data shows that drug can be electrochemically loaded into the wound dressings and released upon electrical stimulation. We have also developed an electrical stimulation paradigm by performing wound healing experiments on indium tin oxide coated glass and applying an electrical stimulus. Fibroblasts demonstrate enhanced wound healing at 50mV/mm DC electrical stimulation.

Discussion

The conductive wound dressings will allow direct electrical stimulation of the wound to achieve pro-regenerative activity. Combined with a drug delivery system, this will allow localised drug release to the wound to stimulate wound healing. The wound

dressings will also provide a direct electrical stimulation to the wound. Overall, we aim to aid the healing of complex wounds by enhancing the endogenous regenerative response of cells in the skin and therefore decrease the recovery period.

Acknowledgements

For financial support we thank the ERSRC and Dstl.

Towards a Cost-Effective Simplified Mechanical Fuse: A Feasibility Study

Pope, V.J*[a], Manna, S.K.[a], Hassanin, H.[a], Rathnayake, G.[a], Wilshaw, M. A.[b]

[a]School of Engineering Technology and Design, Canterbury Christ Church University, United Kingdom

[b]eXroid, Sandwich, Kent, United Kingdom

* Corresponding author(s) e-mail(s): vp406@canterbury.ac.uk & soumyakanti.manna@canterbury.ac.uk

Introduction

Conventional fuses rely on electrical and thermal overload to function, however, there is a gap in the market for a single-use mechanical fuse [1, 2] that fails under controlled shear force and is easy to actuate. This type of fuse can be used in switching circuits for braking systems. In this abstract, the mechanical formation of the fuse is explored along with a comparative analysis of structural material supported by finite element analysis (FEA). Physical testing of the fuse is evaluated using a custom rig breakage force, notch design, and actuator geometry. Results confirm the fuse's viability for applications requiring electrical safety and anti-tampering.

Materials and methods

This project explores a mechanical fuse made from a conductive copper or aluminium core embedded in brittle epoxy resin to provide safer, more predictable operation, particularly in low-powered systems. The fuse is designed to break via a push-button mechanism, interrupting current flow and requiring replacement. Mechanical fuse samples were manufactured using custom silicone moulds. The core material, composed of either copper or aluminium, has a diameter of 0.03 mm, and is encased in a supporting layer with a thickness of 0.10 mm (Fig. 1). The copper wire was placed centrally within the mould, which is filled with epoxy resin using a syringe. A vacuum chamber was used to remove air bubbles, although later batches were produced without the vacuum due to negligible differences in sample quality.

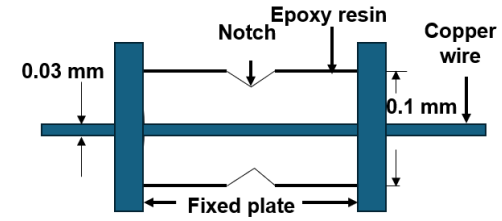

Figure 1. Fuse structure.

Results and Discussion

Finite Element Analysis (FEA) is used to carry out a comparative analysis for different combinations of core and outer materials. Copper and aluminium are analysed in combination with epoxy resin, acrylic, and glass. The sample shown here includes copper embedded in epoxy resin due to its conductive properties and ability to undergo brittle failure under shear force.

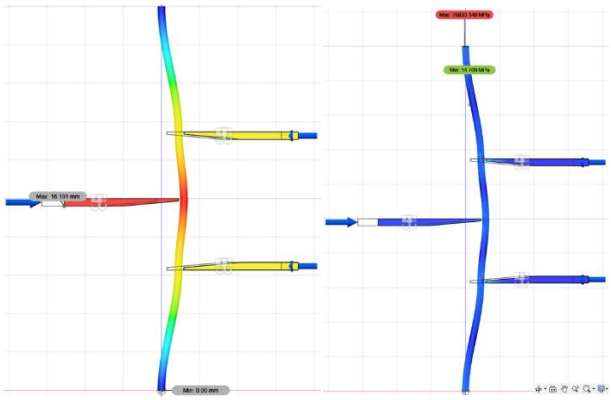

Figure 2. FEA analysis

The FEA analysis (Fig. 2) indicates that it will break under the force of 5N. The displacement is 16.191mm, which is considerable, however limited by the pins and backing, creating more force, and allowing the wire to break with a smaller displacement. The maximum stress on the design is 7.68x10^5 MPa.

A Mechanical test rig (Fig. 3) is designed to apply compressive shear force to break. A range of notch types (including surface slice, ¾ slice, and V-shape) were tested to assess their effect on failure to determine the most effective design for consistent breakage. Conductivity testing confirmed the suitability of the copper-resin combination for current flow prior to mechanical failure.

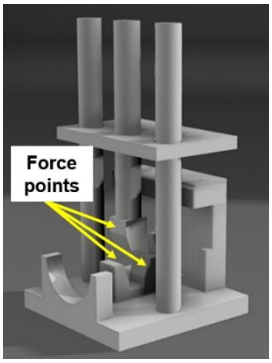

Figure 3. Mechanical Test-rig

Testing proved that copper-resin mechanical fuses consistently failed under the least shear force, with the V-shaped notch design, showing reliable, single-use failure with minimal design complexity. Copper provided reliable conductivity before breakage. The findings demonstrate that integrating a pushbutton with a mechanical fuse can provide electrical functionality alongside mechanical failure, presenting a viable solution for low-voltage safety and single-use mechanical protection applications.

Acknowledgements

This research was funded by Accelerated KTP 2023-24 under Innovate UK.

References

1) Pimenta, A.R. et al, 2020. Journal of Failure Analysis and Prevention, 20, pp.370-375.
2) Leal-Junior, A.G. et al, 2022. Advanced Photonics Research, 3(6), p.2100210.

Tailored Antimicrobial 3D Printed Implants for Periprosthetic Joint Infections.

Bianca I. Ramirez [a], Iván Yuste [a], Francis C. Luciano [a], Carmina Rodríguez [a], Chrysi Rapti [a], Brayan J. Anaya [a], Aikaterini Lalatsa [b], Almudena Ribed-Sánchez [c], Pablo Sanz-Ruiz [c], Elena González-Burgos [a*], Dolores R. Serrano [a*]

[a] Faculty of Pharmacy, Universidad Complutense de Madrid, Plaza Ramón y Cajal s/n, 28040 Madrid, Spain.

[b] School of Pharmacy and Biomedical Sciences, Robertson Wing, University of Strathclyde, 161, Cathedral Street, Glasgow, G4 0RE, Scotland, UK.

[c] Hospital General Universitario, Gregorio Marañón, Doctor Esquerdo 46, 28029, Madrid, Spain.

* Corresponding author(s) e-mail(s): Elena González-Burgos, Email: elenagon@ucm.es
Dolores R. Serrano, Email: drserran@ucm.es
Underlined author name denotes this is the presenter.

Introduction

Periprosthetic joint infections (PJIs) after hip and knee replacements are a serious complication, with current treatments—such as antibiotic-loaded bone cement—facing limitations in drug release and potential mechanical weakening of the implant. This study proposes a personalized 3D-printed implant, externally attached to the prosthesis, designed to deliver amphotericin B (AmB) and vancomycin (VAN) locally in a controlled manner during the critical first 48 hours after surgery to prevent and treat PJIs.

Materials and methods

All other chemicals and solvents were at least of ACS reagent grade and were used without further purification. Spider web-shaped implants were designed to fit the acetabular surface and printed using fused deposition modeling (FDM) with a biocompatible PVA-PEG filament. Drugs were loaded by passive diffusion, optimized via factorial design. Mechanical properties, adhesion strength, UV sterilization, drug loading and release kinetics, hemolytic toxicity, and antimicrobial activity against Candida spp. and Staphylococcus spp. were evaluated in vitro.

Results

The 3D-printed implants were successfully fabricated using fused deposition modeling followed by passive diffusion for drug loading and designed to fit the acetabular component of hip prostheses (fig 1). This achieved a maximum AmB loading of 0.2% and vancomycin (VAN) loading of 0.4%.

Mechanical Testing showed that dry, unloaded implants had the highest hardness. However, once wetted, implants—both loaded and unloaded—exhibited significantly improved adhesiveness. Manual adhesion tests revealed that 60 seconds of wetting were sufficient for strong and reliable adhesion to the acetabular surface.

Drug Loading Kinetics followed different patterns: VAN showed a linear uptake rate (1.1 mg/h), reaching a plateau at 4 hours. In contrast, AmB displayed biphasic kinetics, with slower initial uptake followed by accelerated loading after 3 hours, peaking at 5 hours. Drug Release Profiles showed that VAN was rapidly released (within 1 hour), consistent with its hydrophilicity and surface localization. AmB exhibited a sustained release over 10 hours, followed by a plateau, with saturation levels maintained for up to 48 hours due to its high albumin binding.

Hemolysis Assays showed that AmB-loaded implants had significantly lower red blood cell toxicity (5-fold higher HC50) compared to free AmB. VAN-loaded implants also showed acceptable hemocompatibility.

UV Sterilization of the implants did not significantly reduce the drug content ($p > 0.05$), and no microbial growth was observed after 48 hours of incubation, confirming effective sterilization.

Antimicrobial Efficacy was confirmed via agar diffusion assays. VAN-loaded implants produced inhibition zones ≥15 mm against Staphylococcus aureus and S. epidermidis, comparable to commercial VAN discs. AmB-loaded implants showed robust antifungal activity against Candida albicans, C. parapsilosis, and C. glabrata, with reduced activity against C. krusei.

Minimum Inhibitory and Fungicidal/Bactericidal Concentrations (MIC/MFC/MBC) indicated that the implants were effective at concentrations similar to those of the free drugs. A synergistic effect was observed in AmB+VAN implants, especially against S. aureus, where MIC values decreased (2-fold).

Discussion

The proposed 3D-printed implants provide a novel and personalized solution to PJIs, addressing the drawbacks of conventional antibiotic-loaded cements. The design ensures rapid intraoperative placement, strong adhesion, high biocompatibility, and effective antimicrobial delivery. Despite limited drug loading, it was sufficient for therapeutic activity. Further in vivo validation is needed to confirm their clinical potential, but the approach shows strong promise for improving early PJI management.

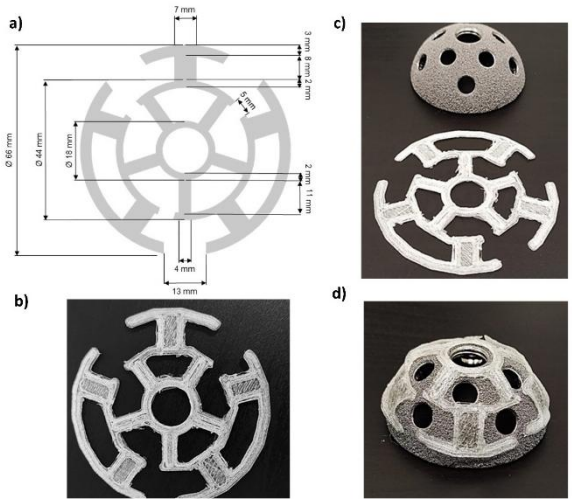

Figure 1. 3D printed implant adapted to the acetabular component morphology. Key: (a) Design and dimensions of the implant, (b) 3D printed implant; c**)** Dimensions of 3DP implant and acetabular component, and (d) 3DP implant adhered onto the surface of the cup.

Acknowledgements

This study has been funded by the Ministry of Science and Innovation – agencia estatal de investigación (award pid2021-126310oa-i00) to Dolores Serrano. Bianca I. Ramirez acknowledges Ministry of Sience and Innovation for the PDI fellowship.

References

1. OECD, Hip and knee replacement, in Health at a Glance 2017: OECD Indicators. 2017, OECD Publishing: Paris. p. 178 - 179.

2. Klug, A., et al., Knee Surg Sports Traumatol Arthrosc, 2021. 29(10): p. 3287-3298.

3. Yuste, I., et al. Antibiotics (Basel), 2023. 12(8).

4. Chen, I.C., et al. Polymers (Basel), 2021. 13(14).

5. Kweon, C., et al., Amphotericin B. Clin Orthop Relat Res, 2011. 469(11): p. 3002.

United Kingdom Society for Biomaterials Annual Conference 2025

BIOINK WITH TUNABLE STIFFNESS: TO INVESTIGATE THE ROLE OF VISCOELASTICITY FOR CELL CULTURE AND PROLIFERATION IN 3D BIO-PRINTED MODEL

Rit, T.[1,2], Das, A. K.[1*], Kalaskar, D. [2*]
[1] Department of Chemistry, Indian Institute of Technology Indore, India, [2] Division of Surgery and Interventional Sciences, University College London, UK

* Corresponding author(s) e-mail(s): apurba.das@iiti.ac.in, d.kalaskar@ucl.ac.uk

Introduction

In recent years, 3D bioprinting has been recognized as an emerging technology in developing in vitro 3D tissue and organ models. There are several reports on the development of bioinks, however most of them are unable to provide the physical and biochemical properties of extracellular environments. To fabricate a bioink with printability of high shape-fidelity with minimum material content and high cell viability is very challenging. 1-2 Moreover, the correlation between viscoelasticity of bioink and cell proliferation in 3D model is an interesting area. 3-4 Here, we aim to investigate the growth of cells inside a hydrogel-based bioink in a 3D-bioprinted model and to check the influence of viscoelastic properties of the hydrogel matrix towards cell proliferation.

Materials and methods

We have developed bioink by mixing Biomatrix® and sodium alginate in different equivalents (1:1, 1:0.75, 1:0.5 and 1:0.25) in PBS (pH 7.4). Composition of both the materials was optimized to get stable and injectable hydrogel. Furthermore, Bio X printer has been utilized to check the printability of bioink and to print various scaffolds. These printed scaffolds have been incubated with various concentrations of calcium chloride solutions to enhance stability by external chemical cross-linking. The long-term stability test of all the scaffolds was performed. To investigate the morphology and mechanical properties of hydrogel FESEM, AFM and rheology experiments were performed respectively. Furthermore, chemical and physical cross-linking in the bioink was investigated by FT-IR spectroscopy and XPS analysis.

Results

To develop 3D bio printed tissue or organ models, most importantly the bioink should be stable for a few weeks to perform various experiments. Hence, we checked the stability of the printed scaffolds in cell culture media, and it indicated that the scaffolds with 1:1 composition are stable till 28 days and other compositions are stable in between 3 to 21 days. The rheological experiments like amplitude sweep, frequency sweep and shear-

thinning tests support the viscoelastic property of the hydrogel. The range of stiffness of bioink is 1 to 10 kPa. It is noteworthy to mention that different compositions of Biomatrix® and alginate give rise to hydrogel formation with different viscoelastic properties, and their stability varies with the mechanical strength. The FESEM and AFM images of xerogel show the porous nature of bioink which could provide the ideal environment for cells to absorb nutrients from culture media. To check cell viability and cell proliferation inside the hydrogel matrix, cells were suspended into bioink and printed the desired scaffolds. The live dead staining was performed to confirm the cell proliferation on day 1, 3, 7, 14, 21 and 28. The live dead images indicate cell survival and proliferation inside the scaffold.

Discussion

Overall, all the experimental data suggest that the efficiency of bioink for 3D cell culture and its versatility in mechanical stiffness supports our hypothesis. Along with the normal cell we expect that dynamic viscoelastic bioink could mimic the stiffness of cancer tissue and help us in better understanding the role of tissue stiffness in cancer progression and malignancy in future study.

Acknowledgements

The authors would like to acknowledge Prime Minister Research Fellowship, India and Commonwealth Split-site Scholarship (Commonwealth Scholarship Commission), UK for funding. Additionally, the authors would like to thank Department of Chemistry, SIC, IIT Indore, India and Division of Surgery and Interventional Sciences, University College London and the Royal Free Hospital NHS Trust, UK for the instrument facility.

References

1. H. Arslan et al. ACS Appl. Bio Mater. 2024, 7, 7040−7050.
2. R. Sharma et al. Gels, 2023, 9, 430.
3. T. Yuan et al. Trends in Biotechnology, 2024, 42, 11.
4. M. Lin et al. ACS Biomater. Sci. Eng. 2023, 9, 3116−3133.

United Kingdom Society for Biomaterials Annual Conference 2025

Health Interventions at the Edge

Austin, H. [a], Richardson, A. [b,*], Gaffney, C. [c,*], Hardy, J. [d,*], Cheneler, D. [b,*], Rust, S. [b,d]

[a] Ultra PCS, Arle Court, Hatherley Ln, Cheltenham GL51 6PN.

[b] School of Engineering, Lancaster University, Lancaster, LA1 4YW

[c] Lancaster Medical School, Health Innovation One, Lancaster University, LA1 4AT

[d] Department of Chemistry, Lancaster University, Lancaster, LA1 4YB

* a.richardson@lancaster.ac.uk, c.gaffney@lancaster.ac.uk, d.cheneler@lancaster.ac.uk, j.g.hardy@lancaster.ac.uk

Introduction

Wearable devices offer instant access to vast amounts of health data; the challenge is knowing how to interpret this into actionable decisions. Often this requires medical / sports science knowledge and the number of medical staff “in the field” capable of making these actionable decisions is limited.

Ultra PCS and Lancaster University have developed an end-to-end system designed to monitor welfare and remotely deliver an intervention from a command post by a trained professional. This aids in reducing the burden on field medical staff by prioritising efforts where most needed.

Materials and methods

A prototype closed loop implementation system has been developed for proof-of-principle demonstration. The system utilises an UltraLYNX power and data hub to receive, combine and categorise data from wearable sensors at the edge. This system can communicate a priority red, amber, or green (RAG) indicator to the designated command post where a trained professional can review the data and authorise the administering of a pre-determined substance via an actuation cuff to the wearer. Physiological monitoring is conducted using a commercial heart rate monitor and a novel potassium sensor created by Lancaster University. The novel sensor comprises of a conductive polymeric membrane containing an ionophore (valinomycin) for potassium selectivity and a solid state PVB reference electrode for stability. On command, the UltraLYNX activates a pneumatic system that applies a transdermal caffeine patch (as a safe analogue to a field-appropriate intervention) to the arm of the end-user. The physiological condition of the user continues to be monitored and communicated by the UltraLYNX system, thus closing the loop.

Results

During bench-top testing, the system was verified against a series of test cases, with successful data transmission, processing and actuation. Calibration of the sensor shows a

near-Nernstian response of 63.2 mV/dec concentration to potassium chloride with a proportion of variance between concentrations of $R^2 = 0.999$. The sensor chip combined with a miniature potentiostat was successfully integrated into the existing hardware, demonstrating a stable response. Further testing, including human trials, are still ongoing.

Discussion

Alongside this work, research is being conducted into the use of hydrogels as an intervention tool, with the intention of integrating this work into the system in the future. Other intentions include integrating an additional array of sensors and exploring other prediction tools such as AI to get a more detailed overall picture of the soldier's wellbeing.[1-5] Numerous ionic species can be detected, including sodium, potassium and chlorine, making them ideal for use in sweat sensors. Furthermore, cortisol as a measure of stress, glucose and lactate as a measure of hyper/hypoglycaemia and fatigue.

Acknowledgements

For financial support we thank UltraPCS and Dstl.

References

1. Q. Al-Gayem, *et al. Journal of Electronic Testing*. **2011**, 27, 1, 57-68.
2. A. Edwards, *et al. Materials Advances.* **2021**, 2, 1600-1605.
3. N. Davison, *et al. Diabetology*. **2022**, 1, 3, 56-71.
4. S. Baldock, *et al. Advanced Materials Technologies.* **2023**, 8, 11, 2201274.
5. M. B. Sharma, *et al. Bioengineering*. **2024**, 11, 7, 649.

United Kingdom Society for Biomaterials Annual Conference 2025

WRINKLING IN THIN POLYMER FILMS FOR PATTERNING APPLICATIONS

Singh, N.[a,*]

[a] School of Engineering, Lancaster University, Lancaster, LA1 4YW, United Kingdom.

* n.singh1@lancaster.ac.uk

Abstract

Self-organized wrinkling instabilities in thin polymer films have instigated a field of versatile surface patterning and have spurred several research efforts in developing micro- and nanopatterned templates for a wide range of applications. Here, we report for the first time a distinct class of wrinkles in a thin polymer (polystyrene) film coated on a substrate under a mixture of organic solvent and aqueous nonsolvent. The solvent softens and swells the polymer and paves the way for wetting of the hydrophilic substrate by the solvent−nonsolvent mixture, leading to wrinkle formation. It is investigated that selective delamination-induced wrinkling is a generic phenomenon and takes place in various polymers as well as different combinations of solvent−nonsolvent mixtures. The surface energy of the substrate and the composition of the solvent−nonsolvent mixture play a critical role as wrinkling is not observed on substrates with lower surface energy. An isotropically distributed yet disordered self-organized wrinkle network of hollow buried channels is formed, and it is illustrated that these can be exploited to generate a mesh of microwires and harnessed to form highly directional patterns using electron beam lithography, which can turn the new leaf for nano- and microfluidic device fabrication platforms.

References

3) N. Singh, A. Sharma and M. Kulkarni, *ACS App. Pol. Mat., Title*, 2021, **3**, 6198-6206.

United Kingdom Society for Biomaterials Annual Conference 2025

Structural polymer as suspending media for lightsheet fluorescent microscopy.

Weightman, J.R.[a], White, P.C.[b], Moakes, R.J.A.[a], Robinson, T.E. [a], Mueller, F.[b] Grover, L.M.[a]

[a] Healthcare Technologies Institute, University of Birmingham, United Kingdom.

[b] Department of Cancer and Genomic Sciences, University of Birmingham, United Kingdom.

* Corresponding author(s) e-mail(s): JRW350@student.bham.ac.uk

Introduction

In recent years, the introduction of lightsheet fluorescent microscopy (LSFM) has provided an outlet to study a host of multidisciplinary areas, ranging from spatial cellular organisation to targeted cancer treatment. However, it is challenging to maintain 3D cell models long term for temporal imaging, due to the absence of suspension materials compatible with cell culture and imaging parameters[1]. In this study, we utilised gellan gum to create optically clear fluid gels and investigated whether these materials could maintain both cell viability and material support necessary for long term 4D imaging.

Materials and methods

Gellan gum formulation

Low acyl gellan gum (Kelco) was dissolved at varying (1-2) w/v% in deionised water, supplemented with 5% PBS and 10 mM NaCl, by heating to 90 degrees and mixing until dissolved. The solution was then autoclaved for 1 hour at 121°C. The hot solution was cooled to 20 degrees under agitation to form the fluid gel, then stored at 4°C until use.

Lightsheet imaging

FUCCI-expressing colorectal cancer organoids encapsulated in gellan gum were imaged using the Z1 Zeiss lightsheet using lasers at 488 and 561nm. Images were processed through imageJ.

Rheometry

Temperature sweep rheological testing was performed on Malvern Kinexus Ultra+ rheometer using parralel plate surface finish geometry. To measure the dependence of the material properties on temperature, the fluid gels were heated from 25 to 40 at 1 deg/min.

Results

Temperature sweeps on varying Gellan gum formulations remained elastically dominant under increasing temperatures. Gellan-embedded organoid models showed continuous

growth and retention of important morphological features. Additionally, gellan-embedding held organoids stable over a 2-week cell cycle study, enabling continuous imaging of the same region over time.

Discussion

Through rheological sweep testing we were able to evaluate and alter the hydrogel microstructure and its response to deformation and temperature. This opens up the potential for gellan gum to be designed to sustain a variety of investigative models. Our initial research has found that gellan gum acts as a suitable medium to support live organoid growth and imaging up to 14 days, allowing for spatiotemporal fluorescent reporter tracking. Our next steps will determine cell viability, followed by expansion into *in vivo* imaging to explore tissue development.

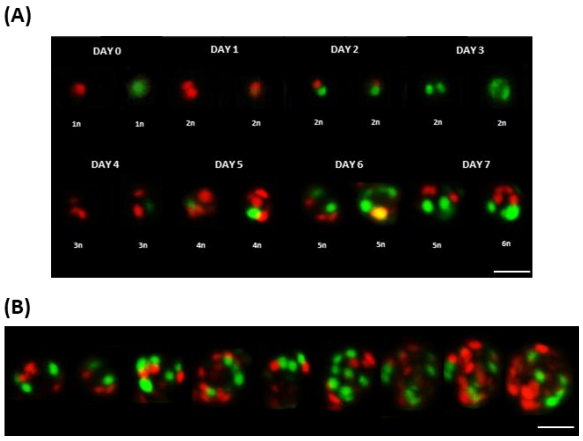

Figure 1. Cell cycle tracking of FUCCI organoid over 14 days. Fluorescent snapshots of nuclear expression of FUCCI fluorescent reporters in the same organoid over 14 days (Post seeding on day 0) using adapted long-term high-resolution imaging protocol in Zeiss Z1 lightsheet. Captured using selected lasers 488 and 561nm at 1.8 and 1.3 intensity and 219.71 millisecond (ms), scale 50μm. (A) Tracking of cell divisions using both fluorescent reporters to distinguish cycle phase and number of nuclei. Same organoid imaged every 12 hours. (B) Same organoid imaged for days 8-14 showing loss of synchronicity and resolution of individual cellular changes.

Acknowledgements

This work was supported by Science Foundation Ireland **18/EPSRC-CDT/3583** and the Engineering and Physical Sciences Research Council **EP/S02347X/1**

References

1) M. Adams, A. Loftus and J. Fitzpatrick, Curr Protoc Cytom. 2015, **1**, 71.

United Kingdom Society for Biomaterials Annual Conference 2025

Toward Deeper Insights into Brain Ageing: Modelling with Explainable Vision Transformers

Zhaonian Zhang [a], Richard Jiang [a,*], John Hardy [b*]

[a] LIRA Centre Lancaster University, Lancaster LA1 4YW, United Kingdom.

[b] Department of Chemistry, Lancaster University, Lancaster, LA1 4YB, United Kingdom.

* Corresponding author(s) e-mail(s): r.jiang2@lancaster.ac.uk

Introduction

Machine learning, particularly through advanced imaging techniques such as three-dimensional Magnetic Resonance Imaging (MRI), has significantly enhanced medical diagnostics—especially in analyzing complex conditions like brain ageing. In this study, we introduce **Triamese-ViT** [1], an innovative tri-structured Vision Transformer (ViT) architecture with built-in interpretability. Triamese-ViT offers structure-aware explainability, enabling the identification and visualization of key features or regions that contribute to its predictions. By integrating information from three complementary perspectives, it enhances the accuracy of brain age estimation while maintaining interoperability with existing methods. When evaluated, Triamese-ViT demonstrated superior performance and produced informative attention maps. These maps were applied to analyze natural ageing and sex differences, and their interpretability was further validated using the traditional explainable AI (XAI) technique of occlusion analysis.

Materials and methods

Figure 1 depicts the architecture of our model, 'Triamese-ViT'. This model processes brain MRI images from three distinct perspectives utilizing the vision transformer to extract unique features. These features are then integrated within a Multi-Layer Perceptron (MLP) framework to generate age predictions. A built-in interpretability function generates 3D-like images to explain different brain regions influence during prediction.

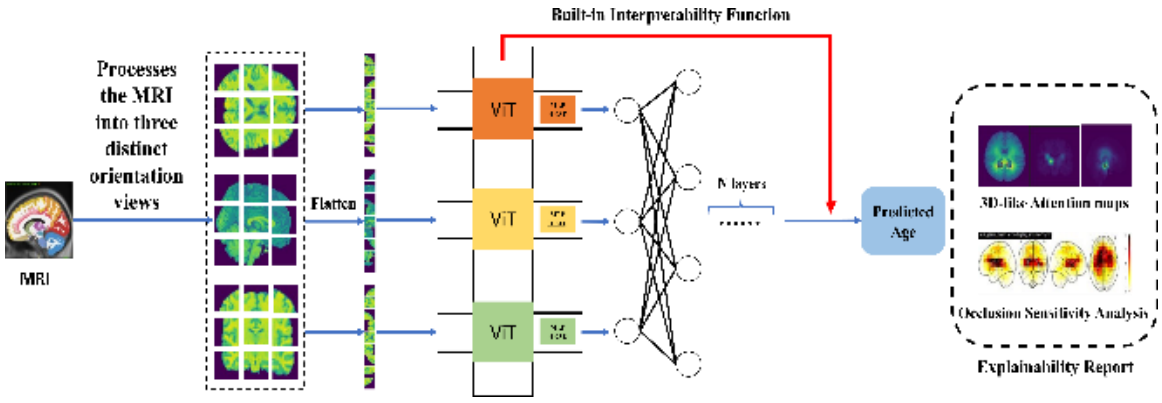

Figure 1. Structure of Triamese-ViT.

Results

The built-in interpretability results (Figure 2) aligned with those from occlusion analysis, identifying the Cingulum, Rolandic Operculum, Thalamus, and Vermis as important regions in normal ageing (Figure 3). And they also revealed pronounced hemispheric asymmetries, especially in females, where left-hemisphere regions were predominantly youth-preserving and right-hemisphere regions—particularly the visual cortex and precuneus, showed age-accelerating effects. In contrast, males exhibited more bilateral and diffuse ageing patterns, with age-accelerating regions notably concentrated in the cerebellum (Figure 4). Over half of the analyzed regions displayed opposite effects between sexes.

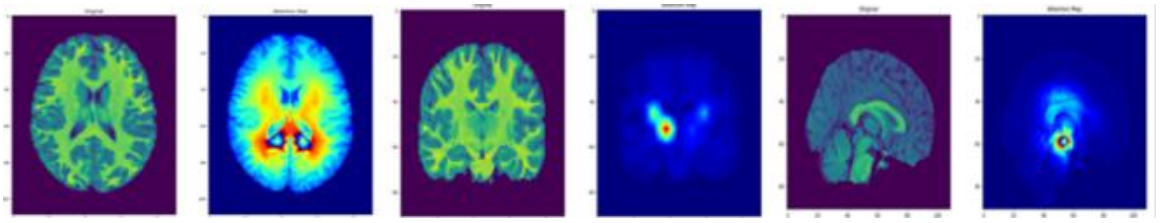

Figure 2. Our built-in interpretability function provides explanations.

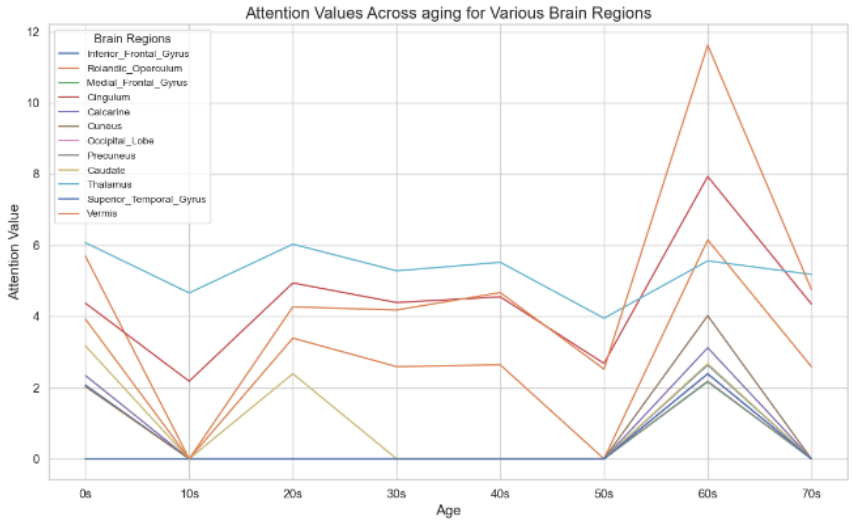

Figure 3. The attention trend lines for the most important regions throughout natural ageing based on the built-in interpretation.

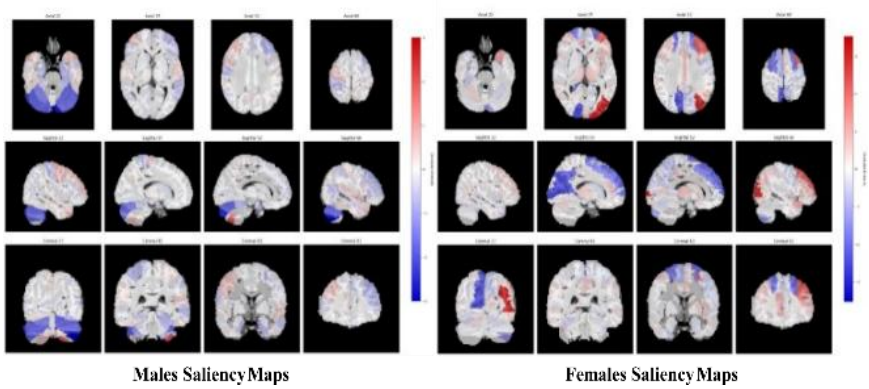

Figure 4. The significant gender difference in different brain regions during ageing.

Discussion

This aspect of our findings paves the way for further research and highlights the profound and reliable insights offered by Tri-ViT. It establishes Tri-ViT as an invaluable tool for advancing our comprehension of brain ageing. Future research could focus on validating these findings in clinical trials, exploring the use of Tri-ViT in personalized treatment plans, and further enhancing its interpretability to better support healthcare professionals in their decision-making processes.

References

1) Z. Zhang, V. Aggarwal, P. Angelov and R. Jiang, "Modeling Brain Ageing with Explainable Triamese ViT: Towards Deeper Insights into Autism Disorder," in *IEEE Journal of Biomedical and Health Informatics*, 2025, in press.